Adhesion and niche residency factors in plasma cell differentiation and neoplasia

Nicole Louise McDermott

Submitted in accordance with the requirements for the degree of Doctor of Philosophy

The University of Leeds Faculty of Medicine and Health

June 2021

The candidate confirms that the work submitted is her own and that appropriate credit has been given where reference has been made to the work of others.
This copy has been supplied on the understanding that it is copyright material and that no quotation from the thesis may be published without proper acknowledgement.
The right of Nicole Louise McDermott to be identified as Author of this work has been asserted by her in accordance with the Copyright, Designs and Patents Act 1988.
© 2021 The University of Leeds and Nicole Louise McDermott

Acknowledgements

When I started my PhD in 2017, I did not expect to be finishing my final year and writing my thesis during a global pandemic. However, throughout this turbulent time and the entirety of my PhD the support received from my supervisor Prof. Reuben Tooze and ad-hoc supervision from Dr.Gina Doody along with support from my lab group was unwavering and for this I am very grateful.

The Doody/Tooze group members past and present made me feel welcome from the outset, I would like the say a special thank you to Sophie Stephenson who is a wonder woman in the lab, who always has time to offer support, knowledge and encouragement and has helped not only me but countless other PhD students. Along with special mentions to Jenny Shrimpton and Emily Robinson who not only became great friends but endured our many random office conversations about baking, TV shows and pretty much everything else. They gave me advise from experimental setup and strange looking results, which usually only Reuben or Gina could make sense of. My time working with the Doody/Tooze group was thoroughly enjoyable, albeit not without its hiccups, but what PhD is. That enjoyment was in part due to the people surrounding me and all I can say to them is thank you.

On a more personal note, thank you to Ann Marie my Aunt who put my entire PhD into perspective and reminded me why I wanted to persue a career in research and the power of staying positive. My final year was a lot tougher than anyone could have anticipated and the encouragement from my parents, which they have with everything I do; I will always be forever grateful.

Abstract

Haematological malignancies are incredibly complex due to the nature of immune cell maturation and the stages that malignancies can arise. Therefore, understanding the underlying mechanisms of survival, homing and migration to the survival niche will aid diagnosis and understanding of disease metastasis. This project aims to investigate cell surface phenotype during plasma cell differentiation of an adhesion signature. This adhesion signature was initially identified using RNA-sequencing and microarray.

The adhesion signature was upregulated in plasmacytoma an isolated, cohesive tumour compared to plasmablastic lymphoma a dispersed, proliferative disorder. Along with a set of niche factors involved in homing and migration, there is a particular focus on the protocadherin-gamma (PCDH-γ) locus which we have shown to be epigenetically regulated in B-cells, this unique mechanism generates an identity code on the cell surface that may influence cell-cell interactions within the bone marrow microenvironment. My work uses a novel *in vitro* differentiation system to investigate the establishment of an adhesion surface phenotype throughout plasma cell differentiation from peripheral blood and malignant bone marrow samples. I aimed to elucidate how this pattern of expression is established in plasma cells and investigate what link this has to the microenvironment.

Expression patterns throughout B-cell differentiation were assessed using an *in vitro* differentiation system to generate antibody-secreting plasma cells from naïve and memory B-cells isolated from peripheral blood of healthy volunteers. A distinct set of patterns for the niche factors was a standard feature of B-cell differentiation, irrespective of the niche conditions stimulating the PC programme with evidence of regulation both transcriptionally and post-transcriptionally. The first evidence for surface expression of the PCDH-γ locus was revealed for 3 of the 22 members of the gamma cluster. The pattern of PCDHGA6, PCDHGB4 & PCDHGB5 expression was consistent between donors and niche conditions. This is consistent with epigenetic regulation determining the expression patterns that are observed at the cell surface. The highest level of surface PCDH-γ expression was at the PC stage of differentiation correlating with mRNA expression. This provides evidence that the PCDHs may indeed act as a unique identity barcode on the surface of PC.

Glossary

ADAM- A disintegrin and metalloproteinase

ALCAM- Activated leukocyte cell adhesion molecule

APRIL- A proliferation inducing ligand

ASC- Antibody secreting cell

BM- Bone marrow

BMSC- Bone marrow stem cell

CCR2- Chemokine receptor 2

CD138- Syndecan-1

CD38- Cyclic ADP ribose hydrolase

CTF- C-terminal fragment

ECM- Extracellular matrix

EMP- Extramedullary plasmacytoma

ER- Endoplasmic reticulum

HSC- Haematopoietic stem cell

IFN-α- Interferon alpha

IL-6- Interleukin 6

IL-21- Interleukin 21

ITGB7- Integrin beta7

LEPR- Leptin Receptor

LLPC- Long lived plasma cell

MM- Multiple myeloma

MMP- Metalloproteinase

MSC-Mesenchymal stem cell

PB- Plasmablast

PBL- Plasmablastic lymphoma

PBMC- Peripheral blood mononuclear cell

PCDHG- Protocadherin-γ

SMM- Smouldering myeloma

SPB- Solitary plasmacytoma of bone

Table of Contents

List of Figures

List of Tables

1 Introduction

1.1 Overview of Cancer and the Immune System

The focus of this thesis will be on cell surface phenotype and how this is affected by gene expression and protein expression at different stages of B-cell differentiation along with changes during plasma cell neoplasia. The aim is to study a set of niche residency factors and assess how their surface expression pattern is affected during B-cell differentiation and identify regulatory mechanisms that may be at play that influence expression at both a transcriptional and post-transcriptional level. The set of niche residency factors were identified in a comparison of differentially expressed genes in plasmacytoma samples compared to plasmablastic lymphoma samples (PBL), this revealed an upregulation in an adhesion signature in plasmacytoma. This was interesting since plasmacytomas from a cohesive isolated tumour in comparison to plasmablastic lymphoma which although derived from a similar differentiation stage is proliferative and often dispersed. This suggested that part of this localisation is a result of expression of a set of niche residency factors. From the list of differentially expressed genes ALCAM, CCR2, ITGB7, LEPR and the PCDH-γ cluster was selected for further investigation at a gene and protein level.

Blood cancers with a B-cell or plasma cell (PC) of origin fall into 3 categories, leukaemia, lymphoma, and myeloma. The most common cancers stemming from the B-cell lineage are lymphomas including DLBCL and CLL that develop from mature B-cells and myelomas developing from terminally differentiated antibody-secreting plasma cells. Our focus will be on myeloma and PC derived neoplasms as they present an interesting area of immune biology. These neoplasms lead to the secretion of monoclonal protein known as M protein and impaired ability to secrete normal antibodies during infection. Myeloma is difficult to treat and follows a course in part due to the heterogeneity seen in the underlying genetic abnormalities. Multiple myeloma gets is name as multiple lesions can often be identified showing a dispersed pattern of disease. However, some patients present with a localised disease pattern of neoplastic PCs. Therefore, understanding migration, localisation and retention of PCs within the survival niche may open a window to unravelling the heterogeneity seen in such a complex disease.

Immune cells already have the ability to circulate and can lead to dispersed tumours around the body. PCs mainly reside in the bone marrow therefore treating PC neoplasms traditionally depends on chemotherapy. This also targets other immune cells causing the patient to be immunocompromised and susceptible to secondary infections. There is an increased effort to move towards tailored treatment for individual patients, which requires in-depth analysis of the phenotype of the neoplastic cells to aid decisions on treatment strategies. Assessing cell surface phenotype provides a way of monitoring the progression and allowing for risk prediction of blood cancers.

1.2 B-cell biology

1.2.1 Overview

B-cells encompass the humoral arm of adaptive immunity and undergo a differentiation process in order to become fully mature antibody secreting plasma cells. They play several roles in the immune response; they not only secrete antibodies but also act as antigen presenting cells and can secrete cytokines that manipulate the immune response. Naïve B-cells develop from haematopoietic stem cells (HSCs) in the bone marrow before migrating to secondary lymphoid organs the lymph nodes or the spleen to undergo maturation and potential engagement in immune responses.

1.2.2 Differentiation

The B-cell lineage is derived from HSCs, which mature into either myeloid progenitors or lymphocyte progenitors. Following the lymphoid lineage, the progenitors can become T- or B-lymphocytes or NK cells and functionally contribute to adaptive immunity. From the lymphoid lineage B-cells into fully mature antibody secreting cells plasma cells.

B-cells can be activated through either T-cell dependent or independent pathways to drive differentiation into terminally differentiated PCs. After activation in secondary lymphoid organs (spleen or lymph nodes) in a T-dependent response, B-cells enter into the germinal centre reaction, here they undergo somatic hypermutation (SHM), class-switch recombination (CSR) and affinity maturation. These processes alter the B-cell receptor (BcR) increasing the specificity of the receptor to the antigen presented which results in a stronger immune response upon exposure to the antigen.

During B-cell ontogeny the process of generating a functional antigen receptor and early B-lymphopoiesis can be separated from subsequent activation and differentiation during a functional immune response. B-lymphopoiesis occurs in the bone marrow and focuses primarily on the acquisition of a fully functional B-cell receptor (BcR). This is the membrane bound form of the immunoglobulin, made up of two heavy and two light chains that will be secreted in an immune response. B-cells undergo rearrangement of the immunoglobulin heavy and light chain through VDJ recombination, which is governed by the recombinase-activating genes (RAG).

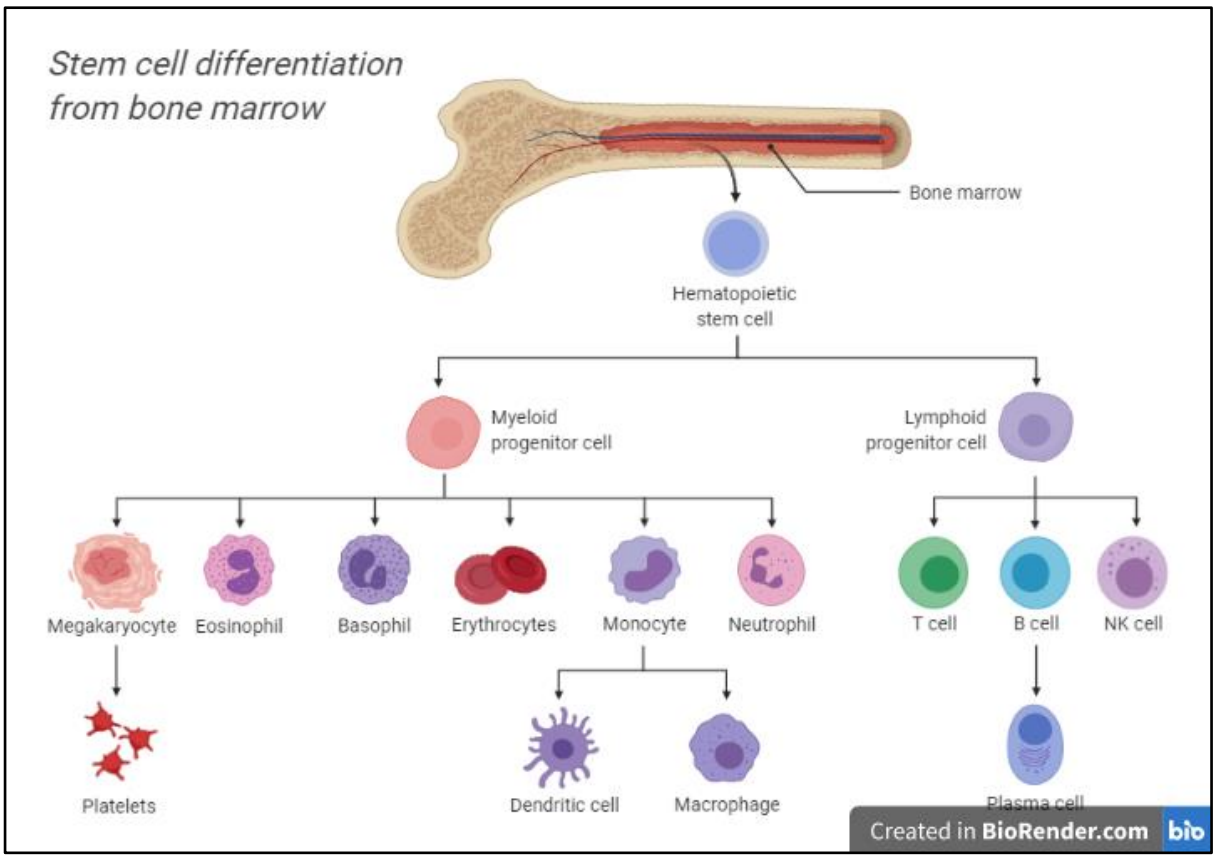

Figure 1.2.2.1 Map of the haematopoietic lineages
Diagram showing the myeloid and lymphoid lineages that a cell can go down from a haematopoietic stem cell and the precursor before fate determination when the cell becomes fully differentiated. (Image from Biorender)

VDJ recombination leads to the formation of the antigen binding site from paired heavy and light chains. This is expressed on the B-cell surface as both IgM and IgD isotypes.

It is the heavy chain that can be identified by different classes (IgH, IgM, IgG, IgA & IgE).

After generation in the bone marrow B-cells pass through transitional stages as they mature into naïve B-cell in the periphery. Here they reside in the secondary lymphoid organs (lymph nodes and spleen and in mucosal associated lymphoid tissue). Further differentiation is initiated by T-cell dependent or independent pathways depending on the nature of the activating stimulus.

Naive B-cells are activated through B-cell receptor (BcR) binding to an antigen which can be soluble or presented by antigen presenting cells (APCs), dendritic cells, macrophages and T-helper (Th) cells. Following activation, naïve B-cells enter the germinal centre in secondary lymphoid organs (lymph nodes and spleen), here they undergo somatic hypermutation (SHM), class-switch recombination (CSR) and affinity maturation. Once selected via affinity maturation they leave the germinal centre either to become a fully differentiated PC that can secrete antibodies or a memory cell that contributes to humoral memory and can re-enter the germinal centre upon a second round of antigen presentation upon a secondary infection.

1.2.3 Germinal centre reaction

Germinal centres (GCs) are formed in the secondary lymphoid tissue, such as the spleen and lymph nodes, following activation of B-cells with T-dependent antigens. After B-cells have been through the GC reaction, they will have undergone SHM, CSR and affinity maturation whereby cells display enhanced levels of affinity to the antigen, cells that are positively selected become either PCs or memory cells. Lymph nodes and the spleen are mainly composed of follicles of IgM/IgD naïve B-cells, T-cell rich zones form borders around these follicles, it is here naïve B-cells interact with the T-cells and the strength of interaction determines whether the B-cell enters the GC. Some of these B-cells rather than enter the GC reaction move to the medullary cords and become short-lived plasmablasts which secrete low affinity antibodies. Whereas B-cells that enter the GC reaction will produce high affinity antibodies against the pathogen (De Silva and Klein, 2015).

Upon exposure to an antigen and entering the GC the naïve mature B-cell undergoes further alterations to the BcR via SHM and CSR. Within the germinal centre the naive B-cell becomes activated in response to signals from Th cells (IL-21) and dendritic

cells which leads to proliferation and clonal expansion. During affinity maturation the B-cell can either be positively selected or if the response to the antigen is too weak or too strong the B-cell can undergo further SHM or apoptosis. Following positive selection, the B-cell will undergo differentiation to become either a memory B cell or an antibody secreting PC and home to the bone marrow to provide long-lived humoral immunity.

As the B-cells undergo these multiple different processes they cycle between the light zone (LZ) and dark zone (DZ) of the GC. If the DZ B-cells go through rapid proliferation and SHM once completed the B-cells migrate back into the LZ whereby they are assessed for affinity maturation and fate determination.

In the LZ the B-cells are exposed to antigens by follicular dendritic cells (FDC), the newly mutated BcR binds to the antigen and internalises it to then present peptide fragments via the MHC-II to T-helper cells (Tfh). The strength of this interaction determines if the B-cell is positively selected, and then differentiates to become either a memory B cell or a PC as it exits. If the interaction is weak the B-cell can cycle back into the DZ for further SHM, at the other end of the scale if the interaction is too strong

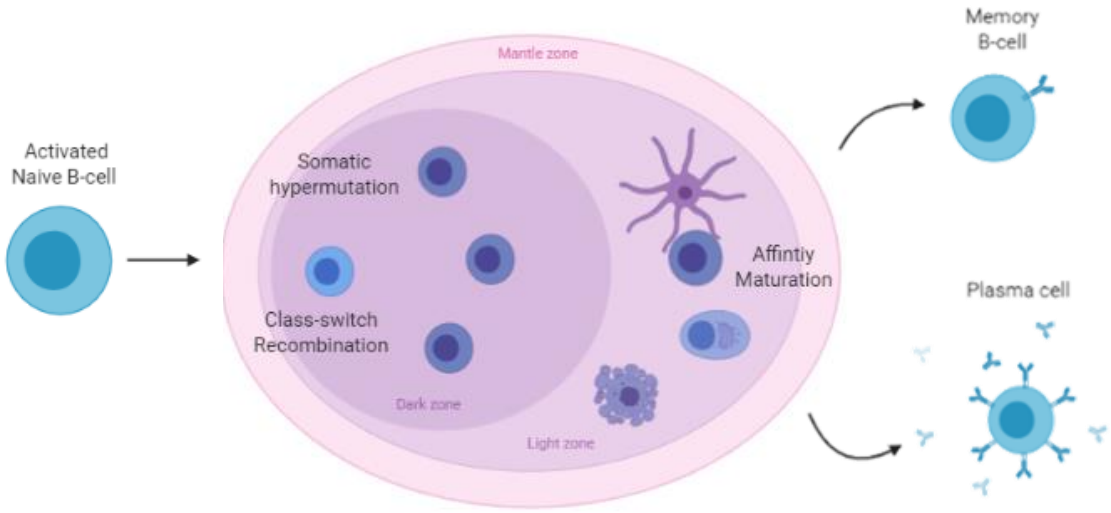

Figure 1.2.3.1 Schematic of the germinal centre reaction

Diagram of the germinal centre showing the dark and light zones that the B-cells cycle between to undergo SHM, CSR and affinity maturation before exciting the germinal centre to fully differentiate as either a plasma cell or a memory B-cell. (Image created using Biorender)

the cell could be autoreactive so it either undergoes apoptosis or becomes anergic. It has been suggested that the level of this interaction is also what decides whether the B-cell becomes a memory B-cell or a PC, having a stronger interaction will drive the cell to become terminally differentiated PCs, a weaker response and the cell becomes a memory B-cell and then an intermediate interaction generates a GC B-cell that will return to cycling in the DZ. (Ise and Kurosaki, 2019; Inoue et al., 2018).

1.2.4 Control of GC exit/cell fate

The decision to become a memory B-cell is generally considered to occur during the GC reaction and this fate decision to become a memory B-cell can be made at two separate stages. The first stage being at the T-B border which is the pre-GC stage as these are activated B-cells that have not yet fully entered the GC (Inoue et al., 2018). Or this fate decision can happen later when a cycling GC B-cell migrates to the LZ and decides whether to become a PC or a memory B-cell. If the decision is made at this stage, then the B-cell has already undergone CSR and therefore there is a subset of memory B-cells that will be IgA and IgG isotypes. The B-cells that make the fate decision to become memory cells at the pre-GC stage will be IgM unswitched and have an unmutated lower affinity BcR. However, this is somewhat controversial and memory B-cells can be classified into multiple subsets. Memory B-cells that are $IgD^{+}IgM^{+}$ double positive, IgM^{+} only or class switched IgG^{+} or IgA^{+} (Palm and Henry, 2019). As well as BcR affinity influencing cell fate, Tfh cells provide survival signals, and the level of cell help may explain how a highly mutated, highly reactive memory B-cell avoids apoptosis. Memory B-cells that are determined at the pre-GC stage can enter the GC reaction during the initial immune response, and due to the early stage they are generated, the pathogen may not have been fully cleared. On secondary exposure or exposure to a similar antigen the low affinity IgM memory cells can act as templates for a more rapid immune response when they develop a secondary GC and mutate their BCR to have a higher affinity. (Inoue et al., 2018) .

Once memory B-cells are generated they reside in areas where they are likely to encounter a pathogen to give them the best chance of responding quickly and effectively. Sentinel memory B-cells reside in the tissue where the pathogen is likely to enter for example mucosal tissues such as the tonsil and lungs, these cells usually express IgA on their surface and IgG respectively (Inoue et al., 2018). Sentinel

memory B-cells will act as the first line of defence having the earliest exposure, this is followed by memory B-cells found in the lymph nodes that will express IgG. Finally, there are memory B-cells located in the bone marrow and spleen that will be the low affinity IgM memory B-cells. These memory B-cells have the ability to re-circulate into the peripheral blood in order to carry out surveillance of other secondary lymphoid tissues, this circulation is controlled by the expression of certain adhesion molecules that control the rolling and tethering of the B-cells to allow migration across the epithelium from the peripheral blood. (Inoue et al., 2018)

1.2.5 Plasma cell bone marrow niche

The bone marrow provides the home of two essential processes; to make blood cells such as RBCs, platelets and neutrophils and to produce and maintain the B-lymphocyte component of the immune system. As well as being the home for HSCs and their differentiation in haematopoiesis, there are other cell types found within this structure. The skeleton itself is maintained by osteoclasts and osteoblasts that constantly turnover bone. These cells are generated from mesenchymal stem cells (MSCs) which are also situated in the bone marrow. The MSCs can also lead to differentiation into other cell types such as chondrocytes and adipocytes. Together the MSC derived lineages leads to the formation of bone, bone marrow, cartilage and fat, all components that support the haematopoietic cells (Comazzetto et al., 2019; Mitroulis et al., 2020). Stromal cells provide direct factor support to HSCs as well as the extracellular matrix (ECM) that provides a framework to allow for cell migration. Stromal cells can also influence lineage commitment, homing, migration and quiescence of the HSCs by contributing to micro-niches within the bone marrow.

The structure of the bone marrow is composed of sinusoids that run through to allow for migration in and out of the bone marrow as well as delivery of survival signals. From here cells can migrate in and out of the bone marrow depending on the chemoattractant signals being received. HSCs are known to reside close to the perivascular regions in the bone marrow where they can receive high levels of CXCL12 (Wilmore and Allman, 2017).

Focusing on the role of the bone marrow in lymphopoiesis, it is the stromal cell support and secretory factors that maintain the HSC population and retain the reserve population of HSCs in the bone marrow. HSCs are mainly quiescent until they receive

signals that initiate differentiation down the myeloid or lymphocyte lineages. Along with the small HSC population there will also be early progenitors for the different lineages (De Grandis et al., 2016; Comazzetto et al., 2019). Stresses within the bone marrow such as inflammation leads to the activation of proliferation of HSCs moving them out of their quiescent state. Activation of HSCs is through IFN-α and other cytokines released by immune cells as well as other cell types at the site of inflammation (Mitroulis et al., 2020). PCs are also in a quiescent state when residing the bone marrow and these PCs are termed LLPCs and continually secrete antibodies. Continual antibody secretion can maintain serological memory through methods that are still poorly understood and is a consideration when it comes to vaccination. Depending on how long memory lasts while determine the time until 'booster' vaccinations are required. A range of factors have been identified that mediate PC survival and longevity within the bone marrow niche such as CXCL12, BAFF, APRIL, TNF-α and IL-6 soluble factors as well as membrane bound factors such as VCAM-1 (Winter et al., 2012).

PCs are exposed to signals in the bone marrow niche via cell-cell interactions. There are also soluble signals playing a part such as secreted cytokines and chemokines as well as signals coming from the endocrine, autocrine and paracrine systems (Lightman et al., 2019; Lindquist et al., 2019; Nguyen et al., 2018; Nguyen et al., 2019). The cell composition and signalling that remains after delivery of cancer treatments can be massively altered in the hope that there is reduced support to the malignant B-cells or PCs, however occasionally some cells are able to persist when treatments are unsuccessful at clearing the entirety of the tumour leading to relapses as in the instance of myeloma. (Mangolini and Ringshausen, 2020).

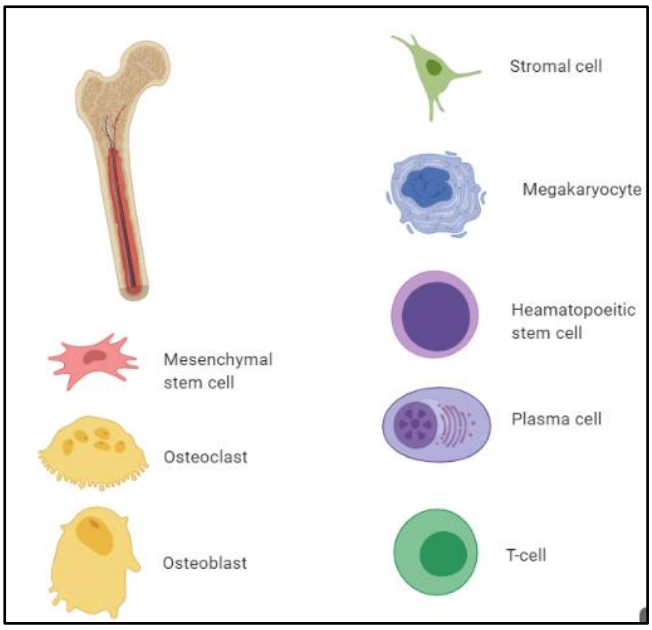

Figure 1.2.5.1 Cellular components of the bone marrow
Diagram of the bone marrow and the cell types that will be found within the bone marrow microenvironment. Cells listed that can provide support to plasma cells within the bone marrow secrete survival signals such as BAFF and APRIL, these include the stromal cells, monocytes and dendritic cells. (Image from Biorender)

Extrinsic signals that the PCs require for long-term survival in the bone marrow niche as well as other niche environments are BAFF and APRIL which signal through BCMA, TACI and BAFFR receptors on the PC, without these PCs undergo apoptosis both *in vitro* and *in vivo*. It is suggested that PC death within the bone marrow is a result of the cells not being able to get access to CXCL12 and APRIL signals as well as IL-6 which are expressed and secreted by stromal cells within the niche. (Wilmore and Allman, 2017). The importance of being able to access these signals from the niche environment for PCs is highlighted in that neoplastic PCs in multiple myeloma (MM) generally can only survive if maintained within the bone marrow niche resulting in bone lesions which are indicative of disease progression. New therapies are now looking to target the niche counterparts to cause disruption and reduce survival of the neoplastic PCs (Asimakopoulos et al., 2017). To this point as novel therapies target the bone marrow niche there may be a push towards extramedullary disease and movement to

other niche environments other than the bone marrow, for example extramedullary plasmacytomas are frequently found in the head and neck.

1.2.6 Homing and migration to the survival niche

As well as survival signals PCs also need signals that help them migrate to the bone marrow but also retain them in the niche environment, this can also be to target tissues such as the gut and other mucosal tissues. Targeting of the differentiated IgG and IgA secreting PCs to their target tissues following the GC reaction requires coordinated effort of chemoattractant cytokines as well as the involvement of adhesion molecules. It is stated that the IgG secreting LLPCs preferentially localise in the bone marrow and sites of inflammation, whereas IgA secreting PCs will migrate to the mucosal sites (Li et al., 2020; Lightman et al., 2019).

Cell homing, and migration are components of leukocyte extravasation which is a series of process that allow cells to move from one tissue into the bloodstream and into a new tissue of residence. These stages involve chemoattraction, rolling adhesion, tight adhesion and transmigration, utilising cytokines and adhesion molecules (integrins and selectins). PCs migrate along a chemotactic gradient to areas of inflammation as well as their survival niche, these chemotactic cytokines are secreted by macrophages and stromal cells, the most prominent of these being CXCL12 secreted by stromal cells, which is the ligand for CXCR4 (Biajoux et al., 2016; Frade et al., 1997; Lindquist et al., 2019). Down regulation of their current adhesion molecules allows the cells to enter the bloodstream.

Once at the site of localisation the PCs start to adhere to selectins on the wall of the blood vessel so that the PCs roll along the endothelial wall of the blood vessel. Rolling slows the travelling speed of the PC and then tight adhesion occurs. The cytokines trigger a switch from low to high integrin affinity on the cell surface creating tight adherence to endothelial layer. Finally, the cell extends pseudopodia through the gap between the endothelial cells and protrude through the basement membrane and allow transmigration out of the bloodstream into the surrounding tissue (Bianchi et al., 2012).

One of the most influential cytokines is CXCL12 the ligand for CXCR4 which acts as a chemoattractant to the GC as well as the PC niche. In order to migrate, PCs upregulate the expression of CXCR4 to the cell surface. Adhesion molecules play a vital role in maintaining the PC population in the bone marrow, aside from this there

are several adhesion molecules that target PCs to their target tissue of residence once leaving the GC (Bianchi et al., 2012). Adhesion molecules that have been well studied are integrins such as VLA-4 and LFA-2. Others are emerging such as ALCAM (CD166) which will be discussed later and is one of the adhesion molecules of interest in this thesis. ALCAM is thought to aid in migration and retention in the bone marrow via homotypic interactions on neighbouring PCs and stromal cells (Wilmore and Allman, 2017). Integrins are well known for their role in cell adhesion and in both mouse and human intergrin α4β7 has been shown to be involved in homing to the PC niche, this is mainly for IgA PCs that are homing to mucosal sites (Inoue et al., 2018). Of interest integrin β7 (ITGB7) which forms a heterodimer with integrin α4 (ITGA4) is one of the adhesion molecules that will be looked at more closely later in this thesis and was found to be upregulated in extramedullary plasmacytoma (EMP) that are found to localise in the head and neck which are mucosal sites.

1.3 Plasma cell neoplasia

1.3.1 Neoplastic B-cells and plasma cells

Plasma cell neoplasms occur when abnormal PCs form cancerous tumours in bone or soft tissue. These PCs often secrete monoclonal antibodies termed M proteins, which can be used as a diagnostic marker. Patients with PC neoplasms have abnormally high levels of this paraprotein which causes hyperviscosity and can lead to kidney damage. There are several stages of PC neoplasms starting with monoclonal gammopathy of undetermined significance (MGUS) which is benign but can develop into malignancy although this risk is around 1% per year, followed by smouldering multiple myeloma (SMM) which is a precursor to multiple myeloma (MM).

MGUS is a stable precursor stage with the same initiating genetic events as myeloma, without the clinical events seen in myeloma which are defined by CRAB, elevated calcium levels, renal failure, anaemia, and lytic lesions in the bone. MGUS patients produce paraprotein that are monoclonal antibodies rather than the full repertoire of functionally class-switched antibodies. MGUS is the first stage in the progression to MM, SMM is an intermediate stage that still is not cancerous but the levels of paraprotein are higher than that seen in MGUS, the transition to MM is the acquisition of the clinical features along with the presence of urinary heavy and light chain in the urine and a higher incidence of neoplastic PCs in the bone marrow.

Plasmacytomas lie on the spectrum of PC neoplasia but are distinguished from SMM and MM by the fact that the neoplastic PCs form an isolated tumour mass in either soft tissue or bone. While in some patients with plasmacytoma a low level of neoplastic PCs is also detected in the background marrow at levels similar to that in MGUS, in some patients no evidence of general marrow involvement is found. By contrast MM neoplastic PCs may form tumour masses in the bone marrow in multiple sites throughout the skeleton and contributing to bone lesions causing the bones to break more easily (Group, 2003). With pathologic fractures being a common complication or presenting sign in patients with PC neoplasia.

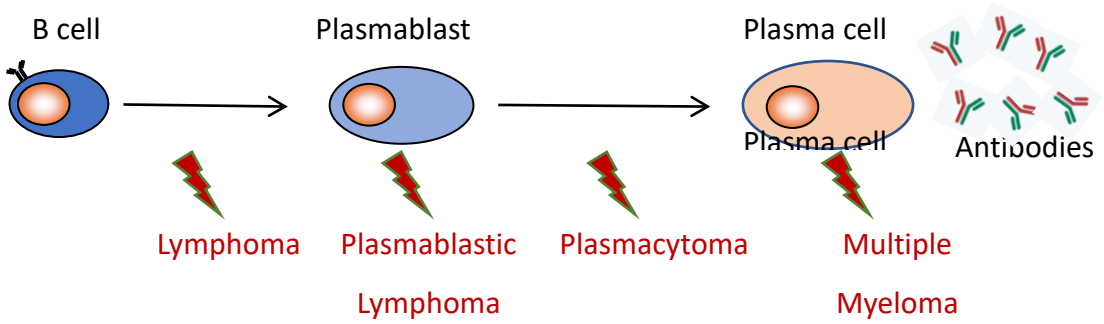

Figure 1.3.1.1 Model of B-cell differentiation and developing neoplasia
Flow diagram of B-cell differentiation showing B-cell and PC malignancies along the differentiation depending on the cell of origin for each malignancy.

1.3.2 Origins of PC neoplasia

Neoplastic PCs arise when certain regulatory pathways become mutated affecting either survival and/or differentiation. When mutations arise, the cells may become halted along the process or once differentiated they retain some plasmablastic functions allowing them to continue to proliferate and have a more immature phenotype. The presence of neoplastic PCs leads to the developments of disorders such as MM when there are multiple tumours and plasmacytoma when only one tumour in bone or soft tissue is present. The aetiology of neoplastic PCs in 50% of patients is from primary translocations affecting the immunoglobulin via aberrant CSR resulting in the insertion of oncogenes in the enhancer regions for the immunoglobulin gene. MM can be split into different types and subtypes. These types are based on the immunoglobulin produced by the myeloma cell, IgG, IgA, IgD, IgE and IgM. The

common translocations in myeloma include t(11;14) being the most common translocation along with t(4;14) and t(14;16), partner genes of these genes include cyclin D genes leading to cell cycle progression (Pawlyn and Morgan, 2017). In the final stages of MM acquisition of these types of mutations leads to a state where the neoplastic PCs have increased proliferation and evasion of apoptosis.

The acquisition of translocations and hyperdiploidy have been identified as the initiating events for the progression of neoplastic PCs from non-symptomatic MGUS and SMM to advanced myeloma, around 20% of patients with MGUS will progress to MM. Understanding the likelihood of acquiring further translocations or mutations that may identify high risk of progressing to MM is key for predicting the progression of neoplastic PCs as well as the chances of metastasis. However, one main feature for risk progression has yet to be identified, and there are a number of factors involved in high-risk sub-groups such as acquisition of further genetic mutation, molecular factors for example mutations in NFκB pathway, along with changes in the bone marrow microenvironment. Frequently mutated pathways that have already been identified for mutations for example the RAS-ERK pathway and certain transcription factors such as MYC, often seen later in the disease process (Pawlyn and Morgan, 2017).

Alongside the acquisition of oncogenic and molecular alterations the microenvironment also aids survival of neoplastic PCs and specific factors, and cytokines can act as indicators as to the likely response of the PCs (Vincent and Mechti, 2005). The bone marrow environment as discussed previously consists of stromal cells which provide support and secretory factors along with the other immune cell populations (Trentin et al., 2007; Agnarelli et al., 2018; Falank et al., 2016; Moschetta et al., 2017). Neoplastic PCs home to the bone marrow microenvironment and due to their ability to proliferate, they compete with the LLPCs for residency in the bone marrow and new plasmablasts entering the bone marrow (Bianchi et al., 2012). The result of the immortalised neoplastic PCs pushing out the healthy resident PCs leads to immunosuppression, known as immuneparesis, with the reduction of healthy PCs that can secrete functional antibodies. As MM progresses the PC population is predominantly neoplastic PCs, increased occupancy in the bone marrow of MM cells effects the normal responses of the immune system. With increased neoplastic PCs

and alterations to the cell populations within the bone marrow leads to the commonly seen clinical symptoms in myeloma (Pawlyn and Morgan, 2017).

Genetic profiles of neoplastic PCs have been studied in detail (Hedvat et al., 2003; Lorsbach et al., 2011; Pawlyn and Morgan, 2017), here we will investigate the cell surface profiles to understand the external interactions and how the surface phenotype can be used in a similar way to predict progression of neoplastic cells from MGUS through the spectrum of PC neoplasms up to myeloma. To gain more insight as to how adhesion molecules play a role in aiding the survival of neoplastic PCs it is important to understand their role and expression patterns in the normal differentiation setting. The hypothesis is that there is an underlying mechanism that distinguishes plasmacytoma in that it is an isolated lumpy disease rather than dispersed like MM. More specifically the hypothesis is that an adhesion mechanism is responsible for maintaining the neoplastic cells in one location either in the soft tissue or bone and may also provide a homing mechanism to a specific niche. As plasmacytoma forms a single tumour of cohesive cells it means that it is easier to treat with radiotherapy and surgical removal of the tumour.

The clonality of PC neoplasia is an area that has been widely debated with a single cell of origin thought the most likely theory and the progeny from this immortalised PC resulting in disease progression (Bianchi and Ghobrial, 2014; Corre et al., 2018; Keats et al., 2012; Manier et al., 2017). This can be seen in myeloma however secondary mutations can lead to a branched evolutionary tree of neoplastic PCs. In the context of relapse and refractory disease such as myeloma, multiple routes of treatment are often required with careful thought over the best plan as the selection pressure placed upon the neoplastic clones can give rise to the expansion of different neoplastic clones with a potentially more aggressive genetic landscape to the previously dominant clone (Keats et al., 2012).

As more work is carried out looking for novel therapies it has become evident that the cell's microenvironment plays a role in survival and drug resistance (Zheng et al., 2016; Vincent and Mechti, 2005). The current treatment as standard uses a combination chemotherapy, protease inhibitors and NSAIDS, this is usually with bortezomib, thalidomide and dexamethasone. Some patients have the option of a stem cell transplant which gives the best prognosis, this is based on age and

underlying health conditions. Extrinsic signals and adhesion are other areas of investigation to help understand disease pathology and identify new targets for treatment. These treatments could act in combination with disrupting the intrinsic biology of the neoplastic cells to help reduce disease progression and relapse.

1.3.3 Multiple Myeloma

Multiple myeloma (MM) accounts for 15% of blood cancers, myeloma develops from MGUS and is characterised by malignant PCs that secrete monoclonal antibodies. These MM cells produce elevated levels of M paraproteins usually IgG or IgA given that MM cells are fully differentiated and therefore have undergone SHM and CSR. MM is given the term ‘multiple’ as it generally affects multiple areas around the body giving a dispersed pattern of disease with multiple bone lesions. MM tends to affect people in their 60s and above and there is a higher incidence in males compared to females. Common treatment for MM has evolved from standard chemotherapy, with chemotherapy drug melphan and steroid prednisone or vincristine, doxorubicin, and dexamethasone (VAD) to an approach with induction using a combination of targeted therapies such as bortezomib, thalidomide and dexamethasone,that are not DNA-damaging, followed by high-dose chemotherapy and autologous bone marrow transplant for younger patients. These deplete the malignant PCs however there currently is no definitive cure and relapse is a common occurrence. For younger patients, the option of an autologous bone marrow transplant which gives one of the better prognoses, along with some emerging new therapies such as anti-CD38, daratumumab and CAR T-cells although these are not widely available, and patients must meet the criteria to be considered for treatment. There are many considerations when deciding on a treatment plan, such as age, underlying health conditions and diagnostic features known as CRAB (C=elevated calcium, R=renal failure, A=anaemia, B=bone lesions).

The cause of MM has yet to be fully elucidated, however genetic profiling has identified chromosomal translocations and other oncogenic mutations as the initiating events in MGUS and MM. Often translocations or hyperdiploidy, usually of the odd numbered chromosomes are the initiating events for progression from MGUS to MM. The chromosomal translocations primarily target the immunoglobulin locus which deregulates the target gene. Some of these translocations can also be identified in

MGUS indicating it as one of the primary genetic alterations at the start of disease progression (Lorsbach et al., 2011; Asimakopoulos et al., 2017).

Having malignant PCs in the bone marrow compartment with proliferative capacity, the balance of cell populations within the niche become disrupted and affects normal haematopoiesis. This alteration within the bone marrow often leads to the common symptoms seen with patients suffering MM such as, anaemia and bone aches due to the lesions that are generated through the changes and stresses on the bone marrow through the residency of the neoplastic PCs. As MM presents in multiple sites within the bone marrow, the homing mechanism of extravasation and localisation to a new survival niche through a chemotactic gradient is important in understanding pathogenicity. Therefore, MM provides a good model for studying cell trafficking and migration to new sites (Ghobrial, 2012). This will help identify therapies that will disrupt the survival cues between MM cells and their bone marrow counterparts to limit relapse often seen following treatment (Bianchi et al., 2012; Moschetta et al., 2017).

It is possible to have the co-incidence of extramedullary plasmacytoma (EMP) in soft tissue which would have developed from MGUS in the bone marrow as well as soft tissue deposits from MM cells that resides in the bone marrow. These MM PCs have developed a mechanism that allows for the migration out of the bone marrow and homing to a new niche environment in soft tissue. To do this the MM PCs also need to avoid detection from immune surveillance and receive the correct survival signals once localised in the new niche environment. Cases showing this type of multi-disease progression have noted that the EMP appears post-treatment for the initial case of MM when the patient relapses. Genetic abnormalities that are associated with the bone marrow disease seen with MM are not thought to be associated with the extramedullary migration suggesting that it is a change in the niche environment interactions possibly caused by treatment to remove the initial MM cells (Bladé et al., 2011).

1.3.4 MM cells in the niche

Within the bone marrow the MM cells are receiving survival signals that help them avoid apoptosis as well as continuing to proliferate, in order to constitutively receive these signals such as IL-6, CXCL12 and TGF-β there needs to be a positive feedback loop between the MM cells and the bone marrow stomal cells. Having a feedback loop keeps signalling pathways such as NF-κB, PI3K-AKT and JAK/STAT pathways active to upregulate anti-apoptotic factors, induce the expression of adhesion molecules as well as matrix metalloproteinases (MMPs). Cell adhesion not only keeps the MM cells in the bone marrow niche to allow for proliferation and survival, it is also one of the mechanisms the MM cells have for developing drug resistance against standard chemotherapy (Vincent and Mechti, 2005; Bianchi et al., 2012).

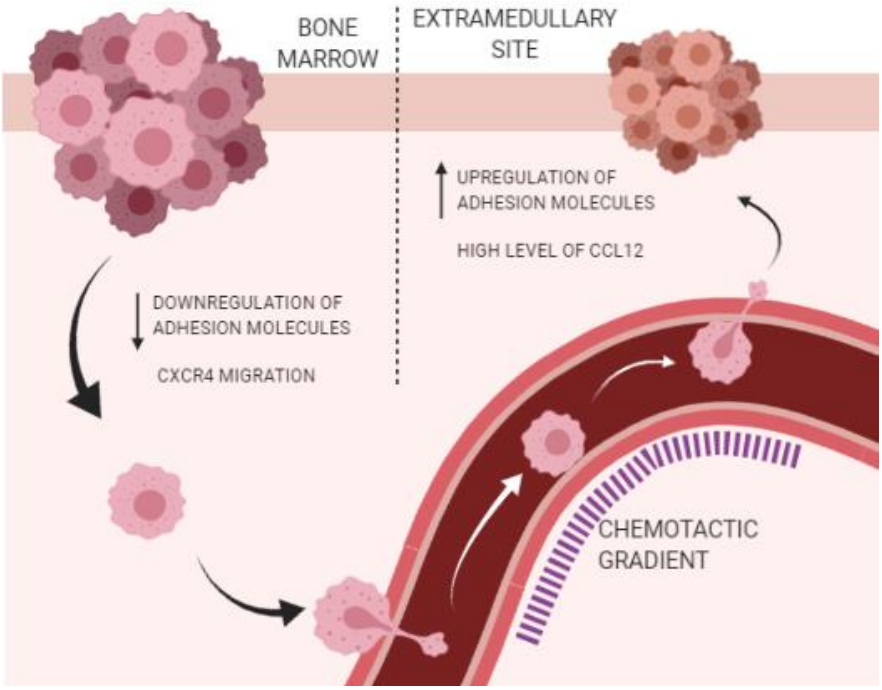

Figure 1.3.4.1 Model of MM metastasis
Diagram representing extravasation of a MM cell from the bone marrow to a extramedullary site induced by alteration in the levels of adhesion molecules as well as chemotactic signals such CCL12 which drives migration via CXCR4. (Image created using Biorender)

MMPs are endopeptidases that are responsible for cleaving the interactions between cell surfaces and the extracellular matrix to aid extravasation and migration as well as metastasis. They are themselves tightly regulated in their activity not only at the

transcriptional and translational level but also by stereotactic interactions and are activated either by cleaving into smaller subunits like in the case of γ-secretase or are transmembrane proteins (Matthews et al., 2017). Cleavage of adhesion molecules on the surface PCs allows for migration out of their current niche and then downregulation of MMPs restores the adhesion molecule expression to the surface of the PCs that can form new interactions with the new niche environment (Bianchi et al., 2012).

Patients can survive for many years with treatment however quality of life is often affected due to the relapse and refractory nature of the disease following treatment. As MM presents as a dispersed disease one could speculate that these malignant PCs have the ability to downregulate adhesion molecules to allow them to migrate and invade new niches within the bone.

MM cell survival is aided not only by genetic alterations but by migration and adhesion. This highlights why looking at more than genetics alone to explain the response to targeting one aspect of MM cell survival is beneficial and helps to explain why treatments may fail to clear all MM cells from the bone marrow. Understanding how cell adhesion affects migrations and localisation to survival niche environments will potentially lead to combination therapies that can target multiple aspects of MM cell survival leading to a reduction in relapse seen in many patients.

1.3.5 Plasmacytoma

Plasmacytoma is a PC neoplasm in which malignant PCs grow in either soft tissue or the skeleton. There are two classifications of plasmacytoma; extramedullary plasmacytoma (EMP) which is localised to soft tissue, often in the respiratory tract, and solitary plasmacytoma of bone (SPB) which presents as lytic lesions in the bone. Other diagnostic factors can be used to determine the risk of progressing to multiple myeloma (MM), such as the serum M protein level, urinary light chain levels, size of the tumour and PC content within the bone marrow (Guo, S.Q. et al., 2013). Plasmacytomas that then go on to develop into MM, approximately 15%, have a poorer prognosis. EMP has a lower incidence but may potentially be a curable disorder when there is low risk of progressing to myeloma (Bladé et al., 2011).

When plasmacytoma presents as a solitary tumour this can be either in the bone or soft tissue but has a rare incidence accounting for 2-5% of all PC neoplasms (Grammatico et al., 2017). When localised to the bone SPB lesions are commonly

found in the vertebral column and for EMP the lesion tends to be present in the respiratory tract. Due to the rarity of solitary plasmacytomas there is limited information available as to whether these neoplastic PCs differ much in terms of genetic programmes compared to MM cells, most likely this will be the migratory and adhesion mechanisms depending on the stroma in the area they are localising to i.e bone or soft tissue. Comparing clinical features between SPB and EMP, which are easier to identify such as tumour size, M protein and risk of progressing to MM has showed that SBP had a poorer prognosis with a higher risk of developing MM. When patients have been given radiotherapy as a treatment method, this shows a better response when applied to EMP compared the SPB (Guo, S.Q. et al., 2013). This is most likely due to the fact any treatment towards the bone marrow also affects the normal haematopoiesis, like that seen when treating MM with other novel therapies such as monoclonal antibodies and chemotherapy. Alongside this there is the possibility of developing drug resistance due to the protective nature of the bone marrow niche.

As mentioned in the previous section EMP can be seen coincident with MM and it is thought that the MM cells have migrated out of the usual niche in the bone marrow and then localised in soft tissue. As genetic alterations are not thought to be involved in the migration to a new niche environment it is suggested that other factors such as adhesion molecules and extrinsic cues are influencing this behaviour (Bladé et al., 2011). Emergence of EMPs have been reported following treatment of patients with MM (Avigdor et al., 2001). Although these findings have not been confirmed, due to the bone marrow niche and extrinsic signals being important for MM cell survival it is conceivable that after disruption of the bone marrow the MM cells are driven to adapt and relocate to a new niche. For MM cells to grow and survive in extramedullary sites, investigation into differences between their gene expression profiles has been analysed to identify if there is a switch in PC programmes that confers an advantage for surviving in a new niche. Analysis of EMP samples revealed expression patterns linked to angiogenesis with high expression of genes such as *NOTCH3, TIE2* and *CD31.* When directly comparing against MM cells there were 156 genes significantly upregulated in EMP that are involved in angiogenesis and cell adhesion (Hedvat et al., 2003). By upregulating gene programmes for new vessel formation and adhesion

molecules many of which were also found to be expressed on endothelial cells will help MM cells moving to extramedullary sites form a new niche.

1.3.6 Plasmablastic lymphoma

Plasmablastic lymphoma (PBL) is a rare aggressive large B-cell proliferative disorder commonly associated with HIV and Epstein-Barr virus (EBV) infection. Patients positive for HIV are at higher risk of acquiring PBL, having co-infection has also shown to affect the pathology of PBL. One case study shows the development of extranodal PBLs associated with EBV (Schichman et al., 2004). Unlike other large B-cell lymphomas that reside in the lymph nodes, PBL is commonly found in extranodal sites such as the oral cavity and digestive tract. PBL cells have a morphology that is plasmablastic and almost identical to other large B-cell neoplastic disorders making it difficult to diagnose correctly and therefore difficult to provide the appropriate treatment (Vega et al., 2005; Lopez and Abrisqueta, 2018).

It is generally considered that PBL cells are at a more immature state of differentiation compared to fully matured PCs. It is thought that PBL develops from a plasmablast that has undergone SHM and CSR and is at the point of transforming to a PC (Castillo et al., 2015). More recent examination of PBL cells has highlighted a genetic characterisation resembling an earlier time point in B-cell differentiation than that of mature PCs. Typically, PBL cells have expression of XBP-1, Blimp-1, CD38, CD138 and IRF4 with a loss of CD20, and PAX5, the latter being used to identify B-cells prior to differentiation. To distinguish between plasmacytoma and PBL a lack of CD56, CD117 and CCND1 would favour PBL as a diagnosis. Along with subtle changes in surface phenotype, cell morphology showing a diffused and aggressive pattern favours PBL over plasmacytoma. Lack of bone marrow infiltration and disease are indicative of PBL over a myeloma diagnosis as well as a lack of translocations that are commonly seen in myeloma. From this analysis it suggests the B-cell has started to switch to a PC programme but is not yet fully differentiated, therefore it has been suggested that the cell of origin of PBL is that of a plasmablast that is an activated lymphocyte and had been through the initial stages of the GC reaction, SHM and CSR (Lopez and Abrisqueta, 2018).

There is an association with immunodeficiency and PBL with many cases reported in patients with HIV and EBV. Interestingly, plasmablasts have been noted to be present

during viral infection such as EBV or HIV. EBV has not only been reported in PBL but also HIV cases suggesting a link with PBL disease pathogenesis. Other than immunodeficiency there has been effort to identify a genetic basis to PBL progression. So far one of the genes identified is *MYC*, a known oncogene, that is frequently found in translocations in PBL cases, causing an over expression of the MYC protein (Lopez and Abrisqueta, 2018). Some cases of PBL have been found to have a MYC translocation, this is also seen in myeloma with tumour progression and thought to be a common pathway of dysregulation in B-cell neoplasms that have a plasmablastic morphology and are clinically aggressive (Taddesse-Heath et al., 2010). Along with these alteration mutations have been identified in *PRDM1,* encoding BLIMP1, which may have an impact on MYC targets but also may be involved in halting differentiation and maintaining the plasmablastic phenotype. In myeloma fully differentiated PCs take on a more plasmablastic phenotype seen in proliferative, aggressive clinical features yet retain normal PC features, the main feature being antibody secretion however due to Ig translocations they secrete monoclonal antibodies known as paraproteins. Therefore, the mutations that give a more plasmablastic phenotype for example MYC will crossover between PBL and proliferative cases of myeloma.

Although PBL, like EMP is found in areas outside the bone marrow niche, due to the proliferative and plasmablastic nature it does not present as an isolated tumour and is an aggressive disease with a poor prognosis, in comparison. Once PBL has advanced to a later stage there is often involvement of the bone marrow. This highlights the difficulties for diagnosis due to these subtle differences in PBL comparted to myelomas or a plasmacytoma therefore it is not seen as a PC neoplasm and generally treated as a lymphoma. There is no standard treatment regime for PBL due to its rarity and difficulty in diagnosing. However, treatment for PBL has been looked at from a few different angles, from traditional therapies such as radio- and chemotherapy which saw the emergence of chemo-resistance with cyclophosphamide, known as CHOP when given with the full treatment regime. Patients with high-risk PBL, where there is bone involvement and the presence of HIV require more aggressive chemotherapy with some evidence for the use of lenalidomide or bortezomib as well as some of the novel approaches such as monoclonal antibodies and small molecules inhibitors (Makady et al., 2021; Castillo et al., 2015; Vega et al., 2005).

1.3.7 Differential gene expression between EMP and PBL

Data obtained from microarray analysis of plasmacytoma and plasmablastic lymphoma samples have revealed a set of genes that are differentially expressed. With 66 genes upregulated in plasmacytomas and 71 genes upregulated in PBLs at FRD=<0.5. Genes upregulated in plasmacytoma were enriched for membrane components and linked to adhesion and secreted growth factor activity. While those upregulated in PBLs were linked to cell cycle and cell division. The PBL and plasmacytoma cases did not differ significantly in features related to core elements of the PC state. This suggested that a set of adhesion genes might be linked to the more quiescent plasmacytoma state.

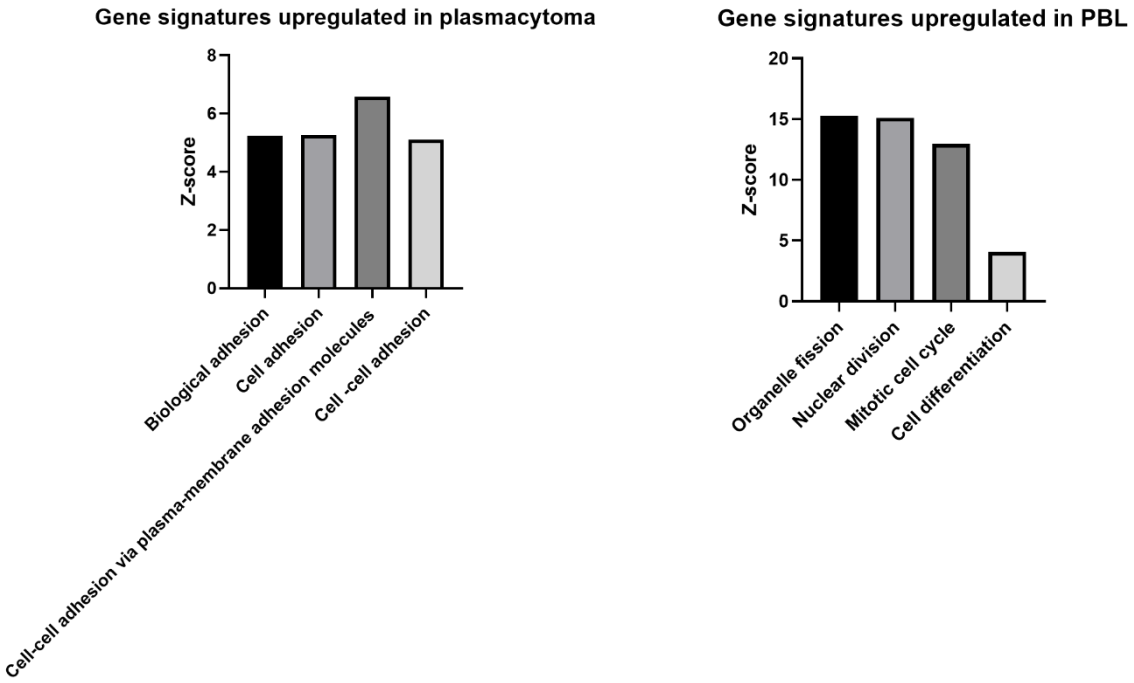

Figure 1.3.7.1 Gene signatures enriched in plasmacytoma vs PBL
Gene ontology performed on plasmacytoma and plasmablastic lymphoma (PBL) samples revealed the gene signatures that are enriched in plasmacytoma in PBL. The Z-scores for the top 4 gene signatures were plotted and revealed that in plasmacytoma adhesion came up in each of the signatures and the signature with the highest Z-score was adhesion via plasma-membrane adhesion molecules. The signatures that came up highest for PBL were linked to cell cycle and division.

RNA-seq from an *in vitro* differentiation series showed similar expression levels of the adhesion molecules but no significant increase in expression throughout differentiation (Mario Cocco & Matthew Care). Of the differentially expressed genes identified the focus was narrowed down to the protocadherin-γ *(PCDH-γ)* family and another 4 genes: *ALCAM, LEPR, CCR2,* and *ITGB7*. These were chosen due them being transmembrane proteins, which was the signature mostly highly enriched in plasmacytoma, we saw differential expression in plasmacytoma compared to PBL and saw positive expression in the *in vitro* differentiation series.

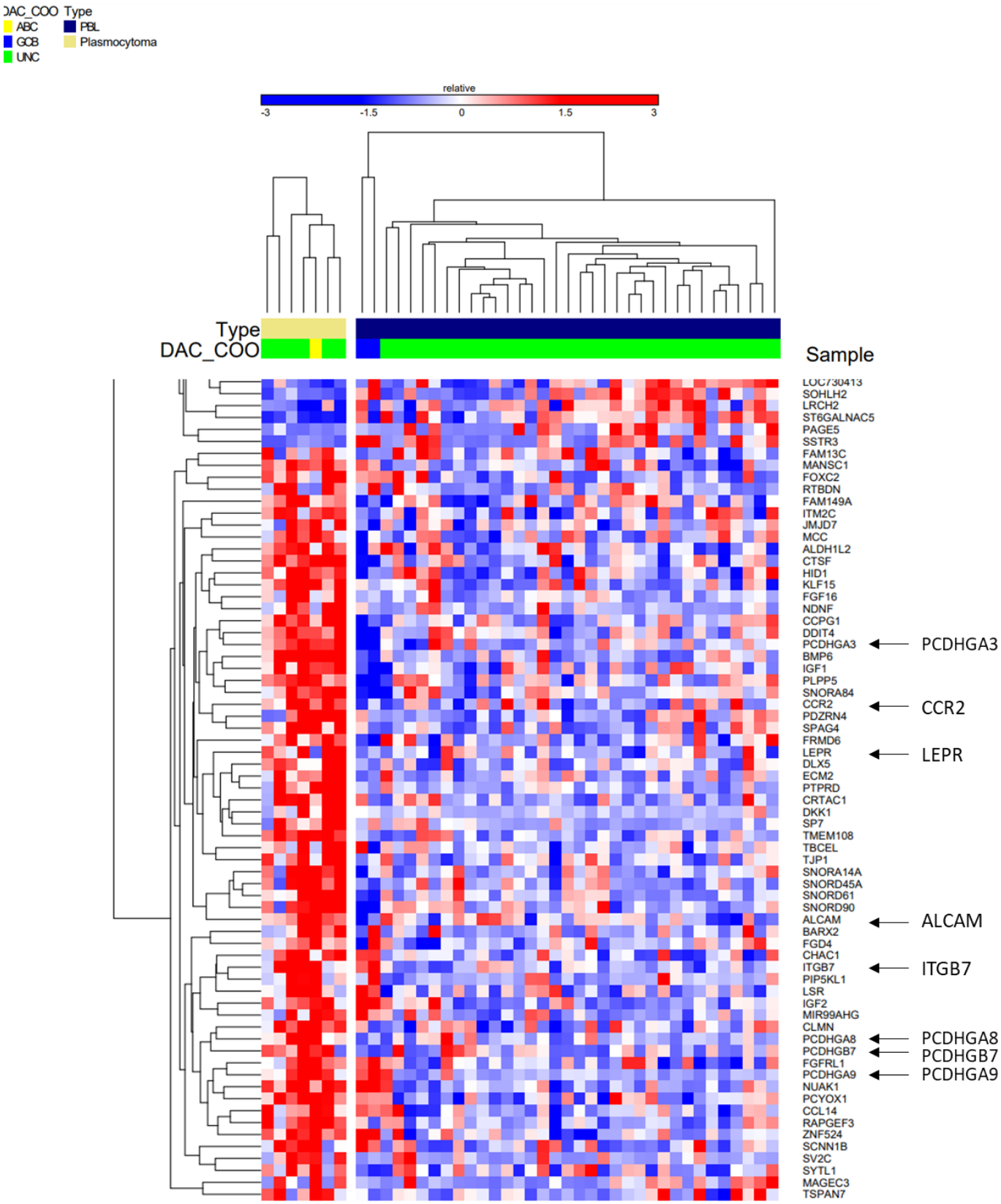
DAC_COO
ABC
GCB
UNC
Type
PBL
Plasmocytoma
relative
-3
-1.5
0
1.5
3
Type
DAC_COO
Sample
LOC730413
SOHLH2
LRCH2
ST6GALNAC5
PAGE5
SSTR3
FAM13C
MANSC1
FOXC2
RTBDN
FAM149A
ITM2C
JMJD7
MCC
ALDH1L2
CTSF
HID1
KLF15
FGF16
NDNF
CCPG1
DDIT4
PCDHGA3
BMP6
IGF1
PLPP5
SNORA84
CCR2
PDZRN4
SPAG4
FRMD6
LEPR
DLX5
ECM2
PTPRD
CRTAC1
DKK1
SP7
TMEM108
TBCEL
TJP1
SNORA14A
SNORD45A
SNORD61
SNORD90
ALCAM
BARX2
FGD4
CHAC1
ITGB7
PIP5KL1
LSR
IGF2
MIR99AHG
CLMN
PCDHGA8
PCDHGB7
FGFRL1
PCDHGA9
NUAK1
PCYOX1
CCL14
RAPGEF3
ZNF524
SCNN1B
SV2C
SYTL1
MAGEC3
TSPAN7
PCDHGA3
CCR2
LEPR
ALCAM
ITGB7
PCDHGA8
PCDHGB7
PCDHGA9

Figure 1.3.7.2 Heatmap of differentially expressed genes that are upregulated in plasmacytoma

Differentially expressed genes from plasmacytoma and PBL samples showed that plasmacytoma samples clustered for a set of genes that are upregulated in plasmacytoma and are downregulated in PBL samples. Of these genes, highlighted with arrows, are the genes chosen for further analysis due to their link to adhesion and are transmembrane proteins, which was the gene signature most highly enriched in the gene ontology analysis.

As plasmacytoma presents as a solitary tumour it is hypothesised that the upregulation of these adhesion molecules could be responsible for isolated tumours with a lower risk of disease progression and metastasis. The four adhesion molecules selected collectively have roles in homing and migration as well as adhesion within the bone marrow niche. The PCDH-γ cluster has mainly been characterised in the nervous system and have a role in adhesion during synapse formation. The combination of PCDH-γ molecules expressed on a cell surface appear to influence cell-cell interactions which may have a similar role in PC neoplasms leading to the generation of monoclonal tumours.

Work carried out previously in the Doody-Tooze lab group has developed an *in vitro* system that allows the differentiation of B-cells isolated from peripheral blood samples into long-lived PCs (Cocco et al., 2012), variations of this system have been used to mimic different niche conditions as well as controlling other processes such as shedding of these adhesion molecules that will be discussed in detail later.

1.4 Adhesion signature of surface adhesion molecules may influence disease progression and pathogenesis

1.4.1 Role of Adhesion molecules in B-cell and Plasma cell neoplasms

Survival of neoplastic cells is dependent on receiving survival signals as well as avoiding apoptosis. As previously mentioned, MM cells can develop drug resistance to treatment or relapse following a course of treatment. Combination therapies that can target multiple aspects of cell survival are starting to be trialled in relapse, refractory disease such as MM and CLL, a hyperproliferative B-cell disorder. By

targeting adhesion molecules MM cells will be less able to respond to the supporting neighbouring cells as well as other support systems like the ECM. Adhesion is one of the factors that is being highlighted as having an important role in the progression of PC malignancies. Along with survival within the bone marrow niche adhesion molecules also play an important role in migration, changes in levels of expression lead to migration to other sites and spread of the disease seen in MM and PBL. Solitary tumours like those in plasmacytoma have better prognosis and are at lower risk of developing into MM a dispersed disease. Investigating the expression of adhesion molecules has revealed variations in the levels of expression between malignancies that may reflect progression and prognosis and an interesting area of research in B-cell differentiation.

1.4.2 ALCAM (CD166)

Activated Leukocyte Cell Adhesion Molecule (ALCAM) also known as CD166, is a transmembrane protein that is a member of the immunoglobulin superfamily. ALCAM binds either homotypically to itself on neighbouring cells as seen with B-cells and PCs or heterotypically to its ligand CD6, which is highly expressed on T-cells. ALCAM is expressed on activated T-cells, activated monocytes and epithelial cells as well as a few others. ALCAM has roles in leukocyte extravasation, stabilisation of the immunological synapse, T-cell activation, proliferation as well as tumour growth and metastasis.

For ALCAM to have a role in extravasation and migration there needs to be a mechanism for up- and downregulation of surface expression, evidence of cleavage by ADAM sheddases of ALCAM has been reported using Raji and Jurkat cells. Cleavage of ALCAM by ADAM17 was shown to be regulated by CD9 and colocalisation (Gilsanz et al., 2013), revealing a regulated mechanism that can dynamically alter the level of adhesion molecules. This will play an important role in disease pathogenesis by having the ability to migrate and metastasise. Where higher levels of ALCAM are seen this could be due to inhibition of ADAM cleavage reducing the risk of cells migrating and spreading, higher levels of ALCAM were seen in EMPs compared to PBL samples which may reflect a reduced capacity to migrate and therefore EMPs having a more favourable prognosis.

ALCAM has also been linked with cellular adhesion in MM within the bone marrow (BM) microenvironment, with migration inhibitory factor (MIF) acting through ALCAM as a surface receptor on MM cells (Zheng et al., 2016). Through the inhibition of MIF MM cells appeared to be more responsive to chemotherapy, possibly due to changes in cellular adhesion. It has been reported to have high expression in MM cell lines. When ALCAM was silenced in *in vivo* models there was less tumour burden and osteolytic lesions as well as better cell survival (Xu et al., 2016). This suggests that ALCAM is a driver of multiple osteolytic disease in the progression of MM.

In breast cancer low expression of ALCAM is associated with poor prognosis and high-grade cancers. Over expression and knockdown expression in breast cancer cell lines has confirmed that low ALCAM expression correlates with reduced adhesion to bone marrow matrix and migration, reflecting what is seen clinically (Davies and Jiang, 2010). In this setting the presence of ALCAM seemed to reduce the cancer cell's ability to adhere and metastasise. For breast cancer ALCAM can be used as a diagnostic marker for bone metastasis and disease progression, the nature of how ALCAM functions in this process has not been elucidated. Targeting ALCAM overexpression may then reduce the risk of bone disease in breast cancer. ALCAM has also been linked to other cancers such as malignant melanoma effecting signalling and expression pathways for example miR-214 is linked to metastasis in malignant melanoma (Penna et al., 2013). ALCAM has also been seen to be highly expressed in malignant mesothelioma, knockdown experiments with shRNA caused a reduction in cell migration and invasion putting forward the idea of ALCAM being involved in cancer metastasis. A soluble form of ALCAM has been reported and when added to the culture medium of WT cell lines reduced cell migration. This shows that the soluble form can have inhibitory effects on the malignant phenotype (Ishiguro et al., 2012).

Overall ALCAM has been shown to have a role in adhesion and homing specifically in the bone marrow and in some instances be a driver of bone lesions and osteolytic disease. Investigating how this adhesion molecule may influence homing and localisation between normal B-cell differentiation and disease settings may highlight potential pathways that can be disrupted to aid treatment plans. Knowing the normal expression patterns and regulation mechanism controlling expression levels of

ALCAM will be a good building block to further investigate the role of adhesion in disease prognosis and progression.

1.4.3 LEPR (Leptin Receptor)

Leptin receptor (LEPR/CD295) is involved in the lymphopoiesis pathway along with many others. Leptin which is secreted by adipose tissue and upon binding LEPR is activated and is involved in controlling pathways such as bone mass, basal metabolism and immune homeostasis. This means that disruption in levels of leptin may have significant effects during infection. There is a positive link between the immune system and the neuroendocrine system during times of stress and inflammation (Abella et al., 2017). T-cell development is thought to be influenced by the presence of leptin causing an increased differentiation into the Th17 phenotype (Reis et al., 2015) which are pro-inflammatory during infection and initiate host defence though recruitment of macrophages and neutrophils.

The interaction between adipokines such as leptin with immune cells and MM cells among other neoplastic B-cells is an area that has previously been somewhat overlooked in disease progression. It is becoming apparent that adipose tissue has a role in maintaining malignant cell growth and survival with secretion of adipokines and other growth factors as well as a protective role to avoid apoptosis-inducing treatments (Falank et al., 2016).

Adipose is one of the components that makes up the bone marrow and is required for survival of the surrounding cell populations, as we age the bone marrow increases the amount of adipose present. Obesity has now been identified as a risk factor of MM, a disease that occurs generally in people in their 60s or older. Therefore, obesity may be linked to an increase in adipose tissue in the bone marrow that provides a survival advantage for MM cells (Thordardottir et al., 2017; Morris and Edwards, 2018; Landgren et al., 2010). Further investigation into the interplay between bone marrow adipose tissue is showing increased complexity in the BM compartment and communication between the cell populations present. MM cells often reside close to bone marrow adipose tissue suggesting potential signalling between the two, also to be considered is the impact having high adipose tissue within the bone marrow has on the bone. Increased levels of adipose tissue can put further pressure on the bone leading to stress and fractures that can be occupied by MM cells and lead to disease

progression from MGUS (McDonald et al., 2017; Morris and Edwards, 2018). LEPR may therefore act as a prognostic marker to aid the likelihood of disease progression.

1.4.4 CCR2 (CD192)

CCR2 is a chemokine receptor 2 (CD192) with 2 isoforms, that mediates monocyte chemotaxis. The family of monocyte chemotactic proteins (MCPs) -1,-2 and -3, are the ligands for CCR2 and have been shown to effect the migration of normal and MM plasma cells and in PBL. Blocking or neutralising antibodies confirmed the link between them and CCR2 as well as their role in migration in vitro. Interestingly blocking only one or two MCPs at a time revealed that the remaining member can compensate as there is still some migration seen. By blocking all three migration of normal and MM cells is greatly reduced but not completely inhibited suggested there are some other factors aiding the process (Vande Broek et al., 2003; Frade et al., 1997). As well as expressing *CCR2* MM cells also express *MCP-1* mRNA upon IL-6 stimulation (Arendt et al., 2002), this may be suggestive of MM cells attracting other MM cells down a chemotactic gradient in a self-homing mechanism for localisation of MM cells to the tumour microenvironment.

Along with the role in migration and homing, CCR2 is a GPCR so has signalling properties. Activation of CCR2 through MCP-1 signals through the MAPK pathway to activate ERK. Activation of ERK is thought to lead to integrin activation and chemotaxis (Jiménez-Sainz et al., 2003). Further investigation into the signalling potential of CCR2 as highlighted expression in cancer cells enhances metastasis, extravasation, and homing of CCR+ monocytes that can provide tumour support. Not only is ERK activated through CCR2 signalling but also JAK/STAT and p38 signalling pathways (Wolf et al., 2012). For a tumour to progress following invasion to a new niche requires support from surrounding cells and stroma, evidence for MCP-1 expression recruiting immune cell support has been reported along with recruitment of myeloid suppressor cells that will aid immune evasion (Huang et al., 2007). Taken together this evidence suggests that CCR2 along with MCP-1 expression by MM cells and other neoplastic B-cells can lead to migration as well as maintaining stromal support following invasion. MM cells often home to areas where there has been bone resorption by osteoclasts (bone lesions), one study looked at the gene expression of the osteoclast/MM cell interaction compared to other cell types, of note they were found to express high levels

of MM cell growth factors such as APRIL and IGF-1 and CCR2-chemokines. CCR2 was more highly expressed on MM PCs compared to healthy PCs and it has been hypothesised that CCR2+ MM cells may enhance bone resorption (Moreaux et al., 2011). This indicates a possible positive feedback loop for homing MM cells to the bone marrow as well as stimulation of bone resorption creating lesions. The MCP-1-CCR2 relationship has been a recent target for treatment in metastatic and solid tumours due to the role in invasion and tumour survival, some trials indicated at adverse effects if this relationship was disrupted causing more rapid metastasis (Lim et al., 2016). Inhibiting CCR2 signalling has not yet been trialled in PC neoplasms nor has the role of CCR2 in migration to extramedullary sites.

1.4.5 Integrin-β7

The integrin-β7 (ITGB7) subunit forms a dimer with α4 and αE chains and is expressed mainly in leukocytes. It has a role in leukocyte adhesion, migration and homing. Integrins are a family of glycoproteins that are known to be expressed on PCs and MM cells and allows them to adhere to ECM proteins and stromal cells in the bone marrow. Integrins that have been identified in PC homing and adhesion to the bone marrow include VLA-4, LFA and NCAM. More specific to MM cells in the bone marrow are the integrins VLA-4 and α4β7 that not only regulate adhesion but also migration, homing, and drug-resistance.

ITGB7 could be used as a marker for poor prognosis in MM which is overexpressed due to either the genetic translocation (t14;16) or due to paracrine stimulation through BAFF/TACI/APRIL signalling (Morito et al., 2011). ITGB7 knockdowns showed loss of adhesion ability of MM cells to fibronectin and human BMSCs, suggesting a role in MM survival in the BM microenvironment (Neri et al., 2011). Other knockdown experiments or blocking ITGB7 in MM adhesion in MM cell lines resulted in reduced ability to invade into Matrigel as well as reduced ability to move along the CCL12 (SDF-1) gradient showing a role for ITGB7 in MM for migration and invasion (Bianchi et al., 2012). A difference between ITGB7 on healthy and MM cells has been identified in that ITGB7 is maintained in the active conformation on MM cells (Hosen, 2020). MM cells have a continually active ITGB7 are likely to lead to disease progression and metastasis.

ITGB7 has been identified as a potential target for treatment of MM to disrupt the bone marrow and the survival advantages of being within the niche environment. Natalizumab is a α4 monoclonal antibody that has been used to disrupt integrin adhesion in MM and was shown to interfere with adhesion to the bone marrow stromal cells as well the ECM. Inhibiting integrins also disrupted angiogenesis and together affected MM cell growth and survival (Hosen, 2020; Podar et al., 2011) highlighting the importance adhesion plays in disease pathogenesis.

1.4.6 Conclusion

In summary each of the adhesion molecules discussed in this section play some role in PC homing, migration, and survival within the bone marrow. There is evidence that these molecules are involved in MM pathogenesis, interestingly these molecules were found to be upregulated in EMPs that are not found in the bone marrow. Evidently an adhesion gene programme is activated in EMPs and understanding how this is associated with the formation of an isolated tumour rather than dispersed disease would provide valuable insight into the process of metastasis and disease dissemination in MM.

1.5 Combinatorial expression of PCDH-γ isoforms on differentiating plasma cells

1.5.1 Characterisation in the nervous system

The protocadherin (PCDH) family are a subfamily of the cadherins, which are cell adhesion molecules involved in the formation of adherens junctions to form cell-cell interactions. The PCDHs can be split into clustered and non-clustered depending on their localisation in the mammalian genome. The clustered PCDHs are split into three separate gene clusters; alpha, beta and gamma, the clusters are organised into variable first exons and distal constant exons, these constant exons encode the intracellular region, and the variable exons encode the extracellular portion, and transmembrane domains and a short intracellular component. Each cluster has a large range of different isoforms that can be expressed, the alpha, beta and gamma clusters contain 22, 13 and 22 members respectively.

Alternate splicing brings together an alternate or a C-type exon together with a constant exon to transcribe a full-length transmembrane protein, this alternate splicing is controlled by CTCF binding and DNA looping described in more detail in the next

section. Once the protein has been translated and expressed on the cell surface it starts to form the combinatorial expression seen in neuronal cells. It is unclear how many isoforms are expressed on different cell types, however the combination of PCDHs determines the type of interaction with the neighbouring cells. PCDHs bind homotypically to their identical partner on the neighbouring cell, these combinations act like a barcode leading to either homotypic repulsion in the case of neuronal cells or homotypic adhesion which is thought to occur on PCs.

The genomic organisation resembles that of the immunoglobulin and T-cell receptor genes, which as discussed previously generate large diversity in the immune system through somatic DNA rearrangement events. The protocadherins provide diversity through surface identity using the combinatorial expression of protocadherin isoforms, the specificity of homophillic interactions between PCDHs plays an important role in the development of the nervous system. The mechanism by which this identity code is established has been of great interest in neurobiology, but its relevance in the immune system has not been appreciated.

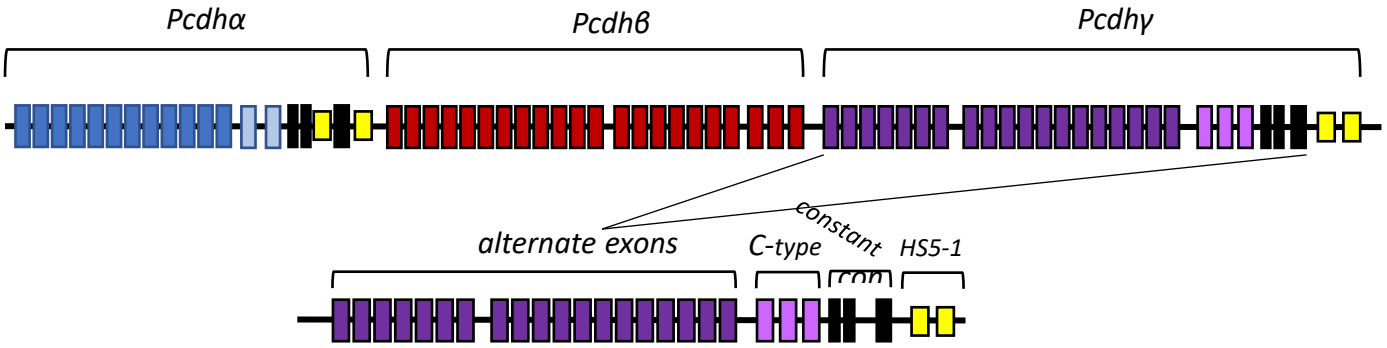

Figure 1.5.1.1 Schematic representing the genomic organisation of the clustered PCDHs

Genomic organisation of the PCDH clusters. Highlighting the PCDH-γ cluster that contains 22 isoforms with 19 alternate (dark purple), 3 C-type (light purple) and 3 constant exons (black) along (black) with the HS5-1 enhancer (yellow). Once transcribed alternative splicing brings together an alternate transcript or a C-type transcript and joins with a constant region to form a transcript encoding for the full transmembrane protein form with the extracellular domain being decided by the alternate or C-type exons.

So far PCDHs have mainly been characterised in neurons in the developing nervous system (Zipursky and Sanes, 2010; Toyoda et al., 2014). In the nervous system PCDHs have been shown to be involved in cell-cell interactions, specifically in neuronal cells for self-avoidance of dendritic trees, during development. The number of varying combinations of PCDHs that can be expressed provides a great range of diversity at the single cell level. Surface expression of PCDHs on neuronal cells results in homophilic repulsion and self-avoidance in order to only allow new synapses to be formed with neighbouring sister dendrites (Lefebvre et al., 2012; Ing-Esteves et al., 2018). Self-discrimination is dependent on the generation of single cell surface code by stochastic expression of surface proteins and a range of PCDH isoforms. Neuronal cells can express a subset of the clustered PCDHs which is determined through a sophisticated mechanism of alternative splicing and promoter choice (Mountoufaris et al., 2018). The self-repulsion mechanism is thought to be dependent on the *trans* interaction between the PCDH extracellular (EC) domains and the internal signalling

cascade leading to intracellular reorganisation (Rubinstein et al., 2017) this explains how in some cell types PCDH binding results in homotypic attraction.

The presence of PCDHs on other cell types can lead to homophilic attraction where the combination of PCDHs needs to be identical in order for a zipper like structure to form with a neighbouring cell, mis-matching isoforms can cause the complex to fall apart (Schreiner and Weiner, 2010). It is hypothesised that there is a tolerance mechanism for mis-matching isoforms, aggregation studies indicate that the level of tolerance is dependent on the number of PCDHs being expressed. For example 3 mismatching isoforms out of 15 would be tolerated whereas 1 mis-match out of 4 isoforms would disrupt adhesion (Rubinstein et al., 2017).

PCDHs can exist as multimeric complexes and it is not clear whether the PCDHs have specific partners like that of the integrins that influences their interactions. Studies investigating PCDH interactions has shown that it is the *trans* interactions that are strictly homophilic, however the *cis* interactions do not show any specificity meaning a PCDH-γ can interact with PCDH-α isoforms. The *cis* interactions are between isoforms that are adjacent to each other on the cell surface and can be either homotypic or promiscuous, the *trans* interactions with neighbouring cells are mediated by the EC 5-6 domains and are limited to homotypic interactions. The formation of PCDH-γ homophilic multimers is thought to provide stability and influences the strength of the heterophilic *cis* interactions as well as the levels of surface expression of the PCDHs (Schreiner and Weiner, 2010; Rubinstein et al., 2017). Aggregation assays show that the PCDH-α isoforms are unable to induce cell aggregation except when in combination with a PCDH-γ. This may be explained by the γ-isoform being a carrier for surface expression suggesting that there may be a dependence on a particular isoform for cell-cell adhesion (Hayashi and Takeichi, 2015).

1.5.2 Epigenetic Regulation and Promoter Choice

The combinatorial expression of PCDHs and the specificity required for cellular adhesion suggest that PCDH expression may generate a barcode to give the cell an individual identity (Kaneko et al., 2006). It is not known whether the expression pattern of the PCDHs is specific to cell types or down to single cells, which has been characterised in neuronal cells. There is literature that provides evidence for epigenetic control of the PCDH locus, and that demethylation allows for long range

DNA-looping. Clustered PCDHs have been linked to cancers when the PCDH promoter is hypermethylated suggesting that their normal action would be as a tumour suppressor (El Hajj et al., 2017). There are also uncertainties as to whether the expression is stable or changes over time and what the potential influences are on expression.

Research into the epigenetic regulation of the PCDH-α locus has revealed a unique mechanism for promotor choice leading to distinct patterns of PCDH expression. This model is underpinned by DNA-looping aided by the CTCF/cohesin complex.

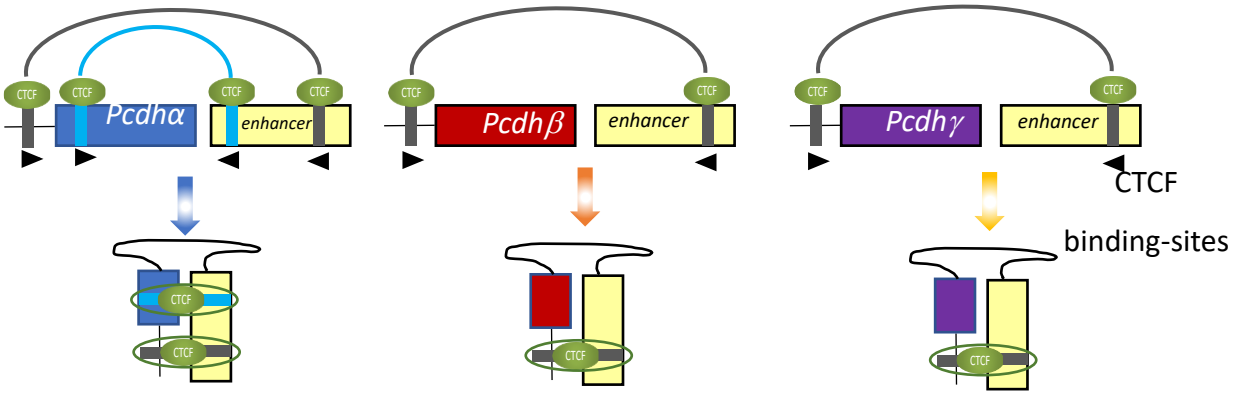

Figure 1.5.2.2 DNA-looping mechanism
Schematic of the DNA-looping, and formation of the CTCF/cohesin complex used for promoter choice across the PCDH gene clusters.

This looping brings together a distal enhancer, hypersensitive site 5 (HS5), and individual variable exon promoters to allow for transcript expression. (Canzio et al., 2019) have elucidated a mechanism of epigenetic regulation that allows for combinatorial expression of multiple different PCDH isoforms, whereby a long non-coding RNA (lncRNA) is responsible for removing methylation from CpG sites. This enables CTCF binding to two sites, one proximal to the promoter and one within the exonic region. The equivalent CpG sites are found in the HS5 enhancer but in the opposite orientation which allows for the formation of a DNA-loop. The CTCF/cohesin complex holds together the enhancer and promoter for transcription of that particular variable exon and PCDH-α transcript shown in both mouse and human (Guo, Y. et al., 2012; Canzio et al., 2019).

The PCDH-γ locus is organised in a similar way to the alpha locus in that the cluster contains variable exons and distal constant exons with a HS5-1 enhancer, the gamma locus differs by only having one CSE and CpG site for CTCF binding. It is conceivable that the same mechanism is employed by the gamma locus for promoter choice. That removal of methylation from the CpG sites allows for the binding of the CTCF/cohesin complex, looping together the HS5-1 enhancer to the active promoter. There was no evidence of lncRNA binding sites on the gamma locus but there may be a different method for demethylation. In the alpha cluster deletion experiments show that the c-type exons are more sensitive to deletion of the HS7 enhancer and only have the CSE in the promotor and not within the exon. At this site it is Rad21, part of the cohesin complex, that binds to the CSE in the HS7 enhancer and in the c-type promoters (Monahan et al., 2012). This demonstrates that expression can still mediated by the DNA-looping mechanism with only one CSE in the promoter region.

1.5.3 Post-translational processing

Once a PCDH had been transcribed and translated it is subject to post-translational processing including correct folding and trafficking to the surface as well as glycosylation modifications. Once expressed on the surface PCDHs can be cleaved, releasing the PCDH-γ ectodomain. Cleavage is carried out by metalloproteases that release a soluble portion as well as a C-terminal fragment (CTF) that has been implicated in intracellular signalling.

PCDHs have been shown to be processed by metalloproteinases (MMPs) which leads to further presenilin-dependent processing to generate a CTF (Bonn et al., 2007). This is a 2-step process where the MMP must act first to cleave and release the ectodomain followed by a second cut by a γ-secretase. For PCDH-α isoforms the MMP has been identified as ADAM10 the same MMP that cleaves AMPA receptors in the nervous system. Once the soluble ectodomain has been cleaved a γ-secretase complex releases the CTF, this fragment can then translocate to the nucleus where it can act a transcriptional regulator (Bonn et al., 2007). It has been suggested that the combinatorial expression of the PCDHs may protect against cleavage. PCDHs can form heteromers which may be a mechanism to avoid processing if the MMP and γ-secretase are unable to reach the cleavage sites (Bonn et al., 2007; Haas et al., 2005). The possible gene targets for the CTF have not yet been identified that may be under

transcriptional regulation of PCDHs. Although the downstream effects of PCDH processing have not yet been identified there is strong evidence to suggest that ADAMs are the proteases responsible.

1.5.4 Functional role of the protocadherins

The main functional role that has been described for PCDHs is cell adhesion through homophilic interactions and self-avoidance in neuronal synapses. The range of combinatorial expression of the PCDH isoforms act as an identity barcode and specificity of the E5-6 domains determines the *trans* interactions. Another functional role for the PCDHs that has been suggested is cell signalling but has not fully elucidated thus far. The intracellular domain that is involved in downstream signalling binds to receptor tyrosine Ret and cell-adhesion kinase Pyk2 and Fak leading to inhibition of kinase activity. It is also thought they may interact with other molecules such as phosphatases, kinases and adhesion molecules (Chen and Maniatis, 2013; Schalm et al., 2010).

PCDH-γ has been implicated in neuronal cell survival, the CTF of the PCDH-γ isoforms has been shown to have an impact on endo/lysosomal trafficking and mice that have PCDH-γ genes disrupted show increased neuronal cell death (O'Leary et al., 2011). The PCDH-γ isoforms appear to have intracellular roles with an indication that they are involved in tubule formation for the recruitment of autophagy markers (Hanson et al., 2010), this involvement links the PCDH-γ family back to having an role in cell survival.

Multiple functional roles have been indicated for the PCDHs although further investigation is needed to understand the role these molecules play outside the nervous system. It is likely that epigenetic regulation seen in neuronal cells will apply in other cell types and combinatorial expression of PCDH isoforms will provide single cell identity barcodes influencing adhesion and potentially downstream signalling.

1.6 Cleavage by ADAM sheddases regulates levels of adhesion molecules on the cell surface

1.6.1 Role and Mechanism

A Disintegrin And Metalloproteinase (ADAM) family are membrane-bound enzymes that cleave extracellular portions of transmembrane proteins, this process is known as ectodomain shedding. The ADAM sheddase family have a large range of targets, often with crossover between family members, such as growth factors, cytokines, chemokines and adhesion molecules. ADAM sheddases have a domain structure which is responsible for giving them proteolytic, adhesive and signalling activities. The catalytic metalloproteinase domain is highly conserved within the ADAM family and requires a Zn-binding motif, the disintegrin together with the cysteine-rich domain are also involved in the catalytic activity as well as cell adhesion and target specificity. The ADAM shedding occurs upstream of γ-secretase releasing the ectodomain fragment which is cleaved further by a γ-secretase. ADAM10 and ADAM17 differ from the rest of the ADAM family in that they do not have an aspartic-acid sequence in their disintegrin domain which would allow cell adhesion via recognition by α4/α9 subfamily.

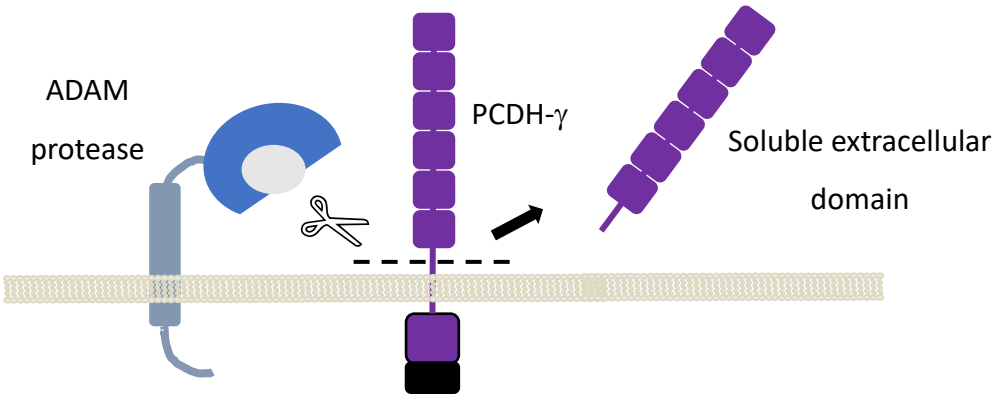

Figure 1.6.1.1 Process of ectodomain cleavage via ADAM sheddases
Example of the proteolytic cleavage by ADAM sheddases on extracellular proteins.

The presence and function of ADAM10 and ADAM17 on B-cells and PCs including links to MM cells has been investigated in a number of different journals. This suggests that the function of ADAM10 and ADAM17 on PCs would be to regulate levels of surface proteins via proteolytic cleavage rather than orchestrating cell-cell adhesion. ADAM10 & ADAM17 activity can have effects on B-cell differentiation via regulation of

levels of TACI, CD138, TNF-α and CD23, along with links to MM cells survival (Lownik et al., 2020; Pupovac et al., 2015; Lemieux et al., 2007; Marchica et al., 2019; Zingoni et al., 2015) .

Some of the most prominent targets of ADAM10/17 are TNF-α and EGFR ligands, cleavage of the ectodomain activates the signalling pathway by releasing peptides that can bind to their receptors. Type I transmembrane proteins are cleaved further at the transmembrane fragment by γ-secretase following release of the ectodomain via ADAM shedding. ADAM10 and ADAM17 appear to be the main sheddases involved in the immune system with links to leukocyte trans-endothelial migration by cleavage of CAMs. Current literature states that ADAM10 and ADAM17(TACE) are responsible for the shedding of the ectodomain of PCDH-γ molecules and ALCAM (Rosso et al., 2007; Reiss et al., 2006; Bouillot et al., 2011; Gilsanz et al., 2013), altering the amount of surface expression on the surface of B-cells and PCs. This process may act as a regulatory mechanism limiting the amount of signalling via the surface expression of the adhesion molecules as well as allowing cell migration by reducing their ability to adhere to the surrounding niche and neighbouring cells.

1.6.2 Role in signal regulation and migration

ADAM cleavage releases an ectodomain segment as well as leaving a cytoplasmic fragment. The cytoplasmic portion is cleaved further by γ-secretase, the C-terminal fragment (CTF) in some instances translocates to the nucleus and alters gene transcription. An example of this is NOTCH signalling that is part of the lymphoid progenitor fate decision, in B-cells NOTCH1 is repressed.

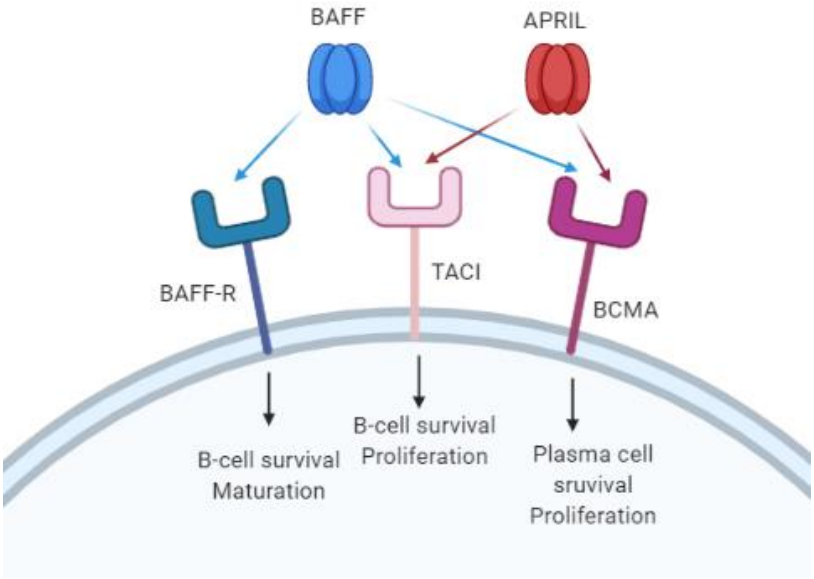

Figure 1.6.2.1 Survival signals involved in B-cell and plasma cell biology.
Diagram illustrating the ligands (BAFF and APRIL) and cognate receptors on the surface of B-cells that are shed by ADAM metalloproteinases. The downstream signalling outcomes are indicated depending on which receptor is signalling. (Image created using Biorender)

ADAM dependent cleavage precedes the activity of the γ-secretase and therefore its activity regulates downstream signalling. NOTCH is cleaved by ADAM10 and then the CTF is released by γ-secretase. The CTF translocates to the nucleus which initiates a T-cell programme and fate determination (Six et al., 2003; Gibb et al., 2010). ADAM mediated surface protein shedding has been shown to be active on B-cells and involved in shedding of surface receptors BAFFR and TACI that impact B-cell differentiation and survival. BAFF induced ADAM17 shedding of BAFFR on B-cells co-expressing TACI. ADAM shedding can also be induced by PMA or ionomycin, with some evidence of specificity to ADAM17 and ADAM10 respectively. Only induction of ADAM17 activity resulted in decreased levels of BAFFR and TACI on the surface of activated B-cells (Smulski et al., 2017; Lownik et al., 2020). The exact mechanism for determining activity of the ADAMs appear to be a combination of substrate conformation and localisation.

As well as surface receptors ADAM10 has been reported to cleave CD23 the low affinity IgE receptor, and NOTCH2. These cleavage events were shown in a murine model to determine the development of marginal zone B-cells. (Gibb et al., 2010; Lemieux et al., 2007; Hammad et al., 2017). More recent evidence for ADAM10's role in commitment to a marginal zone B-cell rather than a follicular B-cell has been linked to Taok3. B-cells require Taok3 to respond to NOTCH ligand Delta-1 and BcR ligation as part of the fate determining decision. BcR ligation leads to an upregulation in ADAM10 expression in a Taok3-dependent manner, B-cells expressing ADAM10 developed into marginal zone B-cells. To summarise B-cells being positively selected in the DZ become receptive to Notch signalling via Taok3-mediated ADAM10 surface expression (Hammad et al., 2017). The interplay of soluble factors and cleavage events during B-cell differentiation induces changes in levels of receptors that in turn alters the intracellular signalling within the cells that eventually results in a terminally differentiated PC.

ADAM10 is thought to be the primary sheddases of ICOSL on B-cells, the ICOS-ICOSL interaction is needed in humoral immunity for ICOS internalisation in T-cells, over expression of ICOS can result in aberrant antibody production in Lupus. Blocking ADAM10 shedding of ICOSL causes excessive internalisation of ICOS in T-cells (Lownik et al., 2017).

ADAM cleavage releases a soluble ectodomain portion, releasing ligands that can initiate signalling by binding to its receptor on cells nearby. ADAM cleavage is involved in releasing cytokines such as EGF ligands that are processed as cell surface transmembrane precursors and the pro-inflammatory cytokine TNF-α (Düsterhöft et al., 2019; Dang et al., 2013). Releasing cytokines such as the EGF ligands activates many downstream signalling pathways involved in cell proliferation, migration, survival, or differentiation. Being able the regulate the release of cytokines and growth factors with the use of commercial inhibitors has been somewhat problematic with the large range of off-target effects due to the diversity of ADAM10 and ADAM17 targets (Saftig and Reiss, 2011). Generally, the activity of ADAM sheddases on adhesion molecules is likely to be involved in migration and homing, increasing cleavage events can lead to a more migratory phenotype by disrupting interactions in the bone marrow

between the PCs and surrounding stroma. The activity of ADAMs may differ between PC neoplasms depending on phenotype and pathogenesis of the neoplasm.

1.6.3 Regulation of ADAM sheddase activity

The ADAM sheddases can act constitutively on a substrate or be induced by certain stimuli to increase activity and intracellular signalling. ADAMs are under regulation by tetraspanins or rhombopoeitins and are dependent on the localisation of the sheddases on the surface and their corresponding regulator (Gutiérrez-López et al., 2011; Matthews et al., 2017). Tetraspanins are a family of transmembrane proteins that associate with themselves and other proteins such as ADAM10 and integrins to form clusters rather than have any signalling or adherent properties. On B-cells the tetraspanin CD81 regulates the glycosylation of CD19 as well as trafficking to the cell surface for BcR signalling (Levy, 2014). Some tetraspanins such as CD9, CD151 and CD63 act as pro-inflammatory leukocyte attractants by clustering adhesion molecules together. Knockout experiments have shown that tetraspanins are required for trafficking ADAMs to the cells surface and release from the ER once the mature form of the ADAM is generated. (Matthews et al., 2017).

CD9 is a transmembrane protein that participates in the cellular organisation with other tetraspanins and interacts with other transmembrane proteins via the LEL domain. CD9 has been shown to interact with ADAM17 and has an inhibitory effect, which in turn affects the levels of ALCAM on the cell surface. This mechanism works in two ways, the inhibition of ADAM17 prevents cleavage from the surface but also causes an upregulation of ALCAM clustering on the cell surface. CD9 forms a direct interaction between ADAM17 and ALCAM, this occurs via co-localisation using the tetraspanin network. CD9 has two enhancing effects on ALCAM, expression is increased as well as a reduction in shedding allowing for cell adhesion via ALCAM interactions (Gilsanz et al., 2013). This highlights the complexity of regulation of transmembrane protein expression on the cell surface, the balance of expression and cleavage allows fine control over cell signalling and adhesion.

Rhomboids are another superfamily of transmembrane proteins often spanning 6-7 transmembrane domains. They have a protease domain within the membrane where the substrates are cleaved. There are also non-protease rhomboids that lack this catalytic domain and have a regulatory function. iRhom1 and iRhom2 are non-

protease rhomboids that have been identified as regulators of ADAM17. Knockout murine studies of iRhoms and ADAM17 showed a remarkably similar phenotype suggesting that the iRhoms affect ADAM17 activity. iRhom2 has been found to interact with ADAM17 in the ER and is involved in ADAM17 maturation with correct folding and trafficking to the cell surface. Both iRhoms promote maturation of ADAM17 and some evidence suggests they can enhance ADAM17 shedding with differential targets depending on the iRhom involved (Matthews et al., 2017). Taken together it is evident that there are multiple levels of regulation that are involved in establishing the cell surface phenotype.

1.6.4 ADAM sheddases link in malignancy

ADAM17 has been linked to several disorders such as myeloma, ovarian cancer and plays a role in tumour progression and angiogenesis (Rosso et al., 2007; Marchica et al., 2019; Tomita et al., 2013; Duffy et al., 2009; Düsterhöft et al., 2019) however ADAM10 has not been studied in as much detail. The ADAMs most established role is the release of TNF-α and EGFR which are implicated in tumour growth and progression, therefore the ADAMs also play a role in tumour pathogenesis. ADAM10 and ADAM17 are upregulated in cancer and correlate with tumour progression and poor prognosis with specific inhibitors being used alongside other therapies (Duffy et al., 2009; Mullooly et al., 2016; Moss and Minond, 2017). One study has linked an upregulation of ADAM10 in multiple myeloma PCs following treatments that induce genotoxic stress. The upregulation of ADAM10 and increased sheddase activity is thought to enable PCs to avoid detections by NK cells by cleaving MIC (Zingoni et al., 2015). This highlights the importance of regulating ADAM shedding as well as surface molecule expression in disease progression and pathogenesis.

There are a range of ADAM inhibitors commercially available that are already being used in clinical applications, for example Marimastat the pan-ADAM inhibitor is used as a cancer treatment to inhibit angiogenesis and metastasis. There are also specific inhibitors available TAPI-2 for ADAM17 and GI 254023x for ADAM10, these types of small molecule inhibitors can be used to assess the level of control the ADAM sheddases are having over the levels of surface proteins of interest.

1.7 Aim and Hypothesis

The current literature and preliminary data leads to the hypothesis that cell surface and adhesion molecules provide an important role in B-cell differentiation and disease pathogenesis. Adhesion and niche residency factors identified to be upregulated in plasmacytoma will be investigated further to understand their expression patterns during normal PC differentiation and how this may be altered in malignant PCs. Surface phenotype on PCs is regulated at both a gene and protein level which can influence homing and adhesion to the survival niche. This thesis aims to study a set of adhesion molecules and niche factors expression levels throughout primary B-cell differentiation and how these levels are affected in malignant patient samples. The regulation of expression will be investigated at a gene and protein level, with focus on the epigenetic regulation of the PCDH-γ and how this expression may provide cell surface identity codes through combinatorial surface expression. Alongside this there will be investigation into proteolytic cleavage of these surface proteins a process that are known to be active on PCs and allow dynamic changes to the cell surface phenotype. The hypothesis is that an upregulation of these niche residency factors generates and cohesive, isolated tumour of neoplastic PCs which ultimately leads to a more favourable prognosis, therefore an understanding of their normal expression patterns and potential factors that influence expression needs to be established.

2 Methods

2.1 Cell lines

Table 2-1 Cell lines

Cell lines	Origin	Growth	Media
RPMI 8226	Multiple myeloma	Suspension	RPMI 1640 (Gibco)/10% FBS (PAA)
H929	Multiple myeloma	Suspension	RPMI 1640 (Gibco)/10% FBS (PAA)
KMS11	Multiple myeloma	Semi-adherent	RPMI 1640 (Gibco)/10% FBS (PAA)
KMS18	Multiple myeloma	Semi-adherent	RPMI 1640 (Gibco)/10% FBS (PAA)
OPM2	Multiple myeloma	Semi-adherent	RPMI 1640 (Gibco)/10% FBS (PAA)
Hela	Cervical cancer	Adherent	RPMI 1640 (Gibco)/10% FBS (PAA)
THP.1	Leukemic monocyte	Suspension	RPMI 1640 (Gibco)/10% FBS (PAA)

2.2 Reagents and Antibodies

Table 2-2 Reagents and Antibodies

Tissue culture reagents	Manufacturer	Catalogue number
Lymphoprep	Allere Limited	1114547
IMDM	Invitrogen	31980048
FBS	Invitrogen	10270106
MACS Rinsing solution (no preservative)	Miltenyi	130-091-222
BSA MACS stock solution	Miltenyi	130-091-376
PBS tablets	Sigma	P4417
Human memory B cell isolation kit	Miltenyi	130-093-546
LD columns	Miltenyi	130-042-901
Amino Acids	Sigma	M550
Lipid Mix	Sigma	L0288
F(ab)2 goat anti-human IgG&IgM	Jackson Laboratories supplied by Statech	109-006-127
hIL-2	Roche	11011456001
hIL-21	Peprotech	200-21
hIL-6	Peprotech	200-06-100
Mega-APRIL (H98)	Adipogen	AG-40B-0088-C010
L-685,458 Gamma secretase inhibitor (GSI)	Tocris	2627

IFN-α	Peprotech	300-02A
TGF-β	Peprotech	100-36E
Marimastat	Tocris	2631
TAPI-2	Tocris	6013
GI254023x	Tocris	3995/1
Ingenio	Mirus	50111
Genejuice	Millipore	70967
Anti-mouse Ig κ comp beads	BD Biosciences	51-90-9001229
Negative control comp beads	BD Biosciences	51-90-900129
4% paraformaldehyde (PFA)	Alfa Aesar	J61899

Table 2-3 Flow cytometry antibodies

Flow Antibodies	Volume used for $1x10^7$ (µL)	Manufacturer	Isotype control	Catalogue number
Anti-human ALCAM(CD1960) -PE	2	Biolegend	Mouse IgG1κ	343904
Anit-human CCR2 –BV421	5	Biolegend	Mouse IgG2aκ	357210
Anti-human LEPR –PE-Vio770	5	Miltenyi	REA Control (S)-PE-Vio770	130-105-212
Anti-human PCDHG pan-APC	5	StressMarq	Mouse IgG1	SMC-454D-APC-SMQ
Anti-human ITGB7 -FITC	2	Biolegend	Rat IgG2aκ	321212
Anti-human CD19 –PE	2	Miltenyi	Mouse IgG1κ	130-113-169
Anti-human CD19 -VioBlue	5	Miltenyi	Mouse IgG1κ	130-120-031
Anti-human CD19-BV510	5	BD Biosciences	Mouse IgG1 kappa	562947
Anti-human CD20-eFluor450	5	Invitrogen	Mouse IgG2b K	48-0209-42
Anti-human CD38 –PE-Cy7	2	BD Biosciences	Mouse IgG_1, κ	335825
Anti-human CD38 –BUV395	5	BD Biosciences	Mouse IgG1 kappa	563811
Anti-human CD138-APC	5	Miltenyi	Mouse IgG1κ	130-117-395

Anit-human CD138-FITC	5	Biolegend	Mouse IgG1, κ	352304
Anit-human CD138-PE-Cy7	5	Invitrogen	Mouse IgG1 K	25-1389-42
Anti-human CD27-PE	2	Miltenyi	Mouse IgG1κ	130-093-185
Anti-human CD27-FITC	5	BD Biosciences	Mouse BALB/c IgG_1, κ	555440
Anti-human IgD - PE	5	BD Biosciences	Mouse BALB/c IgG_{2a}, κ	555779
Anti-human IgM – PE-Cy7	2	Biolegend	Mouse IgG1	314532
Anti-human CD2 –BV605	5	Biolegend	Mouse IgG1, κ	300224
Anti-human CD3 -Viogreen	5	Miltenyi	Mouse IgG2aκ	130-096-910
Anti-human IL6-R -PerCp	5	R&D Systems	Mouse IgG1	FAB227C
Anti-human CD56 –PE-C7	5	BD Biosciences	Mouse BALB/c IgG_{2b}, κ	335826
Anti-human TSPAN8 - PE-Vio700	5	Miltenyi	REA Control (S), human IgG1	130-106-856
Anti-human CD9 – PE-Cy7	5	Biolegend	Mouse IgG1	312115
Anti-human ADAM10	5	Biolegend	Mouse IgG1, κ	352705
Anti-human ADAM17/TACE - PE	5	R&D Systems	Mouse IgG1	FAB9301P
7AAD	5	BD Biosciences	NA	51-689816
UV Zombie	1:1000 dilution	Biolegend	NA	77474
LIVE/DEAD fixable Near-IF Dead cell stain	1:1000 dilution	Invitrogen	NA	L34975
Goat anti-Rabbit IgG (H+L) –Alexa Fluor647	1:100 dilution	Jackson ImmunoResearch	NA	111-604-144

Table 2-4 Western blotting antibodies

Western Antibodies	Manufacturer	Host	Catalogue number
PCDHGB4 [N1N2], N-term	Genetex	Rabbit	GTX117173
PCDHGB5 [N1N2], N-term	Genetex	Rabbit	GTX119181
PCDHGA6 [N1N2], N-term	Genetex	Rabbit	GTX119183
PCDHGA9	Invitrogen	Mouse	MA5-22248
PCDHGA10	Sigma	Mouse	SAB1403308
PCDHGA11	Sigma	Mouse	SAB1411904
PCDHGA12	Sigma	Mouse	SAB1407275
β-actin	Sigma	Mouse	A1978

Table 2-5 Taqman Primers

Assay	Assay ID	Manufacturer
PCDHGA6	Hs00259344_s1	ThermoFisher
PCDHGA9	Hs00259365_s1	ThermoFisher
PCDHGA10	Hs01571699_s1	ThermoFisher
PCDHGA11	Hs00259383_s1	ThermoFisher
PCDHGA12	Hs00259391_s1	ThermoFisher
PCDHGB2	Hs00251715_m1	ThermoFisher
PCDHGB4	Hs00259420_s1	ThermoFisher
PCDHGB5	Hs01107475_m1	ThermoFisher
PCDHGB7	Hs00259445_s1	ThermoFisher
ALCAM	Hs00977640_m1	ThermoFisher
CCR2	Hs00356601_m1	ThermoFisher
LEPR	Hs00174497_m1	ThermoFisher
ITGB7	Hs01565750_m1	ThermoFisher

2.3 Cell culture

Cell lines were cultured in RPMI 1640 medium supplemented in 10% foetal bovine serum and incubated at 37°C with an atmosphere of 5% CO_2.

2.4 In vitro generation of long-lived plasma cells

2.4.1 Collection of peripheral blood samples

Peripheral blood was collected in EDTA tubes and obtained from healthy donors with informed consent. Approval for study granted by the Leeds (East) NHS Research Ethics Committee, REC 07/Q1206/47.

2.4.2 Isolation of PBMCs

50ml of peripheral blood was mixed with an equal volume of sterile phosphate buffered saline (PBS) at RT. Layering of the blood onto the lymphoprep is done using a 3:1 ratio, 34ml of the blood/PBS mix was layered on top of 17ml of Lymphoprep (Allere Ltd.) in a 50ml falcon tube. The layered mixture was centrifuged at 2400rpm for 20 mins at RT (acceleration 5, brake 0). The lymphocyte layer was aspirated and divided between two fresh 50ml falcon tubes containing 10ml cold PBS. The volume was made up to 50ml with cold PBS, the peripheral blood mononuclear cells (PBMCs) were centrifuged at 1800rpm for 15mins at 4°C. Afterwards the cells were combined into one tube, washed with 50ml cold PBS and centrifuged at 1500rpm for 10mins at 4°C. This step is repeated twice more, the PBS is removed, and the cells washed with 15ml of ice-cold MACS buffer. Cells were counted before being centrifuged at 1500rpm for 10mins at 4°C.

2.4.3 Magnetic labelling of cells

A negative selection of B-cells was used to deplete the non-B cell populations, from the PBMCs collected using lymphoprep. B-cell selection was carried out with a Miltenyi memory B-cell isolation kit for $1x10^8$ cells or fewer. The non-B cells were labelled with biotinylated antibodies CD2, CD14, CD16, CD36, CD43 and CD235a, these target the T-cells, NK cells, monocytes, dendritic cells, granulocytes, platelets, and erythroid cells. After incubation with the B-cell cocktail, these cells are magnetically labelled Anti-biotin microbeads for depletion.

Where the PMBC yield exceeded $1x10^8$, quantities of reagents were scaled up accordingly. Using the kits standard protocol, the PBMC pellet was resuspended in 400µl of cold MACS buffer. 100µl of the B-cell Biotin-Antibody Cocktail was added and the mixture incubated for 20mins 4°C. Then 300µl of cold MACS buffer and 200µl Anti-Biotin Microbeads were added to the cells and incubated for 20-30mins at 4°C. 10ml of cold MACS buffer was added and the cells centrifuged at 1500rpm for 10mins at 4°C. The cell pellet was re-suspended in 1ml cold MACS buffer ready to be added to the LD columns.

2.4.4 Magnetic separation of cells

To negatively select for memory and naïve B-cells, magnetic separation is performed using LD columns. LD Columns (Miltenyi) are placed in the magnetic field of a suitable MACS separator and rinsed with 2ml of cold MACS buffer. The cell suspension was

added to the column and the unlabelled cells passing through were collected in a fresh tube. The column was washed 3x with 1ml of cold MACS buffer and flow through collected in the same tube. The cells were counted and re-suspended in IMDM + 10% FBS at 5 x 10^5 cells/ml along with additional cytokines and supplements onto a CD40-fibroblast layer or a further depletion was performed to separate naïve and memory B-cells.

2.4.5 Memory B-cell isolation - CD23 depletion

Before putting cells into the standard differentiation conditions using total B-cells the memory B-cells can be isolated for long-term cultures by using a CD23 depletion to remove naïve B-cells. Isolating memory B-cells from total B-cells uses an anti-CD23-biotin antibody for separation with magnetic biotin beads.

Total B-cells are counted, a cell count <1x10^7 cells required 10µL of the anti-CD23-Biotin antibody is added to cells suspended in 90µL of MACS buffer and incubated at 4°C for 20mins. After the first incubation 20µL of anti-biotin microbeads are added with 80µL of MACS buffer and the cells are incubated at 4°C for 20mins. After the incubation cells were washed with 5ml of MACs buffer and pelleted at 1500rpm for 10mins. Whilst the cells are being centrifuged preparation of the MS columns can be started.

MS columns were prepared by inserting the columns into a magnetic field and rinsed with 1ml of cold MACs buffer. After centrifugation, the labelled cell pellet is resuspended in 500µL of MACS buffer, the memory B-cells are negatively selected and the flow through containing the memory B-cells is collected in a clean 15ml falcon tube, the columns are then washed with a further 1ml of MACS buffer. The final collection volume will be 1.5ml of memory B-cells, cells are counted and seeded according to the differentiation protocol.

2.4.6 Naïve B-cell isolation - CD27 depletion

For comparison between naïve and memory cells the naïve B-cells are isolated using a CD27 depletion to remove any memory B-cells. Following the isolation of total B-cells from PBMCs, cells are stained with anti-CD27 microbeads for 20mins and then washed in 5ml MACS buffers. Cells were resuspended in 500µL in MACS buffer and put onto prepared MS columns. MS columns are prepared as previously described by running 1ml of cold MACS buffer though the column. A clean falcon tube is placed

underneath the columns before the cell suspension is added to collect the flow through which will collect the unstained naïve B-cells. The column is then flushed with another 1ml of MACS buffer resulting in 1.5ml of cell suspension. Cells are counted and seeded with the appropriate differentiation conditions.

2.4.7 Preparation of CD40L-L cells

Murine fibroblasts transfected with irradiated human CD40L (CD40L-L cells) were plated 24 hours in advance. An aliquot of 1 x 10^6 pre-irradiated CD40L-L cells was thawed and added to 10ml IMDM media + 10% HIFBS then centrifuged at 1500rpm for 5mins to remove any traces of DMSO from the freezing media. CD40L-L cells were re-suspended in 12ml fresh IMDM + 10% HIFBS and 0.5ml plated per well of a 24-well plate and incubated overnight at 37°C + 5% CO_2.

2.4.8 *In vitro* Differentiation Conditions

Culture conditions for various stages of differentiation:

Day 0-3: B-cells were cultured in 24-well plates coated with the CD40L-fibroblast layer of cells at 5x10^5 cells/ml in IMDM + 10% HIFBS with the addition of hIL-2 (20 U/ml), hIL-21 (50 ng/ml) and F(ab′)2 goat anti-human IgM and IgG (10 µg/ml). This combination activates CD40 and the BcR as well as providing signals for survival and proliferation via IL-2 and IL-21.

Day 3-6: B-cells were reseeded at 1x10^5/ml in IMDM + 10% HIFBS supplemented with amino acids (1:50) and lipid mixture 1 (1:200) (*supplements)*, with the addition of hIL-2 (20 U/ml) and hIL-21 (50 ng/ml). B-cells were removed from the CD40-L cells by gently pipette mixing.

Day 6-9: Cells were seeded in either a 24-well plate, a 96-well round bottomed plate or a T75 flask depending on the size of the culture. Cells are seeded at 1x10^6 cells/ml in IMDM + 10% HIFBS + supplements with the addition of hIL-6 (10 ng/ml), IhL-21 (50 ng/ml), APRIL (100 U/ml) & gamma secretase inhibitor (GSI) 100nM. The addition of IL-6 drives plasma cell survival, proliferation and antibody secretion from plasma cells. APRIL is a pro-survival signal for plasma cells and the GSI inhibits the cleavage of BCMA to allow for continuous signalling from APRIL.

Day 13 onwards: hIL-21 was withdrawn from the media as the cells at this stage will no longer be proliferative. Supplements + hIL6 + APRIL + GSI were still added to the

media. Cells were fed every 3-4 days by replacing half of the volume of media with a 2x concentration of supplements and day 13 cytokines.

2.4.9 Red cell lysis

Whole blood and bone marrow samples were prepared for analysis by flow cytometry by performing red cell lysis with ammonium chloride.

0.86g of ammonium chloride is dissolved in 100ml of distilled water, this is made up fresh every time. A ratio of 1:10 sample to ammonium chloride was used and once added incubated at 37°C for 5-10mins until samples had turned from cloudy to transparent.

After the incubation, the sample is spun at 2000rpm for 2mins and the supernatant is gently poured off to leave the white cell pellet of PBMCs. Cells are washed 3x with PBS and spun for 5mins at 1500rpm. Before the final wash, a cell count is taken for flow cytometry staining.

2.4.10 Standard flow cytometry staining using conjugated antibodies.

(using ~2x10^5 cells)

Firstly, cells were washed with ~500µL of MACS buffer and then centrifuged for 5mins at 1500rpm to pellet the cells so that the buffer can be removed by gently inverting the tube. The cells are then blocked using 20µL blocking buffer (using mouse serum), the samples were incubated in the fridge at 4°C for 10mins. After incubating, add the phenotyping antibody mix of the conjugated antibodies, incubate at 4°C for 20mins. Finally, wash the cell with ~500µL MACS buffer and centrifuge for 5mins at 1500rpm before gently removing the MACS buffer by inverting the tube. Resuspend the cells in ~100uL of FACS buffer and then samples were run on the Cytoflex S or Cytoflex LX. Data then analysed using FlowJo software.

Table 2-6 Blocking buffer composition

Blocking buffer (1ml)	FACS Buffer
MACS – 933uL	MACS 19ml
hIgG – 17uL	BSA 1ml
Serum – 50uL	-

Table 2-7 listing of components of each of the buffers with corresponding volumes required for making the blocking buffer and FACS buffers used during staining of cell for flow cytometry.

2.4.11 PCDH Secondary staining

2.4.11.1 Final protocol for flow cytometry secondary staining

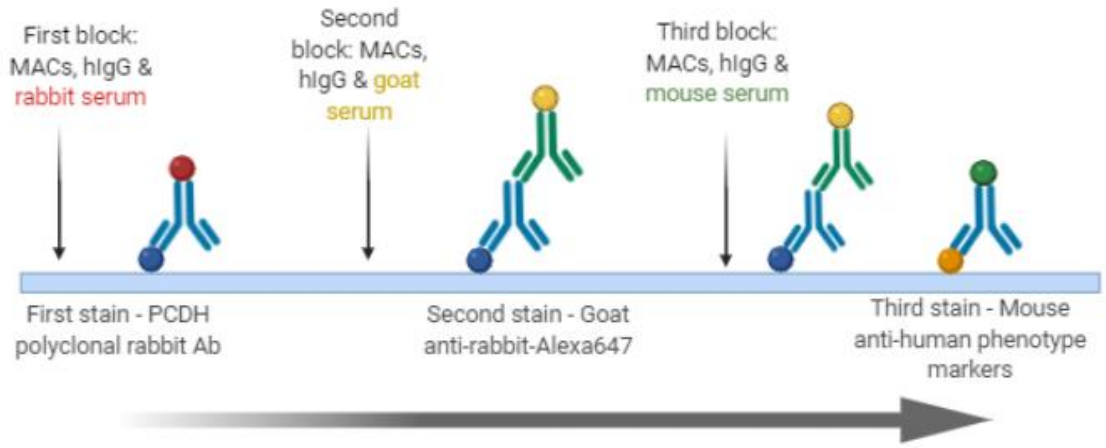

Figure 2.4.11.1 Schematic of the flow cytometry staining protocol for the PCDH-γ isoforms.

The antibodies specific for PCDHGA6, PCDHGB4 & PCDHGB5 are unconjugated rabbit polyclonal antibodies therefore a secondary conjugated antibody is used to allow detection by flow cytometry. The secondary antibody is a goat anti-rabbit antibody conjugated to AlexaFluor647, the staining of the PCDH-γ isoforms was carried out first to avoid non-specific staining with individual blocking steps for each step of the staining. The PC phenotype markers were stained last with standard conjugated flow cytometry antibodies.

Due to difficulties finding commercial antibodies that were specific for the PCDHG proteins suitable for flow cytometry a protocol for staining using unconjugated antibodies was optimised. The final protocol that was generated for the staining of the PCDHG isoforms using unconjugated antibodies, this involved using a secondary antibody towards the PCDHG isoforms that was conjugated with the fluorophore AlexaFluor647.

The final conditions that were established to minimise any non-specific binding split the staining into 3 steps. The first step was to wash the cells with 500µL of MACS

buffer, pellet the cells by centrifuging for 5mins at 1500rpm and remove the MACS buffer by gently inverting the tube. Block the cells using rabbit serum due to the unconjugated PCDHG antibodies being raised in rabbit, cells were blocked using 20µL of the blocking buffer for approx. $1x10^5$ cells for 10 mins at 4°C and then 5µL of the PCDHG antibodies is added respectively and incubated for another 20mins. This is followed by a wash in MACS buffer and the secondary staining step, the blocking buffer for this stage contains goat serum due to the secondary antibody being raised in goat. The same incubation periods are used, and the secondary antibody was used at a 1:100 dilution with 10µL being added per tube. After a final wash with MACS buffer blocking buffer is added containing mouse serum for the final antibodies used for the staining are raised in mouse, a master mix of the PC phenotypic markers is made and then added to the cells for another 20mins. Depending on whether the cells are fixed or not, determines whether the live/dead stain needs to be added prior to fixing along with CD27-FITC which has its staining affected if the cells are fixed in 4% paraformaldehyde (PFA).

2.4.12 LIVE/DEAD staining

For compatibility with fixing the cells with 4% PFA the live/dead staining along with any FITC antibodies was done before the cells were fixed.

The Zombie UV and the fixable near-IF live/dead stains were reconstituted in 100µL DMSO.

Cells were harvested and counted, then washed in PBS. The data sheet from the manufacturer states that the antibodies have a capacity of staining $1x10^6$ cells using the standard protocol before needing to be scaled up. The standard protocol calls for staining with 100µL of a 1:1000 dilution in PBS of the fixable LIVE/DEAD dyes. Cells were stained at room temperature for 15mins along with any other conjugated antibodies that are not compatible with fixing the cells (CD27-FITC) and are then washed in PBS.

After the final wash with PBS cells were either fixed with 100µL of 4% PFA and stained at a later date or the experiment was continued with the blocking and staining conditions needed for that experiment.

2.4.13 ADAM inhibition

Commercial inhibitors were purchased from Tocris, a pan ADAM inhibitor (Marimastat), an ADAM10 specific inhibitor (GI 254023x) and an ADAM17 specific inhibitor (TAPI-2). The inhibitors were dehydrated powders on arrival and were dissolved in either distilled water or DMSO depending on the specification. The inhibitors were made up into a working stock of 100nM per ml and stored as aliquots at -20°C.

The pilot experiments were trialled on differentiating B-cells using 4μM/ml of inhibitor, 4μL per ml was added to the culture media when refeeding cells along with the cytokine cocktail, for example a 2x inhibitor cocktail was made up in 1ml with 1x cytokines to replace 1ml of old media gently removed by pipetting. Inhibitors were in the culture media for 24hrs before the effects on surface expression was analysed by flow cytometry.

Dose responses using the commercial inhibitors used a range of concentrations from the working stocks at 100nM, inhibitors were added to the cytokine cocktail and the culture media. Cells were cultured for 4days in the presence of inhibitors before analysis of surface expression by flow cytometry of adhesion and niche factors.

When testing the effects on the myeloma cells lines (KMS11 & H929) the cells were seeded in a 24well plate at a density of $2.5x10^5$ per well, duplicate wells were seeded for each condition (no inhibitor, Marimastat, TAPI-2 or GI 254023x) and wells pooled for analysis by flow cytometry after being in culture with the inhibitors for 4days.

2.5 Molecular techniques

2.5.1 RNA isolation

To isolate RNA from the cells they are lysed in 800μL TRIzol, here the cells can be stored in the freezer for later use. The first step of the isolation adds 160μL of chloroform to the lysed cells and are shaken by inversion to mix the cell suspension with the chloroform. Samples are centrifuged for 10mins at 12,000g at 4°C. The clear aqueous phase is isolated by gently aspirating and 10μg glycogen is added as a carrier. Following this 400μL of isopropyl alcohol is added to the samples which are incubated at room temperature (RT) for 10mins then centrifuged for 10mins at 12,000g, at 4°C. The supernatant was removed, and the RNA was washed in 1ml of 75% ethanol and centrifuged for 5 mins at 12,000g at 4°C. The supernatant was

removed, and samples left to air dry for 5mins, after the samples have dried, they are dissolved in 44µL of RNAse free water and heated at 55°C for 10mins. Finally, the RNA is treated with DNAseI (Invitrogen) following manufacturer's instructions.

2.5.2 cDNA synthesis-Reagents from Invitrogen

For cDNA synthesis the RNA is added as a 1:1 mixture of RNA to master mix, therefore 5µL of each RNA sample was added to 5µL of the master mix which is made up of random primers, dNTPs and dH_2O.The DNAseI treated RNA and master mix is incubated for 5mins at 65°C. Samples are chilled on ice briefly before the addition of 10µL of the second mastermix (5X Buffer, DTT, $MgCl_2$, SSII RT, RNAse OUT & dH_2O) and were incubated for 50mins at 42°C, samples are inactivated by incubating at 70°C for 15mins. The samples were chilled on ice before being spun to bring down any mixture that had evaporated onto the Eppendorf lid. Finally, RNAse H treatment was done by adding 1µL of RNAse H to the RNA samples followed by a 20min incubation at 37°C. From here samples were either stored at -20°C for later use or used immediately for qPCR analysis.

2.5.3 Taqman Gene Expression

qPCR was carried out on 1:5 dilution of cDNA that was used as the template for the primers and 2µL of cDNA was added to 8µL of the TaqMan Gene Expression mastermix (Taqman Universal PCR Masterm mix) containing the specific gene Taqman primers. Samples, plus a no template control (NTC) using nuclease-free H_2O were ran in duplicate for each gene of interest. Initially PPP6C was trialled as the housekeeping gene in a 96 well plate, however this was expressed as a very low Ct in comparison with the genes of interest meaning that the fold change was difficult to distinguish using PPP6C expression as a control. The following programme was used on a thermal cycler (Aligent Tenchnologies Statagene Mx3005P) to give cycle threshold (Ct) values: 95° (10mins), 95°C (30secs), 60°C (1min) for 40 cycles.

2.5.4 SDS polyacrylamide Gel Electrophoresis (PAGE) and Immunoblotting

To assess protein expression of the niche factors in myeloma cell lines, SDS mini gels were poured on 1mm glass plates at 7.5% or 10% depending on the size of the protein being detected. 10µL of Precision Plus Protein ladder (BIO-RAD) was loaded, and 10-20µL of the samples was loaded depending on the cell number used for the lysate. The samples were prepared in 2x sample buffer in a volume that aimed to generate

an equal cell number so that equal loading volumes could be used for example $1x10^6$ cells would be lysed in 200µL of 2x sample buffer. Once samples were loaded into the well the Bio-Rad Power pack was set at 120V and run for ~1h15mins, again this was dependent on size of the protein. The gel was transferred onto nitrocellulose membrane using a wet transfer system. The blot was incubated in 5% milk/TBS-T overnight at 4˚C. The blot was washed 3x10mins in TBS-T before the addition of primary antibody in 5% BSA/TBS-T, the blot was incubated overnight at 4˚C. The blot was again washed 3x10mins in TBS-T before adding the secondary antibody in 5% milk or BSA/TBS-T and incubated for 1-2hrs at RT. The final set of washes of the blot were done in 1xTBS 3x10mins. Finally, the blot was developed by adding 6ml 1:1 ECL (SuperSignal West Pico Plus, Thermo) and incubated for 5mins at RT. The film was exposed and developed using the x-ray system to visualise protein expression.

2.5.5 PCDHG cloning

Expression vectors for PCDHGA6, PCDHGB4 & PCDHGB5 were bought from Genscript using the pcDNA3.1$^+$/C-(K)DYK vector. The first step was to transform the vectors into competent bacterial cells which grow rapidly to increase the stock of the vectors. The vectors were suspended in 10µL dH_20 then diluted 1:1000 for the working stock. The DH5α competent cells were thawed in ice and 5µL of vector DNA was added to 50µL of DH5α cells and incubated on ice for 20mins. Cells then underwent a heatshock in a 42°C waterbath for 45secs. The cells were chilled on ice for 2mins and 200µL of RT S.O.C media was added to the cells and incubated at 37°C on a shaker for 1hr. 50µL of the cell suspension was then spread on each Ampicillin agar plate and incubated at 37°C overnight.

The second step was colony selection, 4 colonies were selected, and each colony was grown up in 3ml of LB broth with the addition of ampicillin at a concentration of 1:1000, the colonies were incubated on a shaker at 37°C for ~4hours. The culture is then added to 50ml of LB broth containing ampicillin at the same concentration used previously and cultured in the incubator with rotation overnight in a conical flask.

The final part of the vector preparation was to perform a Midiprep. This involved harvesting the DNA from the bacterial culture by centrifuging at 4°C, 4000rpm, 10mins. During this time, the columns from the midiprep kit (Qiagen) were equilibrated ready for the harvested material to be put on the column and from here the manufacturer's

instructions were followed to recover the DNA and elute from the columns ready for transfection into live cells.

2.5.6 Transfection of the PCDHG constructs into HeLa cells

HeLa cells were used for the transfection of the expression vectors of the PCDHG isoforms as they were shown to have no endogenous expression. A confluent T75 flask of HeLa cells were detached using 3ml of trypsin and incubated at 37°C for 5mins, the trypsin was neutralised in 30ml of RPMI media. 2ml of the cell suspension was used to seed to 6-well plate. The 2ml of cells were pelleted and re-suspended in 12ml media to seed a 6-well plate by using 2ml per well. Cells were seeded 24hrs prior to transfection to give them time to adhere to the plate. The transfection mixture contained 4µg of DNA, which was added to 12µL Genejuice per sample, the mixture was incubated together at RT for 5mins prior to the addition and 400µL serum-free media per sample. This mixture was incubated for 20mins at RT and then add dropwise to the cells (scale up for number of wells).

2.5.7 PCDHG Knockdown

siRNA was used to test if PCDHG expression could be knocked down in two myeloma cell lines that had endogenous expression. $2x10^6$ cells of either KMS18 or H929 were seeded per well in a 6-well plate 24hrs prior to the introduction of siRNA using electroporation. On the day of transfection each well of cells was suspended in 100µL of supplemented nucleofection solution and 200nM of the siRNA was added (siRNA 1, 2 or a combination or a scrambled control), each condition was done in duplicate wells. The cell suspension was transferred into a cuvette and electroporated using the AMAXA on program C-13 which had previously been successfully used for other myeloma cell lines. After the electroporation cells were transferred immediately to 2ml RPMI media and plated back into a 6-well plate. The cells were left for 24-48hrs to recover before a lysate was made to assess protein expression of the PCDHG proteins by western blotting.

2.6 Data analysis

2.6.1 FlowJo analysis

All flow cytometry analysis was performed using FlowJo software after importing the FCS files, dot plots and histograms were generated in the layout editor and then exported. The general gating strategy identified the lymphocyte population by size

using SSC/FSC, this population was subject to doublet discrimination before creating a live gate. It was the live cell population that would then be taken forward for further analysis using the B-cell and PC phenotypic markers along with the niche residency factors. The exact gating strategies for each staining panel for different sets of experiments is explained in more detail in the next section (2.5.2). Parameters and measurements regarding percentages, MFI and median were calculated using the table editor function.

Graphpad Prism was used for the quantitative analysis of expression levels observed by flow cytometry as well as any other quantitative data producing the summary graphs for large data sets. A range of scatter graphs and bar graphs were produced to display averages of donors for a range of conditions or the spread of expression between donors.

2.6.2 Staining panels

2.6.2.1 Adhesion signature

Table 2-7 Adhesion signature staining panel

Live/Dead	7AAD
CD138	APC
CD38	BUV395
CD19	BV510
ALCAM	PE
CCR2	BV421
LEPR	PE-Vio770
ITGB7	FITC

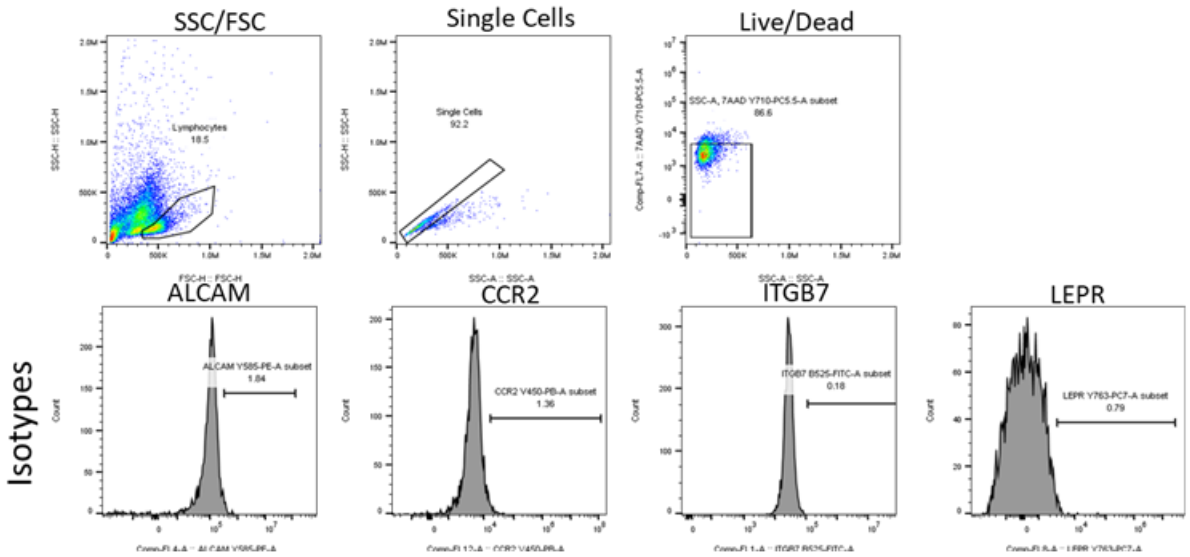

Figure 2.6.2.1 Gating strategy for the niche factors

Flow cytometry plots showing an example of the gating strategy used for analysis of the surface expression of the niche residency factors in the *in vitro* differentiation using different niche conditions. In the example shown plasma cells were differentiated from memory B-cells in APRIL conditions. The histograms show the isotype controls, positive expression was set against the isotypes.

The gating strategy used for assessing the surface expression of the niche factors identified in the adhesion signature was kept simple and used the FSC/SSC to identify the lymphocyte population. As this is an isolated population of differentiating B-cells, there should be very few if any contaminating cells populations, a purity check is done on day 0 of the culture to check this using CD19 and CD20. A doublet discrimination is done on the lymphocyte gate using SSC-H/SSC-A, the single cell gate is taken forward for a live/dead gate using 7AAD. Gating around the 7AAD negative cells creates a live gate, live cells are then assessed for expression of the niche factors using histograms. The B-cell and plasma cell phenotypic markers are there to confirm the cell population is as expected at each stage of the differentiation.

2.6.2.2 PCDH panel

Table 2-8 PCDH staining panel

Live/Dead	7AAD
CD138	FITC
CD38	BUV395
CD19	PE
PCDHGA6	APC
PCDHGB4	APC
PCDHGB5	APC

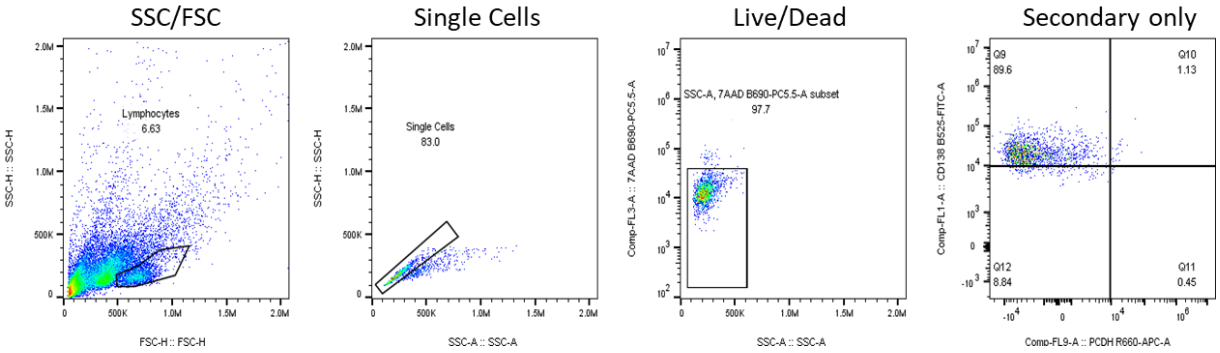

Figure 2.6.2.2 Gating strategy for PCDH staining

The flow plots show an example of the gating strategy used for the analysis for surface expression of the PCDHG isoforms in differentiating B-cells. The gating shown here is of the secondary only condition whereby there was no primary antibody against the PCDHG proteins which was used to set the positive gate for any PCDHG surface expression.

The gating strategy used to assess PCDHG surface expression first identified the lymphocyte population using SSC/FSC, this gate was taken forward for doublet discrimination using SSC-H/SSC-A and then a live gate was generated on the negative 7AAD population. From here expression was assessed using CD138 and PCDG-, the gating was set using the secondary only condition and a CD138 isotype as controls. The top right quadrant showing the subset of cells double positive for CD138 and PCDG isoforms expression. This subset of cells was then used for the quantification and comparison of expression of PCDGA6, PCDHGB4 & PCDHGB5 and the total PCDHG expression seen with the pan-PCDH antibody.

2.6.2.3 Bone marrow panel-adhesion signature

Table 2-9 Bone marrow-adhesion signature staining panel

Live/Dead	Near-IR
CD138	APC
CD38	BUV395
CD19	PE-Cy7
CD27	FITC
CD3	Viogreen
ALCAM	PE
CCR	BV421

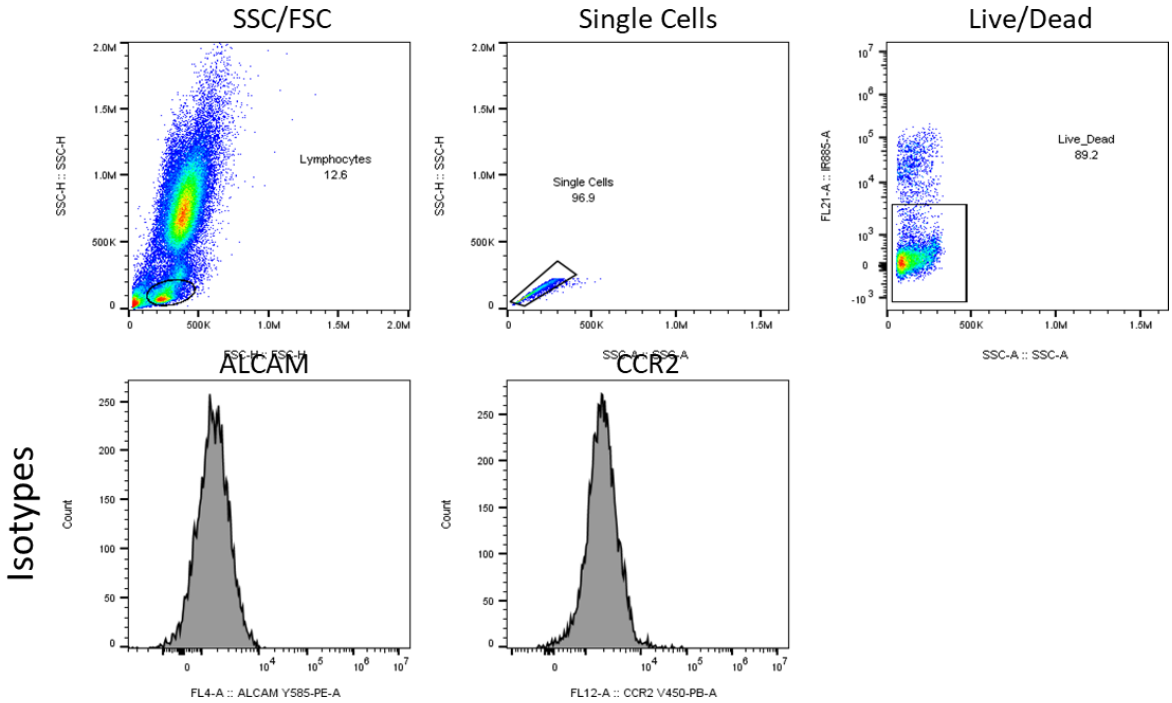

Figure 2.6.2.3 Gating strategy for ALCAM & CCR2 in bone marrow samples

Flow cytometry plots showing the gating strategy used to assess the surface expression of ALCAM and CCR2 on malignant bone marrow samples. Samples were prepared for flow cytometry by red cell lysis and then stained using the panel listed above. The lymphocyte population was identified using SSC/FSC and then doublets excluded by SSC-H/SSC-A. The live cell population was gated on cells negative for the IF-red live/dead fixable stain. Then ALCAM and CCR2 expression was displayed using histograms with the positive gate set from the isotype controls which are displayed above.

ALCAM and CCR2 expression was assessed in malignant bone marrow samples these were prepared for flow cytometry by red cell lysis. The remaining cell population was then stained and the B-cells, PBs and PCs were gated out using the following strategy. The lymphocyte population was selected based on size using SSC/FSC this gate was taken forward and SSC-A/SSC-H was used for doublet discrimination. The live cell population was gated on cells negative for IF-fixable live/dead dye and then any T-cells or NK-cells were excluded from this population using CD3 expression with the CD3 negative population being assessed for ALCAM and CCR2 expression, positive expression was gated on expression seen above the isotype controls, the isotype expression and gating is displayed above. Other B-cell and PC phenotypic markers were included in the staining panel to allow for back-gating on the ALCAM and CCR2 positive population if required.

2.6.2.4 Bone marrow panel-PCDH

Table 2-10 Bone marrow PCDH staining panel

Live/Dead	Near-IR
CD138	PE-Cy7
CD38	BUV395
CD19	BV510
CD3	Viogreen
IgD	PE
PCDHGA6	APC
PCDHGB4	APC
PCDHGB5	APC

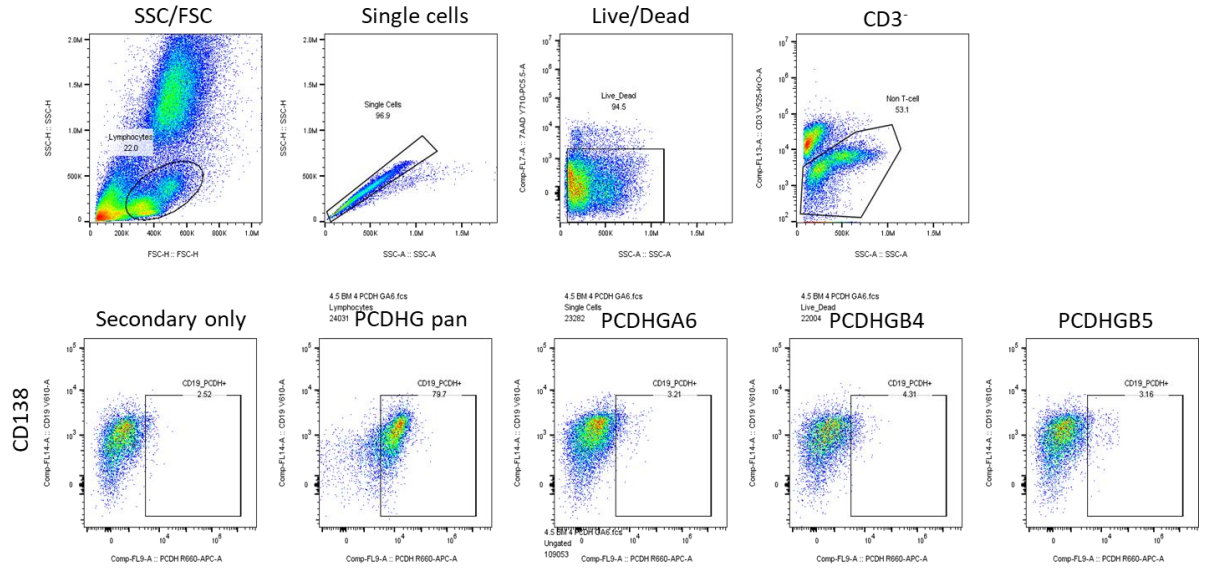

Figure 2.6.2.4 Gating strategy for PCDH staining in bone marrow samples

Flow cytometry gating strategy used for assessing PCDHG expression from malignant bone marrow samples in a mixed population of immune cells following red cell lysis preparation of the bone marrow. A large lymphocyte gate was set using SSC/FSC to capture the B-cells, PCs as well as and slightly larger plasmablasts. This gate was taken forward for doublet discrimination and a then a live gate on the 7AAD negative population. A further gate was set as a non-T cell/NK cell gate using CD3 expression the gate was set over the negative CD3 population. From here PCDHG expression was expression showing expression against CD138 expression.

The gating strategy used for analysis of the bone marrow samples started by setting a large lymphocyte gate to catch both the B-cells and PCs as well as the plasmablast that are larger in size due to their proliferative state, this gate was set using SSC/FSC. From here doublet discrimination was performed using SSC-H/SSC-A and then a live gate selecting cells that were negative for the live/dead fixable dye. The B-cell/PC population was then selected by setting a non-T cell gate on the CD3 negative cells to exclude any T-cells and NK cells. This population of cells was assessed for PCDHG surface expression against CD138 expression as the phenotypic marker of PCs. The PCDH^{+} gate was set using the secondary only control to account for any non-specific staining from the secondary antibody. Total PCDHG expression was assessed using

the conjugated PCDHG pan antibody and the individual isoforms, PCDHGA6, PCDHGB4 & PCDHGB5 were staining using the secondary staining protocol.

2.6.2.5 ADAM inhibition Panel

Table 2-11 ADAM inhibiton staining panel

Live/Dead	7AAD
CD138	FITC
CD38	BUV395
CD19	BV510
ALCAM	PE
PCDH-	APC

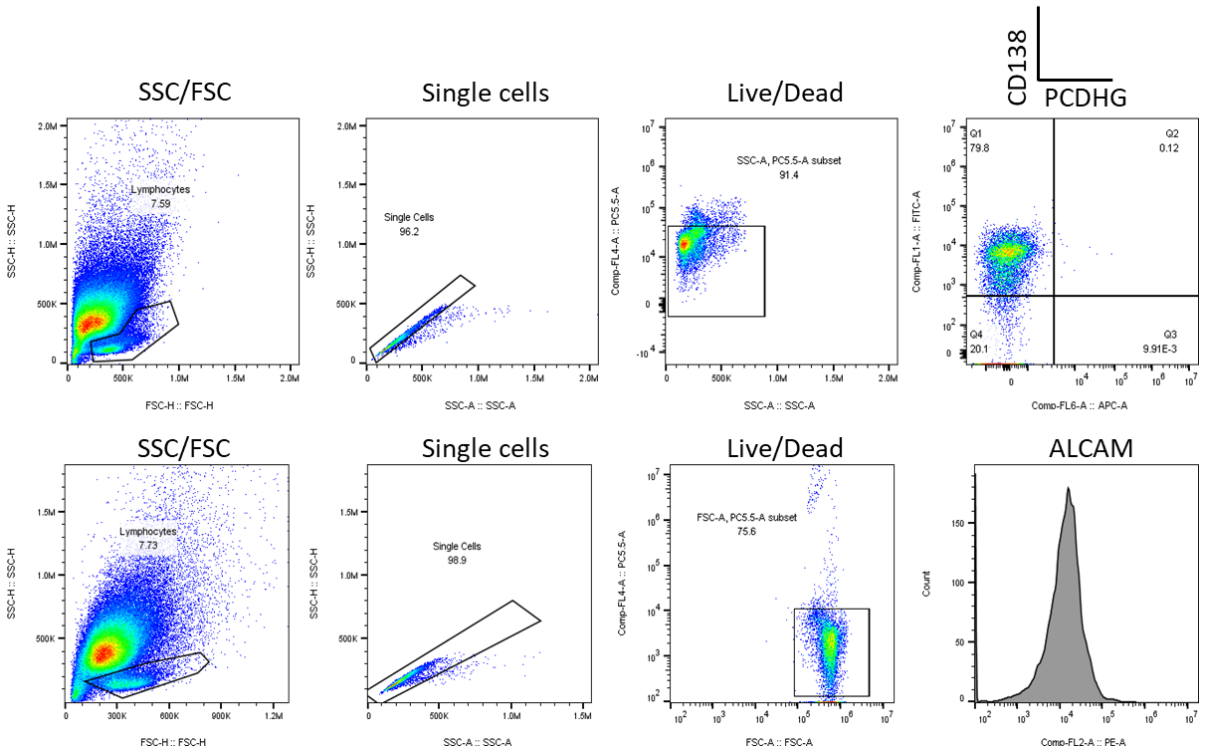

Figure 2.6.2.5 Gating strategy used in the ADAM inhibition experiments.
PCDHG- and ALCAM surface expression was assessed on differentiating B-cells with the use of ADAM inhibition using commercial inhibitors. Surface expression was assessed by flow cytometry and the gating strategy shown above is for two separate assays using the same core phenotypic staining panel but differing in the molecule of interest. The gating strategy identified the lymphocyte population by SSC/FSC and then SSC-H/SSC-A was used to exclude any doublets. A live gate was set on the 7AAD negative population, and this cell population was then assessed for PCDHG- or ALCAM expression. Positive expression of these markers was gated on using the negative controls either secondary only staining or the ALCAM isotype.

The effects of ADAM inhibition of PCDG surface expression and ALCAM expression was assessed by flow cytometry in separate experiments using similar staining panels as listed above and only differing the protein of interest on B-cells and PCs throughout the differentiation system. The gating strategy was similar for each experiment by identifying the lymphocyte population by size using SSC/FSC, doublet discrimination using SSC-H/SSC-A and then a live cell gate over the cell population that was negative for 7AAD. From here the cell population was assessed for either PCDHG- expression or ALCAM expression. The PCDHG positive gate was set against the secondary only control and analysed against CD138 expression. ALCAM positive gate was set using the isotype control.

2.6.2.6 ADAM phenotyping

Table 2-12 ADAM phenotype staining panel

Live/Dead	7AAD
CD138	FITC
CD19	BV510
CD38	BUV395
ADAM10	APC
ADAM17	PE
CD9	PE-Cy7
TSPN8 (added to cell line phenotyping panel)	PE-Vio770

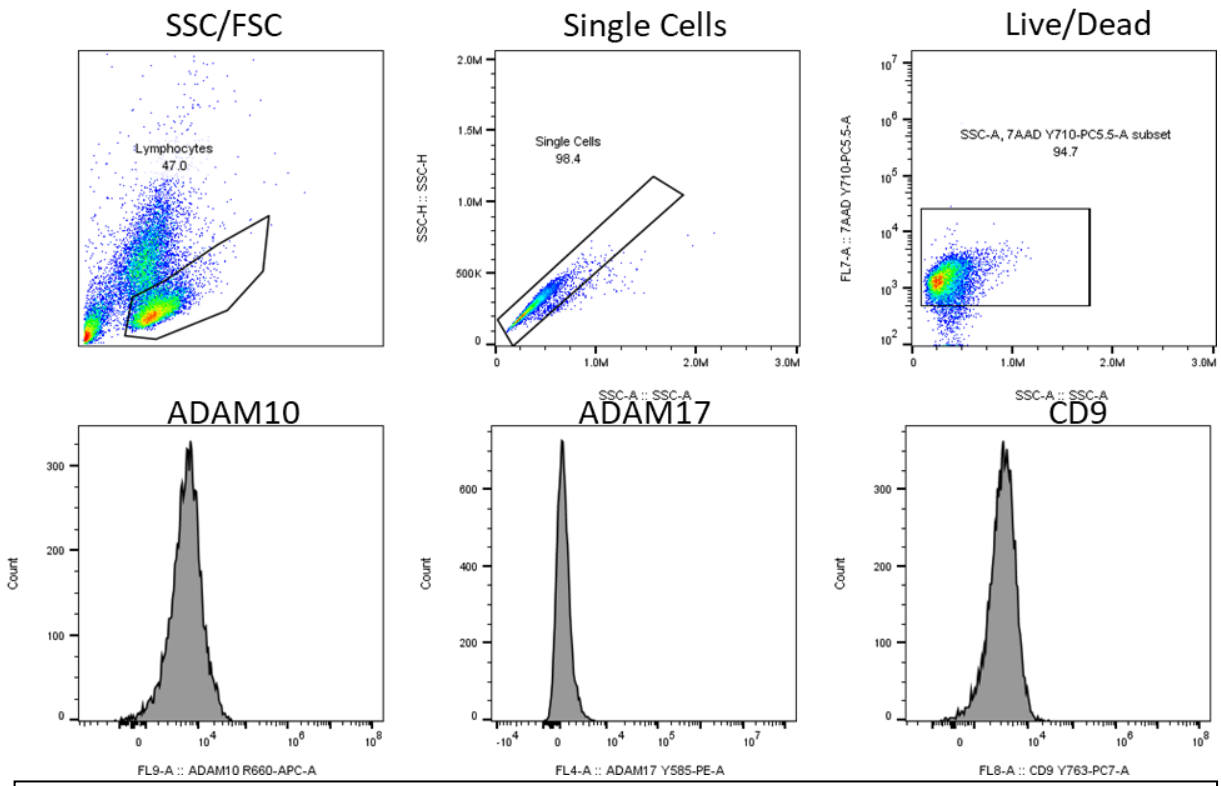

Figure 2.6.2.6 Gating strategy for ADAM phenotyping

Flow plots showing the gating strategy used got the phenotyping of ADAM sheddases, ADAM10 & ADAM17, expression along with some of the known co-factors

To confirm ADAM sheddases surface expression on differentiation B-cells and PCs phenotyping was performed by flow cytometry, the above staining panel was used on primary differentiating B-cells as wells as myeloma cell lines (which had the addition of TSPAN8). The lymphocyte population of differentiating B-cells was identified using SSC/FSC and then any doublets were excluded using SSC-H/SSC-A. A live gate was set over the cell population negative for 7AAD expression, from here this population was assessed for ADAM10, ADAM17 & CD9 expression with positive expression gated above the isotype controls which are displayed above. Other B-cell & PC phenotypic markers were included in the staining panel to allow for back gating to confirm the cell phenotype if required, however the differentiating cells are from an isolated population of total B-cells.

3 B-cells express adhesion molecules in distinct patterns during differentiation

3.1 Introduction

Adhesion molecules play an important role in the development of differentiating B-cells. Adhesion molecules aid naive B-cells in migration and homing out of the bone marrow to secondary lymphoid tissues where they undergo somatic hypermutation and class-switch recombination to increase specificity of the BcR to the antigen being presented. Following a successful T-dependent immune response B-cells may differentiate into either memory B-cells or a long-lived plasma cell (LLPC). PCs need to migrate and home to the bone marrow niche where they reside and receive stromal support and survival signals. Once in the survival niche adhesion molecules maintain retention of PCs within the bone marrow. The surface phenotype can be used to track the transition of differentiating B-cells to the plasmablast and PC stages with changes in surface receptors and niche residency factors. Some of the typical markers used include CD19, CD138 and CD38 and can define subsets of cells through the transition to becoming an antibody secreting PC.

In diagnostic settings these markers are used to assess the PC population in the bone marrow and peripheral blood samples from patients with neoplastic cells that may either lead to a halt in the differentiation for example in the case of Waldenstrom macroglobulemia whereby there is a lack of normal antibody secreting PCs. In myeloma diagnosis is indicated by elevated levels of the paraprotein and bone marrow aspirates reveal neoplastic PCs. Analysing the surface phenotype of PCs can allow monitoring of disease progression and risk factors such as up or downregulation of prognostic markers. Adhesion and niche residency factors play an important role in PC survival and homing to the niche environment in malignancies these can be altered meaning that the standard processes for PC survival and homing can provide the neoplastic cells with an advantage to avoid normal checkpoints. If the cells failed to pass these checkpoints they would naturally be cleared by the immune system and initiate the programmed cell death response.

In this chapter I am going to investigate a set of adhesion molecules and niche factors that have been found to be upregulated in extramedullary plasmacytoma compared to

plasmablastic lymphoma, as plasmacytoma has a better prognosis the hypothesis that this adhesion signature identified may play some role in providing this advantage. Searching the literature is has been shown that these molecules are involved in cell survival, migration and homing to the bone marrow niche. Memory B-cells were differentiated using different niche conditions, APRIL, TGF-β and IFN-α. By culturing with different niche conditions driving the differentiation process I can assess the impact the niche environment has on the pattern of expression and whether this pattern is beneficial for generating cohesive tumours or likely a more dispersed pattern of disease.

ALCAM expression has been linked with homing and migration of PCs to the bone marrow niche and possibly retention once in the niche environment. Immunohistochemistry analysis comparing MM patients with the development of plasmacytoma revealed that ALCAM expression was 4 times higher in bone plasmacytoma compared to EMPs. Higher levels of expression in bone plasmacytomas indicates a role for ALCAM in survival/invasion within the bone microenvironment (Firsova et al., 2020).

Leptin is an adipokine that functions as a hormone and a cytokine. One study has shown that leptin in a concentration dependent manner could induce signalling and secretion of cytokines IL-6, IL-10 and TNF-α from peripheral B-cells (Agrawal et al., 2011), indicating that LEPR is required for signalling that occurs during B-cell differentiation. Leptin leads to increased proliferation in B-cells and a deficiency in leptin has been shown to result in a reduced number of peripheral blood B-cells. The balance of cell populations within the bone marrow is known to be important for normal leukocyte function, LEPR+ cells have been found to affect haematopoiesis of lymphoid progenitors highlighting the influence leptin and adipose tissue can have on maintaining homeostasis in the bone marrow (Comazzetto et al., 2019). Another pathway that leptin promotes is cell survival by inhibiting cell apoptosis through the activation of BCL-6 and cyclin-D, which activates cell cycle (Abella et al., 2017). Given the survival advantages leptin has on B-cells, it may prove beneficial for metastatic PCs to harness this during cancer progression. Therefore, it would be conceivable that leptin may have an involvement during the development of PC disorders.

CCR2 is used as a plasma cell marker and its expression is repressed in B-cells by PAX5 which is then blocked by BLIMP1 once B-cells become fully differentiated. It has been found that osteoclasts secrete CCR2 chemokines CCL2, CCL7, CCL8 and CCL13 in the bone marrow which forms a chemotactic gradient for PCs to migrate to osteoclasts in the bone marrow (Moreaux et al., 2011). This may also provide a link between CCR2+ plasma cells and the number of lytic lesions seen in patients diagnosed with MM. In other studies, the expression of CCR2 on MM cells revealed that down-regulation of CCR2 on the MM cells is indicative of a poorer outcome. With low levels or loss of CCR2 MM cells are not retained in the bone marrow and can migrate into the peripheral blood (Vande Broek et al., 2003; Vande Broek et al., 2006). The presence of MM cells in peripheral blood has been seen with disease progression, this could be explained by loss of adhesion to the stromal support or the development of stroma independent MM cells.

ITGB7 expression seen in MM was correlated with poor outcome for the patients with high expression. *ITGB7* expression is regulated by the *MAF* gene so ITGB7 overexpression can be linked to MAF overexpression that is observed in both MM cell lines and in MM patients. MAF acts as a transcriptional activator or repressor for many downstream targets and is frequently translocated in MM showing this is a pathway utilised by MM cells to enhance growth and survival (Neri et al., 2011; Hosen, 2020). In MAF-translocated cells when either KLF2, IRF4 or KDM3A was knocked down, ITGB7 expression was downregulated. This highlights a signalling axis that MM cells are dependent on. KDM3A maintains expression of KLF2 and IRF4, and KLF2 directly activates IRF4 and vice versa in a positive feedback loop. This signalling axis indicates that upon the initiation of the GC reaction there will be an upregulation of adhesion molecules including ITGB7. Knockdown of these signalling molecules that reduced ITGB7 levels also showed reduced adhesion to BMSCs (Ohguchi et al., 2016). These studies show a specific role in adhesion and homing to the bone marrow and an initiation of an adhesion programme upon differentiation.

It is important to understand the normal expression patterns of these molecules in healthy differentiating B-cells at both a gene and protein level. This will help in understanding the implications expression of these molecules will have in a disease setting, therefore we need to establish knowledge of their standard expression

patterns in healthy B-cells and PCs. Having established a method for analysis and the normal expression pattern the expression in a myeloma cell line model and other myeloma datasets can provide a comparison and give an indication of what role these niche factors may play in disease risk prediction and pathogenesis.

3.2 Gene expression of adhesion molecules in differentiating B-cells

3.2.1 Gene Expression of the niche factors during a differentiation series

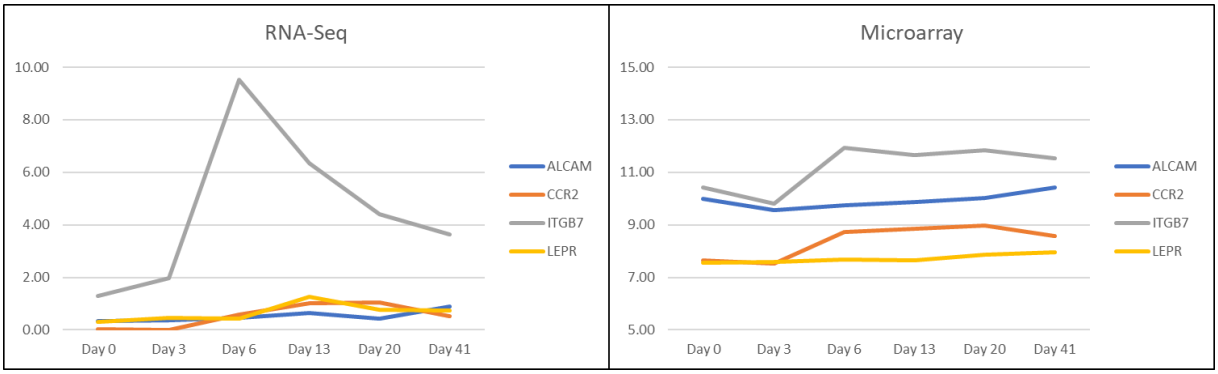

Figure 3.2.1 Gene expression of the niche factors in differentiating B-cells
RNA-seq and microarray analysis was carried out on primary samples from a differentiation series from 3 separate donors. The average expression level of each niche factor was taken across the 3 donors and plotted against each other over the time course of the differentiation.

RNA and microarray data obtained by Mario Cocco showed expression levels of the niche factors across the time course of a 40-day differentiation in IFN-α conditions driving the plasma cell programme (Cocco et al., 2012). The data shows that at a gene level, *ITGB7* expression levels were the highest with most of the niche factors having an increase in gene expression from day 6. This is suggestive that the pattern of expression is present from the plasmablast stage when the B-cell is committed to the differentiation pathway to becoming a plasma cell.

Expression levels were either maintained or reduced to a more basal level once the cells reached day 13 indicating that once established expression of the niche factors is maintained rather than being switched off for a specific stage of the differentiation as the cells transition to the PC gene programme. Maintaining expression of the niche

factors over the time course suggests the role of the niche factors is involved in maintaining the PC survival. The gene expression data mostly correlates with the protein expression, which is not uncommon and can be explained by a lack of the correct processing and trafficking to get the protein to the surface or that the protein is subject to post-translational modifications as well as cleavage or internalisation. These types of events would lead to low levels of protein expression when carrying out flow cytometry analysis of protein surface expression. As the protein expression presented later in this chapter starts from day 6, it shows that the overall trend of higher expression at day 6 and then low-level maintenance in PCs correlates for RNA and protein expression apart from ALCAM. Some variation between the two may also stem from analysis of a bulk population giving an average compared to looking by flow cytometry individual cell analysis.

3.3 Surface expression of adhesion signature molecules in the differentiation system

3.3.1 Model of Differentiation

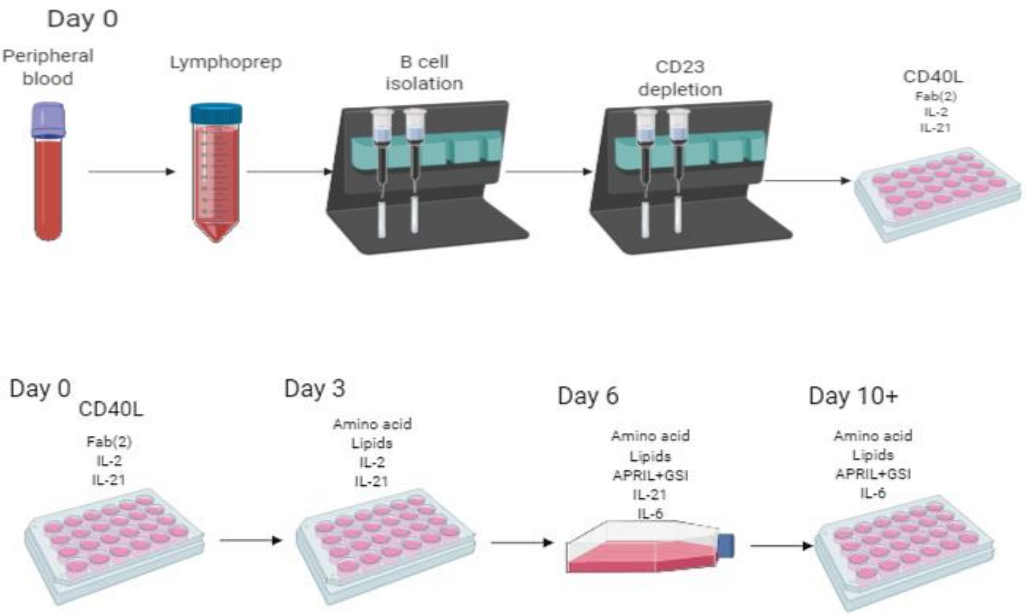

Figure 3.2.1 *In vitro* differentiation system
Schematic showing the setup and process of the *in vitro* differentiation system along with the addition of the different cytokines and supplements at each stage of the differentiation.

In order to study B-cell development an *in vitro* differentiation system has been established (Cocco et al., 2012), this allows for manipulation of culture conditions and phenotyping of the cells as they progress through the differentiation process. Peripheral blood mononuclear cells (PBMCs) are first isolated from peripheral blood using lymphoprep to separate out the layers of the blood by weight and then the PBMC layer is removed and washed before separating the naïve B-cells using magnetic columns and a B-cell isolation kit (Mitenyi) for negative selection. A further isolation step is carried out when wanting to work on memory B-cells which is done using a CD23 depletion to remove the naïve B-cells. Negative selection of the CD27+ memory cells, is achieved by labelling naïve B-cells with anti CD23-biotin antibody and then using biotin microbeads to magnetically separate naïve and memory cells with the

CD23+ cells binding to the column and the CD23- cells being collected in the flow through. Using negative selection of CD23- cell enables completely untouched cells to be used in the differentiation system and therefore have had no prior stimulation through binding of CD23.

Once the isolation steps are complete the B-cells are put into culture with fibroblasts expressing CD40-L to activate the B-cells via CD40 along with BcR activation via the Fab(2) fragment. Along with CD40-L and Fab(2) the B-cells are cultured with cytokines IL-2 and IL-21. As the cells reach day 3 in culture, they are taken off the CD40-L fibroblasts and cultured with a cocktail of amino acids, lipids, IL-2 and IL-21, from here there is a large clonal expansion and increased proliferation up until day 6 by which time the majority of cells enter the plasmablast stage. From day 6 the culture conditions are changed again with cells being stimulated with either APRIL, TGF-β or IFN-α to drive differentiation to long-lived plasma cells (LLPCs). As well as this stimulation the cells are also maintained in media enriched with amino acids, lipids and IL-21 while IL-2 is substituted for IL-6 to support LLPC survival. The cells are refed from day 10/13 onwards with the same cytokine cocktail except for IL-21 which is removed. Once the cells reach day 13 in culture, they will have become quiescent antibody secreting cells fulfilling the definition of a mature plasma cell (PC). From approximately day 20 onwards in the system the bulk of the surviving population are now LLPCs. Throughout the *in vitro* differentiation cells are phenotyped at regular intervals before the culture medium and cytokine cocktail are changed at the different stages, this confirms that the system is working and identifies any low levels of contaminating cell populations, such as T-cells or NK cells.

3.3.2 Phenotype during B-cell differentiation

The *in vitro* differentiation system produces terminally differentiated PCs from CD19+ total B-cells isolated from peripheral blood. The phenotype of the cells is assessed at specific stages of the differentiation to establish the subsets of cells as they transition through the different cell states. Differentiation to mature PCs is confirmed by the gain of CD38 and CD138 expression and the loss of CD20 as the cells move towards the PC phenotype established by day 13.

The cells start off as CD19/CD20 positive with very little expression of either CD38, CD138 or CD27. A small population of CD19- cells at day 0 indicates a slight impurity in the population, usually <5%, which is outgrown as the B-cells differentiate. By day 6 there is a large clonal expansion as the cells become plasmablasts, here the cells gain CD38 expression with some low level CD138 expression. From day 6-13 there is a gain of CD27 expression, a feature of the transition to a mature ASC. A separation in the cell population of CD27 positivity and CD38 expression is seen, it is the CD27+/CD38+ that are thought to be the precursors to ASCs. There is a sub-population of CD27-/CD38+ cells which have not been fully characterised. Once the cells have reached day 20+ in culture they will now be LLPCs as seen by the high expression of CD38/CD138 and high CD38/CD27 and a loss of CD20 expression.

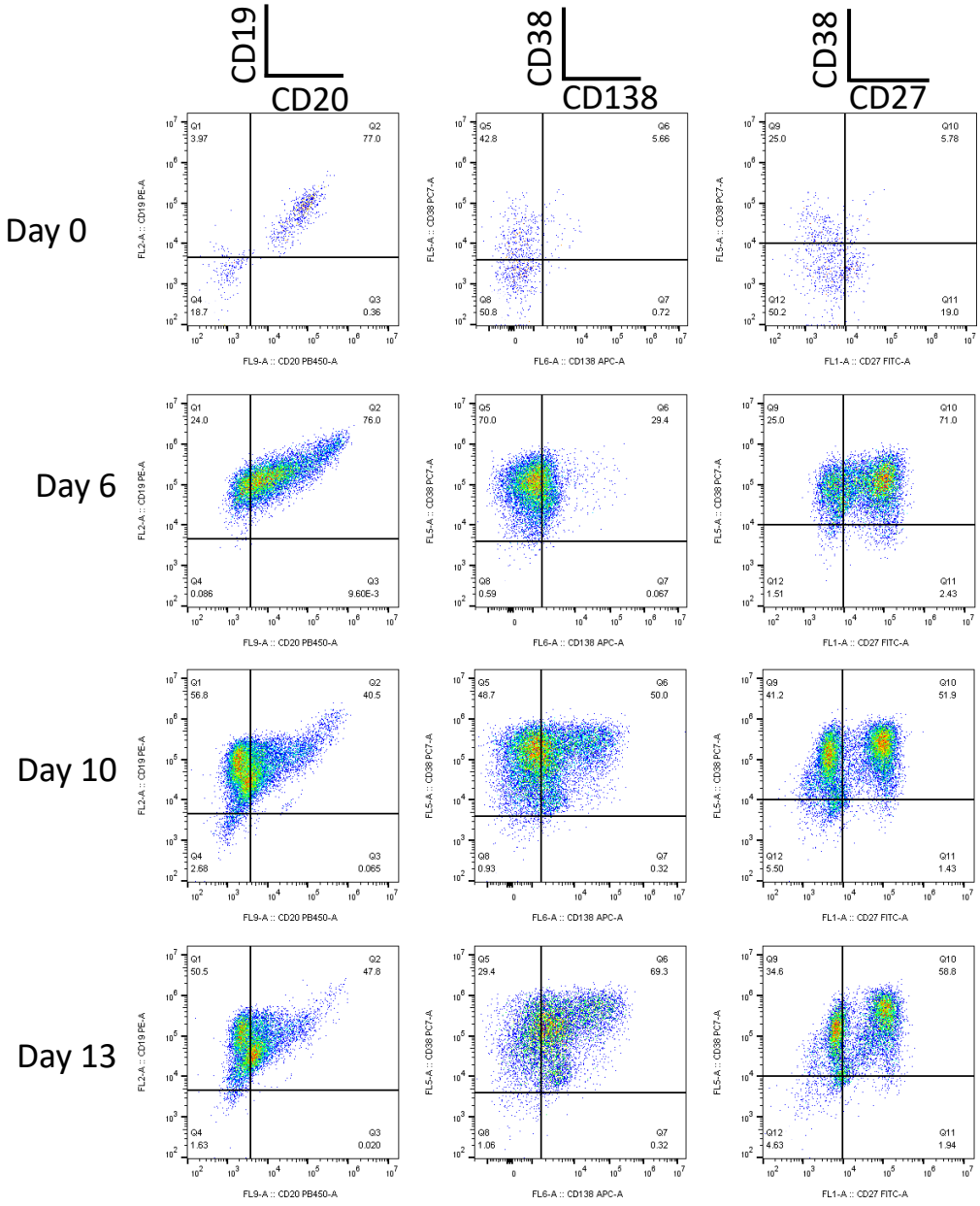

Figure 3.3.2 Standard staining patterns of the phenotypic markers

Total B-cells were isolated from PBMCs extracted from peripheral blood. The B-cells are activated by co-culturing with CD40L-fibroblasts till day 3 and are stimulated with a series of cytokines to drive differentiation. On day 6 APRIL is added to induce the plasma cell programme by day 13 the cells have matured to long-lived plasma cell. At specific timepoints cells are analysed by flow cytometry to assess the phenotype.

3.3.3 Surface expression of adhesion molecules during differentiation

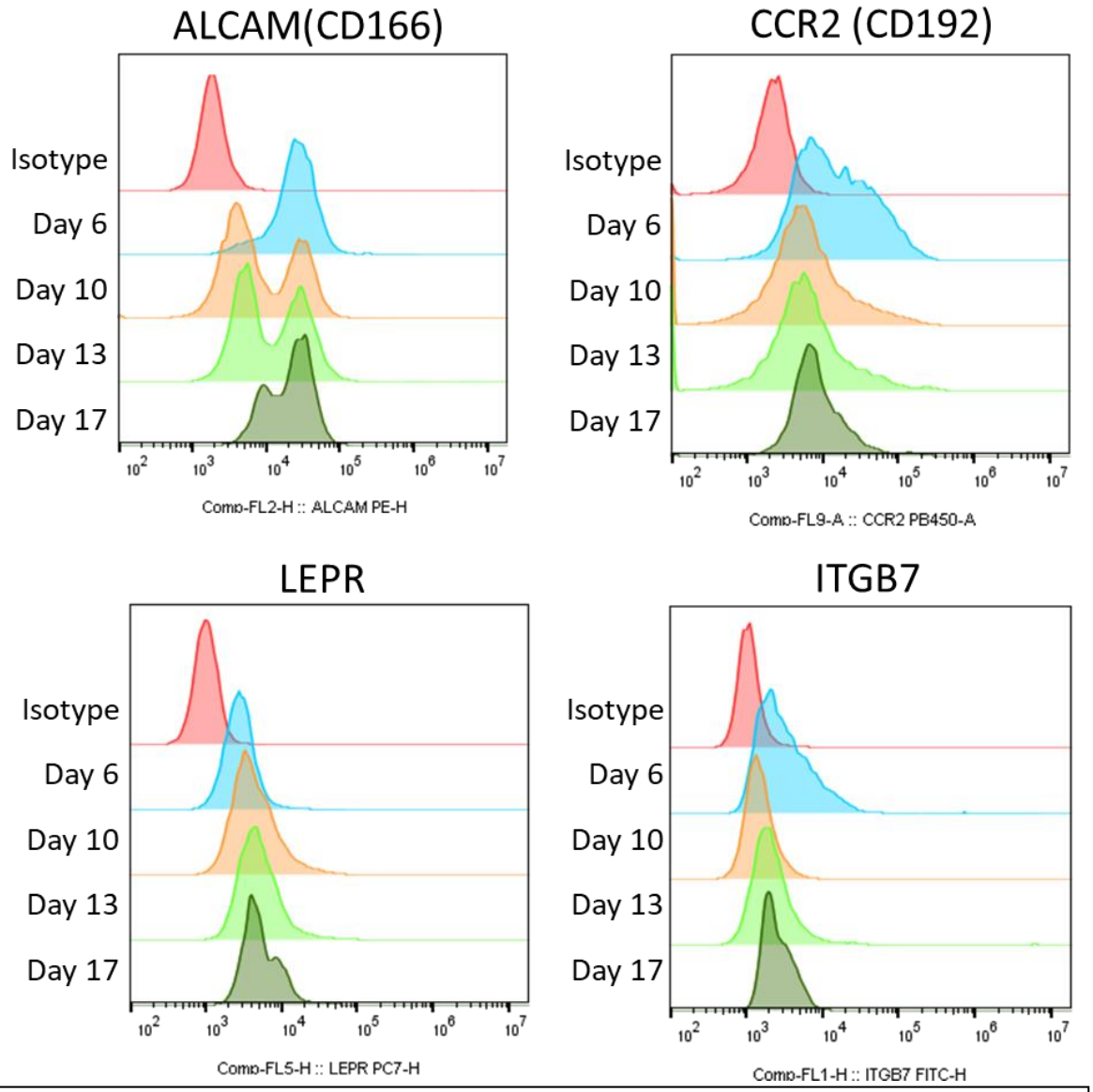

Figure 3.3.3 Histograms of niche factor expression during differentiation
A representative donor where total B-cells were isolated from peripheral blood and differentiated using CD40L and APRIL stimulation, cells were phenotyped at specific time points to assess the expression of different niche factors. Expression was assessed from day 6 at the plasmablast stage through till day 17 when the cells have become antibody secreting PCs. n=1

Expression of the niche factors was analysed by flow cytometry throughout the differentiation. Expression was compared against an isotype control to account for background staining from the antibodies. For each of the niche factors expression was

established from day 6 with positive expression for each of the niche factors which correlated with positive expression seen in the RNA-seq and microarray data (3.2.2). For this donor and initial analysis ALCAM (top left) showed 2 populations of cells differing in expression from day 10 onwards with the ratio of the peak sizes oscillating between time points. This expression pattern does not directly correlate with the mRNA expression seen and may suggest that there is a dynamic pattern of ALCAM expression throughout the differentiation process. From this experiment alone it cannot be ascertained if the split in the population for ALCAM expression is an indicator of cells differentiating more slowly, whether the ALCAM low cells are short lived or if the change in expression is due to a regulation mechanism changing the levels of ALCAM.

For CCR2 expression there is a large shoulder of high expression at day 6 indicating a small proportion of cells with high expression. As the cells moved towards LLPCs at the later time points this shoulder of expression becomes reduced. This suggests that as the cells become more PC like there begins to be a downregulation of CCR2 expression, as CCR2 is involved in the migratory process this may be a standard pattern of regulation as LLPCs typically reside in the bone marrow niche and only migrate out of this niche when there is an immune response. As CCR2 leads to migration down a chemotactic gradient theoretically expression on PCs could result in migration towards any niche that has high levels of CCL2, such as sites on inflammation.

LEPR expression overall has a low level of expression compared to factors like ALCAM, expression steadily increases as the cells age into LLPCs with very little changes in the general pattern of expression. The final niche residency factor tested was ITGB7 expression that also has very low levels of expression during the differentiation, this expression was maintained at a consistent level. There was a slight shoulder of expression at day 6 before the cells then reached the quiescent PCs phase at the later time points.

From this initial experiment it was decided to repeat analysis of the niche residency factors in the differentiation system in multiple donors (3<) and to extend the length of the time course to establish if there is a plateau in expression levels, particularly ALCAM to see if the level of expression becomes homogeneous in LLPCs.

3.3.4 Expression of the niche factors in differentiating B-cells & LLPCs

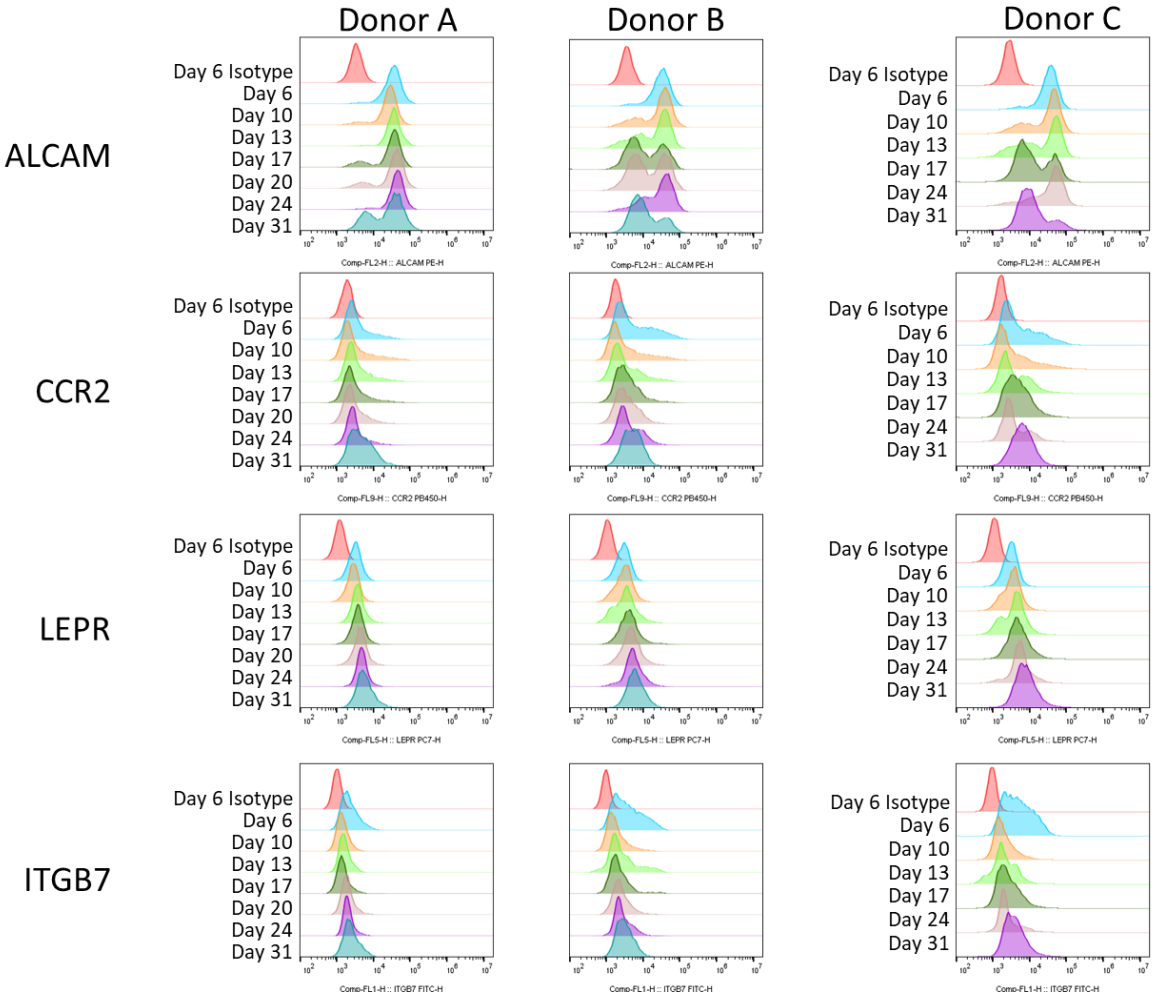

Figure 3.3.4.1 Histograms representing niche factors expression in B-cells & LLPCs Flow cytometry analysis of expression of the niche factors was performed across a B-cell differentiation series. Memory B-cells were isolated from peripheral blood from 3 healthy donors and differentiated in APRIL conditions. Long-term cultures to day 31 were achieved where possible. Equal numbers of cells were used for analysis at each timepoint, and B-cells and PCs were gated using standard phenotypic markers including CD19 and CD138, expression if the niche residency factors from these cell populations were plotted as histograms. n=3

Surface expression of the niche factors was assessed by flow cytometry over an extended time course (day 31) for the B-cell differentiation system to establish at what point the pattern of expression is established and if this is maintained in terminally

differentiated PCs. From here on long-term cultures were differentiated from memory B-cells, this decision was made due to enhanced survival into LLPCs from the memory B-cell cultures compared to cultures started from naïve B-cells. For donors A & B the culture way carried out until day 31, however for donor C the culture was missing the day 20 time point due to low cell number. Expression was analysed in 3 donors to account for individual variation although the general trend for expression patterns appeared to be consistent with a slight difference in the strength of expression.

ALCAM consistently produced a double peak after day 6 in each of the donors as the cells moved toward the PC stage. In the initial time points where there was a split in the population (day 10 & 13) the low expressing population was very small with only a small peak. The low ALCAM populations then varied with the peak of expression increasing to the same level as the high ALCAM population in two of the donors. The peak size of the two populations fluctuates continually throughout the later time points suggesting that the levels of expression are subject to changes at the level of observed populations and time points even after cells are LLPCs.

CCR2 expression is similar between donors and once established in LLPCs is maintained at a consistent level of expression. There is a slight shoulder of expression seen in the peaks that indicates a small proportion of cells with higher CCR2 expression however looking at the maintenance over the longer time course once a pattern of expression is established at day 13 there is very little change in expression levels.

For LEPR there is very little change in expression throughout the extended time course apart from a marginal increase from day 6 to day 20 which is then maintained until day 31. Finally, for ITGB7 there is some variation between donors, but the general trend is that there is a shoulder of expression at day 6 which then decreases slightly, and expression is maintained at a low level through to the later time points.

Overall, there is a standard pattern of expression established for each of the niche residency factors that is consistent between donors. The only niche factor that shows much variation in expression at the later time points following terminal differentiation is ALCAM. Since this factor has previously been associated with myeloma relapse it would be beneficial to know how expression is being regulated, and what changes there are in myeloma to enhance survival and migration of myeloma cells. For

example, looking for changes in activation marks and accessibility using ATAC-seq or looking for post-translational changes.

3.3.4.1 Summary of positive expression of the niche factors

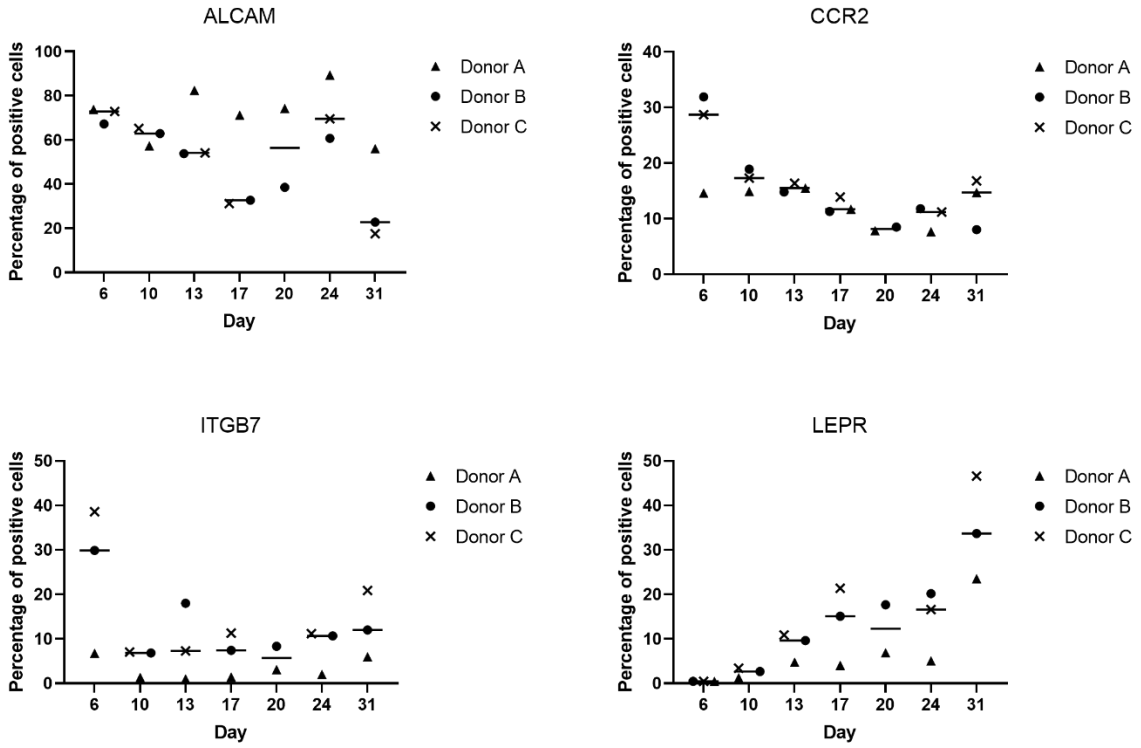

Figure 3.3.4.1 Percentage positive expression of the niche factors during differentiation The percentage of positive cells was quantified using the frequency of parent, generated using the table editor tool in the FlowJo software. Positive cells were set as any cells with expression higher than the isotype control. The frequency of positive cells was plotted for each donor at the time points assessed during the differentiation. Each of the niche factors are plotted separately with the mean of the 3 donors shown for each time point. n=3

The frequency of positive cells from 3 donors was averaged and plotted over the time course of the B-cell differentiation to show the changes in expression levels of the niche factors. The expression of ALCAM is the most variable with the highest expression on day 6 at the plasmablast stage, the variation in the mean value is likely to reflect double peak seen in the histograms, and this may skew the mean and cause the shifts depending on the proportion of the cells that are high expressing at the time of sampling. CCR2 is highest on day 6 of the differentiation, when the cells are

transitioning from the plasmablast stage to fully differentiated PCs. The expression steadily decreases to low level expression as the cells at day 20 & 31 will be LLPCs. LEPR and ITGB7 both follow a similar trend in that expression increases steadily over the course of the differentiation low level expression that is maintained for ITGB7 and for LEPR expression increase up to day 31 indicating a more prominent role in LLPCs. This suggests a there are standard patterns of expression for these niche factors on the cell surface which is maintained past day 13 and seen in LLPCs.

The data from the flow cytometry analysis shows that there are differing patterns of expression for each of the niche factors and that their expression varies from each other at different points during the differentiation. For ALCAM expression is on at a relatively high level throughout the differentiation however the level of expression varies across the time series suggesting there is some form of regulatory mechanism responsible for this fluctuation.

3.3.5 Maintenance of the expression pattern of the niche factors in healthy donors when repeatedly sampled

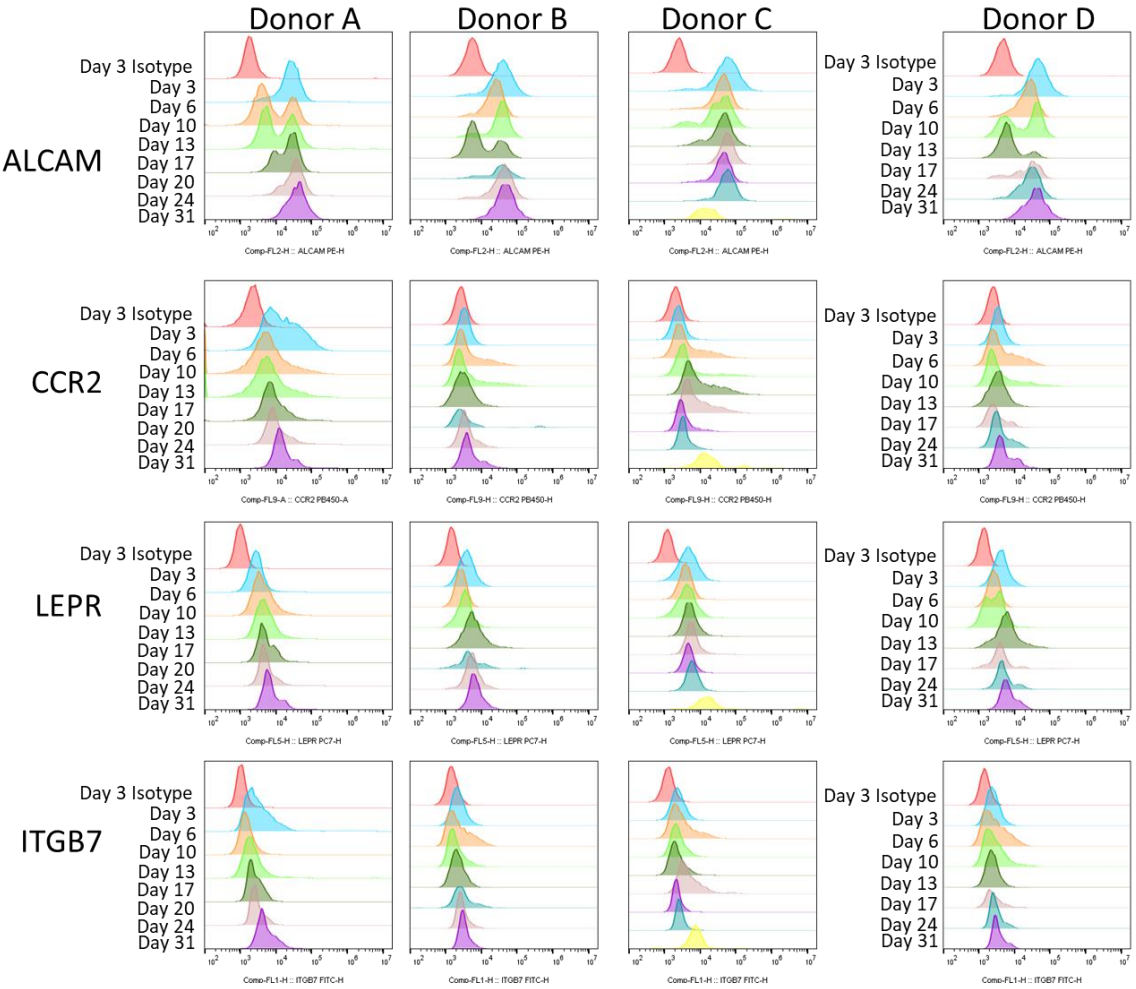

Figure 3.3.4 Maintenance of niche factor expression pattern upon repeat sampling Memory B-cells were differentiated in APRIL conditions from 4 donors over an extended time course to day 31. The surface expression of the niche factors was analysed at specific timepoints by flow cytometry to assess the maintenance of the expression patterns in LLPCs from multiple donors. The gating strategy selects for the lymphocyte population, followed by doublet discrimination and positive gating over the live cells using negative 7AAD expression. The histograms are generated for the entire population of live cells however the populations can be back gated to check the B-cell phenotype using CD19, CD38 & CD138 staining. n=4

B-cells were differentiated up until day 31 to investigate whether the pattern of expression is maintained after the cells have become a terminally differentiated PC at

day 13. The same donors were used as in the previous figure along with one additional donor (Donor D), this is to establish whether the pattern of expression varies depending on the time of sample collection or is specific to the normal differentiation process. The general trend of the expression patterns remained the same. The expression of ALCAM generated two peaks from day 6 onwards the height of the lower peak varied slightly between donors and sampling. The only common feature found from analysing ALCAM expression against the phenotypic markers was that the ALCAM high population were also CD138 high. CCR2 consistently produced a shoulder of high expressing cells but maintained expression throughout the time course of the differentiation. Expression levels of LEPR were low but consistent across the time course and between donors with a marginal increase at the later time points. Finally, ITGB7 expression levels were seen from the start of the differentiation with marginal shifts but overall showed low but consistent expression throughout the differentiation and between donors. From this experiment it has shown that there is a consistent pattern of expression specific to each of the niche factors that is established during normal B-cells differentiation.

3.3.6 Comparison of MFI of adhesion molecules between donors

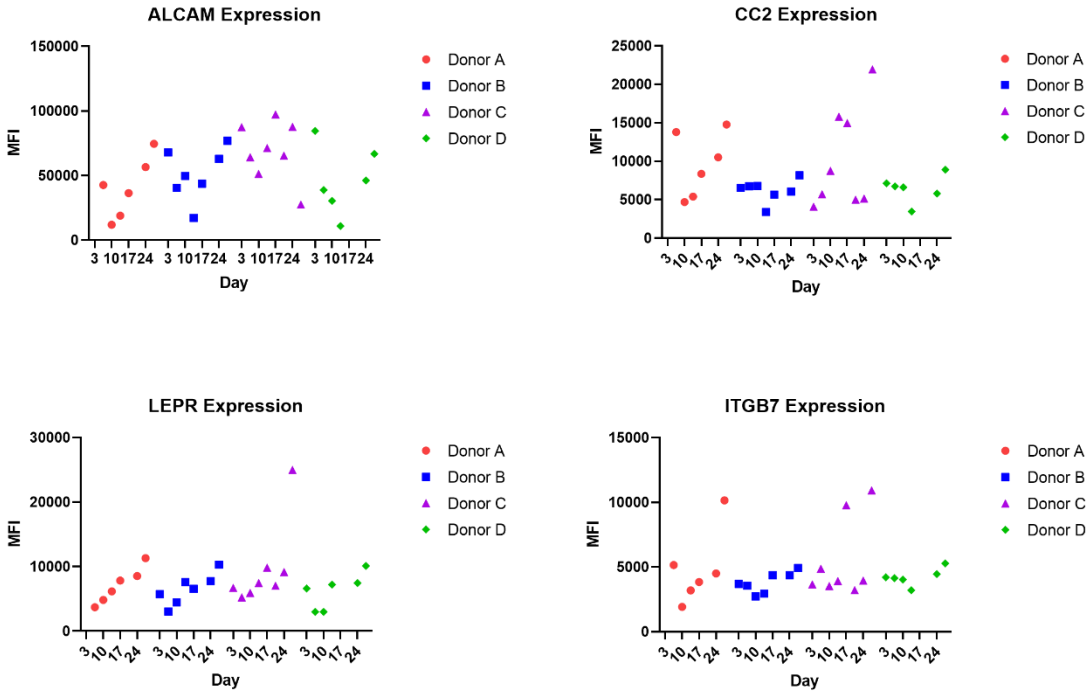

Figure 3.3.6 MFI of the niche factors in individual donors
Memory B-cells were isolated from 4 healthy donors and differentiated in the *in vitro* system using APRIL stimulation. The MFI of the expression for each of the niche factors was plotted across the time course of the differentiation for the whole B-cell/PB/PC population. Expression was plotted individually for each donor to allow a comparison of expression patterns between individuals. n=4

To determine whether there is a trend established for the expression of the niche factors throughout normal differentiation the MFI was plotted for each of the individual donors to see whether there were similarities in the expression patterns and whether any variation could be due to individual donors skewing the average.

ALCAM expression shows the greatest variation between time points for the levels of expression, but this is consistent between donors, suggesting there is something within normal differentiation that is causing the double population. This is seen in the histograms and demonstrates the oscillation of high and low MFI across the time course. CCR2 expression has a general trend of a gradual increase at some of the later time point for donors A and C, however the overall expression tends to remain

low and is maintained across the time course. Some of the points with higher expression levels may be representative of the shoulders of higher expression seen in the histograms, therefore it is difficult to look at an average of the expression level when there appears to be small subsets of cells that express CCR2 at a higher level. This will skew the average; however it highlights the disadvantage of only considering the average rather than looking at the actual spread of data and the benefit of assessing a whole population at a cell level using flow cytometry.

The expression levels of both LEPR and ITGB7 again appear to be similar in that they maintain a low-level baseline expression which does not alter through the time course of the differentiation. There are a couple of outliers with higher expression again in donors A and C for some of the later time points, it is unclear as to whether this is down to the individuals or an artefact that there does tend to be more dead cells and debris in the cultures at the later time points.

3.4 Expression of adhesion molecules in different niche conditions

3.4.1 IFN-α alters pattern of adhesion expression

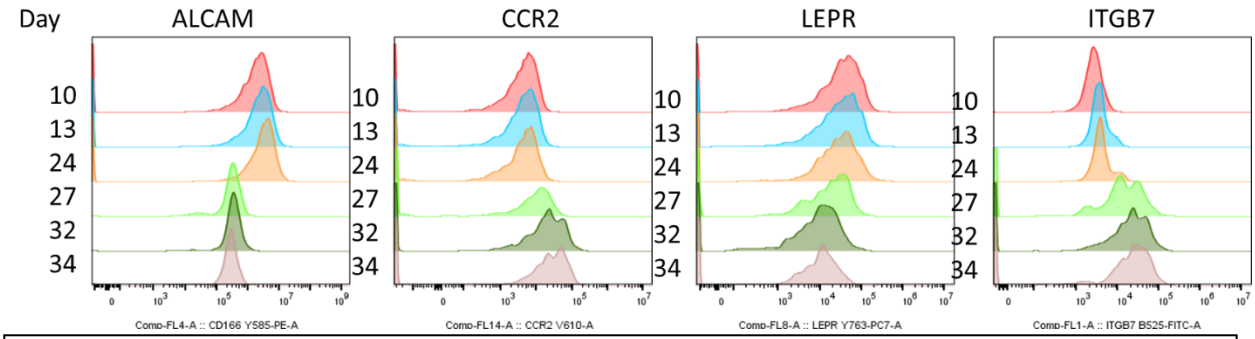

Figure 3.4.1 Pattern of niche factor expression with IFN-α stimulation

Memory B-cells isolated from peripheral blood were differentiated using IFN-α up to day 34 using the *in vitro* differentiation system. Cells we analysed at specific time points by flow cytometry for the surface expression the niche factors. Expression levels for each factor are plotted as histograms. n=1

A pilot experiment was conducted to establish whether the pattern of expression of the niche factors alters depending on the stimulation the cells receive to drive the plasma cell programme. The niche factor tested was an IFN-α stimulation which mimics an inflammatory response compared to APRIL stimulation which was previously used and

initiates and anti-inflammatory response. Most notably the expression of ALCAM became more homogeneous when cells were stimulated with IFN-α producing only a single peak of expression compared to the double peak that is produced in APRIL conditions. The expression of CCR2 marginally increased throughout the differentiation like ITGB7, although ITGB7 showed a wider spread of expression from day 27 onwards. The spread of expression at the later time points is likely an artefact of low cell number slightly skewing the distribution. LEPR expression unlike in the APRIL conditions decreases over the time course.

There is a clear contrast in the expression pattern with IFN-α stimulation in comparison to the pattern seen using APRIL. The expression of the niche factors is more homogeneous which is mirrored in the phenotypic markers. With the IFN-α stimulation there is a tighter population of cells expressing high levels of CD138 which matches with the tight population of ALCAM expression cells. This experiment was only carried out in one donor but is suggestive that the niche condition may affect the pattern of expression. As this was a pilot experiment with one donor I wanted to determine if the results were reproducible. Therefore, I next performed a direct comparison using 3 donors splitting the cells into 3 separate conditions using either APRIL, TGF-β or IFN-α to adequately address the question if the signals received determine the niche factor patterns seen on the PCs and LLPCs.

3.4.2 Long-term differentiation in APRIL niche condition

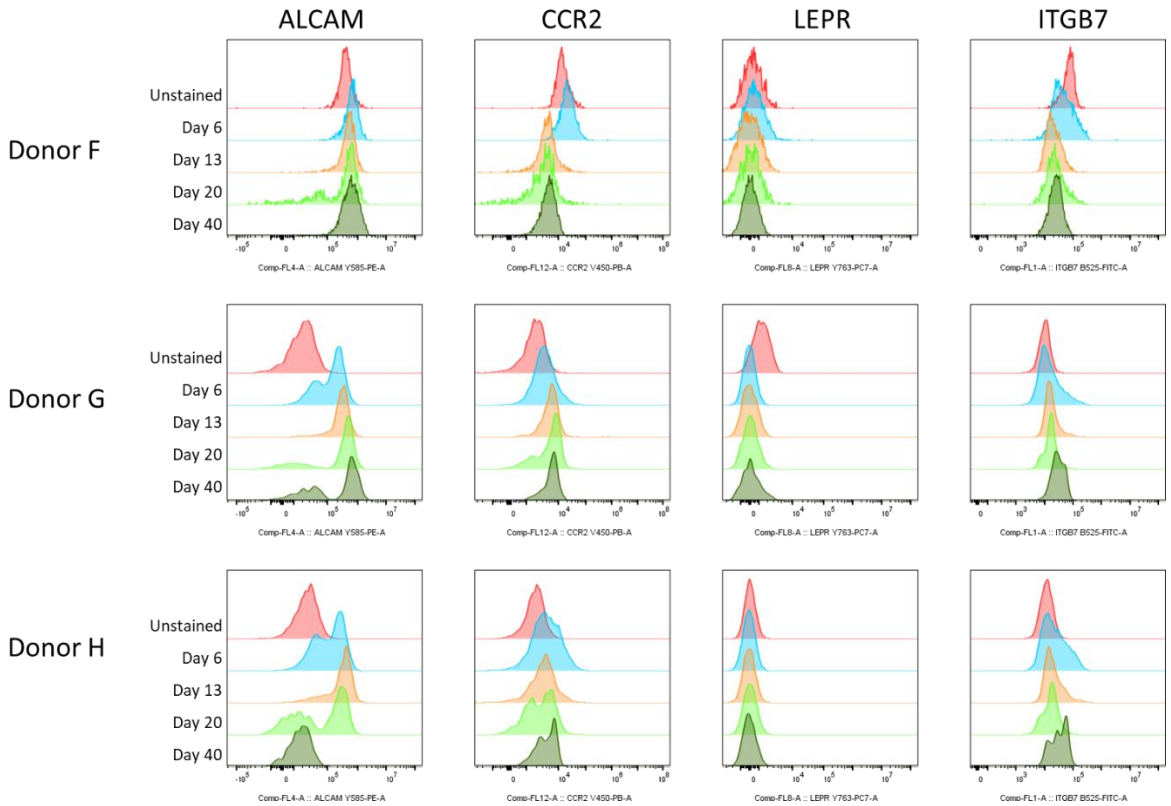

Figure 3.4.2 Niche factor expression with APRIL stimulation
Memory B-cells isolated from blood cones from 3 donors we set up in APRIL niche conditions and differentiated over a long-term time course to generate long-lived plasma cells. At specific time points the expression if the niche factors were analysed by flow cytometry and plotted out as histograms. n=3

A long-term differentiation was set up using 3 donors and the memory B-cells were differentiated into long-lived plasma cells (LLPCs) using APRIL stimulation. Cells isolated from the same donors were also set up in IFN-α and TGF-β conditions. The long-term differentiation showed that once the pattern is established at the plasmablast stage at day 6 the most striking expression pattern was for ALCAM and generated to subsets of cells with high or low expression. This was consistently seen with all donors and correlates with previous experiments (n=10). CCR2 expression shows a small shoulder indicating a small number of cells with higher expression than the general cell population however this does vary between donors. The same level of variation can be seen between donors for ITGB7 expression with a potentially small

number of ITGB7 bright cells. LEPR however maintained a constant low level of expression in each donor.

The main variation in expression levels is ALCAM, double peaks are seen indicating two cell populations, which has been seen previously with APRIL niche conditions. There appears to be a small population of cells with lower ACAM expression with variation in the proportion if low to high expression cells as the cells progress though the differentiation. The cause of this split is not obviously linked to cell phenotype although the CD138+ cells are also ALCAM+, there may be other causes for the split population to be considered. The lower population may be cells that are dying as the general trend show a final single peak of higher expression or it could be due to post-translational processing or endocytosis and recycling. Overall, there does appear to be standard patterns of expression between donors for the niche factors and that establishment of these pattern appears to be a normal feature.

3.4.3 Percentage of positive expression of the niche factors in APRIL condition

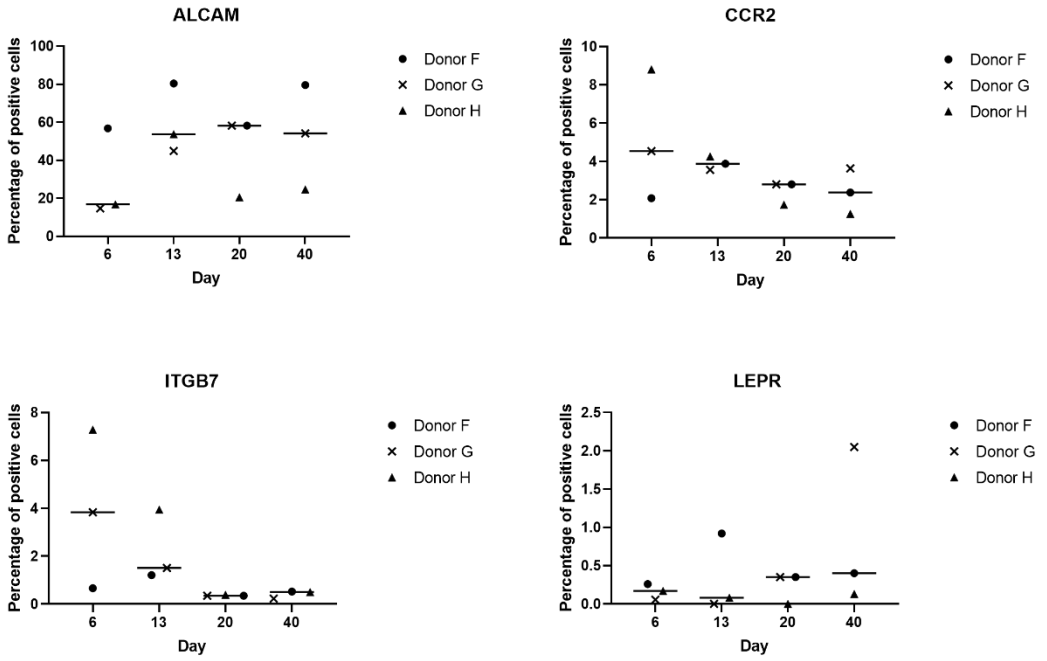

Figure 3.4.3 Percentage of positive expression of the niche factors with APRIL stimulation

Expression of the niche factors over the course of the differentiation was quantified to summarise the expression patterns observed as histograms. The percentage of positive cells from the parent population was calculated from the flow cytometry analysis using the table editor tool in the FlowJo software for each niche factor. The percentage for each donor is plotted across the time course of the B-cell differentiation in APRIL conditions, quantifying the positive population of cells from the parent population of cells. n=3

To summarise the flow cytometry analysis of each niche factor in the APRIL condition, the percentage of positive expressing cells has been calculated. ALCAM expression fluctuated over the time course in each of the donors with oscillating levels of expression. Again, it should be considered that the mean is taking an average of the overall expression level between the donors and a single value may not represent the true distribution of the PC population. Whereas the histograms show that there are two populations of cells with different levels of ALCAM expression which is not represented by the quantification of positive expression. CCR2 and ITGB7 expression is highest at

day 6 with donor H approximately 2-fold higher than the other donors, and then expression decreased throughout the differentiation showing a similar trend to the pattern observed in earlier figures. LEPR and ITGB7 had the lowest levels of expression with some timepoints where no expression was detected at all. Overall, when expression was detected for these niche factors the levels were a lot lower than that of either ALCAM or CCR2.

3.4.4 Long-term differentiation in TGF-β condition

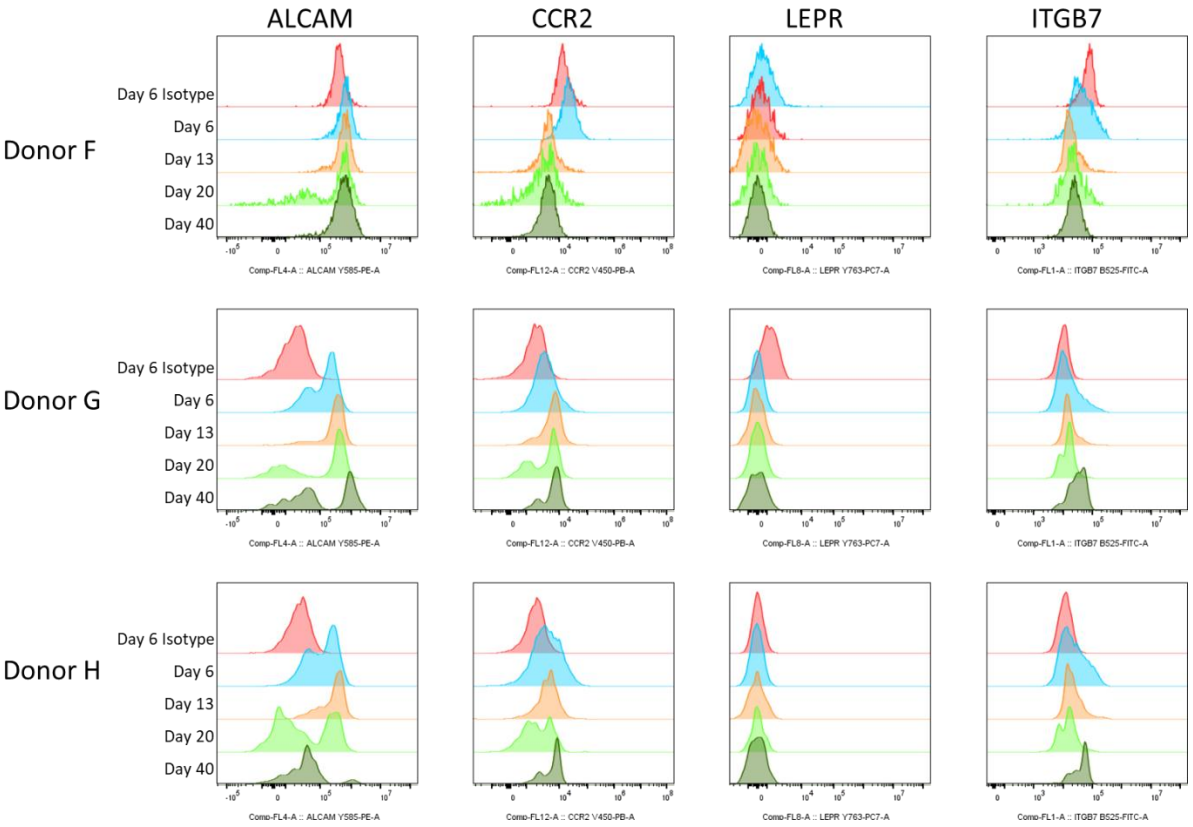

Figure 3.4.3 Pattern of niche factor expression with TGF-β stimulation
Memory B-cells isolated from blood cones from 3 donors was set up in TGF-β niche conditions and differentiated over a long-term time course to generate long-lived plasma cells. At specific time points the expression if the niche factors were analysed by flow cytometry gated for $CD19^+$ B-cells and $CD138^+$ PCs, expression of the niche factors was plotted as histograms. n=3

Expression of the niche factors was analysed across a differentiation series in TGF-β conditions, the pattern of expression for ALCAM did not differ much between donors generated post day 6. However, the proportion of cells in the high and low subsets

differs between donors. A direct comparison of donors between conditions would give the best indication that there is a programme of expression of the niche factors initiated during differentiation and is a consistent feature of normal B-cell differentiation.

TGF-β stimulation produced two peaks of ALCAM expression similar to the expression seen with APRIL stimulation. CCR2 expression appeared to decrease as the differentiation progressed in donor F whereas the other donors the low population was lost leaving a homogeneous cell population in the LLPCs. Minimal LEPR expression was seen compared to the isotype which may be a true result but also possible that there is an issue with the antibody being used for staining which is not binding correctly. Finally, ITGB7 expression also appeared to be very low, with a shoulder of expression at day 6 showing a small subset of cells that have a higher expression which then decreases as the cells transition to PCs.

3.4.5 Percentage of positive expression of the niche factors in TGF-β condition

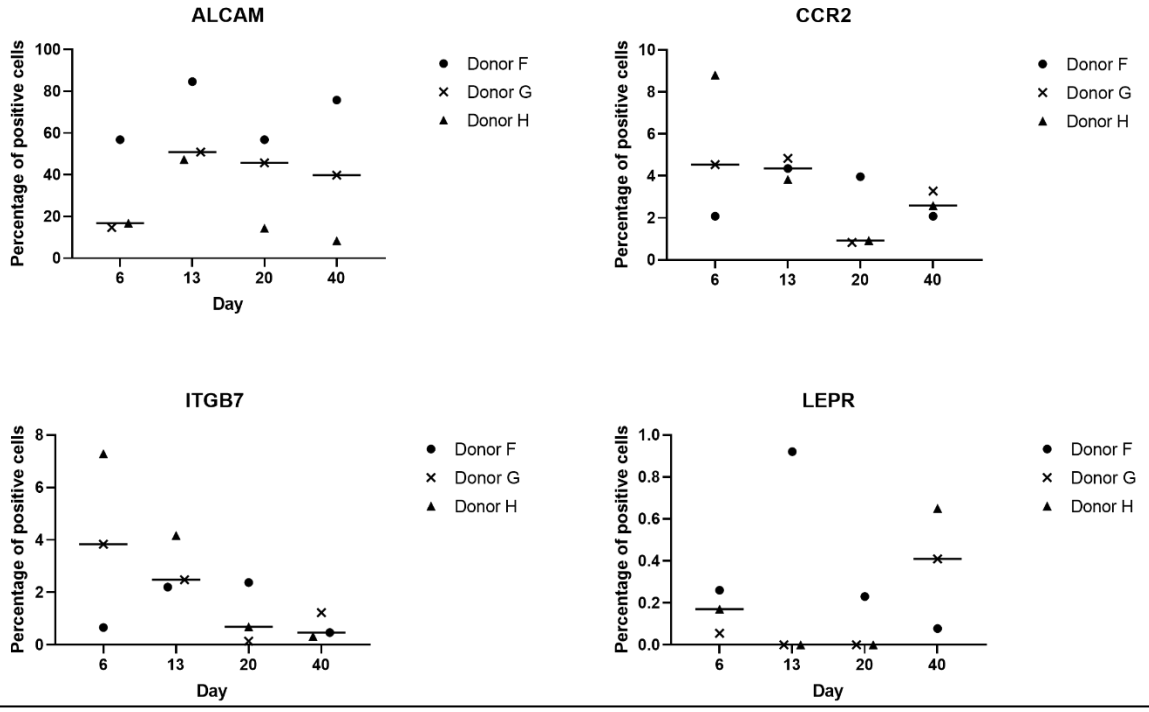

Figure 3.4.4 Percentage of positive expression of the niche factors with TGF-β stimulation

The percentage of positive cells from the parent population was calculated from the flow cytometry analysis using the matching isotype control for each time point. The table editor tool in the FlowJo software quantified the percentage of positive cells for each of the niche factors across the differentiation time course. The percentage for each donor is plotted across the time course of the B-cell differentiation in TGF-β conditions, for each donor the percentage is plotted individually. n=3

Expression of the niche factors in TGF-β conditions was summarised by calculating the percentage of positive cells compared to the isotype control. The isotype was matched for each donor at every time point across the differentiation time course. Similar patterns emerged for the expression of the niche factors with ALCAM oscillating between time points, which may be a due to the double peak and subsets of cells having high or low ALCAM expression or may be a consistent pattern of normal B-cell differentiation. Comparison of expression between all niche conditions for B-cell differentiation will give a clearer picture as the ratio of the populations of high and low

ALCAM expression not only varies between time points but between donors as well. The expression levels for LEPR and ITGB7 very low and at some time points undetectable, for ITGB7 expression levels were highest at day 6 which follows the shoulder of bright expressing cells seen in the histogram data. The quantification of positive expression between donors shows variation between the individual donors albeit the general trend shows there is a relatively standard expression pattern seen during the course of normal B-cell differentiation with TGF-β stimulation.

3.4.6 Long-term differentiation in IFN-α conditions

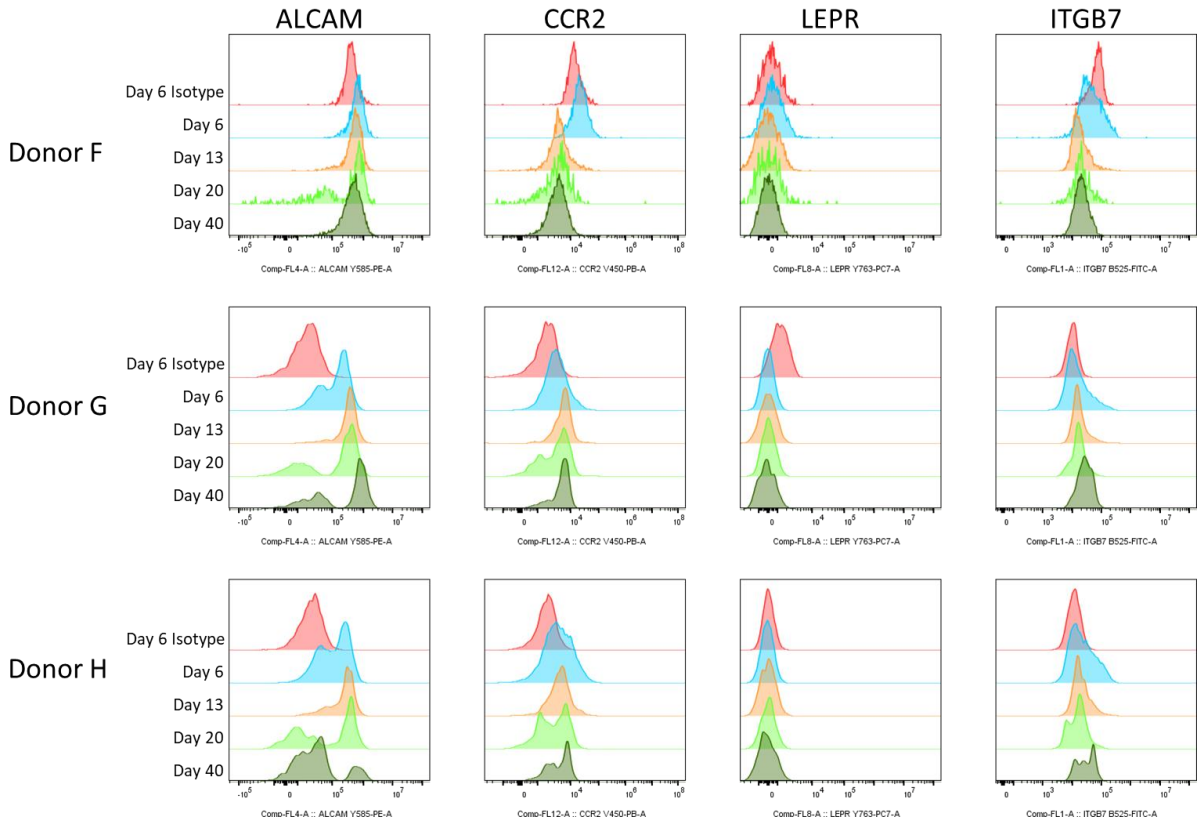

Figure 3.4.5 Pattern of niche factor expression with IFN-α stimulation
Memory B-cells isolated from blood cones from 3 donors were set up in IFN-α niche conditions and differentiated over a long-term time course to generate long-lived plasma cells using the *in vitro* differentiation system. At specific time points the expression of the niche factors were analysed by flow cytometry and expression plotted as histograms. n=3

Expression patterns of the niche factors were analysed when the cells had been differentiated in IFN-α conditions from the same donors as in the previous

experiments. Although there are double peaks for ALCAM expression the ratio of high to low expressing cells favours the high expressing cells apart from in donor H which has a large proportion of low expressing cells at the later time points of day 20 & 40. Although the pattern of producing a double population for ALCAM expression there is donor variability that show differences in the proportion of cells in the high and low subsets. Very low levels were then seen for the other niche factors, CCR2, LEPR and ITGB7. There is evidence of small subsets of cells that may have slightly higher expression indicated by shoulders of expression on the histograms. There is some variability between donors a direct comparison of stimulation condition will provide a better indication as to whether the patterns seen are a feature of differentiation or are dependent on the stimulation from the niche conditions.

3.4.7 Percentage of positive expression of the niche factors in the IFN-α condition

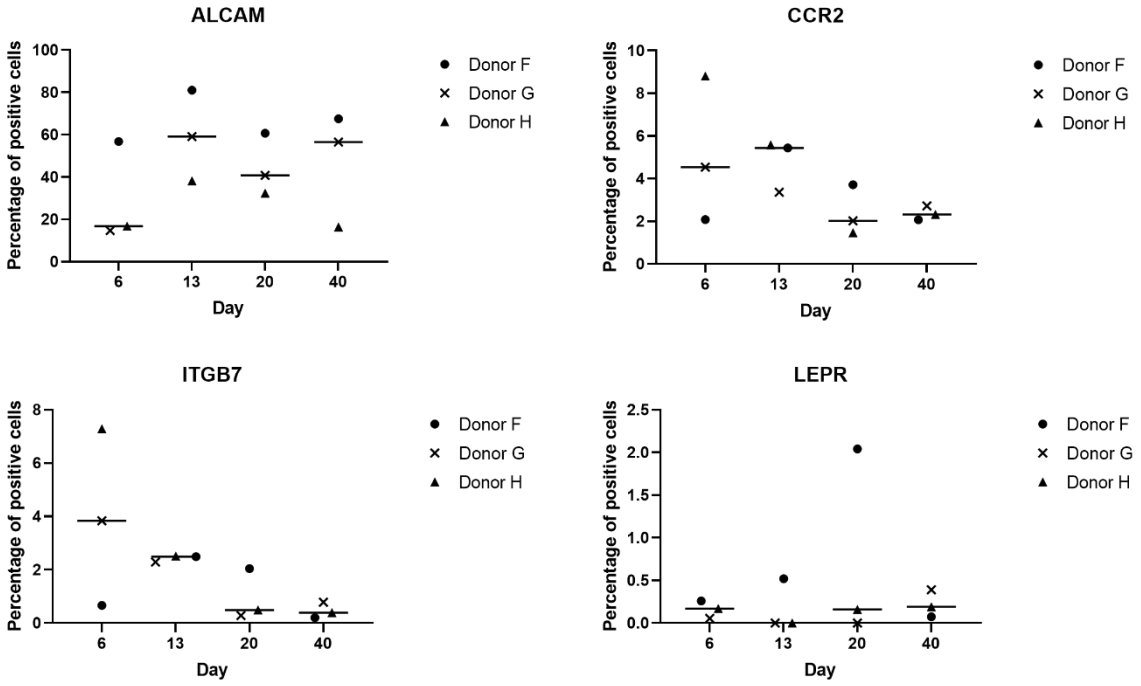

Figure 3.4.6 Percentage of positive expression of the niche factors with IFN-α stimulation

The percentage of positive cells from the parent population was calculated from the flow cytometry analysis using the matching isotype control for each time point. The table editor tool in the FlowJo software quantified the percentage of positive cells for each of the niche factors across the differentiation time course. The percentage for each donor is plotted across the time course of the B-cell differentiation in IFN-α condition, for each donor the percentage is plotted individually. n=3

The expression of the niche factors in IFN-α conditions form 3 donors was summarised by calculating the percentage of positive cells. The positive cells were gated using the isotype controls matched to each donor and time point. The same pattern of expression is seen as the other niche conditions tested albeit there are subtle differences see between the donors, its noted that the IFN-α condition has slightly higher levels of expression. There is a large spread between the donors in the IFN-α condition particularly on day 6 which may reflect on different stages of transition with

some cells moving towards the PC stage rapidly and others remaining closer to the B-cell state.

ALCAM expression shows the same oscillating pattern as the other two differentiation conditions, CCR2 expression is highest at day 6 and gradually decreases with one donor losing any CCR2 expression on days 20 & 40.

The donors show large variations in expression of ITGB7 at day 6 whilst all donors have little or no detectable expression at the two latest time points. From day 13 onwards LEPR expression is low but remains showing a slight increase and donor G is significantly higher at day 40. Again, there is an overall trend seen across the differentiation time course in the patterns of expression however there are differences between donors in the actual levels of expression of the niche factors.

3.4.8 Comparison of expression of adhesion molecules in different niche conditions

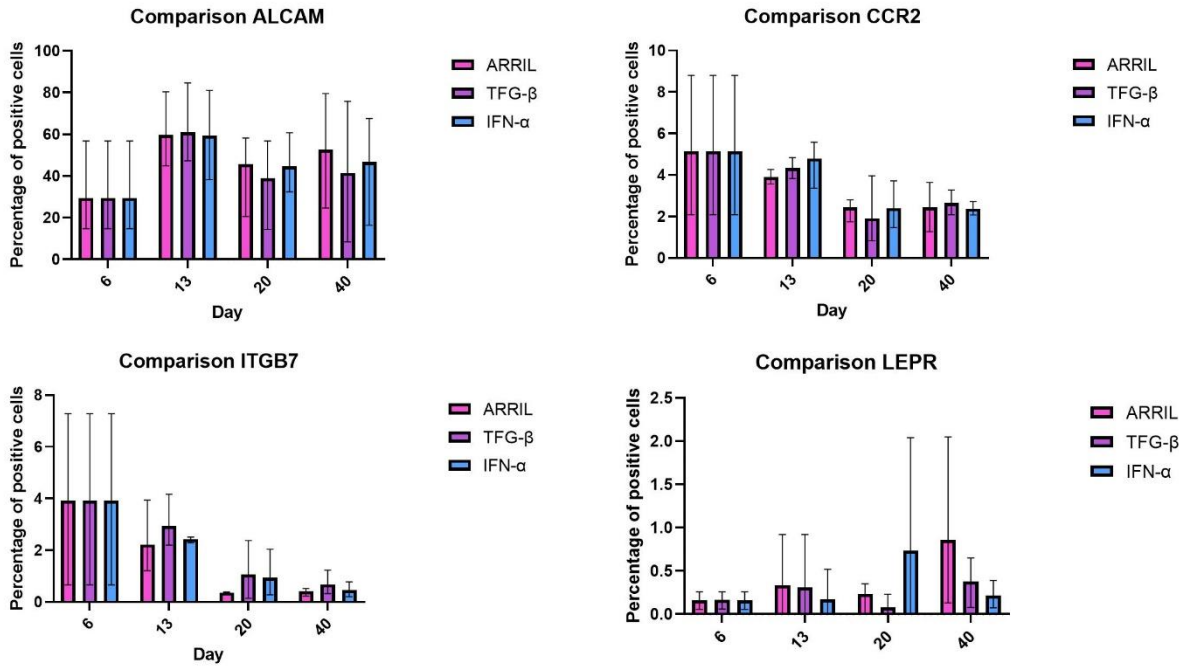

Figure 3.4.7 Comparison of niche factor expression in different niche conditions
The positive expressing cells seen by flow cytometry were quantified using the frequency of parent parameter calculated by setting a positive gate against the isotype control. The average percentage of positive cells of each niche factor from 3 donors was taken for each time point and compared between the 3 niche conditions (APRIL, TGF-β & IFN-α). The frequency averages are plotted for each of the niche factors, ALCAM, CCR2, LEPR & ITGB7 across the differentiation time course from day 6 to day 40, error bars indicate the range seen between the 3 donors sampled.

Memory B-cells from were differentiated in 3 separate niche conditions (APRIL, TGF-β & IFN-α) to compare the effect on the expression levels of the 4 niche factors. This was repeated in 3 donors to account for donor variability. The percentage of positive cells compared to the isotype was calculated and then an average taken from the 3 donors for each time point. Expression was then plotted for each of the niche factors (ALCAM, CCR2, LEPR & ITGB7) comparing the expression levels between the 3 niche conditions.

The general patterns of expression for each of the niche factors does not appear to be affected by the conditions used to generate long-lived plasma cells (APRIL, TGF-β or IFN-α). However, there is a difference in the intensity of expression between donors. ALCAM expression shows an oscillating pattern of expression between time points altering between a high and lower expression level throughout the differentiation. As mentioned previously this may be reflective of the changing ratio of cells in the 2 sub-populations as seen by the histograms. The ratio between these populations varies over the differentiation period and causes a skewing of the percentage of positive cells. As this change in expression is seen in all 3 donors and within all 3 niche conditions it appears to be a standard feature of normal B-cell differentiation.

The expression levels of CCR2 follow the same trend across the niche conditions with the highest expression on day 6 at the plasmablast stage and then decrease gradually at the later time-points as the cells differentiate into LLPCs. This pattern of expression appears to be consistent within normal differentiation and linked to the role CCR2 plays in homing and migration as LLPCs will home to the bone marrow and once residing within the bone marrow will be able to downregulate the levels of CCR2. LEPR expression is a juxtaposition to that seen for CCR2 and steadily increase as the cell become LLPCs, the error bars indicate that there is a large variation in expression seen between the donors. LEPR expression shows the greatest variation in expression between niche conditions, which may indicate that patterns of LEPR expression is due more to the donor than the conditions generating the PCs. The increase in expression as the cells become LLPCs is potentially linked to the bone marrow niche environment that the LLPCs would home to during normal differentiation.

The last niche factor, ITGB7 appears to have highest expression at day 6 which is better displayed as a histogram which reveals a shoulder of high expression. Then a low level of expression is maintained as the cells differentiate to PCs. Most expression is seen at day 20 and is highest in the IFN-α condition however this expression is a lot lower that the other niche factors that have been analysed. Overall, there appears to be a standard pattern of expression specific to the niche factors that is established during normal B-cell differentiation and unaffected by the niche condition the cells are stimulated in.

3.5 Changes of expression of adhesion molecules in malignant plasma cells

3.5.1 Surface expression in myeloma cell lines

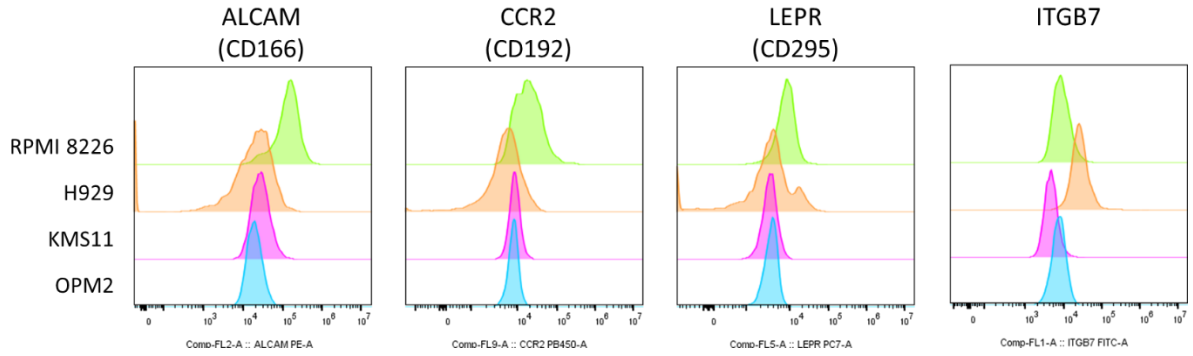

Figure 3.5.1 Niche factor expression on myeloma cell lines
Surface expression of the four niche factors was analysed by flow cytometry on four different myeloma cell lines (RPMI8226, KMS11, H929 & OPM2). Expression of the niche factors was plotted as histograms on the $CD138^{+}$ cell population, expression was set against an isotype control n=1.

The expression of the niche factors was a normal feature of B-cell differentiation and expression was unaffected by the niche conditions stimulating the transition to PCs. Next, we sought to determine if this pattern was seen in myeloma cell lines as a disease model. Although each niche factor had its own distinct pattern of expression these patterns were similar with each stimulation generating a surface phenotype on terminally differentiated PCs. I then tested whether this was sustained in the context of myeloma cells lines that originate from neoplastic PCs. Analysis of the surface expression of the niche factors on myeloma cell lines revealed that the RPMI 8226 cell line had the highest expression of each of the niche factors, except for ITGB7. Overall, the expression of ALCAM was high, particularly for the RPMI 8226 cells and for the other niche factors expression was consistent apart from ITGB7 which was higher in the H929 cells. For CCR2 expression the cell lines RPMI 8226 and H929 produced a shoulder of wider spread of expression compared to the other two cell lines. For LEPR and ITGB7 they both had similar levels of expression in each of the cell lines except

for the LEPR peaks in H929 cells having slightly broader expression and a small second peak.

Although there were marginal differences of expression between cells lines all cells had positive expression of each of the niche factors, of note these expression levels were higher on the log scale in comparison to the primary cells analysed previously, the results may indicate an upregulation of the niche factors in the myeloma cell lines as a model for disease state. Slight differences in ALCAM and CCR2 expression in RPMI 8226 and H929 cell lines compared to KMS11 and OPM2 may reflect differences in disease pathogenesis and prognosis.

3.5.2 Expression of ALCAM & CCR2 in malignant bone marrow samples

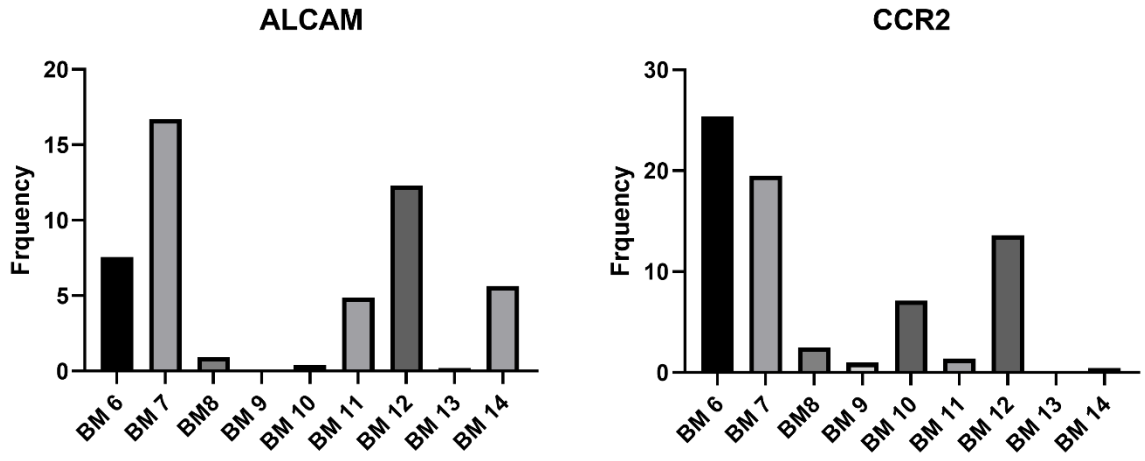

Figure 3.5.2 ALCAM & CCR2 expression in malignant bone marrow

Surface expression of ALCAM and CCR2 was assessed in an array of B-cell and PC populations from malignant bone marrow aspirates. Samples were prepared for flow cytometry by red cell lysis and the staining panel allowed for a gating strategy to positively gate the lymphocytes by size, exclude the T-cells via CD3+ expression and then the remaining PC population was assessed for ALCAM and CCR2 expression, these cells could be back gated using CD19, CD38 & CD138 within the staining panel.

As the surface phenotype of the niche residency factors appeared to show differences between the myeloma cell lines and that seen in healthy primary B-cells and PCs, it was decided to see what the pattern looked like in neoplastic PCs residing in the bone

marrow. Malignant bone marrow aspirates were collected from patients with a range of B-cell and PC neoplasms to assess what levels expression of ALCAM and CCR2 were present on the residing PCs. Red cell lysis was carried out and then the gating strategy used on the flow cytometry analysis on the remaining cell populations used FSC/SSC to positively gate out the lymphocytes followed by doublet discrimination and a live cell gate. CD3 negative populations were then assessed for ALCAM and CCR2 expression. The frequency of positive cells was calculated using the matched isotype control as a negative for background staining. The percentage of positive cells was plotted for each bone marrow sample on the PC population, other markers CD38, CD138 and CD19 were added to the staining panel to identify the population by back gating the ALCAM and CCR2 positive cells.

There was a large range of expression levels seen for both ALCAM and CCRs however it must be noted that there was a range of neoplastic samples analysed to attempt to identify any clustering of differentiation status or disease type using the niche factors to provide additional information for diagnosis or risk prediction. Due to the range of neoplasms tested there is a large range in PC composition expected to be seen therefore making it difficult to draw any direct conclusions (see (Appendix 3.7.1). This is just preliminary look at surface phenotype of these niche residency factors and revealed that the variations seen in the PCs population phenotype is in contradiction to that seen in the primary healthy samples.

Although there were subtle differences between the donors there was an overall trend, for ALCAM there was oscillation and therefore was less surprising to see the variation in surface expression, whereas CCR2 expression in the primary donors there was a shoulder of high expressing cells then maintained at a constant level to LLPCs. There were large differences in the expression levels of CCR2 between the malignant samples and given the role CCR2 play in homing and migration this may represent cells that are transitioning from migratory to localised or vice versa from the bone marrow.

3.6 Discussion

Adhesion and cell-cell interactions in a response to niche signals is essential for plasma cell (PC) survival. Several lines of evidence point to the fact that this dependence is maintained in plasma cell neoplasia, particularly in the early phases of

disease. Plasmacytoma is an example of such an indolent neoplastic phase. In this chapter the experiments presented were focused on exploring the expression pattern of a set of adhesion molecules and niche factor receptors that were preferentially expression on plasmacytoma.

The initial focus was on determining whether the pattern of preferential expression observed in plasmacytoma was or was not a general feature of physiological PC differentiation. To address this a model system of *in vitro* differentiation was used to track the maturation of B-cells to mature into quiescent PCs. The data presented make the argument that while each of the niche factors is regulated during PC differentiation, the pattern of regulation for each factor is distinct.

ALCAM expression consistently shows a split in the cell population in the differentiation system in all stimulation conditions (APRIL/TGF-β/IFN-α) indicating a subset of cells with high ALCAM expression and a subset with low expression. Following the expression levels across the time course of the differentiation shows that the proportion of cells within these subsets oscillates in a manner that does not fit with mRNA expression levels or linked to the stages of differentiation i.e activated B-cell, plasmablast or LLPC. Therefore, there must be another method of regulation at the protein level rather than expression being controlled through transcription, to account for the oscillating expression pattern.

ALCAM has been suggested to have a role in extravasation and migration, therefore there needs to be a mechanism for up- and downregulation of surface expression, evidence of cleavage by ADAM sheddases of ALCAM has been reported using Raji and Jurkatt cells. Cleavage of ALCAM by ADAM17 was shown to be regulated by CD9 and co-localisation (Gilsanz et al., 2013), using a regulated mechanism that can dynamically alter the level of adhesion molecules will play an important role in disease pathogenesis by having the ability to migrate and metastasise. Where higher levels of ALCAM are seen this could be due to inhibition of ADAM cleavage reducing the risk of cells migrating and spreading, higher levels of ALCAM were seen in EMPs compared to PBL samples which may reflect a reduced capacity to migrate and therefore EMPs have a more favourable prognosis.

ALCAM has also been linked with cellular adhesion in MM within the bone marrow (BM) microenvironment, with MIF acting through ALCAM as a surface receptor on MM

cells (Zheng et al., 2016). Through the inhibition of MIF MM cells appeared to be more responsive to chemotherapy, possibly due to changes in cellular adhesion. It has been reported to have high expression in multiple myeloma cell lines. When ALCAM was silenced in *in vivo* models there was less tumour burden and osteolytic lesions as well as better cell survival (Xu et al., 2016). This suggests that ALCAM is a driver of multiple osteolytic disease in the progression of MM.

Overall ALCAM has been shown to have a role in adhesion and homing specifically in the bone marrow and in some instances be a driver of bone lesions and osteolytic disease. The pattern of expression observed in the *in* vitro model argues strongly that ALCAM is subject to dynamic and most likely a post-translational regulatory process in the control of adhesive and cell membrane phenotypic properties of PCs, which may play a role in acutely regulating niche residence by increasing or decreasing adhesion receptors. Investigating how this adhesion molecule may influence homing and localisation between normal B-cell differentiation and disease settings may highlight potential pathways that can be disrupted to aid treatment plans.

The pattern of CCR2 expression decreases as the cells move through the differentiation process and is maintained at a low level from day 13 onwards. The levels of CCR2 expression in myeloma cell lines showed heterogeneity between the cell lines with RPMI 8226 cells having high expression and wide spread of expression along with H929 cells. Whereas the other two cell lines produced a narrow peak indicating a homogeneous cell population with a low level of expression.

In other studies, the expression of CCR2 on MM cells revealed that down-regulation of CCR2 on the MM cells is indicative of a poorer outcome. With low levels or loss of CCR2 MM cells are not retained in the bone marrow and can migrate into the peripheral blood (Vande Broek et al., 2003; Vande Broek et al., 2006). Noticeably in our differentiation model expression of CCR2 was highest at day 6 and then decreased to a constant level being maintained in PCs, therefore low expression on MM cells is in line with this expression and if CCR2 drops below normal levels they lose the ability to respond to CCL2. The presence of MM cells in peripheral blood has been seen with disease progression, this could be explained by loss of adhesion to the stromal support or the development of stroma independent MM cells.

Along with the role in migration and homing, CCR2 is a GPCR so has signalling properties. Activation of CCR2 through MCP-1 signals through the MAPK pathway to activate ERK. Activation of ERK is thought to lead to integrin activation and chemotaxis (Jiménez-Sainz et al., 2003). Further investigation into the signalling potential of CCR2 as highlighted expression in cancer cells enhances metastasis, extravasation, and homing of CCR+ monocytes that can provide tumour support. Not only is ERK activated through CCR2 signalling but also JAK/STAT and p38 signalling pathways (Wolf et al., 2012). For a tumour to progress following invasion to a new niche requires support from surrounding cells and stroma, evidence for MCP-1 expression recruiting immune cell support has been reported along with recruitment of myeloid suppressor cells that will aid immune evasion (Huang et al., 2007). Taken together this evidence suggests that CCR2 along with MCP-1 expression by MM cells and other neoplastic B-cells can lead to migration as well as maintaining stromal support following invasion.
LEPR expression did not show much contrast between primary differentiating B-cells and the myeloma modal due to the low expression detected by flow cytometry. This could be explained as an experimental issue if the antibody had low efficacy, however mRNA analysis also showed low levels of LEPR expression. There is a general trend that there is a gradual increase in LEPR expression, albeit at a low level, throughout the differentiation, the same upregulation is seen at the gene level from RNAseq data. MM cells often reside close to bone marrow adipose tissue suggesting potential signalling between the two, also to be considered is the impact having high adipose tissue within the bone marrow as on the bone. Increased levels of adipose tissue puts further pressure on the bone leading to stress and fractures that can be occupied by MM cells and lead to disease progression from MGUS (McDonald et al., 2017; Morris and Edwards, 2018). LEPR may therefore act as a prognostic marker to aid the likelihood of disease progression.
ITGB7 expression levels were also very low from flow cytometry analysis which contrasts with the gene expression which showed high expression. It is not unusual for gene expression to be higher that protein expression due to post-translational factors such as trafficking to the surface or shedding from the membrane that could account for lower levels. It may need to be considered that low expression is due to a lack of a co-receptor, as integrins typically form dimers. A decrease in expression of

ITGB7 post-day 6 when cells are transitioning from PBs to PCs seems to be a feature of normal B-cell differentiation. Another possibility for the difference in levels of expression between mRNA and protein is that there upregulation early in the differentiation and the shoulder of high expression at day 6 represents late upregulation with the cell population being more heterogeneous at this stage.

ITGB7 in MM is overexpressed due to either the genetic translocation (t14;16) or due to paracrine stimulation through BAFF/TACI/APRIL signalling (Morito et al., 2011), therefore could be used as a marker for poor prognosis. ITGB7 knockdowns showed loss of adhesion ability of MM cells to fibronectin and human BMSCs, suggesting a role in MM survival in the BM microenvironment (Neri et al., 2011). Other knockdown experiments or blocking ITGB7 in MM adhesion in MM cell lines resulted in reduced ability to invade into Matrigel as well as reduced ability to move along the CCL12 (SDF-1) gradient showing a role for ITGB7 in MM for migration and invasion (Bianchi et al., 2012). A difference between ITGB7 on healthy and MM cells has been identified in that ITGB7 is maintained in the active conformation on MM cells (Hosen, 2020). MM cells that have a continuously active ITGB7 are likely to lead to disease progression and metastasis.

In conclusion the data shows that there is a specific pattern of expression for each of the four niche factors. This pattern is established and maintained during B-cell differentiation and is irrespective of the niche condition that the differentiation is stimulated in. Expression patterns in the myeloma cell lines which were used as a disease model showed reduced protein expression of the niche factors when assessed by flow cytometry. Surface expression was a log lower than the expression seen in the LLPCs generated in the long-term differentiations. Although here the niche factors have been looked at on an individual level and not for possible co-regulation or co-expression, taken together it seems that the myeloma model has a downregulation of the niche factors and is a model of a dispersed aggressive disease in contrast to an isolated EMP which has an upregulation in gene expression for the niche factors and consistent with a normal PC differentiation.

3.7 Appendix

3.7.1 Bone marrow samples

Table 3-1 Bone marrow samples

Sample ID	Diagnosis
BM4	Monoclonal gammopathy of undetermined significance (MGUS)
BM5	MDS treated <5% blasts (regenerating marrow post treatment)
BM6	Reactive marrow
BM7	Plasma cell myeloma
BM8	CML chronic phase
BM9	Reactive marrow
BM10	Reactive marrow
BM11	No evidence of disease (regenerating marrow post treatment for AML)
BM12	Plasma cell myeloma
BM13	Plasma cell myeloma
BM14	Plasma cell myeloma

Table 5: List of bone marrow samples. Sample ID and corresponding diagnosis from the diagnostic service following flow cytometry

4 Combinatorial expression of Protocadherin-gamma isoforms have distinct patterns of expression and epigenetic regulation

4.1 Introduction

The initial comparison made between EMP and PBL identified the protocadherin-gamma (PCDH-γ) locus as being upregulated in EMP as part of an adhesion signature. The clustered protocadherin (PCDH@) loci (alpha, beta gamma) are unique locus amongst adhesion molecules, because the epigenetic control of isoform expression can generate high degrees of diversity on the cell surface. Combined with a specific mode of cell surface interaction which has been modelled on the idea of a zipper structure, the combinatorial control of PCDH isoform expression had been proposed to provide a basis for single cell identity codes. We have found evidence of selective epigenetic regulation of the protocadherin-gamma (PCDH-γ) loci in B-cells.

The epigenetic pattern is consistent with that seen in neurons where it is associated with stochastic expression of the PCDH-γ isoforms, of which there are 22 different members. In general, 1-2 variable and 1 constant exon is thought to be expressed from each allele which gives a large diversity for the surface phenotype that can be established. A simplistic calculation the number of combinations that can be produced is in the range of 8000-12000 based on combinations of 4 variable exons from a choice of 22, with or without repetition allowed. The isoforms are similar in structure and only vary in the extracellular domain due to the variable exon coding. As detailed previously the protocadherins interact in a homotypic fashion via a zipper-like structure to mediate homotypic adhesion or repulsion forces depending on cellular context. The hypothesis therefore is that a combinatorial pattern of PCDH-γ expression creates a unique surface barcode that can influence cell-cell adhesion in a homotypic fashion. The number of potential combinations of PCDHs on the cells surface generates a high level of diversity and the potential to provide identity codes for distinct PC populations.

The mechanism for promoter choice of the variable exons characterised in the nervous system identifies a DNA looping mechanism that brings together the enhancer and promoter coding for one of the variable exons. This mechanism uses CTCF/cohesion complex to bind at accessible sites and bring together forming a DNA loop. Here we

show evidence that B-cells may use a similar mechanism for promoter choice generating combinatorial expression of the PCDH-γ locus on the cell surface.

Currently protein expression of the PCDH-γ locus has not been investigated and whether the surface phenotype may be able to provide identity patterns. The pattern of expression will be investigated throughout the stages of B-cell differentiation to elucidate at what stage protein expression established. RNA expression suggests expression is first seen to increase at the plasmablast stage at low levels. Then a significant increase as the cells transition to PCs at day 13 of the differentiation. The question that needs to be addressed is whether expression is maintained providing evidence for a predetermined pattern at an epigenetic level or something that is subject to post-translational and external cues, such and survival signals and niche factors.

4.1.1 Functional role of the PCDH-γ cluster

In the nervous system the role of the PCDHs has been described as homotypic repulsion to matching combinations of PCDHs to avoid the formation of synapses with self-dendrites. In B-cells however it is thought that the PCDHs will result in homotypic adhesion and PCs with identical combinations of PCDHs will adhere forming a zipper-like structure. It has been suggested that there is some level of tolerance for mis-matching combinations and the type of interactions seen. It is not known how many PCDHs a single B-cell expresses therefore assessing the expression of a limited number of individual isoforms will be proof of principle that there is surface expression seen and that expression is not uniform across the entire PC population in an individual.

The hypothesis is that PCDHs will play a role in adhering to neighbouring PCs within the bone marrow niche and restricting interactions depending on the combinatorial surface expression. This may lead to infiltration at a site of infection and inflammation or retention of PCs within the bone marrow depending on whether there is homotypic adhesion or repulsion as a result of matching surface patterns. To date this has not been investigated but the first step in this process is to establish what expression looks like in B-cells and PCs, whether this links between epigenetic activation marks and expression seen in mRNA to the surface protein expression and the functional impact this may have. Functional experiments such as targeted deletion of specific PCDHG

isoforms to see what impact this has on cell survival, state and adhesion are needed to start to characterise the role the PCDHG locus and combinatorial expression has in B-cell biology.

4.1.2 Role of PCDH expression in malignancies

Focusing on the adhesive properties of the PCDHs and the identity codes that they create on single cells, the pattern of expression may influence tumour formation and survival in the niche environment. The PCDH-γ locus was found to be upregulated in plasmacytoma compared to PBL, therefore there may be a pattern of expression of PCDHs on PCs that leads to the formation of isolated monoclonal tumours.

PCDHs have been associated with some forms of cancers, the expression of PCDH-γ can down-regulate signalling through the Wnt signalling pathway and has been found to associate with β-catenin and possibly other cancer associated proteins (Mah and Weiner, 2017). In general the PCDH-γ cluster appears to be silenced in cancers which leads to the idea that PCDH-γ proteins act as tumour suppressors (El Hajj et al., 2017). In gastric cancer PCDHGA9 has been shown to be down-regulated compared to normal tissue and implicated in disrupting Wnt signalling via inhibition of β-catenin translocation to the nucleus. Overexpression of PCDHGA9 leads to reduction in cell migration and an induction of apoptosis and autophagy (Weng et al., 2018). Together this evidence suggests that the PCDH-γ sub-family appear to play a role in tumour suppression and are often down-regulated in cancer, as well as proving to be potential prognostic markers.

The current literature does not fully elucidate the role PCDHs play in disease progression and pathogenesis but has made links to downstream signalling pathways and cell survival. Investigation into the adhesive role the PCDH-γ proteins play in tumour development has not been studied in much detail. Preliminary data shows a difference in the expression levels of PCDH-γ mRNA between EMPs and PBLs. These malignancies vary in prognosis and phenotype which indicates that an upregulation of the PCDH-γ locus in EMPs is beneficial. When comparing the phenotype of these malignancies EMPs present as a cohesive, isolated tumour therefore we hypothesise that PCDH-γ expression may not only provide single cell identity codes in B-cells but also influence adhesion of neoplastic PCs.

4.1.3 Aims

Expression and epigenetic data provide evidence for selective PCDH-γ regulation during B-cell differentiation. However, to support a model in which this regulation and expression has functional significance a key step is to provide definite evidence of protein expression. The aim was therefore to investigate the surface expression of the PCDH-γ proteins, and to determine to what extent this surface phenotype may be able to provide identity patterns. Another question to be addressed is once the pattern of expression is established is it maintained providing evidence for a predetermined pattern of expression at an epigenetic level or something that is regulated by external cues, such and survival signals and niche factors. A comparison will be made between the expression levels seen in primary differentiating B-cells from healthy donors and those from malignant patient samples covering a range of B-cell and PC neoplasms, this will allow for the comparison of expression levels between differentiation states.

This chapter aims to elucidate the expression patterns of the PCDH-γ locus on B-cells and demonstrate the unique mechanism of epigenetic regulation and promoter choice. There is evidence to indicate that this mechanism of epigenetic regulation is active in B-cells and PCs, and we aim to investigate if this translates to the surface phenotype of combinatorial expression of the PCDH-γ isoforms.

4.2 Epigenetic regulation of protocadherin-γ gene cluster in differentiating B-cells

4.2.1 Differentiating B-cells and PCs express the PCDH-γ locus

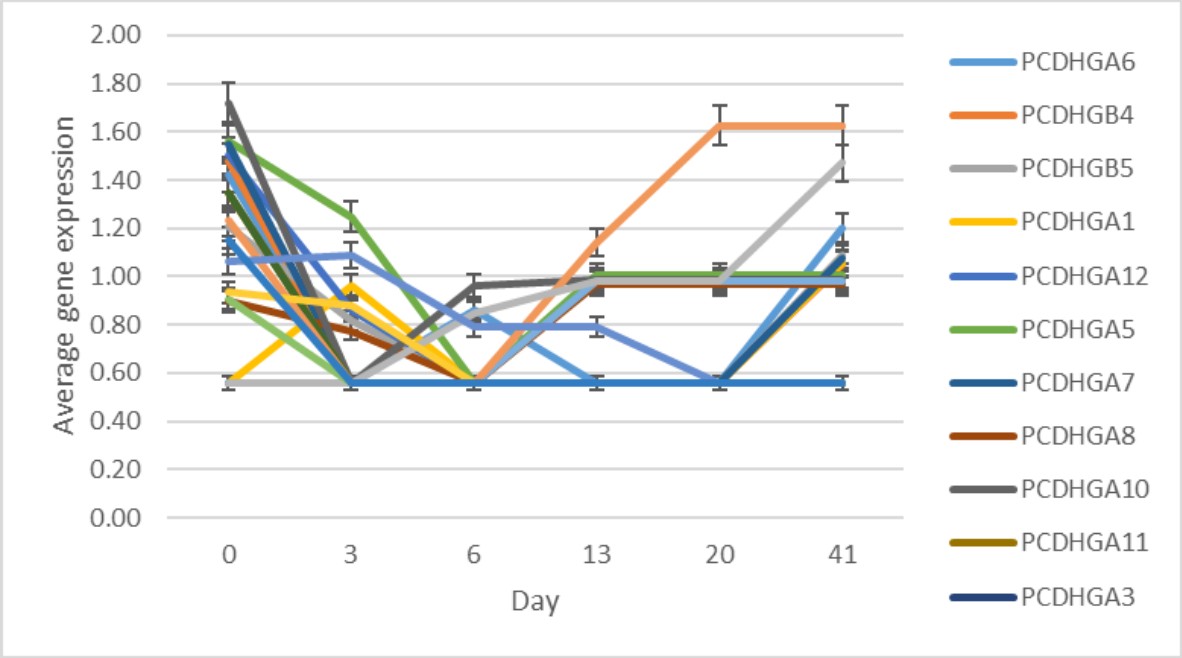

Figure 4.2.1 Expression of the PCDHG locus in differentiating B-cells
RNA-sequencing was performed on differentiating B-cell and PCs from 3 healthy donors. B-cells were isolated from peripheral blood samples and cultured using the *in vitro* differentiation system to generate PCs and LLPCs. RNA was taken at regular time points starting at day 0 and finishing at day 41. RNA-seq was performed on these RNA samples and the expression was taken as an average of the 3 donors and plotted for the individual *PCDHG@* isoforms. Error bars shown as a percentage (Mario Cocco & Matthew Care)

The starting point for investigating the expression if the *PCDHG* loci in B-cells and PCs started with RNA-sequencing of PCs and LLPCs generated in the *in vitro* system to differentiate the B-cells in culture. RNA-seq was performed in samples from 3 healthy donors taken at day 0 of the culture through to the final time point at day 41, this allows for the mapping of expression throughout the different stages of differentiation and in LLPCs. Expression was taken as an average of the 3 donors and plotted individually for each *PCDHG* isoform that revealed a drop in expression from day 0 to day 6. From day 6 onwards in the system, expression increased sharply at day 13 for most of the isoforms, particularly *PCDHGB4* and *PCDHGB5.* This shows that expression is highest once cells are fully differentiated PCs compared to cells that are in the earlier stages of differentiation. With this evidence of RNA expression of the *PCDHG* loci in

PCs further exploration into indications of epigenetic control of this locus, similar to that seen in the nervous system, will be assessed using ATAC-seq and ChIP-seq data (Amel Saadi & Mario Cocco)

4.2.2 Open chromatin over PCDH promoter sites in plasmablasts

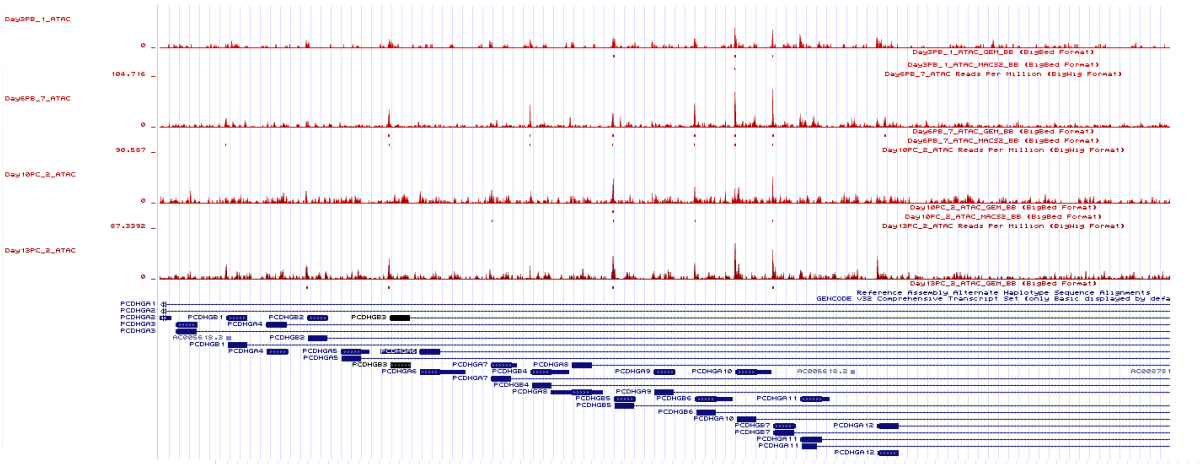

Figure 4.2.1 Accessible chromatin over the promoter sites in primary differentiated plasmablasts

ATAC-seq was performed on differentiating B-cells generated using the *in vitro* differentiation system from 4 donors. ATAC binding to open chromatin indicates accessible sections of the genome that are open to be transcribed, binding is indicated by the peaks and the positioning over the PCDH promoters is shown in blue (Amel Saadi).

Following the RNA-sequencing that shows B-cells and PCs express the *PCDH-γ* locus, investigation into control over this expression via a similar mechanism to that in the nervous system was assessed from existing ATAC-seq data (Amel Saadi). ATAC-sequencing reveals sections of the genome where the chromatin is relaxed and therefore accessible to transcription factors and other transcriptional machinery. Peaks indicate where these sites of accessible chromatin are in the genome and using the genome browser to zoom in over the *PCDH-γ* locus shows that there is accessible chromatin that maps over the promoters for the *PCDH-γ* isoforms. The rows show data from 3 separate donors at the plasmablast stage, the distribution and size of the peaks were comparable between donors. ATAC-seq provides the first step in indicating at a molecular level in plasmablasts, chromatin is accessible to allow for the expression of

individual PCDH isoforms. If the same mechanism were to be used for promoter choice as seen in the nervous system, then having open chromatin over the promoters and enhancer provide the first indication that a similar mechanism of complex binding and DNA-looping could be possible in B-cells and PCs. Further investigation into the binding of the protein components of the CTCF-cohesin complex and other activation marks would further indicate that the same mechanism as described by Maniatis *et al.* may also be used in B-cells (Canzio et al., 2019).

Highlighted are the three PCDHG isoforms, PCDHGA6, PCDHGB4 & PCDHGB5, which are investigated for protein expression later which had commercial antibodies available. Although these isoforms were not the most highly modified of the PCDHG family there is evidence of accessible chromatin and therefore the potential for expression.

4.2.3 ChIP-seq data showing CTCF binding in plasmablasts

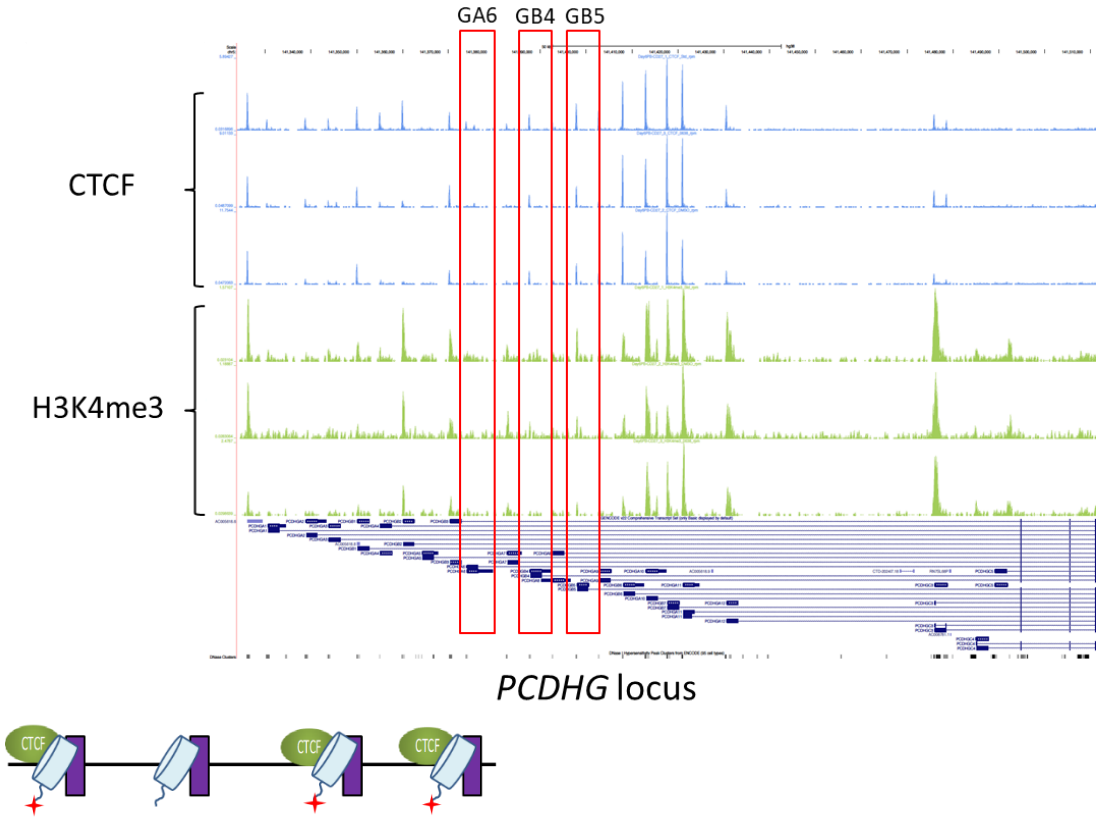

Figure 4.2.3 CTCF binding at PCDHG promoter sites
ChIP-seq was carried out on differentiating plasmablasts to reveal the locations of CTCF binding and active histone mark H3K4me3 (courtesy of Mario Cocco & Matthew Care). The PCDHG locus was viewed on the Genome browser revealing peaks over many of the promoter sites for the PCDH isoforms. Highlighted are the three isoforms investigated in more detail analysing their protein cell surface expression. CTCF binding is shown in blue for 3 separate donors and the H3K4me3 marks are shown in green. Below the peaks is a schematic of CTCF and H3K4me3 binding on active promoters, indicating which variable exons on the PCDHG locus will be transcribed.

ChIP-seq analysis was performed prior to the start of this project on plasmablasts from three healthy donors. The data reveals binding of CTCF at promoter sites along with active histone mark, H3K4me3. Zooming in on the PCDHG locus using the genome browser allows the binding to be seen over the variable exon promoters encoding the

22 members of the gamma locus. Peaks are seen for both CTCF binding and H3Kme3 binding that are positioned over the promoter sites encoding the different PCDHG isoforms. This reveals that in primary plasmablasts there is activation over the PCDHG locus and evidence of epigenetic regulation. The mechanism of promoter choice of the variable exons to be transcribed is achieved through DNA looping, bringing together the HS5 enhancer and the active promoter. DNA looping is created through CTCF binding proximal to the PCDH promoter and binding in the reverse direction at the enhancer this allows for the formation of the CTCF/cohesion complex. Evidence of epigenetic regulation in B-cells indicates the same mechanism of regulation as described by (Canzio et al., 2019) for the alpha locus, although there is no evidence of lncRNA initiating the CTCF binding for the gamma locus the principal of DNA looping likely follows the same methods as described here.

Having a mechanism for stochastic promoter expression means that there can be a combinatorial pattern of expression of PCDHG proteins being expressed. The combinatorial expression in the nervous system is a unique strategy of homotypic repulsion controlling adhesion and synaptogenesis. Identifying the same epigenetic regulation in plasmablasts suggests the unique patterns of expression may be present on the cell surface of PCs and influence their adhesion, it is predicted that the combination of surface PCDHs will lead to homotypic adhesion. Currently it appears that there is only a very low level of expression on the PCs, and it is unknown how many PCDH proteins are expressed by a single PC cell.

4.2.4 mRNA expression of PCDH-γ isoforms GA6, GB4 & GB5

There is evidence for epigenetic regulation of the PCDH-γ locus in B-cells. On the one hand mRNA expression is observed during in vitro differentiation and in ex vivo populations of lymphocytes. Notably mRNA expression increases after the activated B-cell stage (day 3) of the *in vitro* differentiation and is maintained to the PC stage.

A range of epigenetic and accessibility data generated in the lab that I have analysed at the PCDHG@ loci point to epigenetic control, it is not clear at which day the pattern of PCDH-γ expression is established through epigenetic promoter choice as the

individual levels of each isoform vary between time points as to which isoform is the most highly expressed.

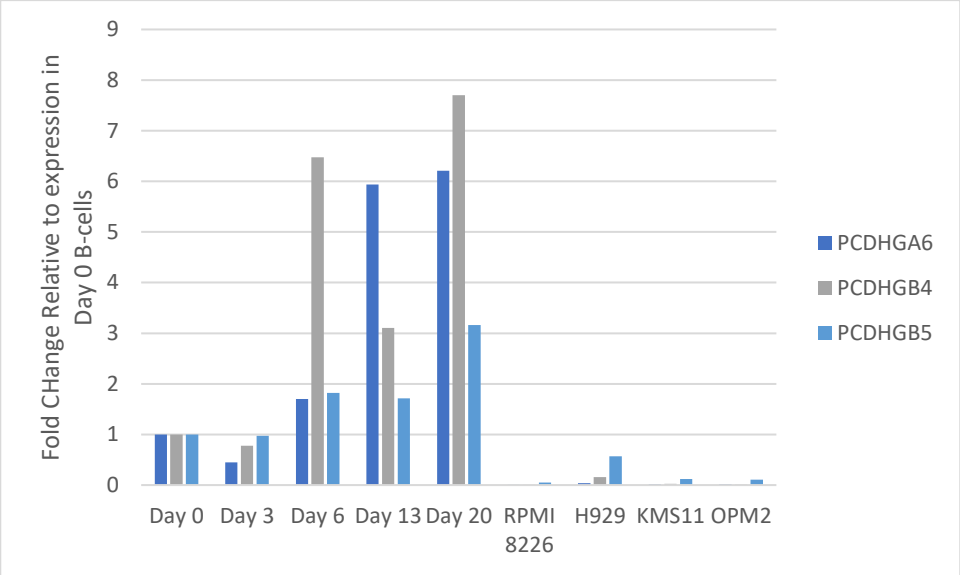

Figure 4.2.4 mRNA expression of PCDHG isoforms in differentiating B-cells and myeloma cell lines

qPCR analysis of PCDH-γ isoforms *PCDHGA6, PCDHGB4 & PCDHGB5* mRNA levels in primary differentiating B-cells and myeloma cells lines. A 1:2 dilution was made of cDNA that was loaded per sample and ran in duplicates. Expression is shown as an average of the two technical replicates for each sample and standardised relative to the expression levels of the day 0 samples from naïve B-cells. n=2

Expression levels are shown relative to the expression seen at day 0 naïve B-cells, which was chosen as the basal expression level of the PCDH-γ locus. An issue was that absolute expression of *PCDHG* isoforms appears low and therefore standard housekeeping genes are expressed so highly in comparison that any differences in fold change between the isoforms is difficult to determine with confidence in qRT-PCR. However, patterns are substantiated in the RNAseq data which highlights the possibility that the issue stems from the sensitivity of the assay. Expression levels for the myeloma cells lines in comparison with the primary B-cells may reflect the data obtained for EMPs and PBL samples that showed there is a down regulation of adhesion molecules in PBL samples which is a more aggressive disease with a

migratory phenotype. From this qPCR analysis it indicates that myeloma cells also have down regulated the niche factors which may be an indicator of an aggressive and dispersed pathogenesis.

4.3 Methods for investigating the protein expression of the protocadherin-γ isoforms

4.3.1 Trial of western blotting antibodies on myeloma cell lines

Table 4-1 Trialled western blotting antibodies

GA6	Invitrogen	x
GA6	Genetex	√
GA9	Invitrogen	x
GA10	Sigma Aldrich	x
GA11	Sigma Aldrich	x
GA12	Sigma Aldrich	x
GB4	Genetex	√
GB5	Genetex	√

Table 4. List of commercial antibodies tested for the PCDH-γ isoforms, the manufacturer and whether they were successful at detecting the protein at the correct molecular weight.

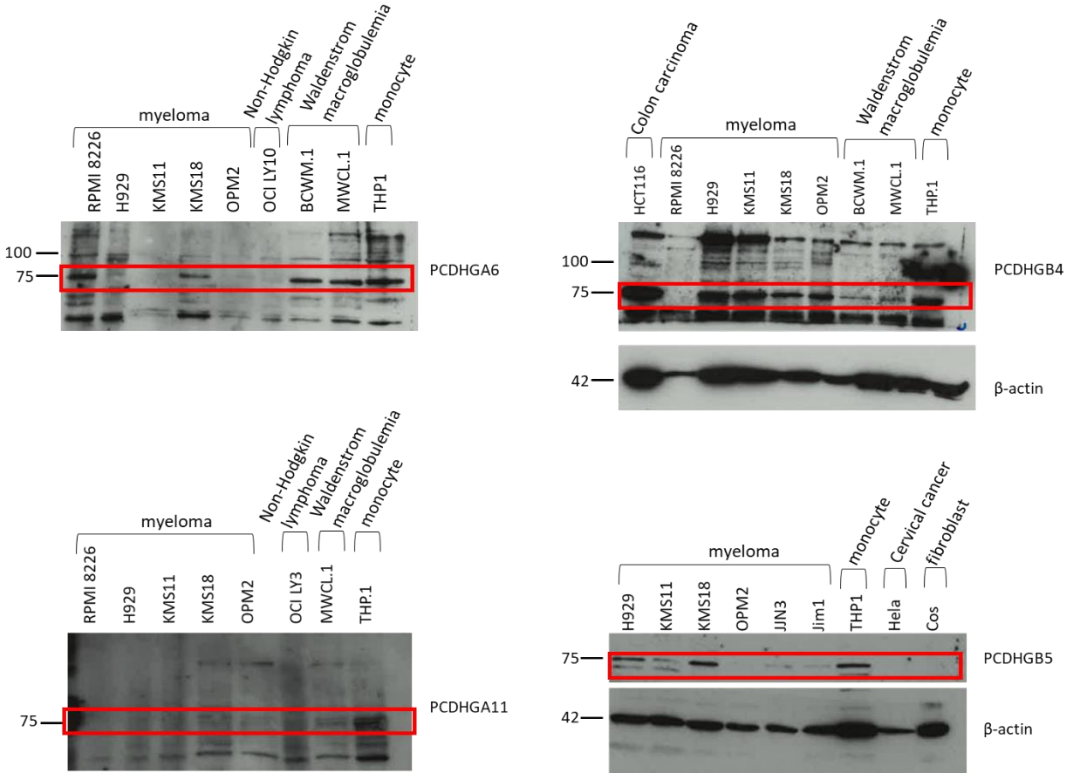

Figure 4.3.1 Protein expression of PCDHG isoforms in myeloma cell lines
Western blots trialling the commercial PCDH-γ antibodies available that produced a band close the expected weight of 75kDa in of a range of myeloma cell lines as well as monocyte and adherent cell. Top left-PCDHGA6 (Genetex) Bottom left-PCDHGA11(Sigma). Top right-PCDHGB4 (Genetex) Bottom right-PCDHGB5 (Gentex). β-actin used as a loading control.

A notable feature of the overall PCDH literature is the paucity of direct protein expression assessments of endogenous protein. There is evidence from IF and or IHC, and some western blots particularly of overexpressed protein, and there is strong evidence of mRNA expression and the importance of the locus from gene targeted mice. However direct evidence of native protein expression by western blot and flow cytometry is considerably sparser.

In part this lack of assessment may reflect a sparsity of reagents. There are very few commercial antibodies available for the PCDH-γ isoforms that produced a band around the correct molecular weight of 75kDa. Often the antibodies detected multiple

bands making it difficult to know which band was specific and whether the smaller bands were a results of proteolytic cleavage events. Another difficulty is that each isoform has the same predicted molecular weight, most likely due the similarity of the structure of the PCDHs which only differ with their variable exon encoding the extracellular domain, however variable glycosylation may impact on detected protein size.

I tested a wide range of antibodies (see Table 4.). My overall ideal strategy to identify specific antibodies was to identify antibodies that 1) detected protein of an expected size in one or more of a panel of cell lines ranging from myeloma and B-cell lymphomas to cells lines used as positive controls of the antibody data sheets. 2) detected an over-expressed protein of suitable size, 3) showed knockdown of the endogenous protein band, 4) allowed detection of expressing and non-expressing populations by flow cytometry in a polyclonal PC population. Of these approaches knockdown failed to generate any meaningful results and over expression was limited to a single isoform. Therefore, my eventual strategy became primarily dependent on detection of an appropriate band size by western blot and distinction between expressing and non-expressing cell populations by flow cytometry using appropriate negative controls. For flow cytometry the negative control was a secondary only sample to aid with distinction between specific and non-specific staining. Given that the antibodies are not always validated across multiple modalities the eventual approach though not ideal was deemed to be adequate to provide the first insight into the levels and expression pattern of endogenous PCDHs.

Of the antibodies tested only 4 produced bands close to the predicted molecular weight of 75kDa. The cleaner blots producing distinct bands were from Genetex (GA6, GB4 & GB5). The bands produced at 75kDa and 100kDa are indicated as being PCDH-γ specific and the difference in size can be explained by post-translational modification such as glycosylation, as well as the larger bands that may be due to dimers that may not have been fully dissociated. There are non-specific bands at smaller molecular weights that may be due to proteolytic cleavage however further investigation would be required to investigate and characterise each of the non-specific bands.

Overall, variation in the levels of PCDH-γ isoforms expression was observed between myeloma cell lines. For example, KMS18 showed strong expression of several proteins and others nearly no detectable protein while other cell lines varied in expression between the isoforms (GA6, GB4 &GB5). The monocyte cell line, THP.1 acted as a positive control for each of the 4 antibodies tested above. In contrast, HeLa and Cos cells were negative for PCDHGB5 expression at 75kDa and could serve as a negative control. This is suggestive that the antibodies may be sensitive for detection of differences in expression levels which would allow them to distinguish between expressing and non-expressing sub-sets within a PC population.

4.3.2 Validation of antibody using expression vector.

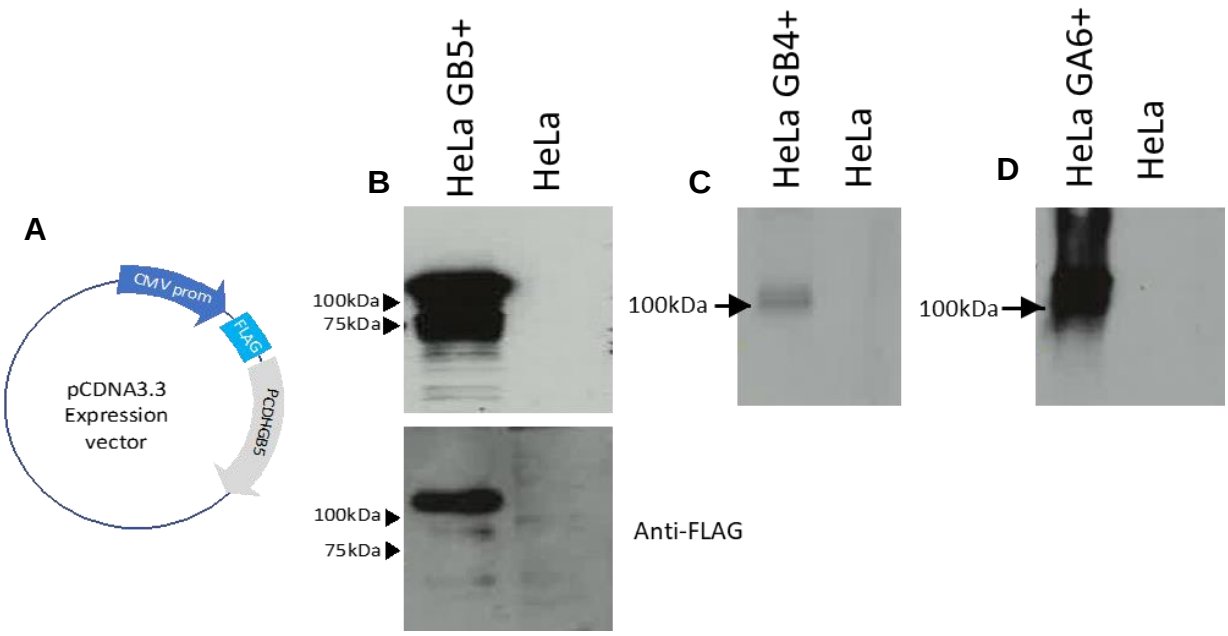

Figure 4.3.2 PCDHG antibody validation

A) Map of the PCDHGB5 expression vector that was transfected into HeLa cells. Expression vectors were transiently transfected into HeLa cells lacking endogenous PCDHG expression, 1µg of DNA was incubated with Genejuice for 20mins prior to addition directly onto the cells. Cells were harvested 48hrs after transfection.

B) Western blots against PCDHGB5 of the transfected HeLa cell lysate next to the GFP-vector control (HeLa)

BOTTOM Western blot against the FLAG-tag in the PCDHGB5 expression vector

C) Western blots against PCDHGB54of the transfected HeLa cell lysate next to the GFP-vector control (HeLa)

D) Western blots against PCDHGA6 of the transfected HeLa cell lysate next to the GFP-vector control (HeLa) n=1

As the second step in validation, it was important to establish that the PCDH antibodies could specifically detect exogenous over-expressed protein. This would also help resolve specific bands amongst the several bands detected by western blot. To

establish this expression vectors with the *PCDHGB5*, *PCDHGB4 or PCDHGA6* sequence inserted into the ORF, containing a FLAG tag upstream of this sequence. Previous western blots indicated that HeLa cells were negative for PCDHGB5 expression as well as being a good cell line to transfect with an expression vector.

Once the expression vectors had been transfected into the HeLa cells, lysates were generated and blotted with an anti-PCDHGB5, GB4 & GA6 as well as an anti-FLAG antibody to confirm the lysate had been positively transfected and was also expressing the PCDHG isoforms. A large band was produced with the anti-PCDHGB5 with heavy bands at 100kDa and 75kDa, the PCDHs are known to form dimers and are also glycosylated which may explain the 2 different sizes of protein being detected. The anti-PCDHGB4 antibody detected a faint band in comparison to the other two vectors, at 100kDa which likely reflects that a lower amount of the vector was taken up by the HeLa cells. The anti-PCDHGA6 antibody detected a large band at 100kDa which extended up to the next marker on the protein ladder approx. 150kDa. Higher molecular weights could represent post-translational modifications such as glycosylation however that relies on the HeLa cells to possess the required molecular machinery or that some of the protein has not fully delineated. The anti-FLAG antibody also detected the FLAG tag at 100kDa confirming that the cells had been positively transfected with the expression vector.

The expression vectors revealed that the antibodies were able to produce a single band at the predicted molecular weights in Hela cells that have no endogenous protein expression. This shows that the antibodies are specific at detecting the targeted PCDHG and that without any post-translational modifications such as glycosylation which band is specific for the full-length version of the isoforms. The transfected HeLa cells produced a single band at the expected molecular weight, as well as seeing variable levels of expression in the cell lines in previous blots (4.3.1) it can be concluded that regardless of multiple bands being produced in the myeloma cell lines that the anti-PCDHG antibodies are specific.

4.3.3 Validation of antibody using siRNA knockdown

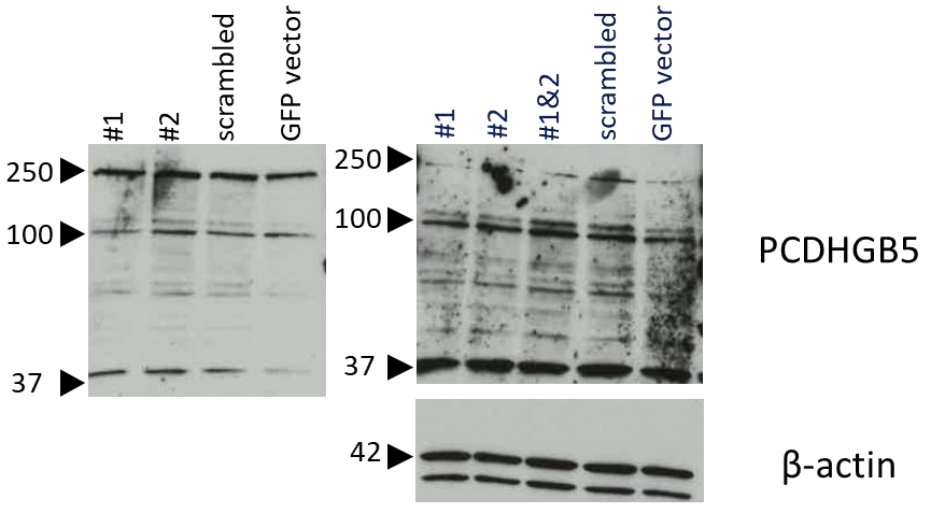

Figure 4.3.3 siRNA Knockdown of PCDGB5
Two PCDHGB5 siRNAs were transfected into KMS18 myeloma cell line to knockdown the PCDHGB5 expression, along with a scrambled control and a GFP vector. This was tried initially at a concentration of 100μM (A) using the siRNAs individually. In the second blot the siRNAs were used at a concentration of 200μM individually and then as a combination with a total concentration of 200μM. Cell lysates were generated and blotted using an anti-PCDHGB5 and an anti-β actin antibody as a loading control. n=3

Following validation of the PCDHGB5 antibody using an expression vector in a negative cell line, the opposite effect was tested using siRNAs to knockdown *PCDHGB5* expression in a positive cell line. The first attempt at knocking down expression is shown in the left blot (A) using single siRNAs at 100μM concentration the specific band at 100kDa does not appear to have been reduced in comparison with the scrambled control apart from a marginal decrease from the siRNA #1. Non-specific bands were detected at 250kDa and 37kDa.

The second knockdown assay combined the siRNAs in one condition and the concentration was increased to 200μM. Lysates were obtained from the transfected cells and blotted for PCDHGB5 and β-actin used as a loading control. Again, bands were detected in all the lanes specific to PCDHGB5 at 100kDa as well as a lower band at 75kDa, there are also non-specific bands at 250kDa and 37kDa. No decrease in the predicted band for PCDHGB5 was observed. The β-actin used as a loading control indicates equal loading therefore any change in expression would be a result of the knockdown. Since the gain of expression experiments supported this as the specific band the results were interpreted as inefficient knockdown with these siRNAs. This line of experimentation was not continued as attention shifted to detection with flow cytometry.

4.3.4 Optimisation of the anti-PCDH antibodies using secondary staining for flow cytometry

4.3.4.1 Schematic of the secondary staining protocol

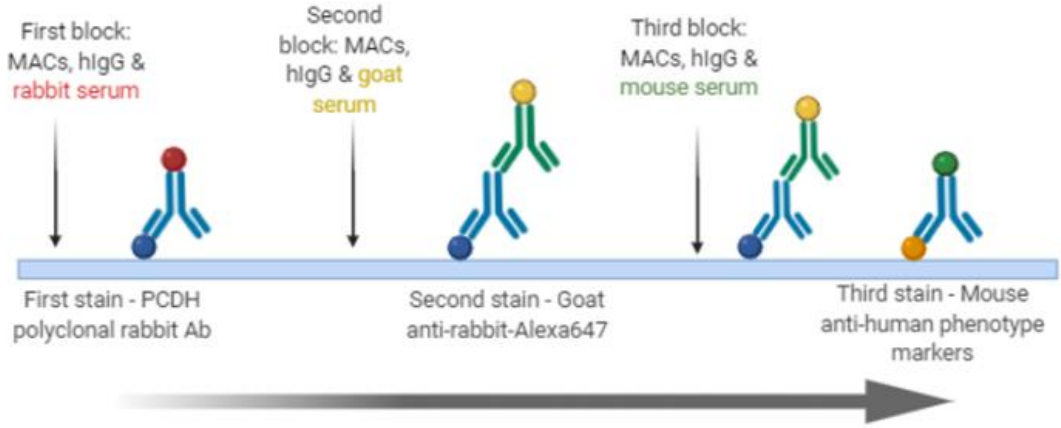

Figure 4.3.4.1 Secondary staining protocol for PCDH staining
Schematic of the flow cytometry staining protocol for the PCDG isoforms. The antibodies specific for PCDHGA6, PCDHGB4 & PCDHGB5 are unconjugated rabbit polyclonal antibodies therefore a secondary conjugated antibody is used to allow detection by flow cytometry. The secondary antibody is a goat anti-rabbit antibody conjugated to AlexaFluor647, the staining of the PCDHG isoforms was carried out first to avoid non-specific staining with individual blocking steps for each stage of the staining protocol. The PC phenotype markers were stained last with the standard conjugated flow cytometry antibodies.

Currently there are no commercially available antibodies for flow cytometry specific to the PCDH-γ isoforms and as the western antibodies detected the isoforms from whole cell lysates, they were tested to see if they could be adapted for flow cytometry. This would then enable the analysis of surface phenotype and provide insight into the pattern of expression of these proteins in individual cells and across cell populations. Each of the three PCDH-γ antibodies (PCDHGA6, PCDHGB4 & PCDHGB5) that had been validated by western blot are rabbit antibodies and are not directly conjugated. Therefore, an indirect staining method is needed and requires antibodies to be stained in individual tubes or the secondary anti-rabbit antibody would bind to all the primary

antibodies and act similarly to a pan antibody showing total PCDH-γ expression. Furthermore, as rabbit antibodies bind to human Fc receptors multiple different blocking conditions were used to avoid any non-specific binding of the antibodies. The blocking conditions were split into 3 steps prior to each staining step, the serum used in each blocking condition was dependent on whether the antibody was rabbit, mouse, or goat. This was done in 3 stages to avoid and cross reactivity between the antibodies. The secondary antibody is conjugated to Alexa647 providing a readout for PCDH-γ expression in this channel of the flow cytometer. This can be multiplexed with other antibodies used to assess plasma cell state. A secondary only condition was included to assess any non-specific binding from the secondary antibody and provide a baseline of background staining.

4.3.4.2 *Optimisation of blocking conditions for flow cytometry analysis of PCDHG expression in primary in vitro generated plasma cells*

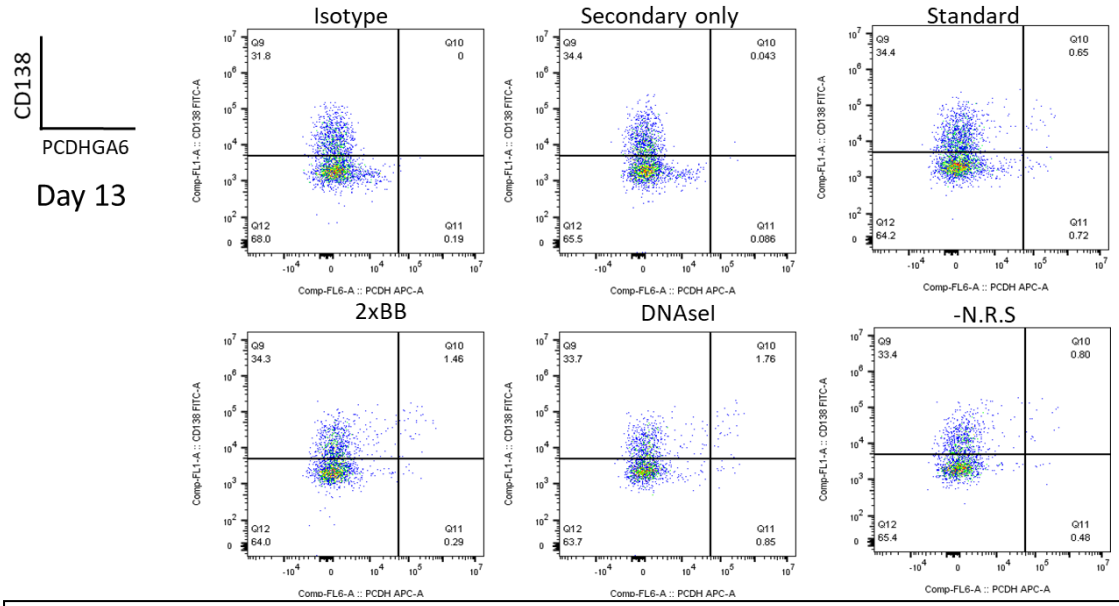

Figure 4.3.4.1 Optimisation of blocking conditions for flow cytometry secondary staining

Memory B-cells were isolated and differentiated using APRIL stimulation and were analysed by flow cytometry at day 13 for PCDHGA6 expression. Different blocking conditions were tested to prevent any non-specific staining form the secondary antibody, this included using 2x the amount of blocking buffer (2xBB) prior to secondary staining, DNAseI treatment and removing the rabbit serum from the blocking buffer. (-N.R.S). As well as the different blocking conditions a isotype (rabibit IgG) and a secondary only condition were also run. Cells are plotted against CD138 on the y-axis and PCDHGA6 on the x-axis.

As an initial step, a further test if multiple different blocking conditions was conducted. The conditions trialled were increasing the amount of blocking buffer 2-fold used in each blocking step, adding DNAseI to the buffer to remove any debris released from dying cells, which is common from day 13 onwards, or to remove the rabbit serum from the first block in case the washes were leaving behind the serum to which the secondary antibody was then binding. Although for this test run the DNAseI treatment gave the highest percentage of positive cells, the benefit over 2x blocking conditions appeared marginal. It was decided that using 2x the amount of blocking buffer would

be used in the final staining protocol and was sufficient at minimising non-specific of the secondary antibody, a goat antibody anti rabbit-Alexa647.

4.3.5 Flow cytometry analysis of PCDHG expression on myeloma cell lines

Representative flow plots of the 4 cells lines in which the PCDH-γ isoform expression (PCDHGA6, PCDHGB4 & PCDHGB5) was analysed. Isotype (rabbit IgG) and secondary only staining was used as controls to set gates and define background or non-specific staining from the anti-rabbit secondary antibody (Alexa647). The gate for positive PCDH-γ expression was set again the background level of expression from the two control conditions.

The top-right quadrant of the flow plots shows the positive PCDH-γ staining, in only a subset of the cell population even for a cell line. This differs for example from the staining pattern of pan plasma cell markers and some of the niche residency factors such as LEPR and ITBG7. There is a spread of PCDH-γ expression levels within the myeloma cell populations and the percentage of PCDHG bright cells shows variation between myeloma cell lines. The percentage of the population that is highly expressing varies between the PCDH-γ isoforms with PCDHGA6 in the H929 cells with 17.8%, PCDHGA6 range to only 2.04% in the OPM2 cells. PCDHGB4 ranges from 3.83%-8.44% and PCDHGB5 ranges from 1.04%-4.73%. There is no trend or pattern of expression of the PCDHG isoforms in the PCDHG that is predominantly expressed or a cell line that has overall higher expression if the PCDHG proteins, although H929 has the highest percentage of bright cells for PCDHGB5 and PCDHGA6.

The staining pattern seen indicates that secondary staining using unconjugated antibodies for the PCDH-γ isoforms is sensitive enough to be able to identify subsets of a cell population with strong positive expression and provides a platform for assessing the surface expression of the PCDH-γ locus.

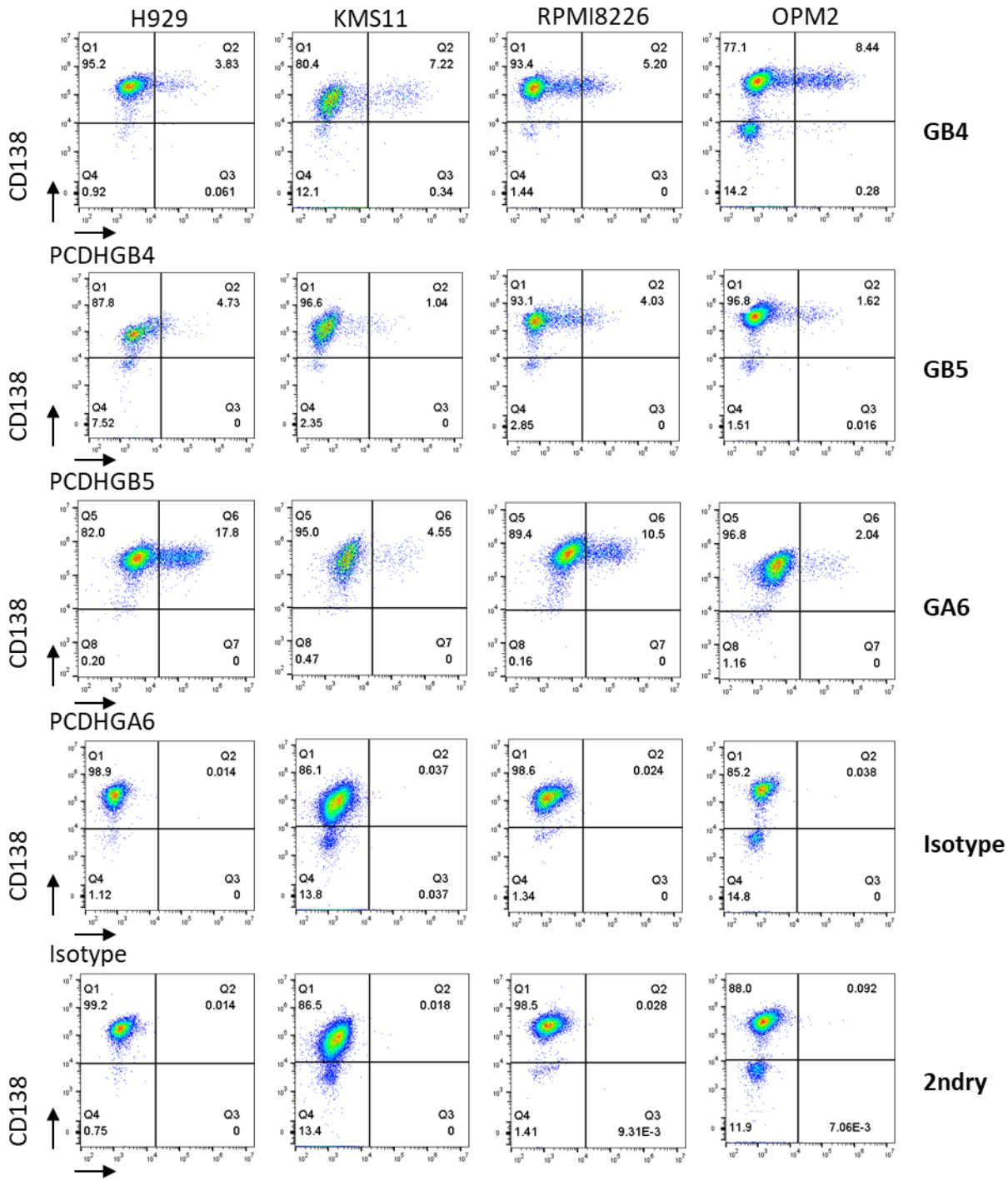

Figure 4.3.5 Surface expression in the PCDHG isoforms on myeloma cell lines

The optimised secondary staining protocol was tested on 4 myeloma cell lines. Flow plots were generated of the PCDH-γ expression for the three individual isoforms, PCDHGA6, PCDHGB4 & PCDHGB5 using the secondary staining protocol and 5µL of the unconjugated antibody for 20mins followed by a 10µL of a 1:10 dilution of the anti-rabbit secondary antibody. Gates were set against the isotype and secondary only controls. CD138-FITC, the plasma cell marker on the y-axis was plotted against the PCDH-γ-Alexa647 expression on the x-axis. n=3

4.3.6 Summary of PCDH-γ expression in myeloma cell lines

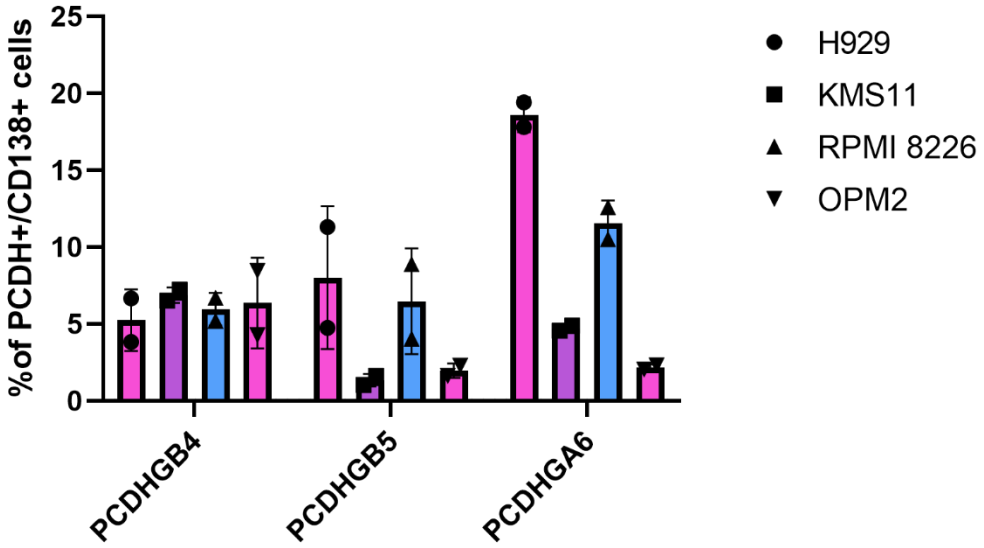

Figure 4.3.6 Variation of PCDHG expression on myeloma cell lines
Average percentage of cells with positive expression of the PCDH-γ isoforms (PCDHGB4, PCDHGB5 & PCDHGA6) showing expression on four myeloma cell lines. Expression was analysed by flow cytometry and plotted against CD138 the plasma cell marker. Percentage is an average from 2 repeat experiments. n=2

Once the staining protocol for the PCDH-γ surface expression was established expression was analysed on four myeloma cell lines (H929, KMS11, RPMI 8226 & OPM2) by flow cytometry. Antibodies for the PCDH-γ isoforms PCDHGA6, PCDHGB4 & PCDHGB5 were used individually due to the same secondary antibody needed therefore the expression between the isoforms cannot be directly compared against each other however cells were from the same passage. Interestingly varying levels of expression were seen not only between the isoforms but also between cell lines which may be due to the clones present in the passage of cells and whether the small subset of PCDHG bright cells, are clonally related which would suggest that the combinatorial pattern of expression is inherited and passed on to the progeny. It is currently unknown as to whether the pattern of expression is determined solely due to the epigenetic regulation and promoter choice and is maintained from parent to daughter cells or if expression is stochastic and influenced by the niche environment. As the myeloma cell lines carry many genetic translocations there is the possibility that this could

impact the normal regulation and expression patterns of the PCDG locus. A dysregulation of this expression may lead to an increased level of mismatching PCDGs on the cell surface and therefore diminishes the ability of the cells to form tight cell-cell interactions which would retain the myeloma cells in the bone marrow.

H929 cells had the highest levels of expression overall and PCDHGA6 having the highest levels of expression out of the PCDHG isoforms. Notably PCDHGB5 and PCDHGA6 expression levels mirrored each other for each of the cell lines with PCDGB5 having lower overall expression. The cell lines RPMI 8226 and H929 had the highest expression of the PCDHG isoforms which may be suggesting of a similar adhesion pattern between the two myelomas.

4.4 Protein expression of protocadherin-γ isoforms show distinct patterns through differentiation of B-cells

4.4.1 Expression pattern of PCDHs in APRIL niche conditions

To determine whether there is a pattern of expression established during B-cell differentiation of PCDH-γ, flow cytometry was carried out on cells from 3 donors in different niche conditions by altering the stimulation driving the plasma cell programme (APRIL, TGF-β or IFN-α). This would not only show whether there is a specific point in the differentiation at which the expression of the PCDHGs is established, if this is then maintained and whether the expression pattern is dependent on the niche condition the plasma cells are generated under. The first condition used was an APRIL stimulation at day 6 of the differentiation to drive the cells from the plasmablast to the plasma cell stage. RNA-seq data previously described shows increased transcript levels from day 13 therefore we anticipated protein expression to also increase once the cells become plasma cells at day 13. To establish whether there is a specific pattern of expression seen in differentiation that is maintained on PCs, expression was analysed past day 13 up until day 40 in a long-term culture.

Since the secondary staining protocol was used for the analysis of PCDH-γ surface expression therefore PCDHGA6, PCDHGB4 & PCDHGB5 had to be tested separately due to the issue with using the secondary antibody not allowing for a direct comparison of their expression. The flow cytometry plots shown identify plasma cells that are $CD138^{+}/PCDH^{+}$ in the top right quadrant, interestingly this shows a sub-population of cells that have strong positive for PCDHG expression and the proportion of cells with PCDHG expression varies depending on the isoform. Overall, the percentage of cells expressing each of the PCDHGs tested increased as the cells become long-lived. This increase correlated with the RNA-sequencing data that shows an increase in the PCDH-γ locus from day 13. At each time point PCDHGA6 had the highest proportion of cells with positive expression and PCDHGB5 the lowest while PCDHGB4 has an intermediate level of expression. The data therefore supported PCDHG protein expression is part of the PC programme and is maintained providing a surface phenotype. As there are only three PCDHG isoforms tested here out of the 22 members it cannot be established whether the subset of cells have an identical barcode of PCDH-γ proteins and are of the same progeny, for example are the

population of PCDHGA6+ cells but PCDHGB4−. This experimental setup does not allow for any analysis of co-expression of the PCDHG proteins. To understand this completely, single cell analysis would be required to show whether there are sub-populations of PCs with identical surface phenotypes for PCDH-γ expression.

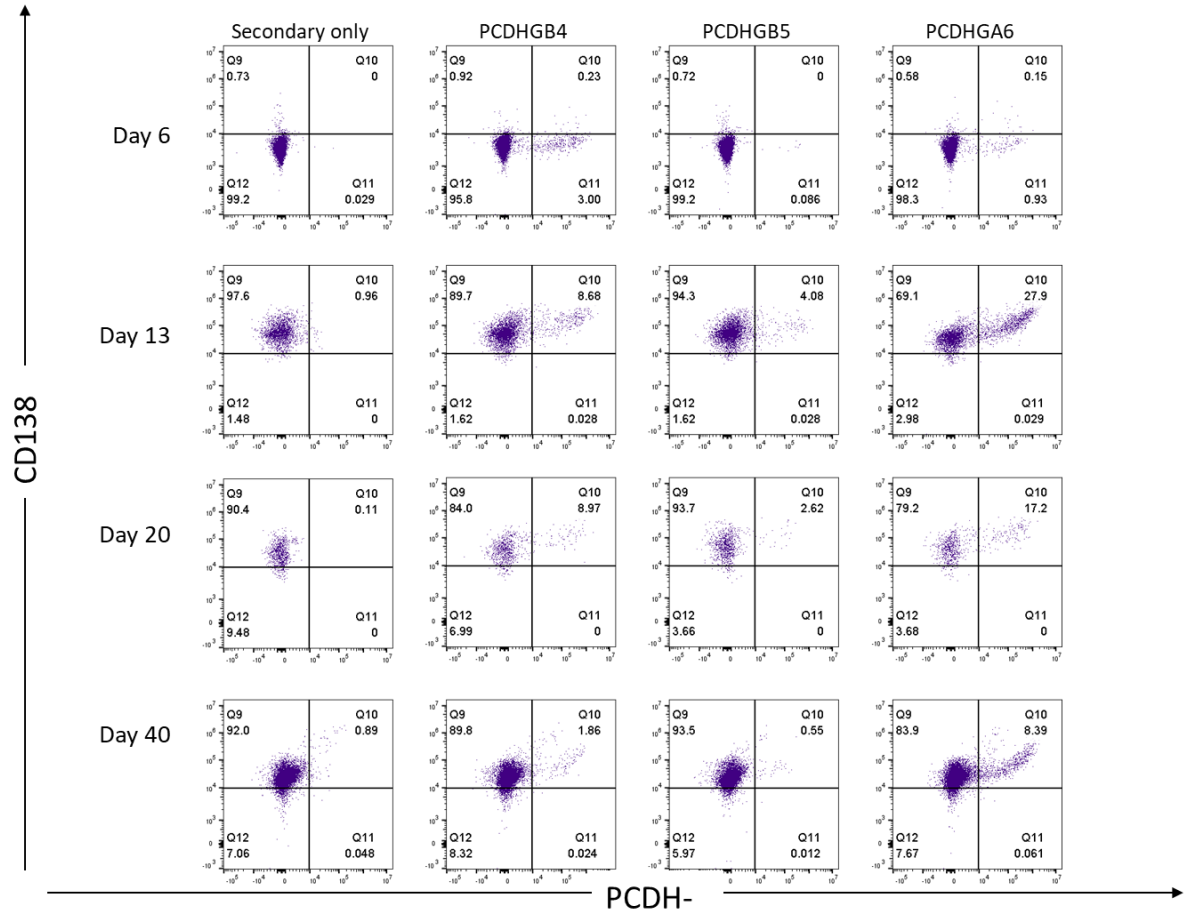

Figure 4.4.1 PCDHG expression in PCs generated in APRIL conditions

Memory B-cells were isolated from peripheral blood from a healthy donor and cultured in the *in vitro* differentiation system using APRIL stimulation from day 6. This is a representative, donor F, out of three donors showing the expression of three of the PCDH-γ isoforms at multiple time points throughout the differentiation from the plasmablast stage at day 6 up until day 40 when cell population will be made up of long-lived plasma cells. Cells were stained for flow cytometry using the secondary staining protocol for the PCDH-γ antibodies, followed by the final staining step of the B-cell and PC phenotypic markers (CD138-FITC, CD38-BUV395, CD19-BV510). The gating strategy used FSC & SSC to identify the B-cell population, followed by doublet discrimination and the live gate using 7AAD negative staining, this gate was then used to analyse expression of the PCDH-surface expression. n=3

4.4.2 Summary of expression in all donors in APRIL condition

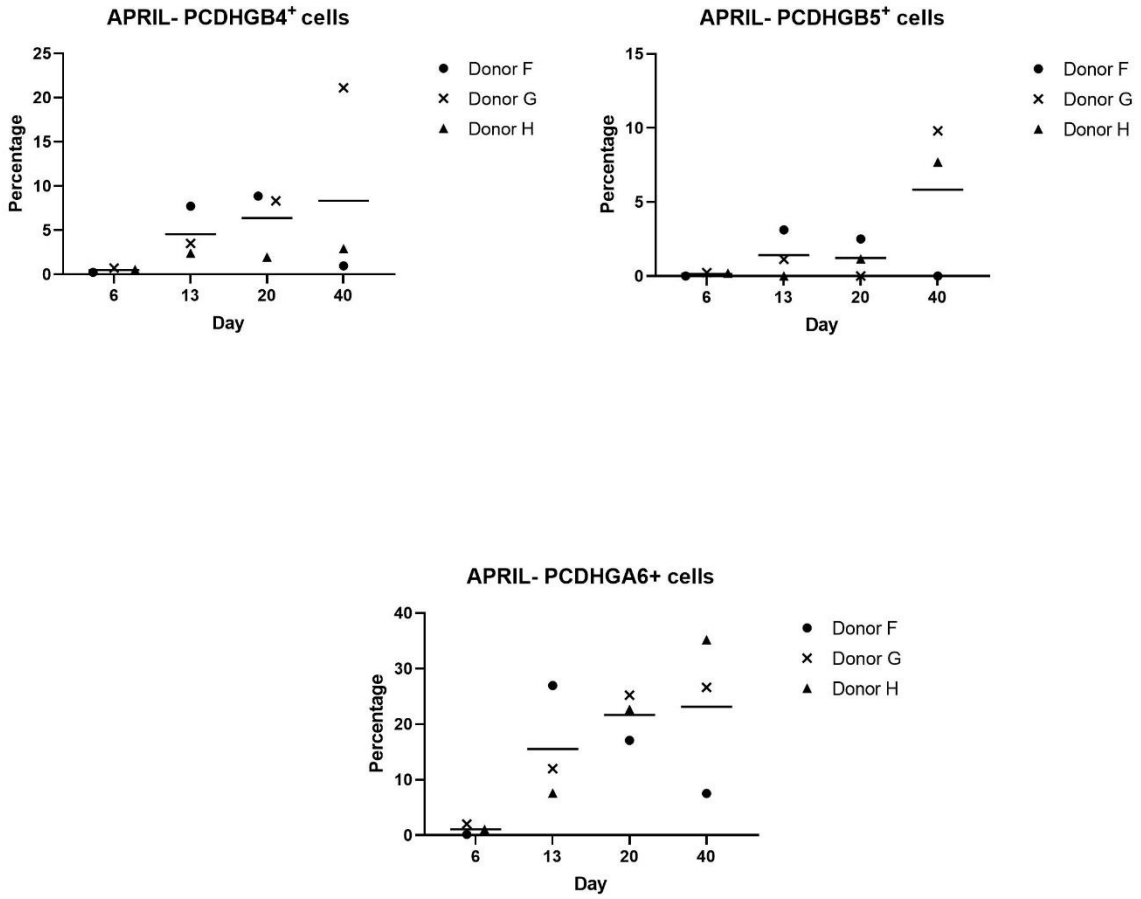

Figure 4.4.2 Donor comparison of PCDHG expression in APRIL conditions
Summary graphs of the percentage of cells positive for both CD138 & PCDH-γ expression. Memory B-cells were differentiated using APRIL conditions in the *in vitro* differentiation system using 3 healthy donors, expression of the PCDH-γ isoforms (PCDHGB4, PCDHGB5 & PCDHGA6) were assessed by flow cytometry at multiple time points during the differentiation. The percentage of cells that were positive for CD138 & PCDH expression were quantified and then standardised to the expression of the secondary only sample.

Three donors were used for the investigation of PCDH-γ expression to account for any clonal variation that may be present between individuals that may alter the pattern of the expression levels. The average levels of expression for each of the PCDH isoforms was calculated and then standardised by subtracting the percentage of PCDH⁺ cells from the secondary only samples from each donor. This provides a level of

background and excludes any non-specific staining from the anti-rabbit secondary antibody in the PCDH+ population.

Expression levels show that the overall trend is that expression of all 3 PCDH-γ proteins tested increased over the time course and that PCDHGA6 is consistently expressed at a higher level in all three donors than the other two isoforms. Although there is some variation in the absolutes levels of expression the pattern is consistent between donors and therefore suggests that PCDHG expression is a feature of normal B-cell differentiation and the highest percentage of cells with positive expression is seen once the cells differentiate into PCs, consistent with mRNA expression.

4.4.3 Expression pattern of PCDHs in TGF-β niche conditions

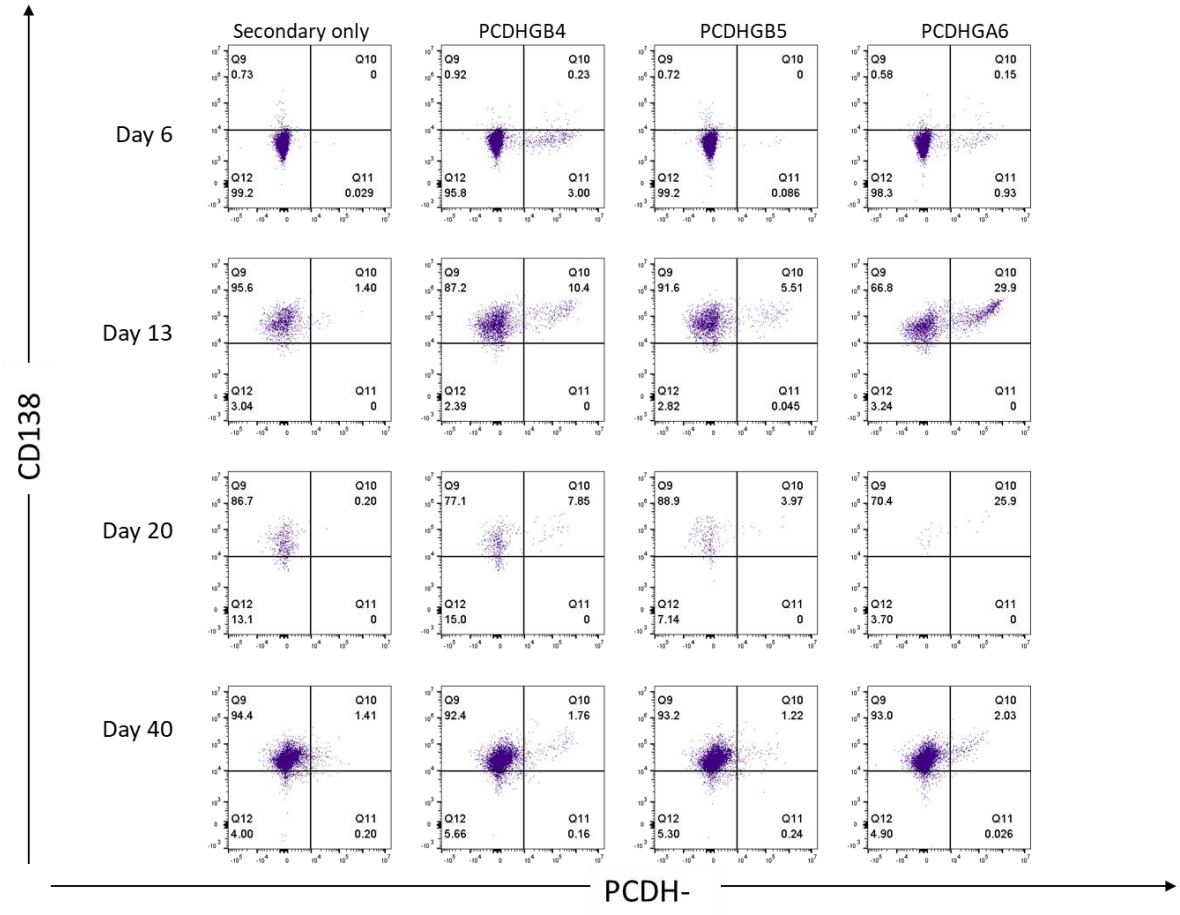

Figure 4.4.2 PCDHG expression on PCs generated in TGF-β conditions
Memory B-cells were isolated from peripheral blood and then cultured in the *in vitro* differentiation system using TGF-β stimulation from day 6. This is a representative donor F out of three donors showing the expression of each of the PCDHG isoforms at multiple time points throughout the differentiation and in long-lived plasma cells. Cells were stained for PCDHG expression using the secondary staining protocol along with the standard panel of B-cell and PC markers. Live cells were gated with negative 7AAD staining and the analysed for PCDH-γ expression. n=3

Memory B-cells taken from the same three donors were cultured with a TGF-β stimulation to compare against the APRIL condition, both of these stimulations are found in an anti-inflammatory niche condition but most importantly act as a survival signal for PCs that would be residing in the bone marrow. With this experimental setup the same three PCDHG isoforms were analysed by flow cytometry throughout the

long-term *in vitro* differentiation to assess whether the niche signals the PCs are exposed to has any influence of the adhesion profile found on the cell surface, including the pattern of expression of the PCDHG locus.

Starting from the same day 6 plasmablast state as shown for the APRIL conditions, the percentage of cells in the CD138+/PCDHG+ subpopulation increased as the cells differentiated into plasma cells. Again, there is a pattern of expression seen for the level each isoform that is expressed, PCDHGA6 has the largest proportion of cells with positive expression this pattern is seen even as early as day 6. PCHGB4 has an intermediate level of expression and PCDHGB5 has the lowest proportion of cells with positive expression. This overall pattern was maintained across all timepoints analysed. This supports a pattern of PCDH-γ expression that is consistent between the two different niche conditions and is maintained on PCs that have entered quiescence to become long-lived.

4.4.4 Summary of expression in all donors in TGF-β condition

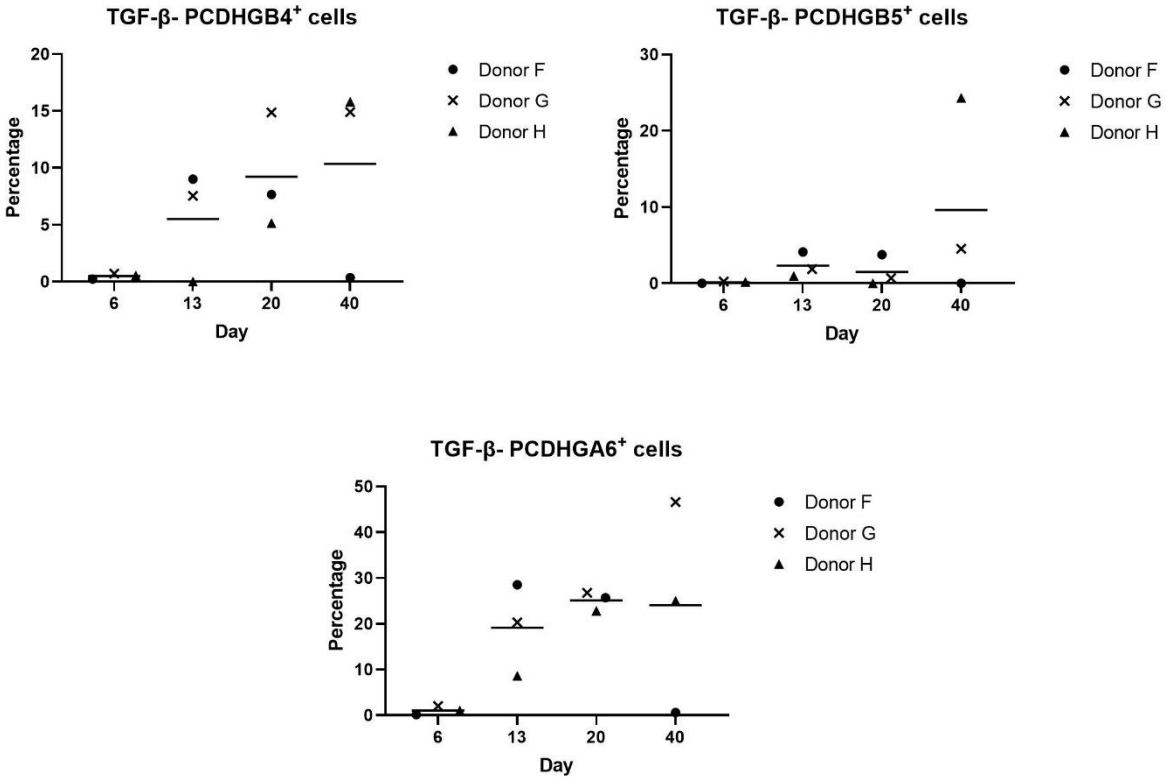

Figure 4.4.4 Donor comparison of PCDHG expression in TGF-β conditions
Average percentage of PCDH+ cells is plotted from 3 healthy donors. Memory B-cells were differentiated using TGF-β conditions in the *in vitro* differentiation system, expression of the PCDHG isoforms (PCDHGB4, PCDHGB5 & PCDHGA6) was assessed by flow cytometry at multiple time points during the differentiation using the secondary staining protocol. The percentage of cells that were positive for CD138 & PCDHG expression were quantified and then standardised to the expression of the secondary only sample.

The mean with standard deviation between the 3 donors is represented as the bars along with the individual points for each donor to show any variability between individuals at each time point of the differentiation. It is noted that on the day 40 time point for donor F had little to no positive expression for any of the PCDHG isoforms, the individual analysis of this this donor showed that there was a very low cell count by day 40 and therefore does not give an accurate representation of the pattern of

PCDHG expression. There is some variation between donors for the percentage of positive cells expressing PCDHG isoforms however the same trend is followed for each donor in that PCDHG of each isoform increases as the cells become long-lived. The overall pattern of expression over the time course is the same for each of the PCDHG isoforms in that expression is low at day 6 and then steadily increases as the cells differentiate into PCs and at the later time points. The pattern of expression appears to be consistent between donors with PCDHGA6 having the highest levels of expression and PCDHGB5 having the lowest.

4.4.5 Expression pattern of PCDHs in Interferon-α niche conditions

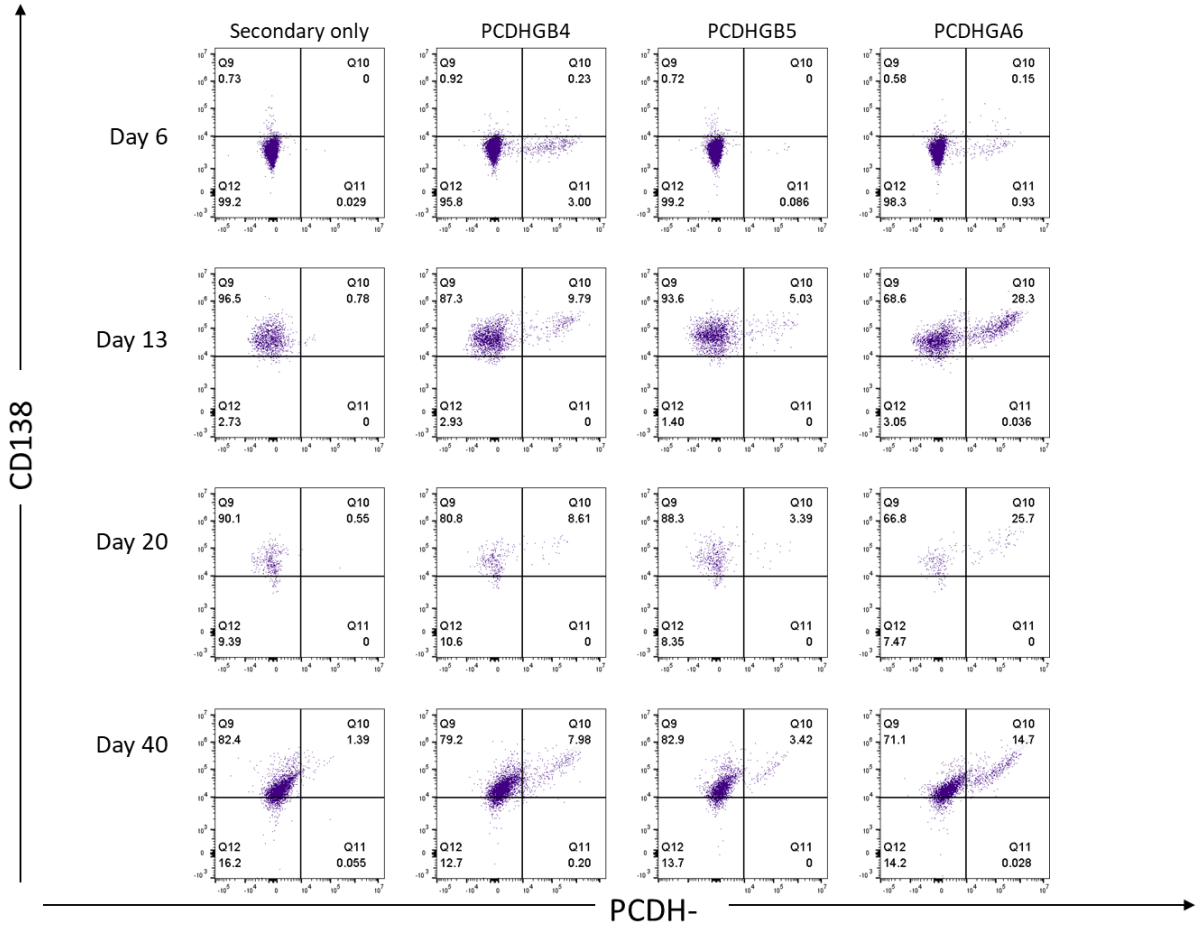

Figure 4.4.5 PCDHG expression on PCs generated in IFN-α conditions

Memory B-cells were isolated from peripheral blood and then cultured in the *in vitro* differentiation system using IFN-α stimulation from day 6. This is a representative donor F out of three donors showing the expression of each of the PCDHG isoforms at multiple time points throughout the differentiation and in long-lived plasma cells. Cells were stained using the secondary staining protocol for PCDHG expression along with the B-cell and PC makers, in the final staining step. Cells were taken from the live gate and plotted using CD138-FITC against PCDHG expression. n=3

The final stimulation used in the differentiation system was IFN-α, a traditionally pro-inflammatory cytokine was tested in comparison to APRIL and TGF-β, to test PCDHG expression when the PCs are receiving a different type of niche signal. Flow cytometry

was carried out during the time course of the differentiation from day 6 at the plasmablast stage up until day 40 analysing the expression of the PCDH-γ isoforms. The same pattern as seen previously in the other two niche conditions was presented with PCDHGA6 having the highest percentage of expressing cells and PCDHGB5 with the lowest percentage of positively expressing cells. Of note the subset of cells with positive PCDHG expression also appear to be high in CD138 expression, this is seen in all three culture conditions. One favoured explanation could be that expression of PCDHG isoforms correlates with a highly differentiated state possibly the most quiescent population and thus strong co-expression of the two markers. There is for example a suggestion that the expression of PCDHGA6 is most consistent under IFN-α conditions which in general drives a more homogeneous plasma cell phenotype than differentiation with APRIL. While a technical compensation issue could contribute, every effort has been made to minimise this and it is anyway unlikely since the fluorophores used on the markers being compared are FITC and Alexa647 which do not have significant issues with overlapping emissions.

4.4.6 Summary of expression in all donors in IFN-α condition

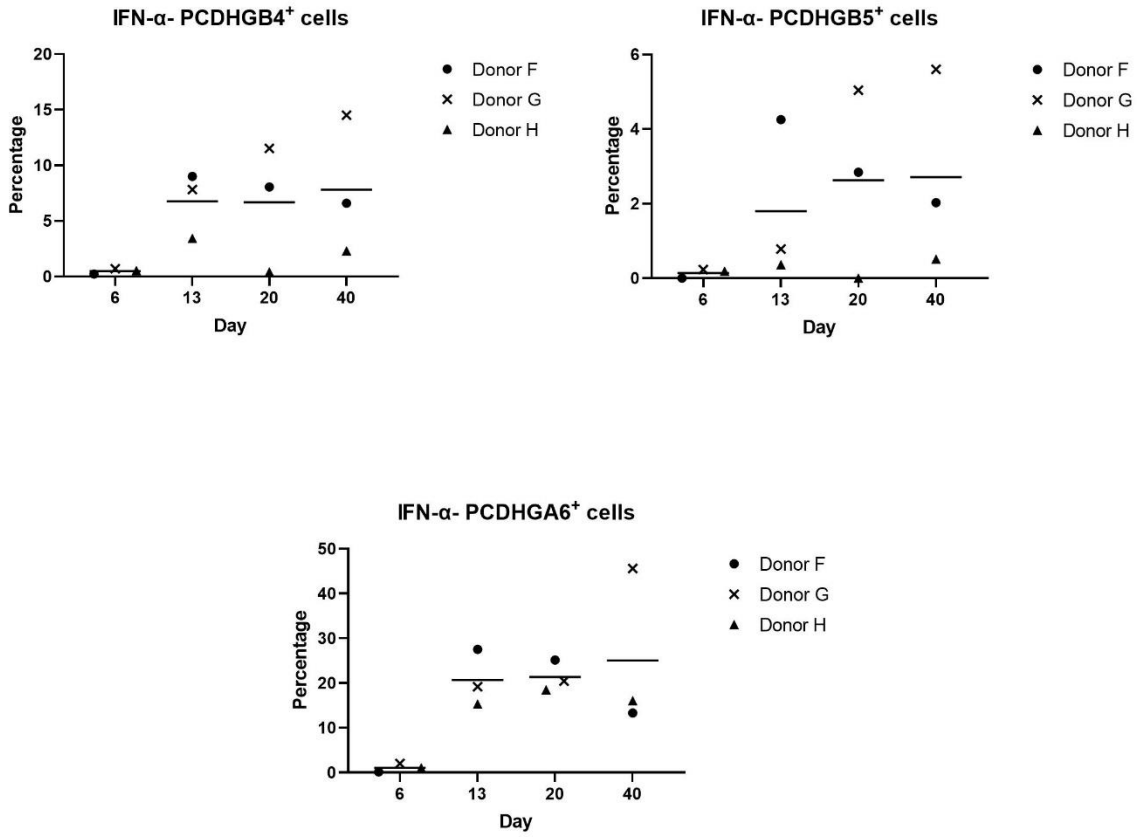

Figure 4.4.6 Donor comparison of PCDHG expression in IFN-α conditions
Averages of the percentage of cells with PCDHG positive expression from 3 donors. Memory B-cells were differentiated using IFN-α conditions in the *in vitro* differentiation system, expression of the PCDHG isoforms (PCDHGB4, PCDHGB5 & PCDHGA6) was assessed by flow cytometry at multiple time points during the differentiation. The percentage of cells that were positive for CD138 & PCDHG expression were quantified and then standardised to the expression of the secondary only sample.

The average pattern of expression from the three donors' shows that the percentage of PCDH positive generally increases at the later time points, the slight difference in the IFN-α condition is that there was very low expression of PCDHGB5. Although PCDHGB5 expression increased from day 6 this was at a very low level which was seen with all three donors when looking at the individual points. PCDHGB4 expression

increases significantly from day 6 and is maintained at a similar level in the later time points. The isoform with the highest percentage of PCDHG positive cells was PCDHGA6, expression levels were similar to the other two isoforms and then rapidly increases from day 6 to around 20% of the cell population being positive for PCDHGA6 expression. This appears to steadily increase up until day 40 however this is skewed slightly by one donor having a much higher percentage of positive cells.

Overall, the pattern of expression appears to be established by day 13 when expression increases and is maintained on the PCs. The levels of each isoform have a similar pattern between donors suggesting that there may be a preferred pattern of expression established during normal B-cell differentiation or pre-existing in memory B-cells and transmitted to their progeny. The latter may be the favoured explanation suggested by accessibility data since ATAC-seg indicates pre-existing accessibility at the locus in B-cells prior to differentiation. The biggest increase in expression is seen between day 6 and day 13 as cells transition from plasmablast out of cell cycle and become quiescent PCs. This is consistent with the mRNA expression data and potentially an association between PCDHG expression and cell cycle quiescence.

4.4.7 Comparison of expression between niche conditions

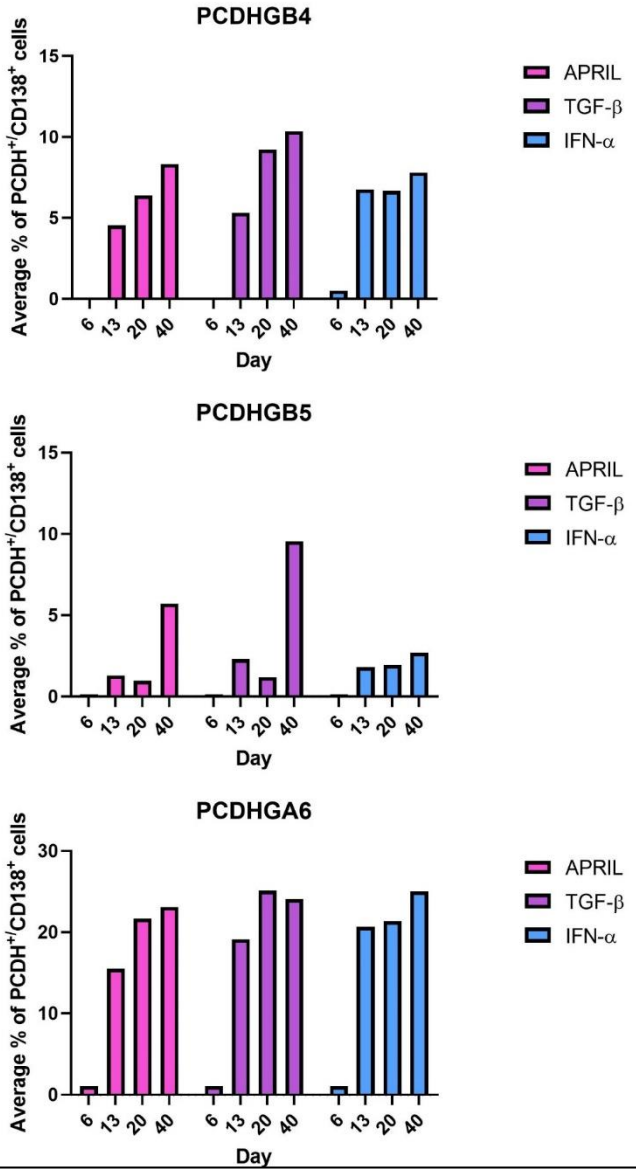

Figure 4.4.6 Comparison of PCDHG expression on PCs generated in different niche conditions

The average percentage of $CD138^+/PCDHG^+$ cells was calculated from 3 donors in each of the three different niche condition signals (APRIL, TGF-β or IFN-α). The percentages had been standardised using the background staining seen from the secondary only condition ran for each individual donor in each condition. The percentages are plotted for each time point analysed from the *in vitro* differentiation system.

When directly comparing the results of differentiation in the 3 different niche conditions (APRIL, TGF-β or IFN-α) the overall trend is further reinforced with expression of the PCDHG isoforms increased as the cells progress from day 6, past day 13 expression continues to gradually increase as the cells become LLPCs and did not show large variation between donors. The trend of PCDHG expression is the same in each of the niche conditions used to generate PCs from the *in vitro* differentiation system, indicating that external signals form the niche environment are not influential on the expression of the PCDHGs. As the increase of expression from day 6 to day 13 matches the increase seen at a mRNA level it likely that the epigenetic regulation mechanism that controls promoter choice and the gene expression influences the protein expression of the PCDHG cluster.

4.5 Protocadherin-γ expression is seen in malignant bone marrow and peripheral blood samples

4.5.1 Expression of PCDHG in whole blood from a healthy control

As a pilot experiment prior to analysing surface expression of the PCDHG isoforms the secondary staining protocol was tested on a whole blood sample from a healthy donor. Prior to staining red cell lysis was performed using ammonium chloride and then the remaining cells were stained with a live/dead stain followed by the secondary staining protocol for the PCDHGs and the PC phenotype markers. As this was a whole blood sample and therefore contained multiple different cell populations the gating strategy used gated out the lymphocyte population using FSC and SSC followed by doublet discrimination and a live cell gate. PCDHG expression was plotted against CD19 the positive gate was set using the secondary only condition.

B-cells from the peripheral blood are equivalent to naïve B-cells at day 0 B-cells in the differentiation system and therefore expression levels of the PCDHG proteins have not been examined at this stage previously. Using the pan-PCDH antibody shows that almost 100% of the cell population is positive for PCDHG expression, however when looking at individual isoforms only a small subset of the population shows strong expression for any of the PCDHG proteins. The positive gate is set using the secondary only condition to account for any background staining, although there is a spread of PCDHG positive expression however there is the emergence of a second population with strong positive expression. This demonstrates that the staining

protocol for PCDHG surface expression can distinguish subtle variations in expression levels from small populations of neoplastic PCs with strong positive cells.

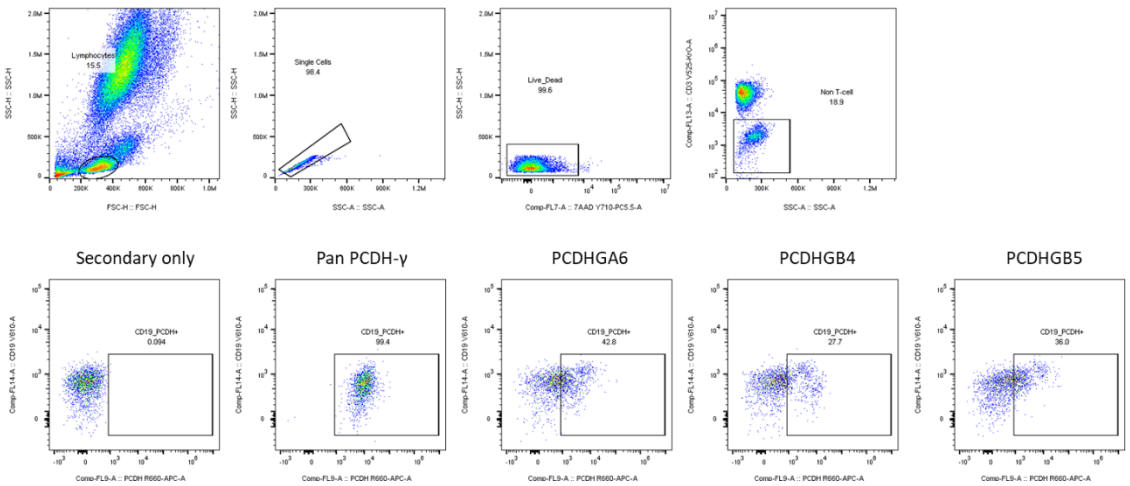

Figure 4.5.1 PCDHG expression in circulating B-cells

Peripheral blood was taken from a healthy donor (donor I) and then red cell lysis performed using ammonium chloride. The cells were stained for PCDH-γ surface expression using the secondary staining protocol along with a staining panel to identify the B-cells and PCs using CD19, CD138, CD38, CD27, IgD and CD3 to separate out the T-cells from the lymphocyte population. The gating strategy used FSC and SSC to gate out the lymphocytes followed by doublet discrimination and a live gate. The cells negative for CD3 were then gated as the non T-cells. PCDH-γ expression was plotted against CD19 for total PCDH-γ expression along with the individual isoforms PCDHGA6, PCDHGB4 & PCDHGB5. n=1

4.5.2 Expression seen in malignant patient samples

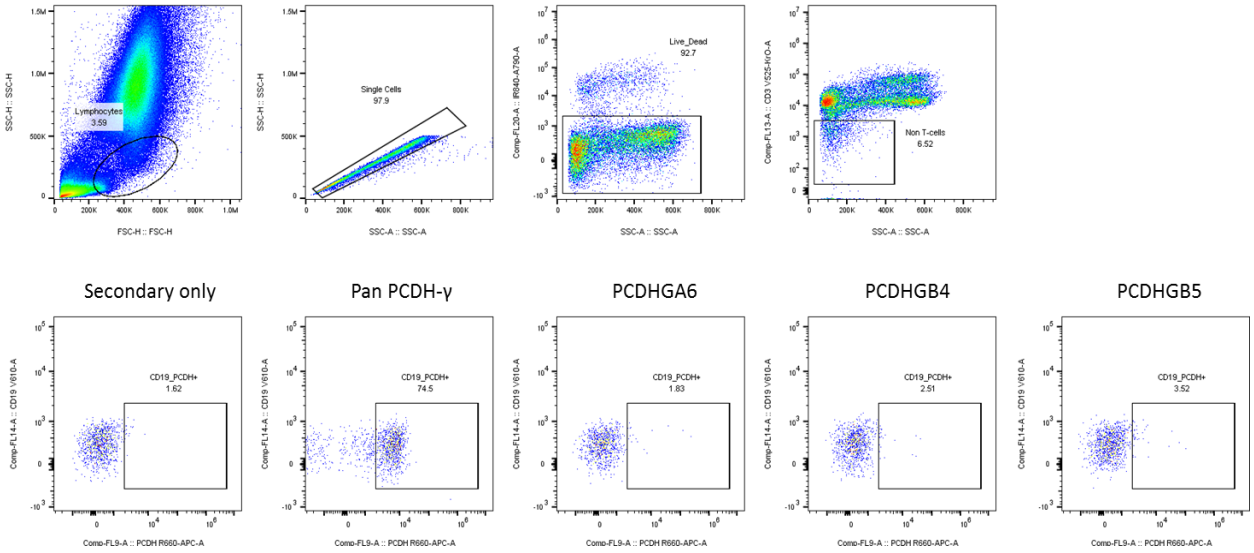

Figure 4.5.2 PCDHG expression on bone marrow PCs from MM patient

A representative bone marrow aspirate from a multiple myeloma patient was analysed the same as all the patient samples run for PCDH-γ surface expression. Before staining was carried out red cell lysis was performed using ammonium chloride and then cells were stained with the live/dead fixable IF-Red dye and CD27-FITC before being fixed in 100µL of 4% paraformaldehyde. Following this, cells were stained using the secondary staining protocol for the PCDH-γ proteins and a panel of B-cell markers (CD138-PE-Cy7, CD38-BUV395, CD19-BV510, IgD-PE) along with CD3-VioGreen to separate out the T-cells. The gating strategy above shows the separation of the lymphocytes and monocytes using FSC and SSC from the sample followed by single cells, a live gate and then non T-cells before gating out the PCDH-γ positive cells. n=11

From the initial sequencing data that revealed an upregulation in an adhesion signature which included the PCDH-γ locus in plasmacytomas compared to PBL. Once a staining protocol was established to analyse surface expression this then allowed for the analysis of surface expression phenotypes in a range of samples from patients with neoplastic B-cells and PCs. Samples were bone marrows aspirates that were all processed in the same manner by using ammonium chloride for red cell lysis before staining a mixed cell population. A live/dead fixable dye and the CD27 staining was done before fixing with 4% paraformaldehyde (PFA) to ensure proper staining as

previously it had been noticed that CD27 staining was affected if cells had been fixed prior to staining. The staining panel that was used allowed for lymphocytes to be gated out and then the B-cells and PCs before expression levels of the PCDHG were analysed.

Samples were analysed for total PCDHG expression using the pan antibody as well as the individual isoforms PCDHGA6, PCDHGB4 & PCDHGB5. For this samples around 70% of the population is positive for PCDHG however when looking at the individual isoforms the percentages are far lower when taking in consideration of the background levels in the secondary only condition compared to what has been seen previously in the healthy donors analysed. As multiple myeloma is a PC neoplasm the cells have reached a stage in differentiation where PCDHG expression is usually seen however the percentage of positive cells is low in fitting with the idea that a more dispersed disease has a down regulation of adhesion markers including the PCDHG locus.

4.5.3 Comparison of PCDH-γ expression levels

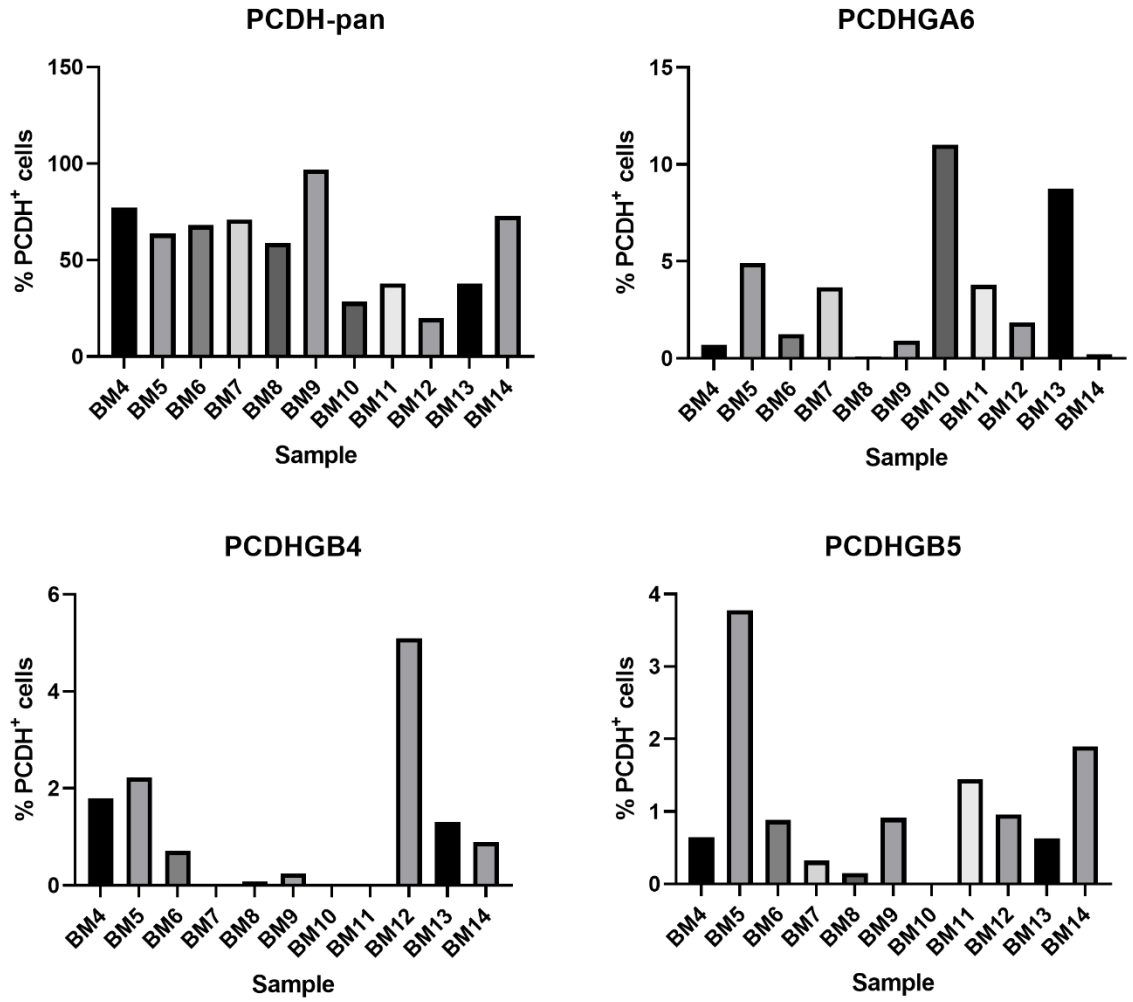

Figure 4.5.2 Percentages of PCDHG⁺/CD19⁺ cells in malignant bone marrows
The percentage of PCDH⁺/CD19⁺ cells from the non T-cells gate that were double positive were compared between bone marrow samples. Percentage of cells was plotted for the total PCDHG expression and the three individual isoforms PCDHGA6, PCDHGB4 & PCDHGB5. Percentage positive cells was calculated individually for each bone marrow samples and standardised for background staining by subtracting the percentage positive cells seen in the secondary only control for each bone marrow, respectively. n=11

Total PCDHG expression identified using the PCDH-pan antibody showed that the majority of samples had at least 50% of their PC population expressing PCDHG

proteins on the cell surface. Four of the samples had lower than 50% of cells expressing (BM10-13) these samples represent a reactive marrow, post-treatment for AML and myeloma. The percentage of cells positive for the individual isoforms is much lower with the highest percentage seen for PCDHGA6 around 10% of cells, for PCDHGB4 and PCDHGB5 this drops to below 5% of cells for the majority of samples. This indicates that the expression of PCDHG uses a combination of isoforms rather than using one single predominant isoform. If the percentages of all isoforms are relatively low, then it is likely that there is a combinatorial expression of the isoforms to account for the full repertoire of PCDHG proteins expressed in the cell surface.

Analysis of the individual isoforms show a large amount of variation between samples in some instances there is a predominant isoform being expression, for example BM10 has no expression of PCDHGB4 or PCDHGB5 whereas ~10% of the cell population is expressing PCDHGA6 from a total of 25% of the population expressing members of the PCDHG locus. Unlike the PCs generated *in vitro* that all follow the same pattern of expression between the three individual isoforms this is not maintained when analysing the expression in malignant bone marrows. There is not a clear clustering of the disease type when looking at the levels of either total PCDHG expression or preference of the individual isoforms being expressed therefore it is unclear how the expression pattern may link to adhesion and what functional affect the expression patterns are having.

4.6 Discussion

The aim of this chapter was to establish if there is a surface pattern of the PCDHG proteins that may provide cells with an identity barcode and whether this pattern is specific to PCs and is this pattern is then disrupted in neoplastic PCs. The data presented here provides strong evidence in support of surface expression of PCDHG protein during plasma cell differentiation *in vitro* and *in vivo* and argue that expression patterns of PCDHG proteins vary within PC populations. PC heterogeneity may stem from separate clones passing on distinct patterns of expression to their progeny or via stochastic promoter choice which has yet to be determined in PCs. Current data shows that there are regions of accessibility over the promotors of the *PCDHG* locus in resting B-cells as well as PCs, and the mRNA data shows that expression is established and maintained in LLPCs. ChIP and ATAC-seq data indicate epigenetic regulation as

characterised in the nervous system is evident in B-cells for the *PCDHG* locus but not the *PCDHA* or *PCDHB* loci, this would provide a mechanism for combinatorial expression. How gene expression translates into protein surface expression has not yet been studied in detail to establish when the combinatorial expression is initiated in B-cell differentiation, or how this correlates with the epigenetic marks. Having a pattern of combinatorial expression of the PCDHG proteins on the cell surface unique to B-cells and PCs could lead to either homotypic adhesion or repulsion, as yet the functional studies to determine this are still required. The hypothesis is that having matching expression patterns would lead to adhesion of PCs within the bone marrow, survival niche or sites of infection.

The first step was to optimise a protocol for identifying the endogenous expression of the PCDHG proteins and be confident that we were indeed identifying individual isoforms. Due to the PCDHG proteins being similar in structure, only varying in their extracellular domain, which is encoded by the first variable exon, meant western blotting was not the best method for distinguishing between the isoforms being expressed. The specificity of the PCDHG western antibodies was confirmed using expression vectors for PCDHGB4, PCDHGB5 & PCDHGA6 being overexpressed in HeLa cells with no endogenous PCDHG expression. Following on from the initial optimisation experiments the antibodies that had been validated were tested for use for flow cytometry which would enable the analysis of cell surface phenotype. PCDHG expression was tested in different niche conditions achieved by using either APRIL, IFN-α or TGF-β stimulation in the *in vitro* system. This revealed that regardless of the niche condition the pattern of expression levels of the isoforms was unaffected. This indicates that for healthy B-cells expression levels of the PCDHG proteins increase at day 13 with a specific pattern which is maintained and correlates with the expression seen at RNA level. Having an assay that can distinguish the different PCDHG isoforms is proof of concept that a PC population can be phenotyped using PCDHG expression, defining subsets of cells rather than expression of a bulk population.

With PCDHGs providing a way of separating subsets of PCs out of the general population further experiments to assess what functional effect this may have on adhesion would be needed. With the premise that having the same surface pattern of PCDHG expression would lead to homotypic adhesion would mean that

subpopulations of PCs with positive expression would be more likely to adhere to each other. To investigate this with only the three isoforms studied here it had been planned to use HeLa cells lacking endogenous PCDHG expression and transfect expression vectors into the cells and then carry out adhesion assays by fluorescently labelling cells depending on the vector to assess whether there is only homotypic adhesion through identical PCDHG expression or promiscuous heterotypic adhesion.

Single cell analysis would be needed to assess whether these subsets of PCDHGA6, PCDHGB4 & PCDHGB5 positive cells have an individual barcode of PCDHG expression and whether these subsets are of the same progeny. Due to the difficulties with staining, the isoform staining had to be done in individually. Therefore comparing the co-expression of the isoforms against each other was not possible which would have confirmed if the subset of expressing cells were double positives for expression of PCDHG isoforms. This would help to elucidate how a barcode of PCDHG expression could cluster subsets of PCs that will have homotypic recognition.

To investigate the idea that PCDHG can be altered on neoplastic cells PCDHG expression was analysed in whole blood and bone marrow aspirates from malignant samples. This showed variation between samples and types of neoplasms and state of the PCs. In myeloma common genetic alterations include translocations of chr5 which carry the clustered PCDHs which may account for variation in expression compared to that seen in normal healthy B-cells. Using PCDHG combinatorial expression to identify subsets of neoplastic cells would provide a good diagnostic tool for monitoring development and progression.

Other links to cancers have been made for the PCDH alpha and the gamma cluster, epigenetic alterations have been identified in their methylation status which affects the CpG sites and accessibility for CTCF binding and prevents DNA looping mechanism for transcription of the promoter. In tissues where there is high expression of PCDHs such as the nervous system, it was seen that there was hypomethylation in the astrocytoma samples, however, in the tissues with low PCDH expression the CpG sites were targeted by DNA methylation (Vega-Benedetti et al., 2019). This provides evidence that the epigenetic profile of the PCDH loci can act as diagnostic biomarkers.

It was shown that the niche condition and stimulation in the *in vitro* system did not appear to affect the expression patterns, therefore where variation in neoplastic PCs

is seen, it may reflect the genetic alterations/translocation commonly seen in neoplastic PCs or if there is a predominant clone where the pattern of PCDHG is passed down to the progeny. Further investigation into factors controlling PCDHG expression, such as PC state and quiescence along with post-translational alterations is needed to fully explain how the PCDHG surface phenotype impacts PC biology and what information this provides us in the context of malignancy.

4.7 Appendix

4.7.1 Bone marrow samples

Table 4-3 Bone marrow samples

Sample ID	Diagnosis
BM4	Monoclonal gammopathy of undetermined significance (MGUS)
BM5	MDS treated <5% blasts (regenerating marrow post treatment)
BM6	Reactive marrow
BM7	Plasma cell myeloma
BM8	CML chronic phase
BM9	Reactive marrow
BM10	Reactive marrow
BM11	No evidence of disease (regenerating marrow post treatment for AML)
BM12	Plasma cell myeloma
BM13	Plasma cell myeloma
BM14	Plasma cell myeloma

Table 5: List of bone marrow samples. Sample ID and corresponding diagnosis from the diagnostic service following flow cytometry

5 Shedding of surface adhesion molecules by ADAM proteases

5.1 Introduction

Cell surface phenotypes are controlled and regulated which enables cells to respond to external cues including niche survival signals. B-cell and PC surface expression can be utilised to provide markers of cellular differentiation state as well as a diagnostic tool in neoplasia. Surface expression can be controlled at gene expression level and represents the gene programme of the differentiation which is potentially further modified by signals from the niche environment. However, in addition to control at the level of gene expression surface phenotypes are subject to extensive post-transcriptional modification. Such mechanisms include variable splicing of mRNA to control exon usage, variable glycosylation, intracellular retention and endocytosis.

In the context of B-cell differentiation, signals from the germinal centre drive the cells to differentiate into antibody secreting PCs or memory B-cells. Upon differentiation PCs need to respond to external cues in order to home to the survival niche in the bone marrow, where they reside potentially for years constitutively secreting antibody. Given the importance of cell surface phenotype for survival and homing post-transcriptional regulatory mechanisms are extensively implicated in the control of these responses. An important mechanism of dynamic modification of the surface phenotype, which is also implicated in signal propagation is proteolytic cleavage. The ADAM sheddase superfamily are responsible for a large range of proteolytic cleavage events. A key example is regulation of the NOTCH pathway, which is responsible for cell fate determination in both B- and T-cell lineages (Gibb et al., 2010; Six et al., 2003). ADAM sheddases are also involved in processing a number of surface adhesion molecules including ALCAM (Gilsanz et al., 2013).

Expression of ADAM sheddases on B-cells and PCs provides the potential for another level of regulation over the cell surface phenotype influencing a cells ability to adhere to the neighbouring cells and extracellular matrix (Bret et al., 2011; Pupovac et al., 2015; Lownik et al., 2020). Surface shedding also impacts responses to cell signalling and migration signals. The main sheddases responsible for cell surface shedding are ADAM10 & ADAM17 which have a crossover of targets and effects on downstream

signalling pathways. ADAM sheddases act by cleaving at the base of the ectodomain releasing an extracellular fragment. This can either lead to indirect external signalling from the extracellular fragment on neighbouring cells or activates internal signalling by allowing further proteolytic cleavage via γ-secretase, which cleaves at the C-terminal. The latter mechanism is exemplified in the control of the NOTCH pathway. The ADAM sheddases themselves can also be regulated via co-factors such as tetraspanins and surface localisation to their targets (Gutiérrez-López et al., 2011; Gilsanz et al., 2013; Matthews et al., 2017)

Since proteases have well defined enzymatic pockets these proteins have been fruitful targets for inhibitor design. Therapeutic and tool compounds have been developed to target specific ADAMs as well as overall pan inhibitors. With the large range of targets of the ADAMs the scope for therapeutic use for these types of inhibitors is compelling due to their ability to disrupt several cell pathways, however an important consideration is the chance of any off-target effects.

From the initial expression analysis of the adhesion signature in the *in vitro* differentiation system the PCDH-γ proteins and ALCAM became the surface molecules of interest. The PCDH-γ proteins showed variable levels of expression between isoforms and were also variable in the myeloma cell lines and malignant bone marrow samples suggesting possible post-translational alterations. ALCAM was interesting due to the distinct high and low expressing populations seen consistently in differentiating B-cells from day 6 as they transitioned into PCs. After investigation into current literature the ADAM sheddases were identified as having both PCDH-γ proteins and ALCAM as targets, specifically ADAM10 targeting the PCDH-γ proteins and ADAM17 being responsible for targeting ALCAM. Additionally, the PCDH proteins may also be targeted by γ-secretase (Rosso et al., 2007; Gilsanz et al., 2013; Bonn et al., 2007; Reiss et al., 2006).

It is already known that the expression of the PCDH-γ locus is epigenetically regulated therefore we wanted to know if the expression pattern is determined at a gene level or if there is further regulation at a protein level, this could be in the form of proteolytic cleavage. For ALCAM expression we wanted to know what the potential cause of generating a double population separating by ALCAM high and low surface expression. It was observed that the ALCAM high population was also CD138 high

which raises the question whether the more mature PCs inherently have more surface ALCAM or whether it may be down to proteolytic cleavage and shedding from the cell surface.

Regulation at both a gene and protein level, provides the potential to fine tune cell surface expression levels and establish more dynamic control over niche interactions relative to control at gene expression level alone. Furthermore, if surface phenotypes are independently and dynamically regulated from the prevailing transcriptionally encoded cell state, it may have significant implications for the evaluation of a phenotypic marker in a clinical context.

5.1.1 Aims

The aim of this chapter is to investigate whether the ADAM sheddases contribute to the control of surface expression of niche factors and adhesion molecules in differentiating B-cells and PCs. A series of inhibition experiments were designed to use a range of commercial ADAM inhibitors, a pan inhibitor (Marimastat) an ADAM10 specific inhibitor (GI 254023x) and a ADAM17 specific inhibitor (TAPI-2) which already have therapeutic applications. These inhibitors were used to assess whether they induced an increase in the expression of surface proteins. If the addition of the ADAM sheddase inhibitors resulted in an increase of surface expression this would provide evidence for a post-transcriptional mechanism of regulation of cell surface phenotype in differentiating B-cells and PCs. Myeloma cells lines were used as a disease model to assess whether the level of expression of the sheddases or their activity is altered allowing for changes in the cell surface expression in the context of neoplastic PCs.

5.2 ADAM sheddase expression in B-cells and Plasma cells

5.2.1 mRNA expression of the ADAM sheddases

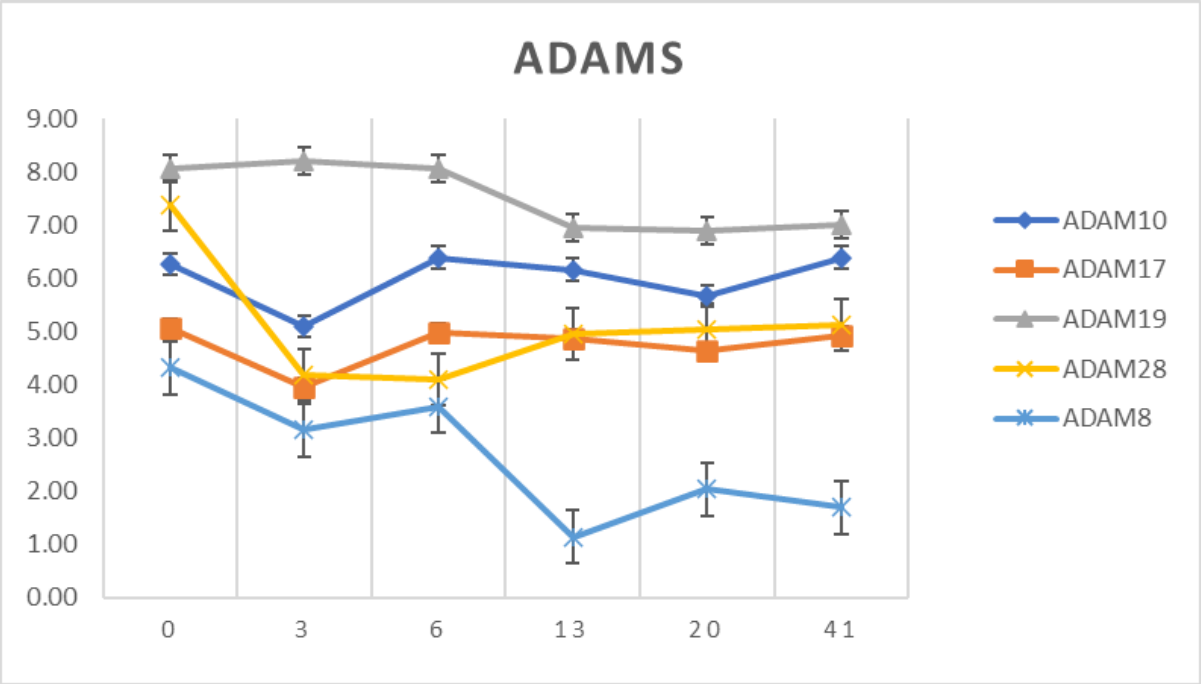

Figure 5.1.1 Gene expression of the ADAM sheddases family in differentiating B-cells

RNA-sequencing data was generated from differentiating B-cells averaged from three healthy donors (Mario Cocco). RNA was taken over a series of time points over the course of the *in vitro* differentiation system, from day 0 consisting of total B-cells out to day 40 when the cell population will consist of long-lived PCs. The averaged expression of the ADAM sheddase family members detected by RNA-sequencing was plotted for each time point. n=3

Initial investigation into the regulation of the cell surface phenotype via shedding of extracellular domains started by looking to see if there was evidence that the ADAM sheddases family was expressed in B-cells and PCs. Existing RNA-sequencing from B-cells differentiation to the PC stage in the *in vitro* system to day 41 was analysed. From this data set the averaged expression levels of any member of the ADAM sheddases family detected were pulled out and then plotted against each other across the time series of the *in vitro* differentiation.

The focus was on expression levels of *ADAM10* & *ADAM17* as these are known to be active sheddases with a common range of targets including NOTCH signalling that can influence cell fate and differentiation status. Therefore, we wanted the know whether these sheddases are expressed during B-cell differentiation and whether they play a role in surface expression. From the RNA-sequencing data we can see that *ADAM17* mirrors the pattern of expression of *ADAM10* just at a slightly lower level in the differentiating B-cells, expression drops from day 0 to day 3 but the increases back up to the initial level of expression from day 6 onward. This fluctuates very slightly at day 20 but overall maintains a relatively consistent level of expression. The pattern of *ADAM10* and *ADAM17* expression for example contrasted with that of *ADAM8* which is repressed progressively during the differentiation process. The RNA data therefore provided evidence of *ADAM10* and *ADAM17* expression in differentiating B-cells. Overall, these genes were maintained at a consistent level regardless of the stage of maturation of the cells and in theory have the potential to be active the entire way through the differentiation. The only time point where there was a modest reduction of expression levels was at day 3 on the activated B-cells which may indicate the necessity to limit surface protein shedding whilst receiving signals to initiate B-cell activation.

Looking at some of the other family members, *ADAM19* has the highest expression out of the ADAM sheddases and decreases from day 6 onwards, *ADAM28* at day 0 had a similar expression level to *ADAM19* however it rapidly decreases at day 3 and is then expressed at a similar level to *ADAM17*. This may indicate a role for different ADAMs at different stage of B-cell maturation with roles in cell-cell interaction, signal transduction and cell migration. It is not implausible to hypothesise that the cells may switch the ADAM they use preferentially depending on the active state and point of differentiation.

5.2.2 Surface expression of ADAMs in the *in vitro* differentiation system

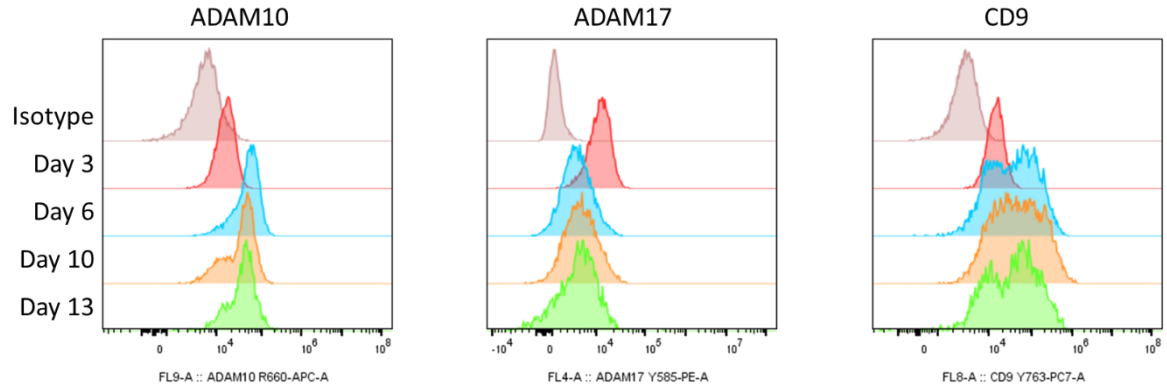

Figure 5.2.1 Surface expression of ADAM10, ADAM17 & CD9 on differentiating B-cells

Surface expression of ADAM10 & ADAM17, along with regulatory protein CD9 was analysed by flow cytometry. Expression levels were assessed on B-cells isolated from a healthy donor and differentiated using APRIL stimulation in the *in vitro* differentiation system. At the major time points, day 3 (activated B-cell), Day 6 (plasmablast), day 10&13 (plasma cells) expression levels were assessed. n=1 (donor C)

Following from the assessment of mRNA expression protein expression was analysed by flow cytometry using the *in vitro* differentiation system. An optimised staining protocol was generated for assessing the surface expression of ADAM10, ADAM17 and the regulatory tetraspanin CD9. Expression levels were assessed on B-cells throughout the *in vitro* differentiation system. It was seen that ADAM10 and CD9 are likely to be co-expressed as they share the same expression pattern over the time course, this observation fits with the literature which indicates CD9 as a co-factor and regulator of ADAM10 activity. CD9 has an inhibitory effect on ADAM10 when co-localised in the cell surface (Gilsanz et al., 2013). Day 3 has the lowest level of expression which increases by day 6 and then is maintained until day 13 when the cells will be terminally differentiated PCs. ADAM10 and CD9 expression differs slightly in that ADAM10 produces a tight peak with only a small shoulder of cells that have lower ADAM10 expression this then reduces by day 13 suggesting most of the cell population has the same level of ADAM10. Whereas the peak created post-day 3 for CD9 expression is very broad, this may indicate varying levels of CD9 activity within

the cell population. ADAM17 on the other hand has the highest level of expression at day 3 and then decreases from day 6 and maintains expression at this level to day 13, this may indicate a preference towards ADAM10 activity in plasmablasts/plasma cells compared to B-cells and the reciprocal use of ADAM17 in B-cells over the use of ADAM10.

Interestingly if there is a preference of ADAM usage at specific time points within the differentiation this may link to ADAM10 and ADAM17 being dominant for specific targets even though it is reported that there is often target cross-over. Activation of the ADAM sheddases by phosphatidyl serine has been specifically linked to ADAM17 function (Sommer et al., 2016) which is present on PCs. A switch from ADAM17 to ADAM10 having the predominant levels of expression reflects a transition of the cells from activated B-cells to plasmablasts and progression along the differentiation process.

5.2.3 Surface expression of ADAMs in the myeloma cell line model

To further assess the ADAM sheddases expression in B-cells and PCs surface expression was analysed in two myeloma cell lines, KMS11 and H929 cells, to provide a disease model. If ADAM sheddases play a role in normal B-cell differentiation their activity or expression levels may be impacted in a disease setting and therefore expression levels were examined in cell lines representing an aggressive myeloma model that is often dispersed with multiple sites of occurrence. If ADAM sheddases can influence differentiation or impact on the levels of surface adhesion molecules or niche factors, then they may be dysregulated in neoplastic cells that have either changed differentiation state or migratory behaviour.

From looking at only two cells lines the full picture of ADAM sheddases cannot be elucidated however the results show that differences can be seen between only two myeloma cell lines. ADAM10 is expressed in both cell lines but with stronger expression relative to the isotype in KMS11. In contrast to ADAM10, ADAM17 staining was no different from the isotype in H929 and at most marginally elevated in KMS11. This pattern appears broadly consistent with the expression data suggested by RNA-seq data in normal plasma cells in which ADAM17 is more highly expressed at day 3 in activated B-cells. Co-factors also differed in expression. CD9 is normally co-expressed with ADAM10 and acts as a regulatory protein that can limit the activity of

ADAM10. In KMS11 cells CD9 and ADAM10 were strongly co-expressed. By contrast in the H929 cell line CD9 expression was not detectable which may result in altered levels or activity of ADAM10. TSPAN8 another potential tetraspanin co-factor was not detected in either cell line, albeit a positive control was lacking and therefore we cannot rule out the antibody having weak binding.

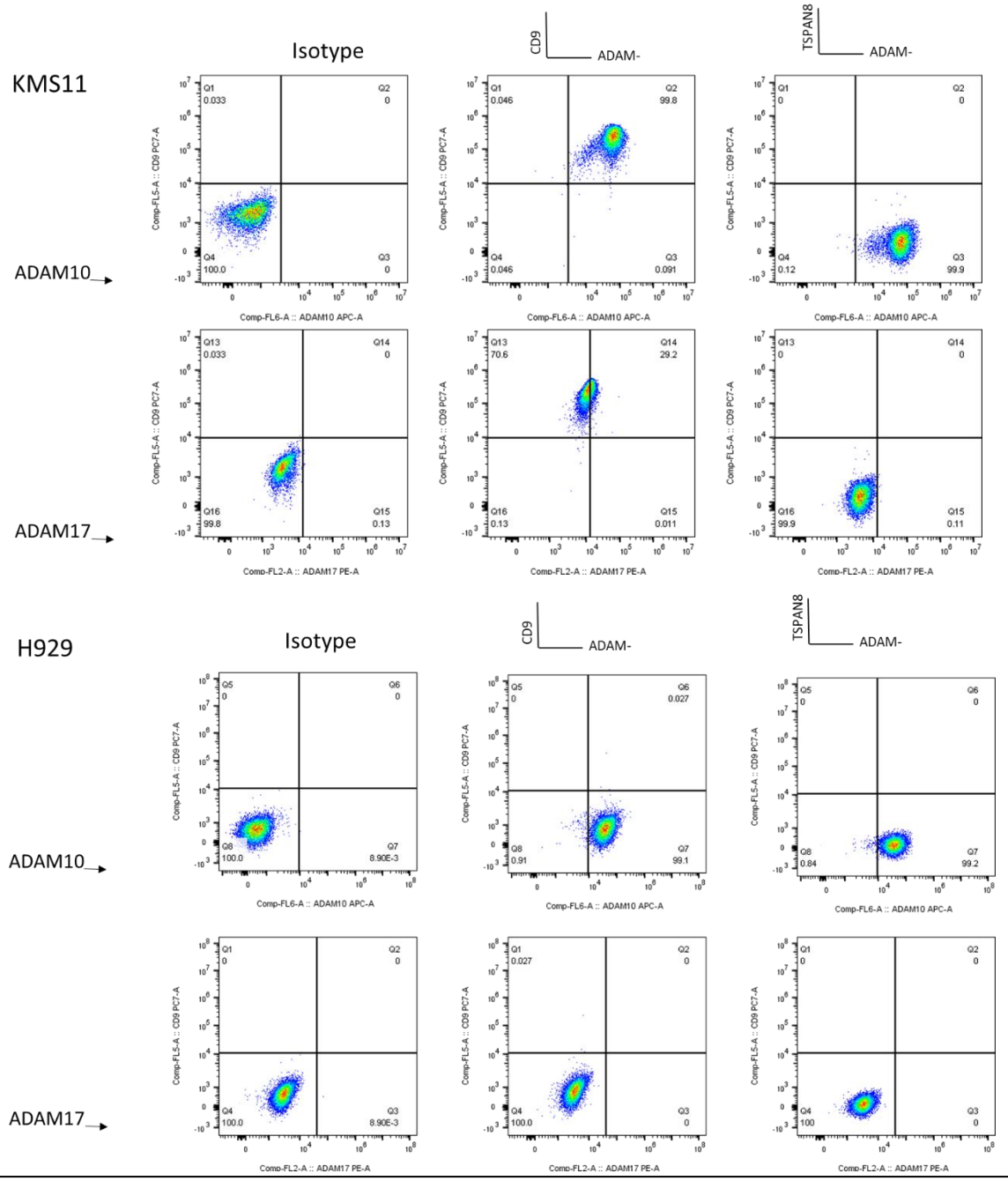

Figure 5.2.3 ADAM10, ADAM17 & cofactor surface expression on myeloma cell lines Using myeloma cell lines (KMS11 & H929) as a disease model. Surface expression of ADAM10, ADAM17 and the tetraspanins CD9 & TSPAN8 were analysed by flow cytometry in KMS11 & H929 cell lines. An isotype control was used to set the gating for positive expression in each of the cell lines. n=2 flow cytometry data shown are representative of two biological repeats

5.3 ADAM shedding of surface ALCAM

5.3.1 Inhibiting ADAM shedding of ALCAM for 24hrs (4μM)

ALCAM surface expression was of interest as previous analysis had revealed two cell populations in the standard differentiation and dynamically changes throughout the time points (See Chapter 3, Figure 3.3.5). One possibility for this dynamic pattern was a process of active ALCAM shedding. To investigate the activity of ADAM sheddases on the surface expression of ALCAM, inhibitors were added to the culture medium to see if blocking their activity would lead to an increase in the level of surface ALCAM. A pan ADAM inhibitor, Marimastat was tested alongside TAPI-2 an ADAM17 specific inhibitor as ALCAM has been identified as a target of ADAM17. The inhibitors were added at 4μM for 24hrs, which had been used in current literature, and then the effect of the level of surface ALCAM was assessed by flow cytometry.

At day 10 and 13 the spread of CD38/CD138 expression was plotted showing the usual spread of CD38 and CD138 although it is evident that adding the inhibitors reduces the percentage of CD138 high expressing cell. Although there is a decrease in the CD138 high cells, the overall patterns of the cell population were maintained in the presence of ADAM inhibitors. The inhibitors at the tested concentration therefore did not substantially impair the differentiation system and the effects seen on ALCAM are likely to reflect direct impact by ADAM inhibition.

The flow cytometry data showed that there were only small changes in the levels of ALCAM surface expression and no large differences between inhibition with Marimastat or TAPI-2 for ALCAM expression. However, it was observed that when Marimastat was added to the culture medium there is a slight reduction in the level of CD138.

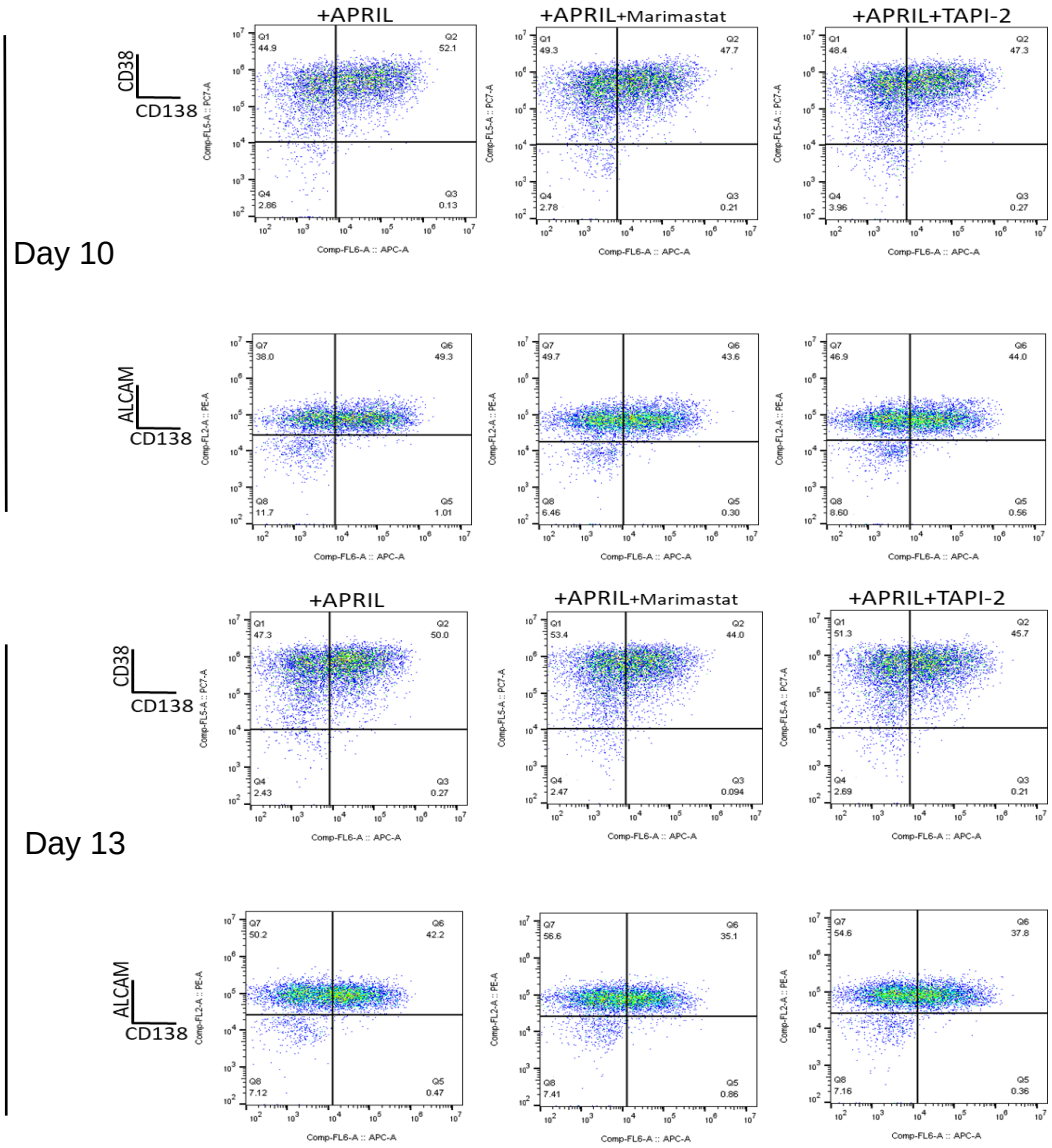

Figure 5.3.1 Inhibiting ADAM sheddases activity for 24hrs effects ALCAM surface expression

Naïve B-cells were differentiated using APRIL stimulation and then cultured with 4μM of either Marimastat (pan) or TAPI-2 (ADAM17) inhibitors and a no inhibitor control condition. Inhibitors were added to the culture medium for 24hrs prior to analysis on day 10 & day 13. Equal numbers of cells were taken and analysed by flow cytometry for ALCAM expression as well as phenotyped for B-cell and PC makers to indicate differentiation state. Flow plots are of one representative donor. Expression was plotted for CD38 against CD138 and with ALCAM against CD138 expression. n=2 representative donor-Donor C

5.3.1.1 *Summary of ALCAM expression levels after 24hrs of ADAM inhibition*

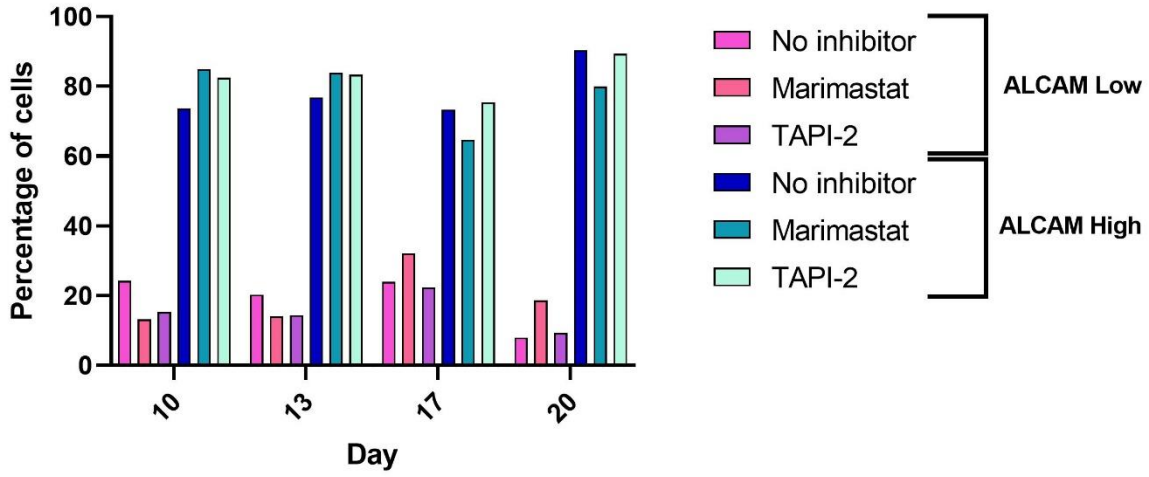

Figure 5.3.1.1 ADAM inhibition for 24hrs effects the ALCAM high/low expressing PC populations

Total B-cells were isolated from 2 healthy donors and differentiated in the *in* vitro system using an APRIL stimulation, the cells were cultured up to day 20. Effects of 24hrs of ADAM inhibition with either Marimastat (pan) or TAPI-2 (ADAM17) or a no inhibitor control condition were used to investigate the shedding of ALCAM. The effects were summarised by plotting the average percentage of ALCAM high and ALCAM low expressing cells after analysis by flow cytometry for time points between day 10 & day 20. n=2 donors B&C

The effects of adding either the pan inhibitor, Marimastat or the ADAM17 specific inhibitor, TAPI-2 on ALCAM shedding and surface expression levels were investigated over the course of a longer B-cell differentiation. Inhibitors were added to the culture medium for 24hrs prior to each time point for flow cytometry analysis, this ranged from day 10 to day 20, at this stage the majority of the cell population will be PCs with a mix of PCs and PBs at the first time point, day 10.

The trend seen for day 10 &13 is that the addition of either ADAM inhibitor marginally increases the percentage of ALCAM high expressing cells and decreases the percentage of ALCAM low expressing cells. This reflected a shift in the cell population to ALCAM high expression levels suggesting that ADAM inhibition may impact on the

level of surface ALCAM expression. There is only a small difference between the increases in ALCAM expression for the cells treated with Marimastat or TAPI-2 may suggest ADAM17 is the most likely sheddases to target ALCAM as the pan inhibitor, Marimastat, did not increase the surface levels any further. However as stated these differences were only small and previous analysis of ADAM surface expression would indicate that ADAM10 is the predominant sheddases on PCs. At the time points for day 17 & 20 the addition of Marimastat the pan ADAM inhibitor decreases the percentage of ALCAM high expression cells below the percentage seen in the condition with no inhibitor, this can be but down to Marimastat having a negative effect on cell viability as it was noticed that the cell number was lower in the Marimastat conditions compared to cells with no inhibitor or with the addition of TAPI-2. Therefore, the earlier time points at days 10 &13 are more informative for revealing the effects on the shedding of surface ALCAM, at these time points in the previous figure using the inhibitors revealed a reduction in the percentage of CD138 high cells and ACLAM high expressing cells are usually also positive for CD138 expression. Therefore, at the later timepoints the decrease in the percentage of ALCAM high is most likely a reflection of the loss of CD138 high expression cells.

5.3.2 Dose response Inhibiting ADAM17 on ALCAM surface expression on differentiating B-cells and plasma cells.

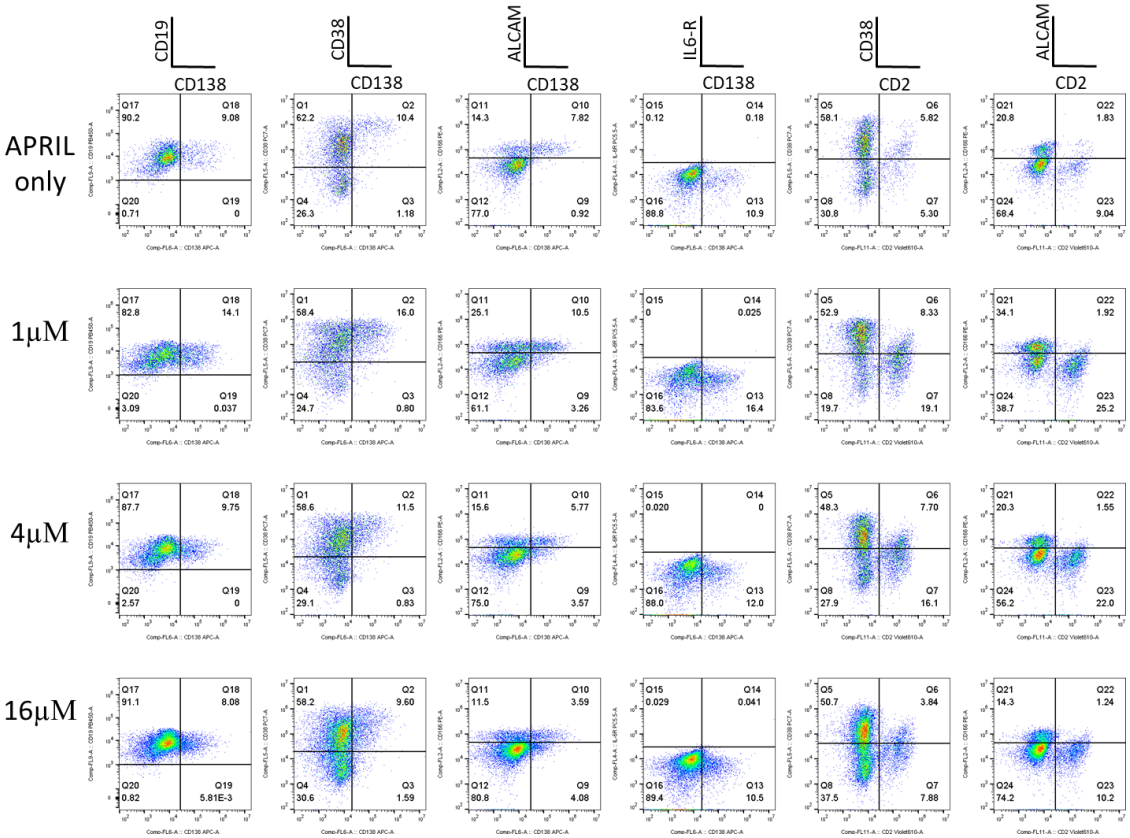

Figure 5.3.1 Dose response of TAPI-2 to inhibit ALCAM shedding on PCs
The ADAM17 specific inhibitor TAPI-2 was added to the media of differentiating B-cells for 4 days at a range of concentrations (1µM, 4µM & 16µM). Above is a representative donor at day 13 of the differentiation after being cultured with the varying doses of TAPI-2 as well as a control condition grown with no inhibitor. The plasma cells were analysed by flow cytometry using a panel of markers to assess the levels of ALCAM as was as the PC state and if there was a presence of any contaminating cell populations. n=1 Donor B

Since ADAM17 inhibition marginally increased surface ALCAM after 24hrs at 4µM a dose response was set up to see if increasing the concentration effected the shedding of surface ALCAM. In addition, the duration of treatment was extended to 4-days rather than 1-day previously tested. Concentrations were chosen that are 4fold higher and 4fold lower that the initial concentration tested (4µM), to assess the effect on ALCAM

shedding and see if a higher concentration and/or a longer treatment duration can enhance the increase in surface ALCAM. An extended staining panel was designed to try and elucidate the cause of the double population generated when plotting with ALCAM expression, the main theory was that the high and low subsets of ALCAM expressing cells reflect active surface shedding at the stages of the differentiation as the high ALCAM subset is double positive for CD138 expression.

The flow plots show that compared to cells cultured alone the addition of TAPI-2 increases the surface expression of ALCAM, specifically that 1μM of inhibitor was the most optimal at increasing the level of ALCAM. Of note was that at the higher concentration at 16μM there is a negative shift in the population in the level of CD138 the main plasma cell marker.

Other markers that were analysed were CD2 for any T- and NK populations. A variable proportion of T and NK cells can be observed in differentiations, which generally reflects expansion after day 6 of culture of small populations of contaminating cells. This can be detected in the core antibody panel as a CD19/CD20 double negative population also lacking CD138. In the example shown these are additionally detected with CD2 and demonstrates that, this population does not account for the ALCAM high expressing cells indicating that the effect we see by inhibiting ADAM17 is a result of inhibition on the B-cells and PCs. Furthermore, CD138 which is co-expressed with ALCAM is not a marker of human T-cells or NK-cells. Another marker that was added into the flow cytometry panel, this was IL6 receptor (IL-6R) which has been reported as a target of ADAM proteases and thus might provide a positive control for the ADAM inhibition. Unfortunately, there was no positive staining in any of the conditions for IL-6R, which may be a result of poor staining by the IL-6R antibody. Overall, this data suggests that the effects of TAPI-2 impacted on the surface expression of surface ALCAM indicating the ADAM protease activity is responsible for at least some of the shedding seen on PCs.

5.3.3 Dose response of Pan-inhibition of ADAM shedding on ALCAM surface expression on differentiating B-cells and plasma cells

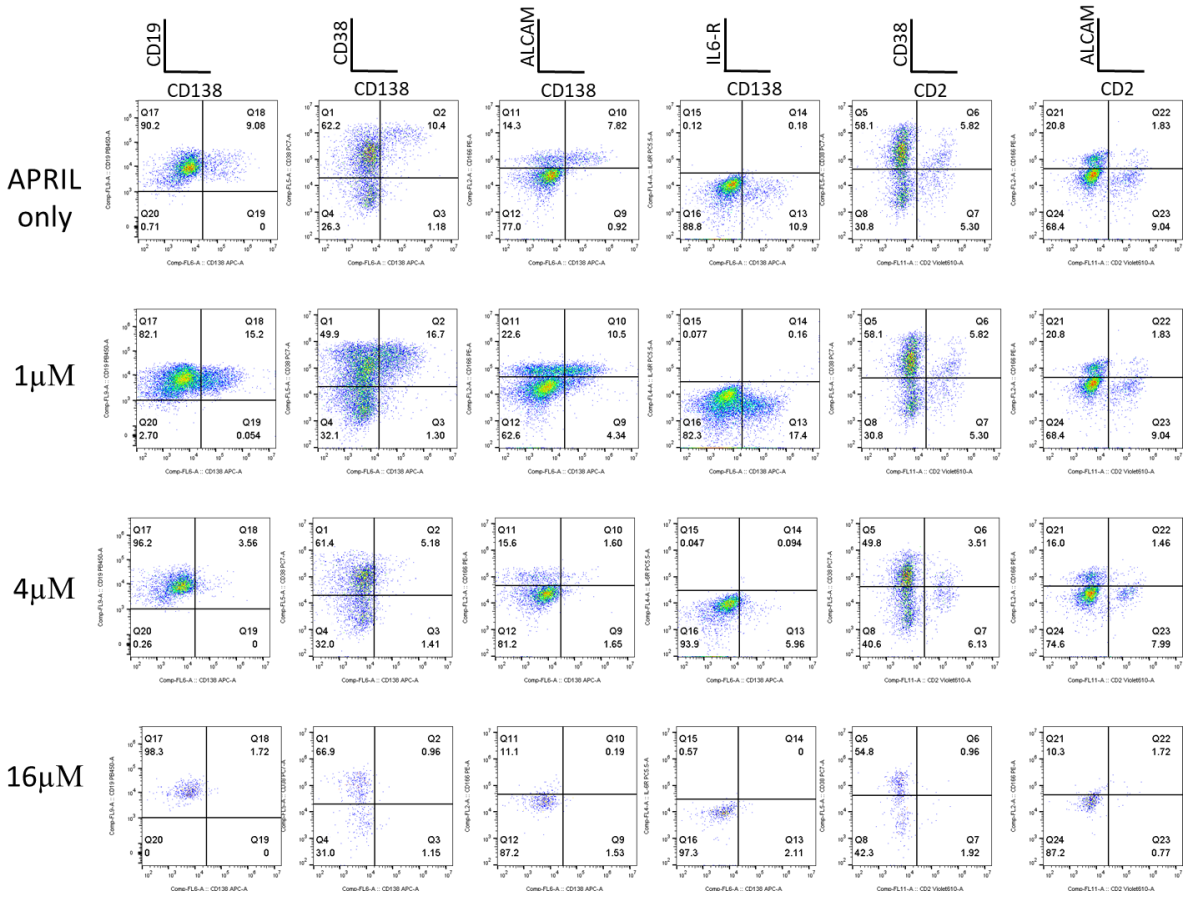

Figure 5.3.2 Dose response of Marimastat to inhibit all ADAM sheddase activity on ALCAM surface expression

Representative donor of plasma cells generated in the *in vitro* differentiation system, that were cultured with or without the pan ADAM inhibitor, Marimastat. A range of concentrations of Marimastat from 1μM-16μM were used for a dose response. The level of surface ALCAM along with PC makers and non-B-cells markers were analysed by flow cytometry at day 13 after the cells had been in culture with Marimastat for 4days. n=1 Donor B

Alongside, testing the effects of inhibiting the dose response using the ADAM specific inhibitor TAPI-2, the pan ADAM inhibitor Marimastat was tested. The same set up was used with the same donor (B) to test the effects of Marimastat on ALCAM surface expression. Concentrations were used 4fold lower and 4fold higher than the initial 4μM

and rather than having the inhibiters in the culture medium for 24hrs, Marimastat was in the culture media for 4days prior to analysis of ALCAM levels by flow cytometry.

The level of surface ALCAM expression was analysed to assess the effect of inhibiting the shedding activity of the ADAM sheddases, cells were analysed on day 10 & day 13 of the differentiation, shown above is day 13 when the bulk of the cell population will be PCs. It was noticeable the after having a higher dose of Marimastat in culture for 4days by day 13 the viability of the cells had been affected in the conditions with a concentration of 4μM and 16μM. The cell population affected most significantly by Marimastat was the $ALCAM^{+}/CD138^{+}$ double positive population in the higher concentration showing a reduction in the percentage of cells as well as a decrease in cell number. However, in the 1μM condition there was an increase in this population similar to that seen with the TAPI-2 inhibitor. This suggests that while at high doses ADAM sheddases inhibition is poorly tolerated by PCs, as a lower dose inhibiting ADAM sheddases can increase the ALCAM high subset of cells. This would be consistent with a model in which ADAM mediated shedding contributes to the generation of differential ALCAM expressing subsets observed in the differentiating PC population.

Treatment with the pan inhibitor, Marimastat increased the ALCAM high population to a similar level to that observed with TAPI-2. Since TAPI-2 is reported to be relatively specific for ADAM17 over ADAM10 it suggests a predominant control via ADAM17. However, at the dose used it is conceivable that both ADAM17 and ADAM10 were inhibited, and a definitive statement is not possible, particularly given the preferential expression of ADAM10 at this time point. Marimastat appears to significantly affect the $CD138^{+}$ cells which may be an off-target effect whereby another ADAM sheddases other than ADAM17 that may be involved in another signalling pathway that impacts B-cell differentiation.

The extended staining panel that was used when assessing the effects of TAPI-2 on ALCAM expression was also used when assessing the effects of Marimastat. Comparing control to inhibitor treated cells using 1μM of Marimastat indicated that inhibiting ADAM sheddases enhanced B-cell differentiation when considering the distribution of cells from CD38 expression against CD138. There is a higher percentage of double positive cells when 1μM of Marimastat is added to the culture

whereas the higher concentrations had a negative impact suggesting that there is a fine balance of sheddases activity during the differentiation process.

5.3.4 Percentage change of ALCAM expression on plasma cells with ADAM inhibition

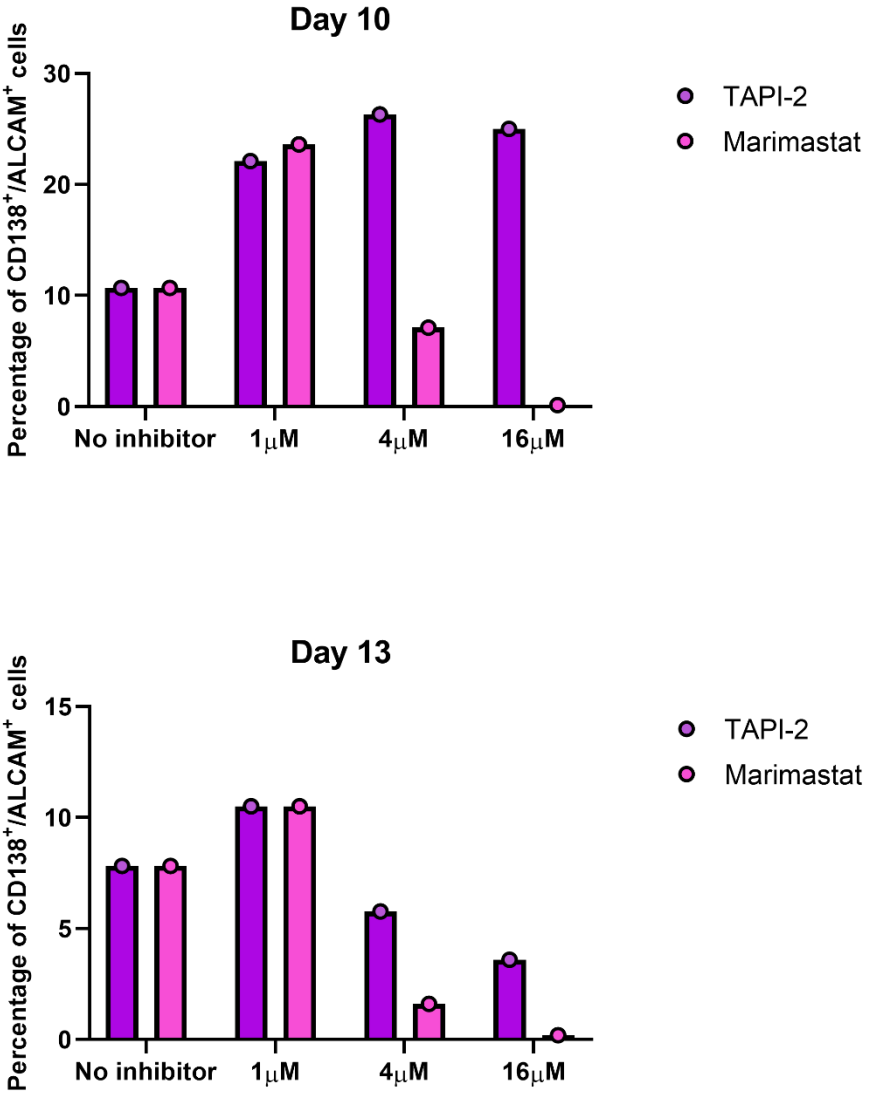

Figure 5.3.3 Percentage of ALCAM⁺ plasma cells following ADAM inhibition with either TAPI-1 or Marimastat

Summary of the ADAM inhibitor dose response on the effect of surface ALCAM, at day 10 and day 13 of the differentiation system. Percentage of CD138⁺ and ALCAM high expressing cells was plotted for each inhibitor (Marimastat and TAPI-2) in accordance with the doses of inhibitor used. Graphs were generated for the expression levels recorded on day 10 & 13 after the inhibitors had been in the culture for 4days. n=1 tested in one healthy donor-donor B.

The percentage of cells in the ACLAM high population was quantified using the Flowjo analysis software, the percentage of cells double positive for ALCAM and CD138 expression was measured in the top right quadrant of the flow plots. The change in percentage of the ALCAM high population shows and increase in surface expression from the condition where the cells were cultured without an ADAM inhibitor therefore the changes seen are in response to the blocking of ADAM activity. The levels of ALCAM expression at day 10 after having the ADAM inhibitors, TAPI-2 and Marimastat in culture for 4 days revealed that TAPI-2 successfully increased ACLAM levels by at least 40% with the lowest concentration of 1μM and this was slightly higher at 4μM & 16μM, this however was not seen at day 13 which saw the largest increase using 1μM of TAPI-2 of 20%.

In comparison to day 10 using the higher concentrations of TAPI-2 at 4μM and 16μM at day 13 did not increase the levels of ALCAM above that seen using 1μM. Using 4μM of TAPI-2 increased ALCAM above the percentage with no inhibitor, however adding 16μM had a lower percentage of cells expressing high levels of ALCAM than the cells with no inhibitor in culture. This may in part be due to the addition of inhibitor added at day 10 before the analysis at day 13, continued exposure to the ADAM inhibitors may have started to have a toxic effect on the cells. The effect on cell viability was more prominent on the cells cultured with Marimastat, but this inhibitor also increased the percentage of ALCAM high cells at the lower concentrations where viability was less impacted.

5.3.5 Effect of ADAM inhibition of ALCAM surface expression on differentiating plasma cells

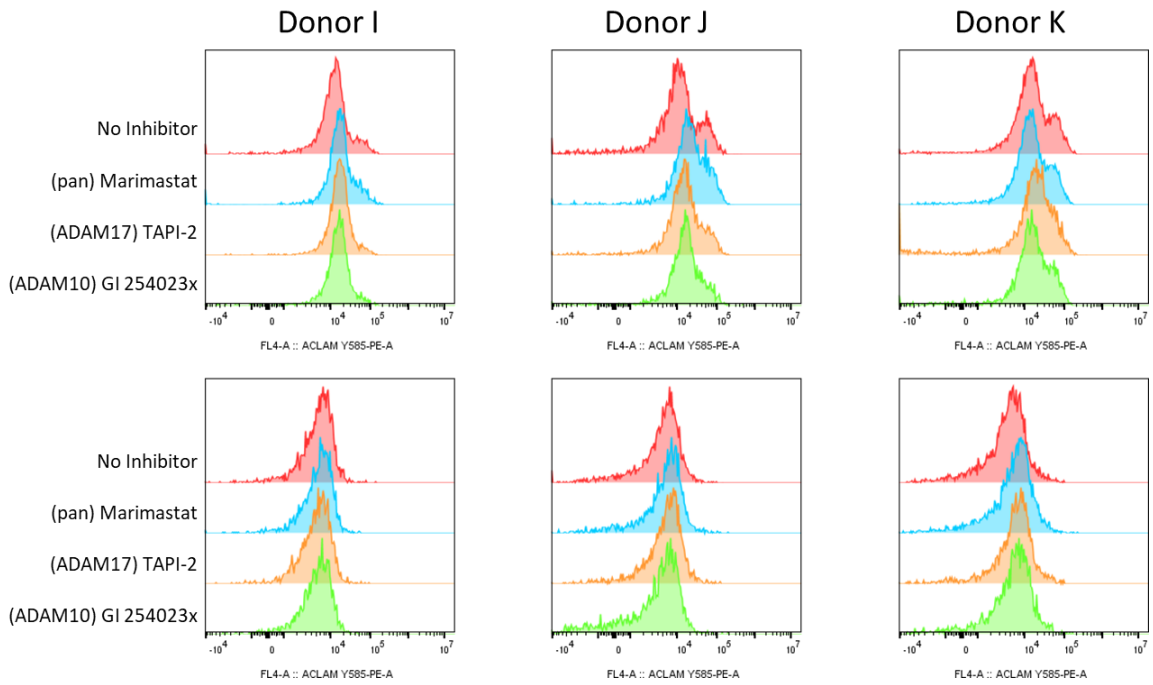

Figure 5.3.4 ACLAM expression on PCs cultured with either TAPI-2, GI 254023x or Marimastat

Total B-cells were isolated from peripheral blood from 3 healthy donors and differentiated to plasma cells using the *in vitro* differentiation system with an APRIL stimulation. The effect of inhibiting ADAM shedding on the surface expression of ALCAM, the pan ADAM inhibitor, Marimastat, ADAM17 specific inhibitor TAPI-2 and the ADAM17 specific inhibitor GI 254023x were used at a 1μM concentration. The inhibitors were added to the culture media for 4 days before ALCAM surface expression was analysed (day 10 & day 13), along with a control condition with no inhibitor added to provide a baseline level of ALCAM surface expression.

Following on from the dose response experiments using varying concentrations of the ADAM inhibitors, Marimastat, TAPI-2 and GI 254023x, it was evident that there is a significant effect on cell viability using the higher concentrations and therefore the effect on ALCAM surface expression is lost. Therefore, the ADAM inhibition experiment was repeated using a concentration of 1μM for each of the inhibitors to assess to the effect on inhibiting surface shedding of ALCAM. Total B-cells were

isolated from peripheral blood from 3 healthy donors and differentiated into PCs using APRIL stimulation. The cells were cultured in the presence of the ADAM inhibitors for 4-days before analysis of ALCAM surface expression by flow cytometry. ADAM inhibitors were added to the culture media on days 6 and day 10 as previous analysis has shown that the highest levels of ALCAM expression was seen on $CD138^{+}$ therefore surface expression was analysed at day 10 and day 13 when the cell population will transition from plasmablasts to PCs.

Surface expression of ALCAM was analysed by flow cytometry and then plotted as histograms for each donor on days 10 & 13 against a control condition where the cells were cultured without the presence of an ADAM inhibitor. Levels of ALCAM surface expression were similar between donors however there was a small shoulder of expression seen which indicate a small population of ALCAM high expressing cells and this is where the donors vary slightly in the proportion of ALCAM high population. With the addition of the ADAM inhibitors by day 10 this shoulder of expression is reduced compared to the no inhibitor control with a slight shift in the entire cell population towards the level of the high expressing cell population. This shift is seen more prominently with the addition of TAPI-2 inhibitor which is specific for ADAM17 which has been indicated as the main sheddases for ALCAM expression, this shift is also seen with the use of the pan inhibitor, Marimastat. The shoulder of expression is not seen at the day 13 time point, which reflect of the effect that the cells had previously been exposed to the presence of ADAM inhibitors prior to the day 10 time point. There is a marginal shift of the entire population in the ADAM conditions to suggest a reduction in the amount of ALCAM shedding causes an increase the overall level of ALCAM expression.

Although the change in ALCAM surface expression is only subtle with the addition of ADAM inhibitors a 1μM in this experiment the previous dose response shows that surface expression of ALCAM can be increased with the addition of ADAM inhibitors indicating that ADAM sheddases are active on PCs and ALCAM is one of the targets however the difficulty of the experimental design is the effect on cell viability which means looking at the effects in a long term culture becomes problematic with a trade-off between efficacy of the inhibitor and the toxicity to the cells.

5.3.6 Dose response of ADAM inhibitors in cell lines

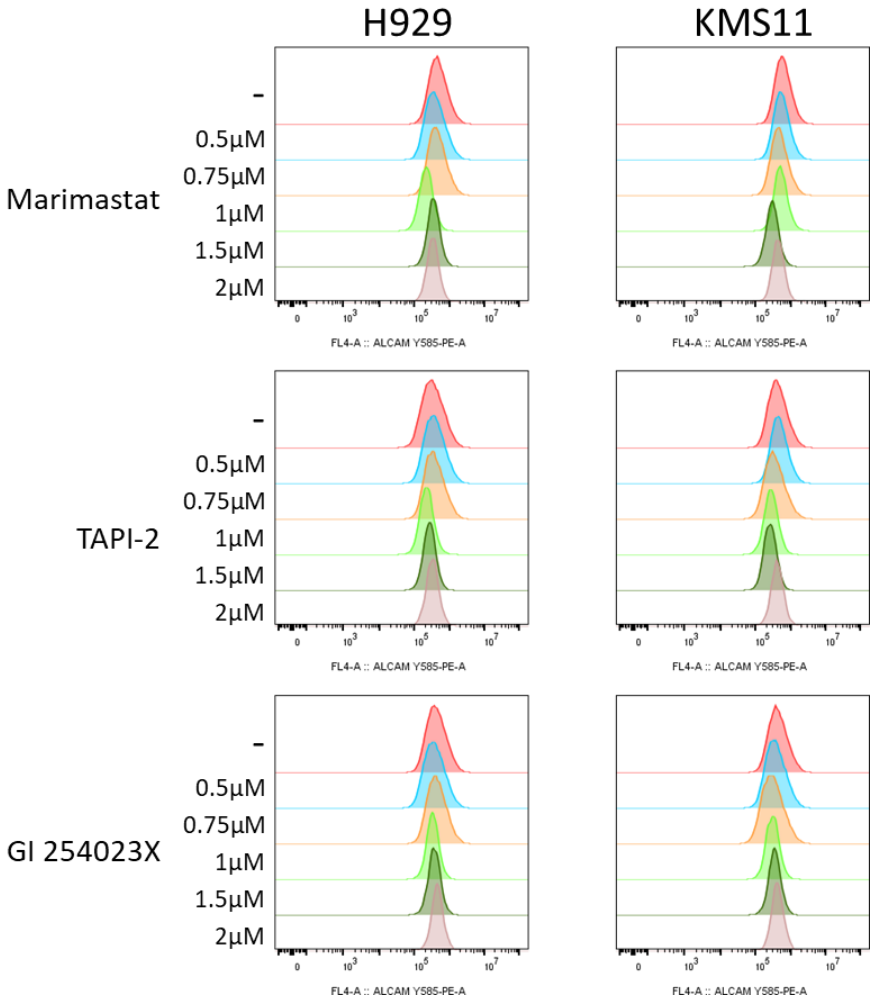

Figure 5.3.6. Dose response of the effects of the ADAM inhibitors on ALCAM expression in myeloma cell lines

Myeloma cell lines H929 & KMS11 were cultured either alone or with the addition of ADAM sheddase inhibitors, Marimastat (pan), TAPI-2 (ADAM17) or GI 254023x (ADAM10). A dose response was created by adding the inhibitors at varying concentrations ranging from 0.5µM-2µM. Inhibitors were added to the culture media 4days prior to analysis of ALCAM expression by flow cytometry.

Having observed the effects of ADAM sheddases inhibition in in primary B-cell differentiation it was interesting to determine whether the effects on ALCAM expression could be observed in myeloma cell lines. I therefore tested all three ADAM sheddases inhibitors we had available, Marimastat (pan), TAPI-2 (ADAM17) & GI 254023x (ADAM10) and see how this affected ALCAM surface expression.

Previous experiments showed that the addition of Marimastat and TAPI-2 inhibitors at concentrations at 4μM and higher impacted cell viability without enhancing the efficacy of the ADAM sheddases any further. Therefore, a dose response was set up using much lower concentration of the inhibitors that started at 2μM and decreased from there down to 0.5μM. As done with earlier inhibition experiments the inhibitors were added into the culture medium for 4 days before the effect on expression was assessed.

The same two myeloma cell lines, H929 and KMS11, were used to assess the effects of ADAM inhibition in surface expression. From the earlier figure (Figure 5.2.3) of the ADAM phenotyping experiments, we know that the levels of ADAM10 & ADAM17 vary between the cell lines as well as the level of ALCAM expression seen on the cell lines (Figure 3.5.1). Here we wanted to know whether the lower doses of the ADAM inhibitors would affect the expression of ALCAM on the cell lines in a similar manner to that seen on the differentiating B-cells. This dose response was set up using all three commercial inhibitors purchased Marimastat (pan), TAPI-2 (ADAM17) and GI 254023x (ADAM10). The ADAM10 inhibitor GI 254023x was introduced as ADAM10 was found to be more highly expressed in the myeloma cell lines but also on the PCs in the *in vitro* differentiation system suggesting that although ADAM17 is thought to target ALCAM, it is likely that ADAM10 is the most active sheddases on PCs.

The surface expression of ALCAM was assessed by flow cytometry and revealed that there was no increase of expression with any inhibitor regardless of the concentration used. From the results testing the inhibitors on the primary PCs concentrations above 1μM if anything resulted in a reduction of the ALCAM high population and may also be seen here will the loss of the shoulder of the peak and most of the population having slightly lower ALCAM expression than the no inhibitor condition.

The small changes in ALCAM expression seen from blocking the ADAM activity was surprising particularly with the GI 254023x inhibitor specific for ADAM10 which we know is expressed to on the cell lines from the initial phenotyping experiments. However, since the overall expression level of ALCAM is very high in the myeloma cell lines it suggests that despite surface expression ADAM sheddases may not be active against ALCAM or are dysregulated on the myeloma cell lines. This could be due to regulation of the sheddases by co-factors such as tetraspanins like CD9 or the

dependency of localisation on the cell surface to the ADAM targets. It could also be due to a lack of activation such as phosphatidyl serine exposure which is high on PCs but may be lower in the context of the myeloma cell lines.

5.3.7 Inhibiting ADAM shedding affects cell viability.

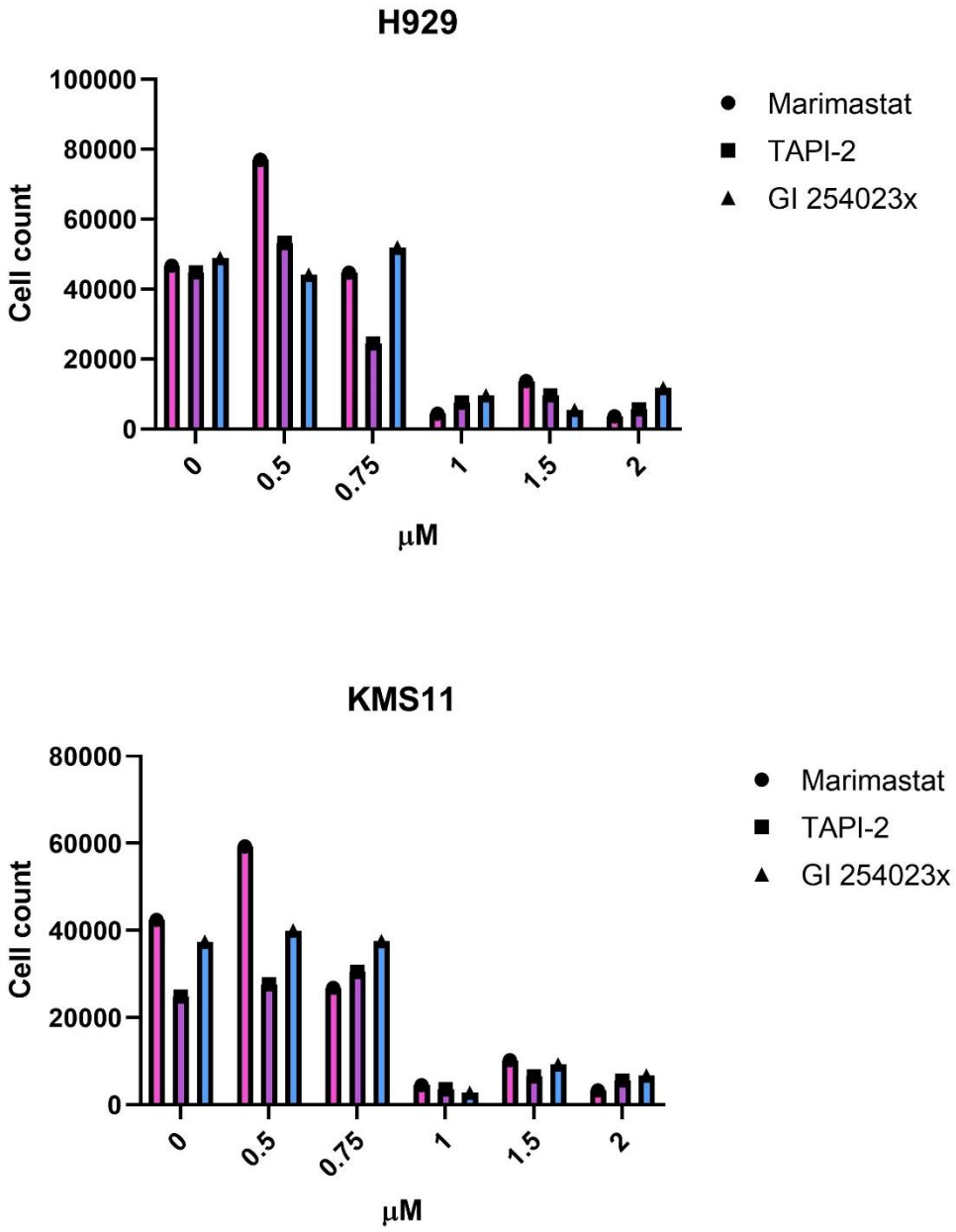

Figure 5.3.6 Cell viability is affected by the use of ADAM inhibitors
Cell counts were taken for cell lines H929 & KMS11 when cultured with or without the range of ADAM inhibitors (Marimastat, TAPI-2 or GI 254023x). Inhibitors were added as a dose response starting at 0.5µM and ranging up to 2µM, the cells were cultured for 4days with the inhibitors before analysis and cell counts taken.

Cell viability was assessed when cultured with or without the 3 different ADAM inhibitors (Marimastat, TAPI-2 or GI 254023x), the inhibitors were added as a dose response ranging from 0.5μM-2μM. Cell counts were taken after the inhibitors had been in the culture medium for 4 days, counts were plotted for one single repeat. For both cell lines H929 & KMS11 the cell number drops significantly once all three inhibitors reach 1μM. There does not appear to be much difference between the effect of the inhibitors whether it is specific for ADAM10 (GI 254023x), for ADAM17 (TAPI-2) or the pan inhibitor (Marimastat). From this dose response it appears that using the inhibitors at a concentration of 0.75μM would be the optimal concentration for cell viability but the efficacy may be lower than the higher concentrations.

The effects on cell number confirm observations in previous experiments that there is a loss of cell viability using higher concentrations of inhibitors, due to some form of toxic effect. However, the contrast between cell viability at 0.75μM compared to 1μM is quite striking and the drop in cell viability follows the same trend for each of the ADAM inhibitors given the small increment the drug concentration was increased by. It is unclear whether this is a genuine effect of the inhibitors on a survival pathway or whether an issue with the efficacy of the aliquots of drugs used, for example too many freeze thaw cycles may have contributed if multiple aliquots were used to set up the dose curve. As a control it would have been beneficial if there were a downstream target of the ADAMs included in the flow cytometry panel, this would have indicated whether the activity of the ADAMs had been inhibited. It is unknown whether this is a blockade of a specific cell signalling pathway that would otherwise be activated or switched off, had the cells maintained their usual level of ADAM activity.

5.4 ADAM shedding of surface PCDH-γ proteins

5.4.1 Effect of Inhibiting ADAM10 and total ADAM sheddases on PCDHG in cell lines

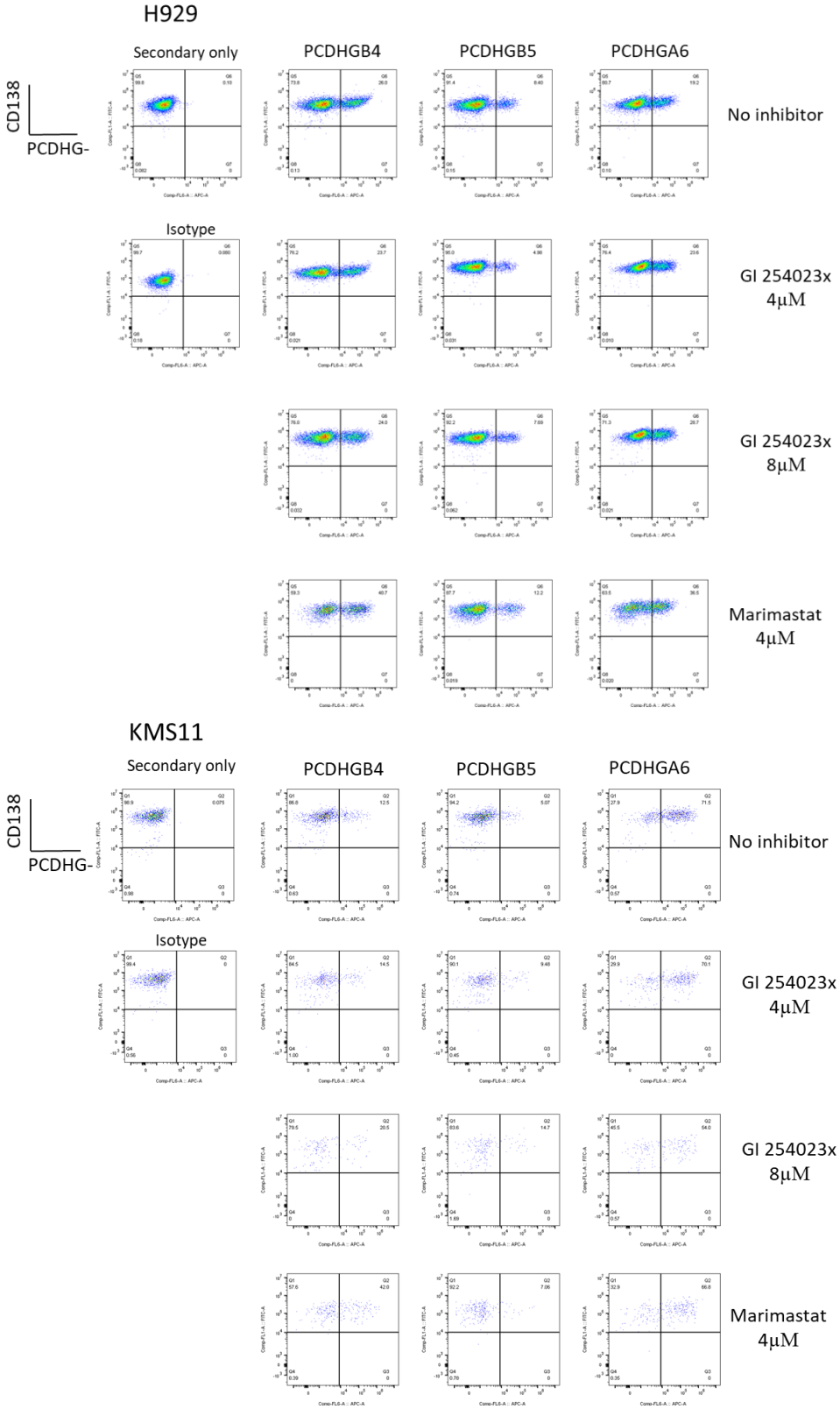

Figure 5.4.1 Effect on PCDHG surface expression on myeloma cell lines following ADAM inhibition.

The effects on PCDHG surface expression were assessed by inhibiting the ADAM sheddases in myeloma cell lines KMS11 & H929. ADAM shedding activity was inhibited with 4μM of GI 254023x (ADAM10) or Marimastat (pan) and then a higher dose of 8μM of GI 254023x was also trialled. The effect of inhibiting ADAM10 or all ADAM sheddases for 4 days was assessed by flow cytometry to see the effect on surface expression of PCDHG isoforms, GB4, GB5 & GA6. The staining of the PCDHs was validated using a secondary only stain and rabbit IgG as an isotype control.

Since the sensitivity of different surface proteins to sheddases activity may vary, a pilot experiment was conducted to test if the PCDHG surface proteins are subject to proteolytic cleavage by the ADAM sheddases using myeloma cells lines, and the pan ADAM inhibitor, Marimastat and the ADAM10 specific inhibitor GI 254023x. The ADAM10 specific inhibitor was trialled as it has been identified to target the clustered and non-clustered PCDHs (Bouillot et al., 2011; Reiss et al., 2006). The effect of inhibiting ADAM10 with GI 254023x on the surface expression if the PCDHG isoforms was initially trialled on myeloma cell lines H929 and KMS11 at 4μM and 8μM. Due to the PCDHG proteins being expressed at such a low percentage, using higher concentrations were chosen in order to increase any effects seen. The pan inhibitor Marimastat was also used at the trialled concentration of 4μM in case ADAM10 was not the main sheddase of the PCDHG proteins.

The inhibitors were added to the culture media for 4-days before the effects were analysed by flow cytometry. The flow plots reveal that the highest level of endogenous expression was of PCDHGA6 followed by PCDHGB4 while PCDHGB5 had the lowest expression in KMS11 cells. Upon addition of either of the inhibitors there was an increase in the percentage of cells with positive expression and it was also noticeable that the spread of CD138 expression was increased particularly with the higher dose of GI 254023x and with Marimastat. The other effect seen with the pan and higher dose of ADAM inhibition was that there was a decrease in cell number suggesting that the inhibitors were having a negative effect on cell viability.

Specifically looking at the effect of the shedding activity on the expression PCDHG isoforms there is a clear shift in the cell population in comparison to the distribution of cells in the no inhibitor condition. Increasing the concentration of GI 254023x does appear to increase the expression of PCDHGA6 however the change in expression for PCDHGB4 & PCDHGB5 is less obvious, which may indicate preferential targeting of ADAM10 for PCDHGA6.

5.4.1.1 Summary of percentage increase with surface shedding inhibition

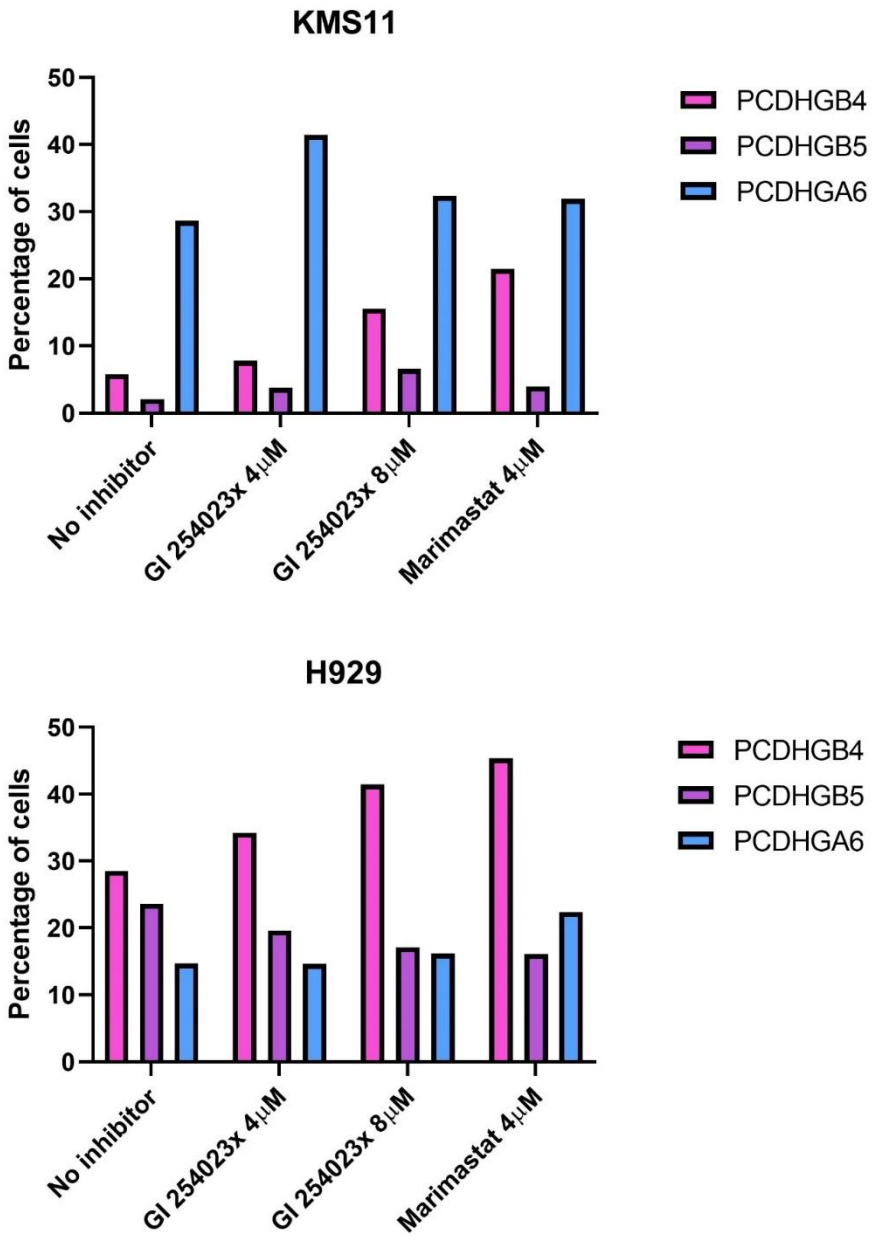

Figure 5.4.1.1 Percentage change of PCDHG^{+}/CD138^{+} cells when the myeloma cells are cultured with ADAM inhibitors.

The effects of the dose response were summarised by plotting the percentage increase of the PCDHG isoforms. The percentage of cells that had positive PCDHG expression for each of the three isoforms analysed were quantified above to show the effect on expression with the inhibition of the ADAM sheddases with either GI 254023x (ADAM10) or Marimastat (pan) after 4days in the culture media. An average percentage was calculated from three repeat experiments. n=3

To summarise the effects seen on the myeloma cell lines by inhibiting the ADAM sheddases and assessing the effect on PCDHG expression the percentage positive cells was plotted for each isoform. The ADAM inhibitors GI 254023x and Marimastat, were added to the myeloma cell cultures 4-days prior to analysis by flow cytometry. Expression on the PCDHG isoforms was plotted against CD138 expression, and gating was set using a secondary only control to provide a background level of staining. The percentage of CD138/PCDH double positive cells was used to assess the effect of blocking ADAM shedding activity for each PCDHG isoforms, PCDHGA6, PCDHGB4 and PCDHGB5. The percentages are an average of three repeat experiments to account for any variations in the passage of cells used for the analysis. Using two different concentrations of the GI 254023x inhibitors, 4μM and 8μM, had differing effects on the two myeloma cell lines. The expression of PCDHGB4 shows a small increase in expression when ADAM shedding activity is inhibited, this increase gradually rose with an increase in GI 254023x concentration from 4μM to 8μM in both cell lines. The KMS11 cells overall appeared to be more responsive to ADAM inhibition than the H929 cells displaying the largest increases in PCDHG expression. PCDHGA6 expression on KMS11 cells was increased using the ADAM10 inhibitor at the lower concentration of 4μM proving to be more effective than the 8μM concentration, this shows that there is a threshold at which increasing the dose of the inhibitor does not further increase the level of surface expression. PCDHGB4 was selectively increased in both cell lines but the other two proteins, PCDHGB5 & PCDHGA6, were not significantly affected.

These results confirm that the ADAM sheddases do target the PCDHG proteins however PCDHGB5 expression was not significantly impacted in either cell line whereas PCDHGB4 and PCDHGA6 did show an increase with the blockade of ADAM10. This indicates that even within the same family ADAM sheddases show selectivity over their targets which can be explained by localisation on the cell surface which is known to limit ADAM activity as well as regulatory proteins. Further investigation into surface localisation would be needed to confirm this and the finer details of the dynamic between surface expression and shedding by the ADAM family.

5.4.2 Dose response of ADAM inhibitors in cell lines

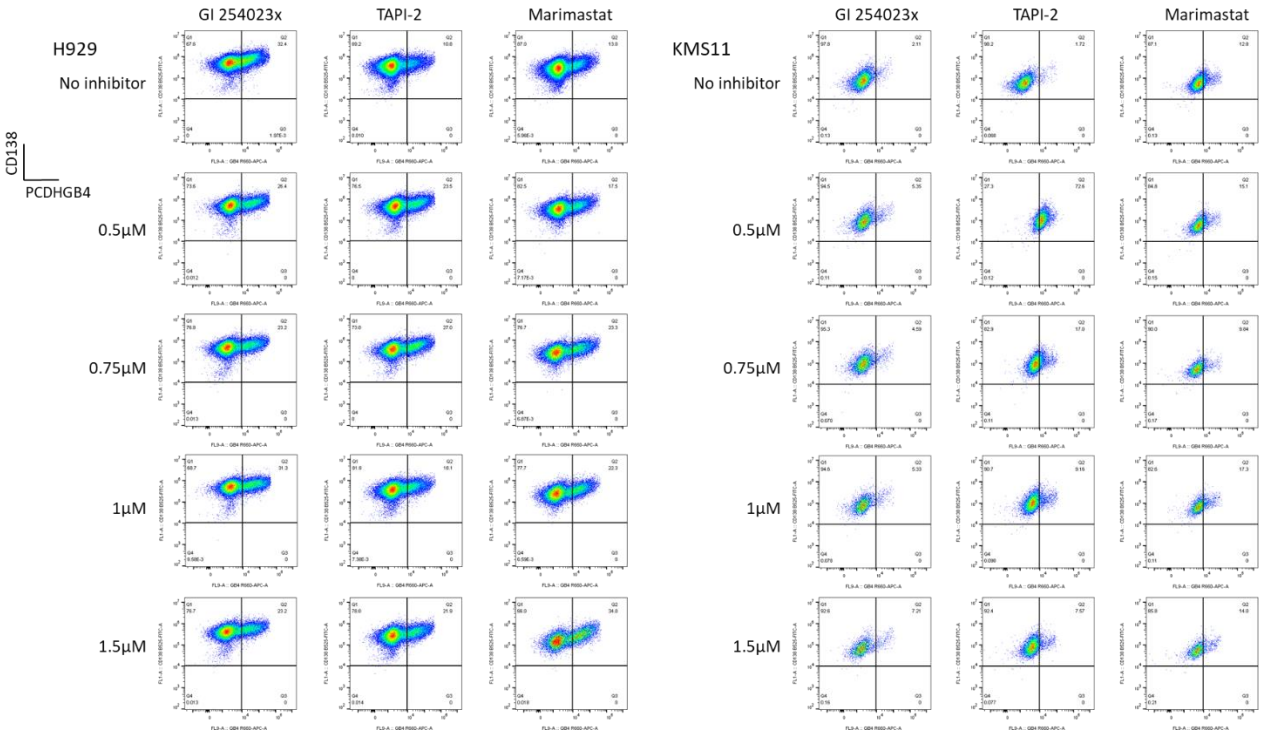

Figure 5.4.1 Effects of the dose response of the ADAM inhibitors on PCDHGB4 surface expression on cell lines

A dose response using three ADAM inhibitors (GI 254023x, TAPI-2 & Marimastat) was tested in two myeloma cell lines H929 and KMS11 for the effect on PCDHGB4 surface expression. Concentrations ranged from 0-1.5µM and were added to the culture medium for 4days before analysis by flow cytometry. PCDHGB4 was used as the readout for inhibiting shedding from the cell surface using the secondary staining protocol. n=2

Previous pilot experiments had shown that having high concentrations of ADAM inhibitors in the culture medium for a prolonged period had an impact on cell viability. Therefore, a dose response around a concentration of 1µM which had previously seen to be effective at reducing cell surface shedding was tested on myeloma cell lines. The myeloma cell lines chosen, H929 and KMS11 were chosen as they differ in that KMS11 cells are semi-adherent whereas H929 cells grow fully in suspension. Therefore, we anticipated that KMS11 cells may express a higher level of adhesion molecules and therefore we may see slight differences when adding the ADAM

inhibitors to the culture media. A dose response had been carried out using ALCAM as the readout of shedding inhibition however this revealed that the myeloma cell lines were not responsive to ADAM inhibition, therefore the dose response was repeated using PCDHGB4 as the readout. All three ADAM inhibitors were trialled in this dose response to account for both ADAM10 and ADAM17 activity as well as using the pan inhibitor. Using both the specific inhibitors will indicate if there is any redundancy between ADAM10 and ADAM17. Although the phenotyping experiments suggest that ADAM10 is more likely to be the predominant sheddases in mature PCs as these are myeloma cells lines their behaviour and responses may be quite different to healthy PCs.

Two different myeloma cell lines were used as cell lines are known to behave quite differently depending on the genetic abnormalities they harbour. H929 and KMS11 cells were chosen as they grow differently in culture, H929 cells grow in suspension whereas KMS11 cells appear to be semi-adherent in that they form small clusters of cells in suspension. The amount of shedding seen varied between the two cell lines with H929 cells having a higher percentage of PCDHGB4 expressing cells but did not appear responsive to the inhibitory effect from the ADAM inhibitors. The KMS11 cells had a lower percentage of PCDHGB4 expressing cells but did appear responsive to the ADAM inhibitors. It was noted that the KMS11 cells responded better to the specific ADAM10 & ADAM17 inhibitors, GI 254023x and TAPI-2 respectively.

The percentage of cells positive for PCDHGB4 expression in the KMS11 cell line gradually increased with the addition of the ADAM inhibitors at increasing concentrations compared to the no inhibitor control. However, due to the variability these results were inconclusive in at identifying a concentration with optimal efficacy. Therefore, the next question to be addressed is how does the concentration effect cell viability. When the inhibitors are to be used in the primary differentiation system this will be important as the inhibitors are added sequentially over a long-term culture. Another factor to consider is that there is only a very small percentage of cells that have positive expression for an individual isoform therefore using a concentration that will show the greatest effect is needed.

5.4.2.1

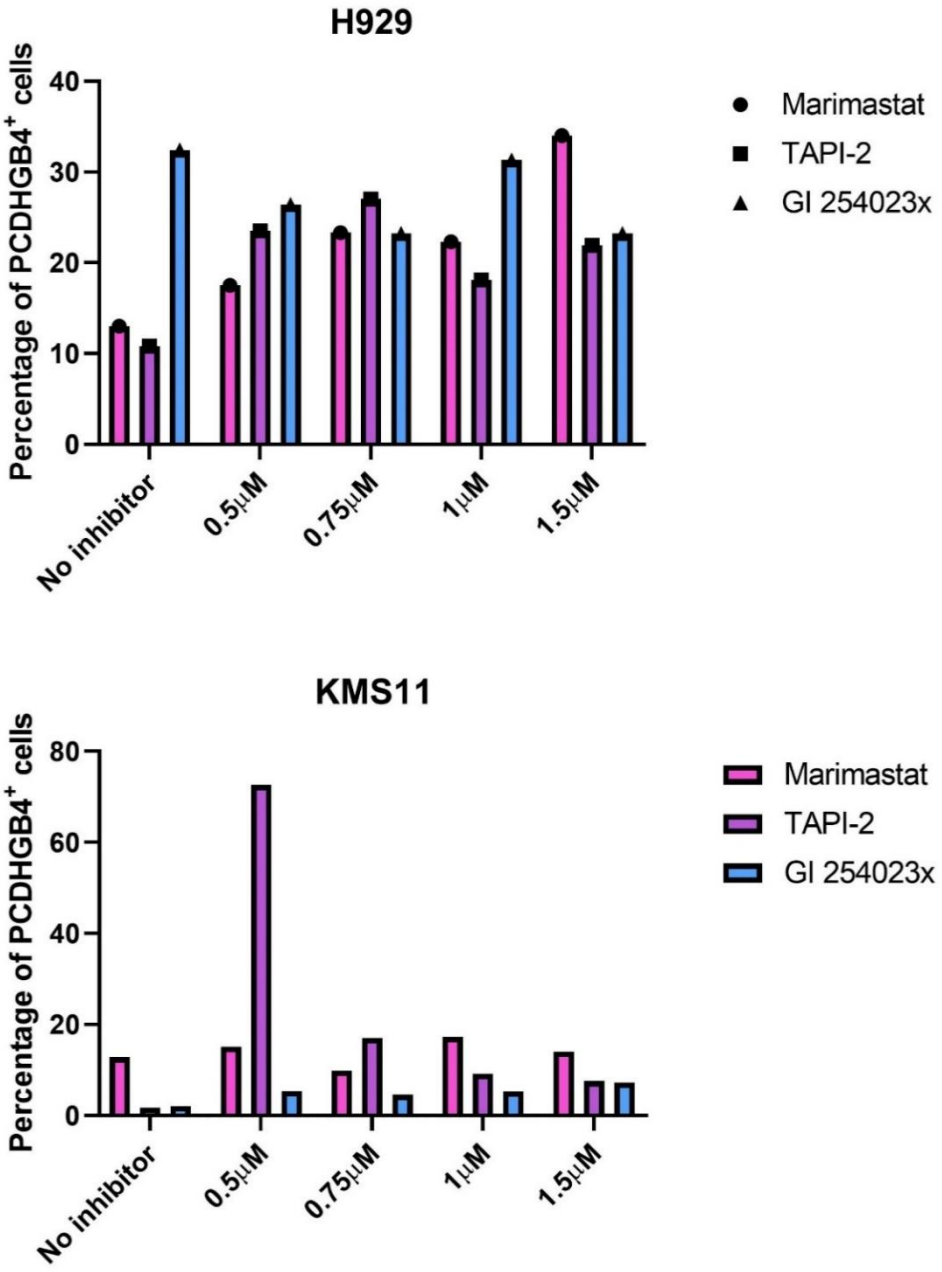

Figure 5.4.2.1 Change in percenoage pf PCDHGB4^{+} with the use of ADAM inhibitors as a dose response

Summary of the effects of the ADAM inhibitor dose response on PCDHGB4 surface expression. The percentage of PCDHGB4 positive cells for each concentration including the control condition, no inhibitor added, was plotted for each ADAM inhibitor (Marimastat (pan inhibitor), TAPI-2 (ADAM17) & GI 254023x (ADAM10)). Cells were cultured with or without the inhibitor for 4days and then analysed for PCDHGB4 surface expression to test whether inhibiting the ADAMs reduces surface shedding of adhesion molecules.

The effects of the ADAM dose response were summarised for each cell line, H929 and KMS11. The effectiveness of blocking ADAM shedding activity was measured using the percentage of PCDHGB4/CD138 double positive cells. Plotting the percentage of surface PCDHGB4 following culture with or without the ADAM inhibitors revealed the effect of the dose response in two different myeloma cell lines, H929 and KMS11 cells. It was observed that there are varying levels of surface expression in the condition with no inhibitor for both cell types indicating that expression levels are dynamic and can change even within the same cell population.

In the H929 cell line the percentage of cells expressing PCDHGB4 increased with the addition of each of the ADAM inhibitors, regardless of concentration. If comparing directly against the no inhibitor control, there is an enhanced increase using 0.5μM and 0.75μM this dips marginally as the concentration increases. The effect on PCDHGB4 fluctuates between the inhibitors which is also reflected in the no inhibitor controls which is likely due to sampling selecting a population of cells that inherently have more PCDHGB4 expression regardless of the activity of the ADAM sheddases.

The expression on KMS11 cells is significantly lower than that seen in the H929 cells line with only small increases in the percentage of PCDHGB4 positive cells with the use of ADAM inhibitors even with the highest concentration of 1.5μM. However, the specific ADAM inhibitors GI 254023x (ADAM10) and TAPI-2 (ADAM17) consistently increases PCDHGB4 more than the pan inhibitor, Marimastat. Literature indicates that ADAM10 is the prevalent sheddases responsible for PCDH shedding, however the ADAM17 inhibitor also increases PCDHGB4 surface expression showing some cross over between the two ADAM sheddases.

The results from the dose response does not indicate an obvious concentration that the most efficient for inhibiting the shedding of surface PCDHGB4 using the ADAM inhibitors. As all the doses increased expression to some extent the main factor to consider is the effect on cell viability which has previously shown to be affected with doses over 1μM.

5.4.3 Percentage increase of surface PCDHGB4, GB5 & GA6 with ADAM inhibition on differentiating plasma cells.

The effect of inhibiting ADAM shedding on differentiating B-cells from 3 healthy donors was assessed by the surface expression of the PCDHG isoforms, PCDHGA6, PCDHGB4 and PCDHGB5. Literature suggests that ADAM10 should be the primary sheddases involved in cleavage of the PCDHG surface proteins however as there is a lot of crossover of targets for ADAM10 and ADAM17 both specific inhibitors, GI 254023x and TAPI-2 were tested along with the pan inhibitor Marimastat. Following the pilot experiments using myeloma cell lines a concentration of 0.75μM was used to account for any effects on cell viability.

Percentage of cells with positive PCDHG expression is averaged from 3 donors and plotted for each inhibitor as well as a control condition cultured without the addition of any ADAM inhibitor. Memory B-cells were isolated from peripheral blood and differentiated using the *in vitro* system using APRIL stimulation for the PC programme. Cells were assessed on day 6 of the differentiation pre-ADAM inhibition and again after 4-days with the ADAM inhibitors in the culture media at day 10. Cells were refed with fresh media containing the inhibitors 4-days prior to day 13 and day 20 when PCDHG expression was analysed. Expression of the PCDHG locus increases when the cells differentiate into PCs from the plasmablast stage which is seen as an overall pattern between days 6 to 13. Expression increases further once the remaining cell population will mainly consist of LLPCs by day 20 where expression is approximately three times higher the level seen on day 13. Overall, the expression pattern of the PCDHG proteins is increased as the cells increase their CD138 expression linking PCDHG expression to plasma cell state. At the day 20 the overall level of PCDHG expression is much higher and it is by this time that we expect that most of the cell population to be LLPCs at this stage correlating PCDHG with a quiescent phenotype. Although the expression level seen with the ADAM inhibitors is lower than the no inhibitor control this can be contributed to the toxic effect the inhibitors appear to have on cell viability after prolonged exposure in the culture.

As PCDHG is known to be higher on plasma cells compared to B-cells at an earlier stage of differentiation the inhibitors were added from day 6 at the plasmablast stage. Overall, it can be concluded that the addition of the inhibitors had no consistent effect

over the surface expression of the PCDHG proteins. The changes in the effectiveness of the inhibitors may be due to the activity of the ADAM sheddases at the time of analysis as localisation on the cell surface to their target can influence activity as well as regulatory proteins such as tetraspanins on the cell surface.

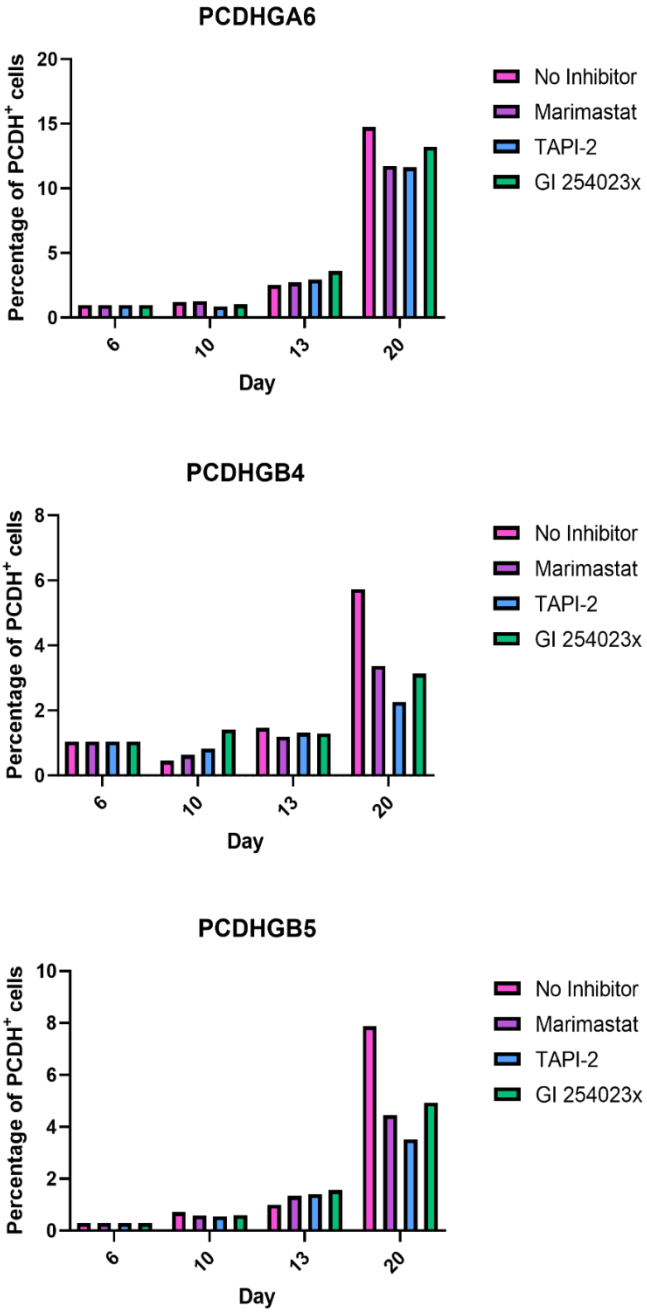

Figure 5.4.3 Effect on PCDHG surface expression by inhibiting ADAM sheddases activity on differentiating B-cells and PCs

Average expression of the PCDHG expression from 3 healthy donors where memory B-cells were isolated from peripheral blood samples and differentiated using the *in vitro* differentiation and APRIL stimulation. Expression was analysed by flow cytometry from day 6 pre-ADAM inhibition and then again at day 10, 13 & 20 following 4days in the presence of the 3 different ADAM inhibitors. Each inhibitor (Marimastat-pan, TAPI-2-ADAM17 specific & GI 254023x-ADAM10 specific) was used at a concentration of 0.75μM/mL

5.5 Discussion

The ADAM sheddases are responsible for the cleavage of many surface proteins which gives them a role in many cell processes such as adhesion and cell signalling. Cleavage of cell surface proteins enable the activation of internal signalling events as well as releasing cytokines to provide external signalling as well as altering cell-cell interactions. Having the ability to dynamically alter cell surface phenotype allows cells to respond to external cues and their microenvironment. Being able to respond rapidly to changes in cell microenvironment enhances cell survival and ability for cell migration (Smulski et al., 2017).

The aim of this chapter was to elucidate if ALCAM and the PCDHG proteins are indeed targeted by the ADAM sheddases on B-cells and PCs and may explain the two PC populations generated by ALCAM expression in the *in vitro* differentiation system.

ADAM sheddases function by cleaving the ectodomain and therefore are located on the cell surface with their activity depending on localisation to their target. Surface expression of the ADAM10 & ADAM17 the predominant sheddases for proteolytic cleavage and a large range of targets, was assessed by flow cytometry and revealed the presence of the two sheddases, of note ADAM10 expression increases from day 3 and then is maintained till day 13 on PCs, in comparison ADAM17 has the highest expression at day 3 on B-cells and then decreases as the cells transition into plasmablast and then PCs. This may indicate a dominance of ADAM17 activity in B-cells and then a switch to ADAM10 as the cells differentiate in PCs. When expression was analysed in a diseased model using myeloma cells lines this showed that both cells lines expressed ADAM10 in line with what was seen in the PCs generated from healthy donors.

The direct effects of ADAM mediated shedding were analysed by flow cytometry for ALCAM and PCDHG surface expression levels. The pilot experiments used the pan ADAM inhibitor, Marimastat, and the ADAM17 specific inhibitor, TAPI-2, to see the effects on ALCAM and the generation of a double population. The inhibitors were added at a concentration of 4μM for 24hrs as used in (Smulski et al., 2017), to inhibit cell surface expression. In the pilot experiment a small increase in surface expression of ALCAM was seen. To test this further a dose response was set up 4fold lower and 4fold higher than the initial 4μM trialled as well as leaving the inhibitors in the culture

for 4days over the weekend. This revealed that the effect of the inhibitors does reduce shedding and increases surface expression on PCs however it also revealed that a higher concentration became toxic and resulting in a decrease in cell number which consequently was reflected by a reduction in the frequency of cells in the ALCAM high population. This dose response not only revealed the regulation of surface ALCAM by ADAM sheddases specifically ADAM17 but also that ADAM sheddases likely play other roles in B-cell and PC survival. ADAM10 has been identified to control PC differentiation by acting on transcription factors *PRDM1, XBP1 & IRF4* required for the transition to PCs although the mechanism of ADAM10 on these transcription factors has not been elucidated (Chaimowitz et al., 2012). As well as differentiation ADAM10 has also been linked to survival in a BAFF-dependent manner (Smulski et al., 2017). ADAM sheddases were also revealed to be responsible for surface shedding of the PCDHG proteins with a preference of ADAM10 as the main sheddase (Reiss et al., 2006; Bouillot et al., 2011). Due to PCDHG isoforms being individually expressed on such a small percentage of the PC population and the toxic effects previously seen at concentrations above 1μM the results were inconsistent. As very little effect was seen in healthy PCs it suggests that the ADAMs do not directly target the PCDHG proteins however in the controlled *in vitro* system we lacked a positive control to confirm the activity of the sheddases. Therefore, the PCDHG may be a target of ADAM shedding providing the correct activation conditions and localisation to allow shedding activity. The effect of inhibiting the ADAM sheddases had a less of an impact when tested on the myeloma cell lines, phosphatidyl serine is known to activate the sheddases and is present on normal PCs in the cell lines this may be reduced presence of phosphatidyl serine. The endogenous expression of ADAM10 and ADAM17 was not dissimilar from the healthy PCs although ADAM17 expression was not significant on the myeloma cells. Using the myeloma cell lines as a disease model for neoplastic PCs, the small increase in surface expression suggests that the ADAM sheddases activity appears to be down regulated indicating they are lacking the correct activation conditions. Along with the genetic abnormalities and translocations seen in multiple myeloma alterations in ADAM activity may enhance myeloma cell survival by affecting normal surface protein expression and transcription factors required for normal PC survival and regulation (Lambrecht et al., 2018).

6 Discussion

6.1 Overview

The initial aims for this project were to assess the pattern of surface expression of a range of niche factors, these factors play a role in the migration and retention of PCs in the bone marrow (Zheng et al., 2016; Vande Broek et al., 2006; Agrawal et al., 2011; Gorfu et al., 2010; Neri et al., 2011). The niche factors were initially identified using microarray analysis comparing patient samples with either plasmacytoma or plasmablastic lymphoma (PBL), an upregulation in the plasmacytoma samples identified a possible signature that identifies a less aggressive subset of neoplastic PCs with a phenotype that favours adhesion over migration and metastasis.

To investigate the role these niche factors may play in PC differentiation, analysis of their expression patterns and changes within malignancy is essential to better improve our understanding of the many interconnections involved in PC survival within the bone marrow niche. This was carried out using a range of techniques but predominantly flow cytometry, which provides in depth analysis of protein expression on the cell surface as well as comparative analysis for co-expression. The focus of the expression analysis was to establish whether there is a standard pattern of expression seen in healthy differentiating B-cells and how this correlates with gene expression. Establishment of patterns of expression was examined from day 6 at the plasmablast stage and focused on the expression in developing PCs. The data shows multiple levels of regulation at both a gene and protein level. The transcriptional and post-transcriptional regulation investigated shows subtle changes on the PCs suggesting that these regulation mechanisms allow for dynamic changes in response to external cues and changing survival signals received from the bone marrow microenvironment. From the current data so far, it looks likely that the pattern of surface expression is determined at a gene level for example the PCDH-γ locus follows the gene expression data with protein expression. However, there is some discordance between the gene and protein expression levels for some of the niche factors, which can be explained by post-translational processing.

The effect of malignancy on the established patterns was hypothesised to cause a dysregulation in the expression and therefore normal survival and homing would be affected. This is thought to most likely be a downregulation in metastasising cells by

allowing for neoplastic PCs to become more migratory by reducing retention within the bone marrow. It is seen that neoplastic PCs become plasmablast-like and acquire a phenotype seen earlier in the differentiation process. Thereby giving the cells attributes that are intrinsically more proliferative and migratory in comparison to differentiated PCs that is linked to localisation, stable residency within the niche and cohesive growth. In the context of an upregulation of these niche factors there may be the emergence of cohesive tumours with tight cell-cell interactions that can provide a survival advantage by blocking any apoptotic factors or targeted treatments aimed at reducing the tumour burden. Albeit the data generated here fails to elucidate the exact functionality that niche factors have in PC homing due to a lack of migration studies, it has provided a basis on which to compare standard patterns of expression to those dysregulated in PC neoplasms. It is hypothesised that dysregulation in malignancies will have direct effects on the niche factors and how the PCs can respond to their survival niche.

6.2 Establishment of a pattern of expression of niche factors

Surface expression analysis by flow cytometry revealed that there is a standard pattern of expression seen in differentiating B-cells for several niche residency factors. The expression of these niche factors increases once the cells transition from the PB stage to PCs, this correlates with the PBs preparing to establish residency in the bone marrow following migration. Typically, this involves processes such as rolling, tethering and transmigration via selectins, integrins and chemokines. The function of the niche factors combined may provide the PCs with a more tailored response in terms of their migration, homing and residency within the survival niches. Current literature identifies each of the niche factors being expressed on immune cell types influencing the interactions and behaviours within the niche environment, such as ALCAM which is expressed on T-cells and binds to CD6 as wells as being expressed in B-cells but only showing homotypic adhesion (Nelissen et al., 2000), CCR2 is shown to be involved in chemotactic migration on B-cells as well as monocytes (Huang et al., 2007; Vande Broek et al., 2003) revealing a combination of mechanisms these niche factors are a part of. All of which has been linked to tumour progression and migration particularly in the bone marrow. Flow cytometry analysis provides evidence that the pattern of some of the niche factors for example ALCAM, is not as linear as being either on or

off and that there are subsets within the PC population displaying heterogeneity. ALCAM expression was found to be dynamic and revealed to be under multi-layered levels of regulation. Post-translational alterations are present in the form of ectodomain shedding from the ADAM sheddases. Whereas expression of LEPR was very homogeneous with low expression in PCs that gradually increased in LLPCs. Monitoring levels of surface expression of these niche factors can allow for predictions to be made on how neoplastic cells will respond to the microenvironment and likely responses to treatment. For example, disrupting the niche with treatment may induce changes in migration to a new niche. Here surface phenotypes can provide a strong diagnostic tool to identify proliferative or more quiescent, cohesive subsets or clones of neoplastic cells. Albeit the four niche factors did not correlate with their expression patterns in showing co-expression, this was not expected given their varying roles in PC development in either migration or residency. Expression of LEPR and ITGB7 was a lot lower than expression of ALCAM and CCR2 for example which this is more representative of the role they play in PC survival and homing.

We know that LEPR and ITGB7 play a role in retention within the bone marrow and receiving signals from stromal cells which are missing in the *in vitro* differentiation system, may mean that high expression of these factors may not be induced. It is however shown that there is a standard pattern of expression of these niche residency factors in healthy PCs which is part of normal B-cell differentiation. Establishing patterns of standard expression allows for comparison of expression in a number of different B-cell and PC disorders compared to normal B-cell differentiation stages. Healthy PCs reside in the bone marrow niche therefore plasmacytomas likely reflect the expression pattern of niche factors in normal PCs and neoplasm with plasmablastic-like cells will have a surface phenotype resembling that seen in B-cells and PBs at the early stages of differentiation.

6.3 Effects of different niche conditions

Since PCs may reside in different niche conditions in physiological and pathological states, the expression patterns were investigated using different niche conditions in the *in vitro* differentiation system. This was achieved by using APRIL, TGF-β and IFN-α stimulations as IFN-α generates a pro-inflammatory response whereas APRIL and TGF-β generates an anti-inflammatory response. Given the different niche conditions

reflect different environments for PCs to reside it was hypothesised that this may lead to subtle differences in the surface phenotype between the niche residency factors. For example, tumour progression and proliferation can be linked to inflammatory cytokines released by the surrounding cells within the niche, therefore a downregulation of adhesion molecules would be advantageous for a malignant phenotype (Musolino et al., 2017). Outside of the bone marrow in extramedullary sites, an increase in adhesion molecules at sites of inflammation aid with the infiltration of immune cells. Traditional adhesion molecules that are known to be upregulated are ICAM-1 and VCAM-1 to attract circulating T-cells via extravasation. The effect of the niche conditions and PC stimulation received by the cells was assessed by flow cytometry to see if the surface phenotype reflects the niche environment. The pattern of expression of the niche factors develops across the course of the differentiation as the cells become PCs. The pattern seen for each of the niche factors investigated, ALCAM, CCR2, ITGB7 & LEPR revealed that it was unaffected by the alteration of the niche conditions in all three donors. This indicates that the niche factors are expressed as a standard feature of normal B-cell differentiation.

The function of the 4 niche factors analysed all play a role in either homing, migration or retention in the bone marrow which correlates with the theory that an upregulation of this type of signature can indicate a more localised, isolated tumour. Strong expression of factors would aid adhesion and retention in the survival niche. A dysregulation of niche factors on neoplastic PCs for example in myeloma may lead to migratory cells that can emerge from the bone marrow and metastasise to a new niche environment. By identifying niche factors that could predict the likelihood of cells having a more migratory phenotype, analysis of certain niche factors could be added to traditional diagnostic panels to aid risk prediction and disease progression.

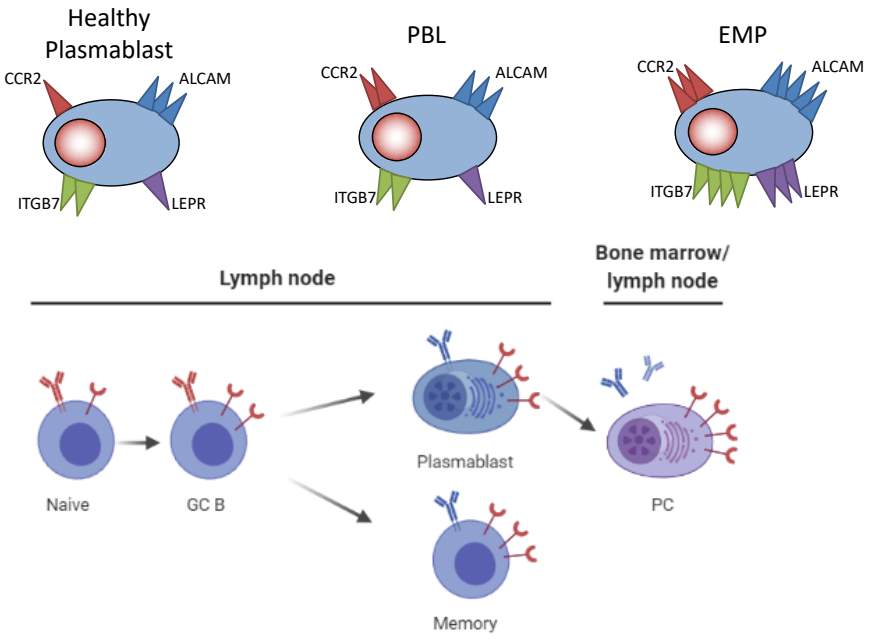

Figure 6.3 Model of surface expression of the niche factors during differentiation and neoplasia

Model of niche factor expression in a healthy plasmablast, plasmablastic lymphoma (PBL) and extramedullary plasmacytoma (EMP) indicated from the initial gene expression comparison identifying the upregulation of an adhesion signature in EMP. Hypothesised that the gene expression will correlate with increased surface expression of the niche factors. Below is a representation of expression throughout B-cell differentiation, expression is low on naïve and germinal centre B-cells, this increases as the cells differentiate into plasmablasts and plasma cells (PCs) or memory B-cells.

Further investigation is required to fully elucidate the true function the niche residency factors in PC survival and migration however the more understanding we have of the interactions within in the survival niche the more informed treatment plans and targeted therapy can be. For PCs to survive within the bone marrow niche they require access to blood vessels to receive survival signals and nutrients along with stromal cell support. ALCAM has been identified as a homing factor for PCs to the bone marrow and helps in retaining them within the survival niche. MIF acts on myeloma cells and upregulates ALCAM from and can lead to chemoresistance via tight adhesion of the myeloma cells (Zheng et al., 2016). Therefore, highlighting the impacts

niche factors can have in malignancy, two roles are happening here ALCAM is retaining the myeloma cells in the bone marrow niche which may reduce spread and metastasis but also then causes myeloma drugs to be less effective as neoplastic cells are potentially more resistant to therapy in survival niches. ALCAM in other cancers such as breast and prostate cancer has also been linked to tumour metastasis (Hansen et al., 2014; Davies and Jiang, 2010) driving the malignant cells to metastasise to bone. CCR2 has also been shown the respond to MCP-1 secreted by IL-6 induced myeloma cells along with osteoclasts expressing CCR2 targets to promote myeloma cell to migrate to the bone marrow (Arendt et al., 2002; Moreaux et al., 2011). By establishing the pattern of niche residency factors, we can better understand the overall picture of cell-cell interactions between PCs and the stromal support along with the neighbouring immune subsets.

6.4 Epigenetic regulation and protein expression of the PCDH-γ locus

The PCDH-γ locus has a characterised role in the nervous system in synaptogenesis by the combinatorial expression achieved by stochastic promoter choice (Hirayama and Yagi, 2017; Lefebvre et al., 2012; Mountoufaris et al., 2018). This combinatorial expression provides a surface identity code to avoid self-adhesion of synapses forming on the same neuron. Here the results show for the first-time epigenetic activity over the promoter choice in differentiating B-cells to provide a surface identity code on PCs. The epigenetic control was seen specifically in the PCDH-γ locus with evidence of CTCF binding proximal to the promoters of the gamma isoforms that is similar to that described in neurons. This type of epigenetic activation could allow for distinct combinations of the PCDH-γ locus to be expressed on the cell surface, further investigation into the effects of the CTCF binding on PCDH-γ isoform expression is required to confirm specific epigenetic control. Therefore, identifying the surface proteins being expressed was critical in revealing whether there may by a surface identity code present on PCs. The biggest difficulty was finding antibodies that were specific to the individual PCDH-γ isoforms, this was due to the similarity in structure of the gamma isoforms as they all have the same constant regions and only differ by the ectodomain. The similarity in structure means that their molecular weights are all approximated to be around 100kDa making detection by western blot less conclusive.

Using the expression vectors in the HeLa cell line confirmed specificity of the three PCDHG antibodies that produced the cleaner more specific blots. This led to the development of using these antibodies for flow cytometry to be able to assess surface expression.

Within the PC population there is only a small percentage that have positive expression for the individual isoforms however with the use of a pan antibody this percentage increased significantly. This shows that distinct subsets can be identified within the PC population and given that there are 22 members of the gamma cluster that can be expressed this likely makes up and the total percentage expressed. Currently it is undetermined how many isoforms a cell can express at any one time to indicate the diversity of patterns that could be expressed on the surface of the PCs. The consistent pattern of PCDHG expression on the PCs post-day 6 suggests that once an expression is established it is then maintained on LLPCs. Therefore, surface patterns of the PCDHG isoforms are likely to be unique to that small subset of PCs and providing a barcode for surface identity. Unfortunately, flow cytometry was limited in that all three PCDHG antibodies required an anti-rabbit secondary antibody therefore co-expression could not be assessed. To investigate fully if the surface expression pattern of PCDH isoforms can generate unique identity codes single-cell analysis would be required to see combinations of PCDH-γ expression on PCs, sequencing of single cells would also be able to identify if PCs that have identical combinations are of the same progeny which would indicate that the expression pattern in inherited.

Expression of PCDH-γ isoforms was assessed in malignant bone marrow with a range of diagnoses including myeloma and samples with normal bone marrow microenvironment. A large variation in the levels of expression were seen between the bone marrow samples even between those samples with the same diagnosis. The functional role of the PCDH-γ proteins in PCs has not yet been fully elucidated although they are likely to play a role in PC survival within the bone marrow niche as protein expression correlates with gene expression showing the increase after day 13 in the *in vitro* differentiation system when the cells are terminally differentiated. This appears to be altered in neoplastic PCs which may then affect their retention in the bone marrow. Along with the evidence of epigenetic regulation there is also regulation

of protein surface expression via ectodomain shedding which was seen most strongly in the myeloma cells lines as there was the biggest increase in the percentage of positive cells when the activity of the ADAM sheddases was inhibited.

Ideally a more extensive analysis of the PCDH-γ would have been carried out to cover more members of the locus and better show the combinations of expression seen and identify any monoclonal populations. Single-cell analysis would better identify whether the PCDH-γ pattern of expression is inherited and determined at a gene level and elucidate the number of combinations seen within a PC population. The disadvantage of trying the assess the PCDH-γ locus in B-cells and PCs is that expression is very low and therefore the read depth required for sequencing would need to be very large. This is to account for the number of reads taken up by IGHV expression in PCs, along with other genes expressed at a high level. This type of experiment is under development and delayed due to the impact of the COVID pandemic as it may reveal correlations between specific gene programmes for example quiescence associated with fully differentiated PCs. Initial attempts to isolate single PCs for surface expression analysis were trialled using single cell sorting into 96-cell plates. The plan had been to carry out single cell sequencing on these PCs to establish the combinatorial expression patterns. This would tell us not only how many isoforms can be expressed but also if the pattern of expression is inherited and passed on from a parent cell to its progeny. Difficulties were encountered ensuring we had accurately sorted 1 cell per well, I tried to overcome this by fluorescently tagging the cells however as the cells are cultured in suspension imaging the cells proved problematic and did not produce any usable images. A fibronectin coated plate was also trialled to attempt to overcome the imaging problem however generating a cell number high enough from the *in vitro* differentiation was not only time consuming but by the time the cells reached the PC stage which has the highest expression of the PCDH-γ locus, cell viability is very low. After initial optimisation experiments were trialled, it was decided that the first steps needed to be having an assay that could identify some of the PCDH-γ isoforms in a PC population. And to be able to confirm that surface expression can be seen on PCs which builds upon our knowledge of gene expression and epigenetic regulation.

6.5 Post-translational regulation of surface expression

The initial identification of niche residency factors was from RNA-sequencing data and analysis of surface expression showed that they are also expressed in protein form on the cell surface. Although there is genetic control over the expression of certain niche factors and adhesion molecules such as the PCDH-γ locus, post-translational regulation is also an important factor in determining cell surface phenotype. Gene expression analysis tells you that cells have the capacity to express gene transcripts at different stages in B-cell differentiation but not how this translates to functional protein expression. Varying levels of protein expression compared to gene expression can be due to problems translating the protein or post-translational modifications. For some of the niche residency factors varying levels of expression were seen such as ALCAM which saw two subsets of cells with the PC population. Expression here did not correlate with gene expression nor was the PC population homogeneous in its expression level. Cell surface proteins can be regulated by cleavage events and ectodomain shedding, which can result in downstream signalling events and further proteolytic cleavage by γ-secretase.

The observation of two subsets of ALCAM expression in the PC population led to the investigation of shedding activity from the ADAM sheddases. The subsets of ALCAM high or low subsets was shown to be attributed to some extent ectodomain shedding, specifically by ADAM sheddases. Through blocking the activity of ADAM10 & ADAM17 a shift in the ratio of cells into the high expressing subset was seen. Evidence that ADAM sheddases are active on differentiating B-cells and PCs gives a mechanism for a dynamic pattern of expression. Outside of the *in vitro* system this mechanism will play a role in PCs ability to respond to signals within the germinal centre as well as migrating and homing to the bone marrow niche. This activity provides a survival advantage for the PCs by being able to respond to the signals and environment but also creates a point of dysregulation that can be manipulated in neoplastic PCs.

Plasmacytoma samples had an upregulation of niche factors that retained PCs within the bone marrow niche, activation of mechanisms such as ectodomain shedding in neoplastic PCs allows for more migratory behaviour. This is seen in more aggressive neoplasms such as myeloma where multiple tumour sites and lesions can be seen within the skeleton therefore downregulating the expression of niche factors gives an

advantage for metastasising myeloma cells (Wen et al., 2017; Avigdor et al., 2001; Bianchi et al., 2012; Bladé et al., 2011). The neighbouring cells and extracellular matrix surrounding the neoplastic PCs influence PCs survival and behaviours, shedding activity of ADAM proteases can alter cells surface phenotype which in turn may impact PC responses to their environment and ability to receive external signals (Hosen, 2020; Vincent and Mechti, 2005). Currently the link between ADAM shedding and the functional effects on the niche residency factors still needs further investigation.

ADAM sheddases were also shown to target the PCDH-γ proteins (Reiss et al., 2006; Bouillot et al., 2011; Buchanan et al., 2010) and the effects were most prominent when using the ADAM inhibitors on the myeloma cell lines. This result was not too surprising given that expression of the PCDH-γ expression tended to be higher in the myeloma cell lines given that they are a monoclonal population in comparison to the PC populations generated in the *in vitro* differentiation system. There was also higher expression of the ADAM sheddases on the cell surface of the myeloma cell lines and given that localisation of ADAM sheddases to their target on the cell surface affects increased activity on the myeloma cell lines makes sense that there is enhanced shedding as there is a higher chance of being near a target. Targets of ADAM10 and ADAM17 could have been confirmed by ELISA had supernatants been collected with and without the presence of the ADAM inhibitors to assess the levels of soluble ALCAM and the PCDH-γ proteins. Another experiment that would have confirmed targeting these niche factors by ADAM sheddases would have been fluorescent microscopy to assess the localisation of the ADAM proteins to the niche factors ALCAM and PCDH-γ on the cell surface as localisation of the ADAMs is a limiting factor for their activity. Along with localisation ADAM activity is regulated by co-factors as discussed in the introduction, activity can also be induced with ionomycin and PMA. Therefore, it is likely that specific conditions may alter the targeted shedding of the ADAMs and is context dependent rather than ubiquitous shedding of all targets.

6.6 Dysregulation of surface expression in malignancy

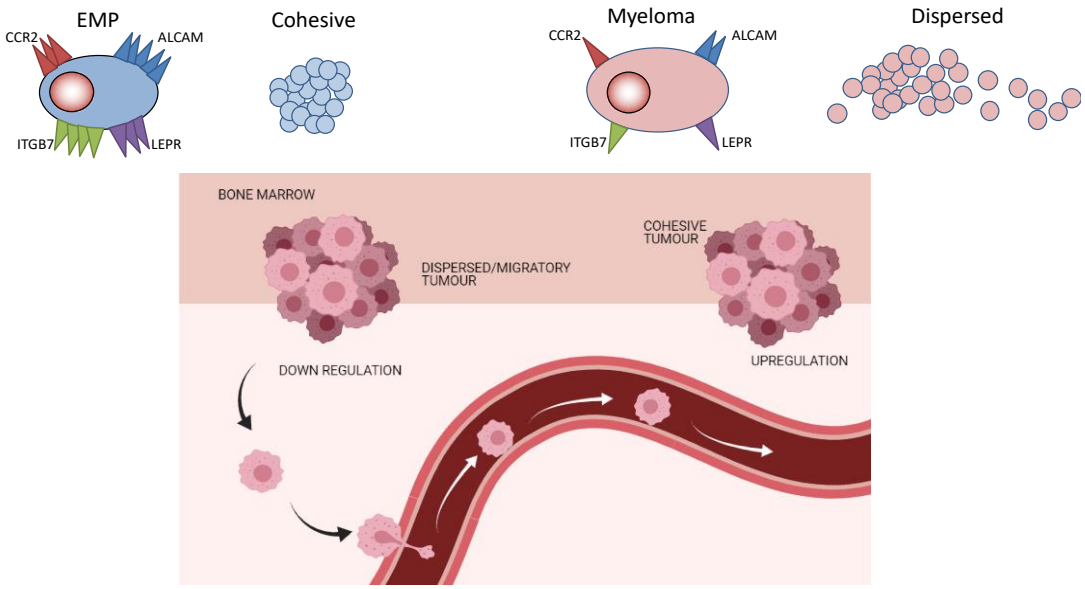

Figure 6.6 Model of neoplastic PC migration depending on the surface phenotype Schematic hypothesising the effect of an up and downregulation of the niche residency factors and the predicted expression pattern on different forms of PC neoplasm. EMPs have and upregulation of niche residency factors and for a cohesive, isolated tumour whereas myeloma will have a down regulation resulting in a dispersed disease pattern. This behaviour is explained in part by either an up or downregulation of niche residency factors that aid in homing and retention within the bone marrow. A downregulation of these niche factors can allow for PCs to migrates out of the bone marrow to new sites of localisation in the skeleton or to extramedullary sites.

Expression of the nice factors was initially tested on a disease model using myeloma cell lines and then progressed to analysis using bone marrow aspirates from patients. The bone marrows tested were representative of a range of PC and B-cells disorders to provide a better insight how the pattern of expression seen *in vitro* translates to *in vivo* samples. The niche factors analysed were the PCDH-γ isoforms along with ALCAM and CCR2 due to the patterns of expression and levels being higher and more distinct than ITGB7 and LEPR. The functions of the factors assessed are linked to homing, migration and retention within the survival niche and therefore are more likely to be altered in neoplastic cells.

There was a large variation seen in the expression of the niche factors in the 10 bone marrow samples analysed, ideally the number of samples would have been greater however the impacts of the COVID-19 pandemic affected time and access to samples and laboratory facilities. Had the sampling been greater better clustering of diseases may have been achieved or revealed an overall trend for an up or downregulation of the niche factors. Although the samples analysed do not indicate any clear patterns of PCDH-γ surface expression with disease classification, this does not rule out that the combination of PCDH-γ isoforms may impact the adherence of the PCs depending on the compatibility of the pattern of isoforms being expressed.

For ALCAM and CCR2 expression seen in malignant PCs was unclear whether the expression is unique enough to classify PC neoplasms. However the role of ALCAM and CCR2 in myeloma as well as other cancer cells types have been commented on, for example there is a strong link that ALCAM is a driver of metastasis to bone and CCR2 upregulation promotes migration if myeloma cells to the bone marrow (Davies and Jiang, 2010; Hansen et al., 2014; Zheng et al., 2016; Ishiguro et al., 2012; Vande Broek et al., 2003; Vande Broek et al., 2006). Together these studies identify a role for ALCAM and CCR2 in malignancy and homing to the bone marrow niche however their diagnostic value may be more indicative for disease progression over classification of sub-types of B-cell and PC neoplasms. Migration studies would elucidate the role ALCAM and CCR2 in normal PCs and therefore alterations in expression levels may then help in the monitoring of PC responses to treatment.

Further investigation into the combinatorial expression of the PCDH-γ locus is needed to fully elucidate what affect the pattern of expression has on the PCs and the exact role they play in survival and disease pathogenesis. As PCDHs are known to be involved in synaptogenesis it is likely that they play a similar role in adhesion of PCs to each other and the microenvironment. The theory is that the combination of the PCDHs being expressed form a zipper like structure when adhering to the identical combination of PCDHs on a neighbouring cell. Any mismatching PCDHs weakens the strength of the adhesion (Schreiner and Weiner, 2010), therefore a downregulation of PCDHs would allow cells to become migratory therefore it was predicted we would see lower levels of expression in myeloma samples.

PCDHs in the nervous system display homotypic repulsion not adhesion (Mountoufaris et al., 2018; Hirayama and Yagi, 2017; Lefebvre et al., 2012; Peek et al., 2017) showing that depending on the context PCDHs can have two very distinct behaviours, it is hypothesised that the nervous system is unique in the mechanism used for self-avoidance and that in PCs it is likely that it is adhesion between the PCDG proteins. Especially due to the upregulation seen in the plasmacytoma samples which form cohesive tumours, in healthy PCs homotypic adhesion would maintain the PC population within their survival niche. Another factor to be considered is whether identical combinations of PCDH expression arise from the same progeny which could result in the formation of monoclonal tumours. Further studies into how the combinatorial expression of PCDHs effects PCs retention in the bone marrow as well as adhesion and migration to the survival niche could reveal a unique mechanism of providing individual surface identity codes achieved through stochastic promoter choice.

The main aims for targeting neoplastic cells are to reduce stromal support and access to blood vessels using anti-angiogenesis factors, disrupting growth and replication by causing DNA damage or to promote toxic stress via protease inhibitors, blocking clearance of proteins. For diseases such as myeloma which are known to relapse having an arsenal of different drug treatments and targets is imperative for extending a patient's chance of survival (Bolzoni et al., 2013; Nishida and Yamada, 2019; Di Bernardo et al., 2010; Castella et al., 2018). There are many combinations of therapies currently available however having a plethora of targets such as niche residency factors that can either aid in treatment or help monitor disease progression will be extremely beneficial for those patients who have relapsed following previous treatment options (Ge et al., 2021). Understanding changes to the bone microenvironment or the capacity for neoplastic cells to respond to it by monitoring niche residency factors may open up additional measures during routine check-ups and provide further insights into how the drugs are interacting and what the effects of long-term use are.

6.7 Concluding remarks

Identifying surface expression patterns on differentiating B-cells and PCs demonstrates how dynamic a cells phenotype can be, meaning they can rapidly respond to external cues and home to their survival niche. Specific patterns of

expression were identified throughout the course of the *in vitro* differentiation system for each of the niche factors which will mirror their role in PC survival. Although the direct function of the niche factors was not tested, the previous analysis showing an upregulation at a gene level in cohesive tumours compared to proliferative and migratory tumours indicates that there is an advantage for prognosis in having an upregulated adhesion signature.

Analysis carried out so far shows that there is a correlation in the gene and protein expression of the PCDH-γ locus and that there are small subsets of the PC population that have positive expression of the individual isoforms suggesting that there are differing combinations of PCDHG expression in a polyclonal PC population. Adhesion assays would conclude whether the combinations expressed lead to homotypic adhesion and what level of tolerance there is for mismatching pairs.

The niche environments tested included stimulating with TGF-β, APRIL and IFN-α to mimic pro and anti-inflammatory signals, this did not impact the expression patterns meaning that the adhesion signature is not linked to the signals driving the differentiation response but are more likely a feature of standard differentiation. For the investigation into the niche conditions all differentiations were started from isolated memory B-cells which have previously been through the germinal centre reaction and class switching unlike naïve B-cells. Therefore, these cells will have been exposed to one of the niche conditions previous and may account for some of the donor variability in their memory B-cell populations. It is hypothesised that these niche factors aid with adhesion and migration to the survival niche as expression increases post day 6 when the cells transition from plasmablasts to PCs. Features of normal differentiation become disrupted in neoplastic PCs that can cause them to re-enter cell cycle and potentially change expression programmes to features that are characteristic of earlier stages of differentiation (Agnarelli et al., 2018; Vega et al., 2005; Slomp and Peperzak, 2018; Ryu et al., 2016)

By highlighting the regulation at a transcriptional and post-translational level provides an insight into processes that may then be dysregulated in neoplastic PCs. In order to better diagnose and predict disease progression identifying such adhesion signatures and niche factors can provide new diagnostic tools for more accurate diagnosis (Vande Broek et al., 2006; Mykytiv et al., 2019). By analysing samples by flow

cytometry and developing a novel staining protocol to newly identify surface expression of the PCDH-γ proteins, there is the opportunity to further investigate the combinatorial expression providing a unique identity code. The use of flow cytometry is in line with current diagnostic methods and therefore translatable for diagnosis and monitoring progression either using a new panel or being incorporated into the standard diagnostic markers already used. However, for the analysis of the PCDH-γ locus surface expression requires further optimisation to account for the issue with using secondary antibodies for staining and limited ability to distinguish the unique identify codes created by combinatorial PCDH expression.

Overall, we have shown the importance of looking at surface phenotypes not only to identify the stage of differentiation using traditional biomarkers such as CD138 and CD19 but also identified a set of niche residency factors with distinct patterns during differentiation and that have levels of regulation transcriptionally and post-transcriptionally. Having an idea as to how cells are likely to respond depending on cell surface expression profiles can aid disease risk prediction, progression, and response to treatment. Trials using combinations of treatments to best target the neoplastic cells need to be able to monitor multiple parameters of a cells surface phenotype. This will tell us how the cells are responding and what treatments are best suited at different stages of disease progression. Many current therapies targeting B-cell disorders particularly myeloma use a combination of chemotherapy and proteosome inhibitors, along with steroids such as dexamethasone to dampen the immune response. A consideration of using the niche residency factors as a targeted treatment is that this may disrupt other cell populations within the bone marrow for example CCR2 is expressed highly on monocytes and therefore there may be many off-target effects however targeting niche residency factors specific to the PCs may drive the neoplastic cells out of the bone marrow making them susceptible to clearance by the immune system or allowing anti-myeloma drugs to work more effectively.

From the data generated the investigation of surface phenotypes has been identified and an adhesion signature of niche residency factors shown to be expressed in distinct patterns throughout B-cell differentiation and therefore provides a basis for normal expression. An upregulation of this adhesion signature was first identified in plasmacytomas to generate a cohesive tumour in comparison to PBL a proliferative

disorder with a plasmablastic phenotype representing an earlier stage of differentiation to the PCs. I have shown there are subtle changes in expression between these niche residency factors between PBs, PCs and LLPCs, that are unaffected by the niche conditions. This showed that PCs and LLPCs had higher expression than the earlier stage PBs and confirms the observation that in PBL when the neoplastic cells take on a phenotype of an earlier stage in differentiation correlates with a down regulation of niche residency factors. We have shown a novel mechanism for regulation over the PCDH-γ locus in B-cells and PCs which is then translated to show surface protein expression of the PCDHG isoforms which had not yet been investigated in many cell types outside of the nervous system. This revelation showing a novel mechanism for controlling promoter choice and stochastic expression by epigenetic regulation indicates that PCs can produce unique combinations of *PCDHG* expression. Expression was then proven to be translated to surface protein expression, although more extensive investigation into number of distinct patterns seen in a PC population is needed. This leads to the exciting and novel idea that PCs can use combinations of PCDHG expression to create unique identity codes that can be used to identify rare subsets of PC populations and clones. Combinatorial expression of the PCDHGs involvement in cell-cell adhesion may lead to homotypic adhesion or repulsion as well as evidence in the literature of strong homotypic *trans* interactions and promiscuous *cis* (Schreiner and Weiner, 2010) generating a large range of potential interactions between the PC population impacting their residency within the bone marrow. The scope for the PCDHGs impact on PC behaviour is enormous given the number of potential combinations given there are 22 members in the PCDH-γ locus, and more work is needed to fully understand the mechanism of adhesion of the PCDHGs on the PC surface and their tolerance for mis-matching interactions.

Regulation transcriptionally and post-transcriptionally has been shown for several of the niche residency factors showing the dynamic nature of expression throughout B-cell differentiation. This highlights the importance at looking at multiple avenues of analysis for gene expression and epigenetic factors along with proteins expression and their potential for proteolytic processing. Further investigation in neoplastic cells would be needed to elucidate the exact changes in expression for specific neoplasms and how this would then translate into the diagnostic setting, however the current work

has provided a framework for the expression and regulation of these important niche residency factors in normal B-cell differentiation.

7 References

Abella, V., Scotece, M., Conde, J., Pino, J., Gonzalez-Gay, M.A., Gómez-Reino, J.J., Mera, A., Lago, F., Gómez, R. and Gualillo, O. 2017. Leptin in the interplay of inflammation, metabolism and immune system disorders. *Nat Rev Rheumatol.* **13**(2), pp.100-109.

Agnarelli, A., Chevassut, T. and Mancini, E.J. 2018. IRF4 in multiple myeloma-Biology, disease and therapeutic target. *Leuk Res.* **72**, pp.52-58.

Agrawal, S., Gollapudi, S., Su, H. and Gupta, S. 2011. Leptin activates human B cells to secrete TNF-α, lL-6, and IL-10 via JAK2/STAT3 and p38MAPK/ERK1/2 signaling pathway. *J Clin Immunol.* **31**(3), pp.472-478.

Arendt, B.K., Velazquez-Dones, A., Tschumper, R.C., Howell, K.G., Ansell, S.M., Witzig, T.E. and Jelinek, D.F. 2002. Interleukin 6 induces monocyte chemoattractant protein-1 expression in myeloma cells. *Leukemia.* **16**(10), pp.2142-2147.

Asimakopoulos, F., Hope, C., Johnson, M.G., Pagenkopf, A., Gromek, K. and Nagel, B. 2017. Extracellular matrix and the myeloid-in-myeloma compartment: balancing tolerogenic and immunogenic inflammation in the myeloma niche. *J Leukoc Biol.* **102**(2), pp.265-275.

Avigdor, A., Raanani, P., Levi, I., Hardan, I. and Ben-Bassat, I. 2001. Extramedullary progression despite a good response in the bone marrow in patients treated with thalidomide for multiple myeloma. *Leuk Lymphoma.* **42**(4), pp.683-687.

Biajoux, V., Natt, J., Freitas, C., Alouche, N., Sacquin, A., Hemon, P., Gaudin, F., Fazilleau, N., Espéli, M. and Balabanian, K. 2016. Efficient Plasma Cell Differentiation and Trafficking Require Cxcr4 Desensitization. *Cell Rep.* **17**(1), pp.193-205.

Bianchi, G. and Ghobrial, I.M. 2014. Biological and Clinical Implications of Clonal Heterogeneity and Clonal Evolution in Multiple Myeloma. *Curr Cancer Ther Rev.* **10**(2), pp.70-79.

Bianchi, G., Kumar, S., Ghobrial, I.M. and Roccaro, A.M. 2012. Cell Trafficking in Multiple Myeloma. *Open J Hematol.* **3**(Suppl 1).

Bladé, J., Fernández de Larrea, C., Rosiñol, L., Cibeira, M.T., Jiménez, R. and Powles, R. 2011. Soft-tissue plasmacytomas in multiple myeloma: incidence, mechanisms of extramedullary spread, and treatment approach. *J Clin Oncol.* **29**(28), pp.3805-3812.

Bolzoni, M., Storti, P., Bonomini, S., Todoerti, K., Guasco, D., Toscani, D., Agnelli, L., Neri, A., Rizzoli, V. and Giuliani, N. 2013. Immunomodulatory drugs lenalidomide and pomalidomide inhibit multiple myeloma-induced osteoclast formation and the RANKL/OPG ratio in the myeloma microenvironment targeting the expression of adhesion molecules. *Exp Hematol.* **41**(4), pp.387-397.e381.

Bonn, S., Seeburg, P.H. and Schwarz, M.K. 2007. Combinatorial expression of alpha- and gamma-protocadherins alters their presenilin-dependent processing. *Mol Cell Biol.* **27**(11), pp.4121-4132.

Bouillot, S., Tillet, E., Carmona, G., Prandini, M.H., Gauchez, A.S., Hoffmann, P., Alfaidy, N., Cand, F. and Huber, P. 2011. Protocadherin-12 cleavage is a regulated process mediated by ADAM10 protein: evidence of shedding up-regulation in pre-eclampsia. *J Biol Chem.* **286**(17), pp.15195-15204.

Bret, C., Hose, D., Reme, T., Kassambara, A., Seckinger, A., Meissner, T., Schved, J.F., Kanouni, T., Goldschmidt, H. and Klein, B. 2011. Gene expression profile of ADAMs and ADAMTSs metalloproteinases in normal and malignant plasma cells and in the bone marrow environment. *Exp Hematol.* **39**(5), pp.546-557.e548.

Buchanan, S.M., Schalm, S.S. and Maniatis, T. 2010. Proteolytic processing of protocadherin proteins requires endocytosis. *Proc Natl Acad Sci U S A.* **107**(41), pp.17774-17779.
Canzio, D., Nwakeze, C.L., Horta, A., Rajkumar, S.M., Coffey, E.L., Duffy, E.E., Duffié, R., Monahan, K., O'Keeffe, S., Simon, M.D., Lomvardas, S. and Maniatis, T. 2019. Antisense lncRNA Transcription Mediates DNA Demethylation to Drive Stochastic Protocadherin α Promoter Choice. *Cell.* **177**(3), pp.639-653.e615.
Castella, M., Fernández de Larrea, C. and Martín-Antonio, B. 2018. Immunotherapy: A Novel Era of Promising Treatments for Multiple Myeloma. *Int J Mol Sci.* **19**(11).
Castillo, J.J., Bibas, M. and Miranda, R.N. 2015. The biology and treatment of plasmablastic lymphoma. *Blood.* **125**(15), pp.2323-2330.
Chaimowitz, N.S., Kang, D.J., Dean, L.M. and Conrad, D.H. 2012. ADAM10 regulates transcription factor expression required for plasma cell function. *PLoS One.* **7**(8), pe42694.
Chen, W.V. and Maniatis, T. 2013. Clustered protocadherins. *Development.* **140**(16), pp.3297-3302.
Cocco, M., Stephenson, S., Care, M.A., Newton, D., Barnes, N.A., Davison, A., Rawstron, A., Westhead, D.R., Doody, G.M. and Tooze, R.M. 2012. In vitro generation of long-lived human plasma cells. *J Immunol.* **189**(12), pp.5773-5785.
Comazzetto, S., Murphy, M.M., Berto, S., Jeffery, E., Zhao, Z. and Morrison, S.J. 2019. Restricted Hematopoietic Progenitors and Erythropoiesis Require SCF from Leptin Receptor+ Niche Cells in the Bone Marrow. *Cell Stem Cell.* **24**(3), pp.477-486.e476.
Corre, J., Cleynen, A., Robiou du Pont, S., Buisson, L., Bolli, N., Attal, M., Munshi, N. and Avet-Loiseau, H. 2018. Multiple myeloma clonal evolution in homogeneously treated patients. *Leukemia.* **32**(12), pp.2636-2647.
Dang, M., Armbruster, N., Miller, M.A., Cermeno, E., Hartmann, M., Bell, G.W., Root, D.E., Lauffenburger, D.A., Lodish, H.F. and Herrlich, A. 2013. Regulated ADAM17-dependent EGF family ligand release by substrate-selecting signaling pathways. *Proc Natl Acad Sci U S A.* **110**(24), pp.9776-9781.
Davies, S. and Jiang, W.G. 2010. ALCAM, activated leukocyte cell adhesion molecule, influences the aggressive nature of breast cancer cells, a potential connection to bone metastasis. *Anticancer Res.* **30**(4), pp.1163-1168.
De Grandis, M., Lhoumeau, A.C., Mancini, S.J. and Aurrand-Lions, M. 2016. Adhesion receptors involved in HSC and early-B cell interactions with bone marrow microenvironment. *Cell Mol Life Sci.* **73**(4), pp.687-703.
De Silva, N.S. and Klein, U. 2015. Dynamics of B cells in germinal centres. *Nat Rev Immunol.* **15**(3), pp.137-148.
Di Bernardo, A., Macor, P., Guarnotta, C., Franco, G., Florena, A.M., Tedesco, F. and Tripodo, C. 2010. Humoral immunotherapy of multiple myeloma: perspectives and perplexities. *Expert Opin Biol Ther.* **10**(6), pp.863-873.
Duffy, M.J., McKiernan, E., O'Donovan, N. and McGowan, P.M. 2009. Role of ADAMs in cancer formation and progression. *Clin Cancer Res.* **15**(4), pp.1140-1144.
Düsterhöft, S., Lokau, J. and Garbers, C. 2019. The metalloprotease ADAM17 in inflammation and cancer. *Pathol Res Pract.* **215**(6), p152410.
El Hajj, N., Dittrich, M. and Haaf, T. 2017. Epigenetic dysregulation of protocadherins in human disease. *Semin Cell Dev Biol.* **69**, pp.172-182.

Falank, C., Fairfield, H. and Reagan, M.R. 2016. Signaling Interplay between Bone Marrow Adipose Tissue and Multiple Myeloma cells. *Front Endocrinol (Lausanne).* **7**, p67.
Firsova, M.V., Mendeleeva, L.P., Kovrigina, A.M., Solovev, M.V. and Savchenko, V.G. 2020. Plasmacytoma in patients with multiple myeloma: morphology and immunohistochemistry. *BMC Cancer.* **20**(1), p346.
Frade, J.M., Mellado, M., del Real, G., Gutierrez-Ramos, J.C., Lind, P. and Martinez-A, C. 1997. Characterization of the CCR2 chemokine receptor: functional CCR2 receptor expression in B cells. *J Immunol.* **159**(11), pp.5576-5584.
Ge, M., Qiao, Z., Kong, Y., Liang, H., Sun, Y., Lu, H., Xu, Z. and Liu, H. 2021. Modulating proteasome inhibitor tolerance in multiple myeloma: an alternative strategy to reverse inevitable resistance. *Br J Cancer.* **124**(4), pp.770-776.
Ghobrial, I.M. 2012. Myeloma as a model for the process of metastasis: implications for therapy. *Blood.* **120**(1), pp.20-30.
Gibb, D.R., El Shikh, M., Kang, D.J., Rowe, W.J., El Sayed, R., Cichy, J., Yagita, H., Tew, J.G., Dempsey, P.J., Crawford, H.C. and Conrad, D.H. 2010. ADAM10 is essential for Notch2-dependent marginal zone B cell development and CD23 cleavage in vivo. *J Exp Med.* **207**(3), pp.623-635.
Gilsanz, A., Sánchez-Martín, L., Gutiérrez-López, M.D., Ovalle, S., Machado-Pineda, Y., Reyes, R., Swart, G.W., Figdor, C.G., Lafuente, E.M. and Cabañas, C. 2013. ALCAM/CD166 adhesive function is regulated by the tetraspanin CD9. *Cell Mol Life Sci.* **70**(3), pp.475-493.
Gorfu, G., Rivera-Nieves, J., Hoang, S., Abbott, D.W., Arbenz-Smith, K., Azar, D.W., Pizarro, T.T., Cominelli, F., McDuffie, M. and Ley, K. 2010. Beta7 integrin deficiency suppresses B cell homing and attenuates chronic ileitis in SAMP1/YitFc mice. *J Immunol.* **185**(9), pp.5561-5568.
Grammatico, S., Scalzulli, E. and Petrucci, M.T. 2017. Solitary Plasmacytoma. *Mediterr J Hematol Infect Dis.* **9**(1), pe2017052.
Group, I.M.W. 2003. Criteria for the classification of monoclonal gammopathies, multiple myeloma and related disorders: a report of the International Myeloma Working Group. *Br J Haematol.* **121**(5), pp.749-757.
Guo, S.Q., Zhang, L., Wang, Y.F., Sun, B.C., Zhang, L.Y., Zhang, J., Wang, G. and Zhang, Y.Z. 2013. Prognostic factors associated with solitary plasmacytoma. *Onco Targets Ther.* **6**, pp.1659-1666.
Guo, Y., Monahan, K., Wu, H., Gertz, J., Varley, K.E., Li, W., Myers, R.M., Maniatis, T. and Wu, Q. 2012. CTCF/cohesin-mediated DNA looping is required for protocadherin α promoter choice. *Proc Natl Acad Sci U S A.* **109**(51), pp.21081-21086.
Gutiérrez-López, M.D., Gilsanz, A., Yáñez-Mó, M., Ovalle, S., Lafuente, E.M., Domínguez, C., Monk, P.N., González-Alvaro, I., Sánchez-Madrid, F. and Cabañas, C. 2011. The sheddase activity of ADAM17/TACE is regulated by the tetraspanin CD9. *Cell Mol Life Sci.* **68**(19), pp.3275-3292.
Haas, I.G., Frank, M., Véron, N. and Kemler, R. 2005. Presenilin-dependent processing and nuclear function of gamma-protocadherins. *J Biol Chem.* **280**(10), pp.9313-9319.
Hammad, H., Vanderkerken, M., Pouliot, P., Deswarte, K., Toussaint, W., Vergote, K., Vandersarren, L., Janssens, S., Ramou, I., Savvides, S.N., Haigh, J.J., Hendriks, R., Kopf, M., Craessaerts, K., de Strooper, B., Kearney, J.F., Conrad, D.H. and

Lambrecht, B.N. 2017. Transitional B cells commit to marginal zone B cell fate by Taok3-mediated surface expression of ADAM10. *Nat Immunol.* **18**(3), pp.313-320.
Hansen, A.G., Arnold, S.A., Jiang, M., Palmer, T.D., Ketova, T., Merkel, A., Pickup, M., Samaras, S., Shyr, Y., Moses, H.L., Hayward, S.W., Sterling, J.A. and Zijlstra, A. 2014. ALCAM/CD166 is a TGF-β-responsive marker and functional regulator of prostate cancer metastasis to bone. *Cancer Res.* **74**(5), pp.1404-1415.
Hanson, H.H., Kang, S., Fernández-Monreal, M., Oung, T., Yildirim, M., Lee, R., Suyama, K., Hazan, R.B. and Phillips, G.R. 2010. LC3-dependent intracellular membrane tubules induced by gamma-protocadherins A3 and B2: a role for intraluminal interactions. *J Biol Chem.* **285**(27), pp.20982-20992.
Hayashi, S. and Takeichi, M. 2015. Emerging roles of protocadherins: from self-avoidance to enhancement of motility. *J Cell Sci.* **128**(8), pp.1455-1464.
Hedvat, C.V., Comenzo, R.L., Teruya-Feldstein, J., Olshen, A.B., Ely, S.A., Osman, K., Zhang, Y., Kalakonda, N. and Nimer, S.D. 2003. Insights into extramedullary tumour cell growth revealed by expression profiling of human plasmacytomas and multiple myeloma. *Br J Haematol.* **122**(5), pp.728-744.
Hirayama, T. and Yagi, T. 2017. Regulation of clustered protocadherin genes in individual neurons. *Semin Cell Dev Biol.* **69**, pp.122-130.
Hosen, N. 2020. Integrins in multiple myeloma. *Inflamm Regen.* **40**, p4.
Huang, B., Lei, Z., Zhao, J., Gong, W., Liu, J., Chen, Z., Liu, Y., Li, D., Yuan, Y., Zhang, G.M. and Feng, Z.H. 2007. CCL2/CCR2 pathway mediates recruitment of myeloid suppressor cells to cancers. *Cancer Lett.* **252**(1), pp.86-92.
Ing-Esteves, S., Kostadinov, D., Marocha, J., Sing, A.D., Joseph, K.S., Laboulaye, M.A., Sanes, J.R. and Lefebvre, J.L. 2018. Combinatorial Effects of Alpha- and Gamma-Protocadherins on Neuronal Survival and Dendritic Self-Avoidance. *J Neurosci.* **38**(11), pp.2713-2729.
Inoue, T., Moran, I., Shinnakasu, R., Phan, T.G. and Kurosaki, T. 2018. Generation of memory B cells and their reactivation. *Immunol Rev.* **283**(1), pp.138-149.
Ise, W. and Kurosaki, T. 2019. Plasma cell differentiation during the germinal center reaction. *Immunol Rev.* **288**(1), pp.64-74.
Ishiguro, F., Murakami, H., Mizuno, T., Fujii, M., Kondo, Y., Usami, N., Yokoi, K., Osada, H. and Sekido, Y. 2012. Activated leukocyte cell-adhesion molecule (ALCAM) promotes malignant phenotypes of malignant mesothelioma. *J Thorac Oncol.* **7**(5), pp.890-899.
Jiménez-Sainz, M.C., Fast, B., Mayor, F. and Aragay, A.M. 2003. Signaling pathways for monocyte chemoattractant protein 1-mediated extracellular signal-regulated kinase activation. *Mol Pharmacol.* **64**(3), pp.773-782.
Kaneko, R., Kato, H., Kawamura, Y., Esumi, S., Hirayama, T., Hirabayashi, T. and Yagi, T. 2006. Allelic gene regulation of Pcdh-alpha and Pcdh-gamma clusters involving both monoallelic and biallelic expression in single Purkinje cells. *J Biol Chem.* **281**(41), pp.30551-30560.
Keats, J.J., Chesi, M., Egan, J.B., Garbitt, V.M., Palmer, S.E., Braggio, E., Van Wier, S., Blackburn, P.R., Baker, A.S., Dispenzieri, A., Kumar, S., Rajkumar, S.V., Carpten, J.D., Barrett, M., Fonseca, R., Stewart, A.K. and Bergsagel, P.L. 2012. Clonal competition with alternating dominance in multiple myeloma. *Blood.* **120**(5), pp.1067-1076.
Lambrecht, B.N., Vanderkerken, M. and Hammad, H. 2018. The emerging role of ADAM metalloproteinases in immunity. *Nat Rev Immunol.* **18**(12), pp.745-758.

Landgren, O., Rajkumar, S.V., Pfeiffer, R.M., Kyle, R.A., Katzmann, J.A., Dispenzieri, A., Cai, Q., Goldin, L.R., Caporaso, N.E., Fraumeni, J.F., Blot, W.J. and Signorello, L.B. 2010. Obesity is associated with an increased risk of monoclonal gammopathy of undetermined significance among black and white women. *Blood.* **116**(7), pp.1056-1059.
Lefebvre, J.L., Kostadinov, D., Chen, W.V., Maniatis, T. and Sanes, J.R. 2012. Protocadherins mediate dendritic self-avoidance in the mammalian nervous system. *Nature.* **488**(7412), pp.517-521.
Lemieux, G.A., Blumenkron, F., Yeung, N., Zhou, P., Williams, J., Grammer, A.C., Petrovich, R., Lipsky, P.E., Moss, M.L. and Werb, Z. 2007. The low affinity IgE receptor (CD23) is cleaved by the metalloproteinase ADAM10. *J Biol Chem.* **282**(20), pp.14836-14844.
Levy, S. 2014. Function of the tetraspanin molecule CD81 in B and T cells. *Immunol Res.* **58**(2-3), pp.179-185.
Li, Y., Jin, L. and Chen, T. 2020. The Effects of Secretory IgA in the Mucosal Immune System. *Biomed Res Int.* **2020**, p2032057.
Lightman, S.M., Utley, A. and Lee, K.P. 2019. Survival of Long-Lived Plasma Cells (LLPC): Piecing Together the Puzzle. *Front Immunol.* **10**, p965.
Lim, S.Y., Yuzhalin, A.E., Gordon-Weeks, A.N. and Muschel, R.J. 2016. Targeting the CCL2-CCR2 signaling axis in cancer metastasis. *Oncotarget.* **7**(19), pp.28697-28710.
Lindquist, R.L., Niesner, R.A. and Hauser, A.E. 2019. In the Right Place, at the Right Time: Spatiotemporal Conditions Determining Plasma Cell Survival and Function. *Front Immunol.* **10**, p788.
Lopez, A. and Abrisqueta, P. 2018. Plasmablastic lymphoma: current perspectives. *Blood Lymphat Cancer.* **8**, pp.63-70.
Lorsbach, R.B., Hsi, E.D., Dogan, A. and Fend, F. 2011. Plasma cell myeloma and related neoplasms. *Am J Clin Pathol.* **136**(2), pp.168-182.
Lownik, J.C., Luker, A.J., Damle, S.R., Cooley, L.F., El Sayed, R., Hutloff, A., Pitzalis, C., Martin, R.K., El Shikh, M.E.M. and Conrad, D.H. 2017. ADAM10-Mediated ICOS Ligand Shedding on B Cells Is Necessary for Proper T Cell ICOS Regulation and T Follicular Helper Responses. *J Immunol.* **199**(7), pp.2305-2315.
Lownik, J.C., Wimberly, J.L., Takahashi-Ruiz, L. and Martin, R.K. 2020. B cell ADAM17 controls T cell independent humoral immune responses through regulation of TACI and CD138. *Biochem Biophys Res Commun.* **522**(2), pp.442-447.
Mah, K.M. and Weiner, J.A. 2017. Regulation of Wnt signaling by protocadherins. *Semin Cell Dev Biol.* **69**, pp.158-171.
Makady, N.F., Ramzy, D., Ghaly, R., Abdel-Malek, R.R. and Shohdy, K.S. 2021. The Emerging Treatment Options of Plasmablastic Lymphoma: Analysis of 173 Individual Patient Outcomes. *Clin Lymphoma Myeloma Leuk.* **21**(3), pp.e255-e263.
Mangolini, M. and Ringshausen, I. 2020. Bone Marrow Stromal Cells Drive Key Hallmarks of B Cell Malignancies. *Int J Mol Sci.* **21**(4).
Manier, S., Salem, K.Z., Park, J., Landau, D.A., Getz, G. and Ghobrial, I.M. 2017. Genomic complexity of multiple myeloma and its clinical implications. *Nat Rev Clin Oncol.* **14**(2), pp.100-113.
Marchica, V., Toscani, D., Corcione, A., Bolzoni, M., Storti, P., Vescovini, R., Ferretti, E., Dalla Palma, B., Vicario, E., Accardi, F., Mancini, C., Martella, E., Ribatti, D., Vacca, A., Pistoia, V. and Giuliani, N. 2019. Bone Marrow CX3CL1/Fractalkine is a New

Player of the Pro-Angiogenic Microenvironment in Multiple Myeloma Patients. *Cancers (Basel).* **11**(3).
Matthews, A.L., Noy, P.J., Reyat, J.S. and Tomlinson, M.G. 2017. Regulation of A disintegrin and metalloproteinase (ADAM) family sheddases ADAM10 and ADAM17: The emerging role of tetraspanins and rhomboids. *Platelets.* **28**(4), pp.333-341.
McDonald, M.M., Fairfield, H., Falank, C. and Reagan, M.R. 2017. Adipose, Bone, and Myeloma: Contributions from the Microenvironment. *Calcif Tissue Int.* **100**(5), pp.433-448.
Mitroulis, I., Kalafati, L., Bornhäuser, M., Hajishengallis, G. and Chavakis, T. 2020. Regulation of the Bone Marrow Niche by Inflammation. *Front Immunol.* **11**, p1540.
Monahan, K., Rudnick, N.D., Kehayova, P.D., Pauli, F., Newberry, K.M., Myers, R.M. and Maniatis, T. 2012. Role of CCCTC binding factor (CTCF) and cohesin in the generation of single-cell diversity of protocadherin-α gene expression. *Proc Natl Acad Sci U S A.* **109**(23), pp.9125-9130.
Moreaux, J., Hose, D., Kassambara, A., Reme, T., Moine, P., Requirand, G., Goldschmidt, H. and Klein, B. 2011. Osteoclast-gene expression profiling reveals osteoclast-derived CCR2 chemokines promoting myeloma cell migration. *Blood.* **117**(4), pp.1280-1290.
Morito, N., Yoh, K., Maeda, A., Nakano, T., Fujita, A., Kusakabe, M., Hamada, M., Kudo, T., Yamagata, K. and Takahashi, S. 2011. A novel transgenic mouse model of the human multiple myeloma chromosomal translocation t(14;16)(q32;q23). *Cancer Res.* **71**(2), pp.339-348.
Morris, E.V. and Edwards, C.M. 2018. Adipokines, adiposity, and bone marrow adipocytes: Dangerous accomplices in multiple myeloma. *J Cell Physiol.* **233**(12), pp.9159-9166.
Moschetta, M., Kawano, Y., Sacco, A., Belotti, A., Ribolla, R., Chiarini, M., Giustini, V., Bertoli, D., Sottini, A., Valotti, M., Ghidini, C., Serana, F., Malagola, M., Imberti, L., Russo, D., Montanelli, A., Rossi, G., Reagan, M.R., Maiso, P., Paiva, B., Ghobrial, I.M. and Roccaro, A.M. 2017. Bone Marrow Stroma and Vascular Contributions to Myeloma Bone Homing. *Curr Osteoporos Rep.* **15**(5), pp.499-506.
Moss, M.L. and Minond, D. 2017. Recent Advances in ADAM17 Research: A Promising Target for Cancer and Inflammation. *Mediators Inflamm.* **2017**, p9673537.
Mountoufaris, G., Canzio, D., Nwakeze, C.L., Chen, W.V. and Maniatis, T. 2018. Writing, Reading, and Translating the Clustered Protocadherin Cell Surface Recognition Code for Neural Circuit Assembly. *Annu Rev Cell Dev Biol.* **34**, pp.471-493.
Mullooly, M., McGowan, P.M., Crown, J. and Duffy, M.J. 2016. The ADAMs family of proteases as targets for the treatment of cancer. *Cancer Biol Ther.* **17**(8), pp.870-880.
Musolino, C., Allegra, A., Innao, V., Allegra, A.G., Pioggia, G. and Gangemi, S. 2017. Inflammatory and Anti-Inflammatory Equilibrium, Proliferative and Antiproliferative Balance: The Role of Cytokines in Multiple Myeloma. *Mediators Inflamm.* **2017**, p1852517.
Mykytiv, V., Alwaheed, A. and Mohd Hashim, N.A. 2019. Double CD38. *Hematol Oncol Stem Cell Ther.* **12**(1), pp.64-66.
Nelissen, J.M., Peters, I.M., de Grooth, B.G., van Kooyk, Y. and Figdor, C.G. 2000. Dynamic regulation of activated leukocyte cell adhesion molecule-mediated homotypic cell adhesion through the actin cytoskeleton. *Mol Biol Cell.* **11**(6), pp.2057-2068.

Neri, P., Ren, L., Azab, A.K., Brentnall, M., Gratton, K., Klimowicz, A.C., Lin, C., Duggan, P., Tassone, P., Mansoor, A., Stewart, D.A., Boise, L.H., Ghobrial, I.M. and Bahlis, N.J. 2011. Integrin β7-mediated regulation of multiple myeloma cell adhesion, migration, and invasion. *Blood.* **117**(23), pp.6202-6213.
Nguyen, D.C., Garimalla, S., Xiao, H., Kyu, S., Albizua, I., Galipeau, J., Chiang, K.Y., Waller, E.K., Wu, R., Gibson, G., Roberson, J., Lund, F.E., Randall, T.D., Sanz, I. and Lee, F.E. 2018. Factors of the bone marrow microniche that support human plasma cell survival and immunoglobulin secretion. *Nat Commun.* **9**(1), p3698.
Nguyen, D.C., Joyner, C.J., Sanz, I. and Lee, F.E. 2019. Factors Affecting Early Antibody Secreting Cell Maturation Into Long-Lived Plasma Cells. *Front Immunol.* **10**, p2138.
Nishida, H. and Yamada, T. 2019. Monoclonal Antibody Therapies in Multiple Myeloma: A Challenge to Develop Novel Targets. *J Oncol.* **2019**, p6084012.
O'Leary, R., Reilly, J.E., Hanson, H.H., Kang, S., Lou, N. and Phillips, G.R. 2011. A variable cytoplasmic domain segment is necessary for γ-protocadherin trafficking and tubulation in the endosome/lysosome pathway. *Mol Biol Cell.* **22**(22), pp.4362-4372.
Ohguchi, H., Hideshima, T., Bhasin, M.K., Gorgun, G.T., Santo, L., Cea, M., Samur, M.K., Mimura, N., Suzuki, R., Tai, Y.T., Carrasco, R.D., Raje, N., Richardson, P.G., Munshi, N.C., Harigae, H., Sanda, T., Sakai, J. and Anderson, K.C. 2016. The KDM3A-KLF2-IRF4 axis maintains myeloma cell survival. *Nat Commun.* **7**, p10258.
Palm, A.E. and Henry, C. 2019. Remembrance of Things Past: Long-Term B Cell Memory After Infection and Vaccination. *Front Immunol.* **10**, p1787.
Pawlyn, C. and Morgan, G.J. 2017. Evolutionary biology of high-risk multiple myeloma. *Nat Rev Cancer.* **17**(9), pp.543-556.
Peek, S.L., Mah, K.M. and Weiner, J.A. 2017. Regulation of neural circuit formation by protocadherins. *Cell Mol Life Sci.* **74**(22), pp.4133-4157.
Penna, E., Orso, F., Cimino, D., Vercellino, I., Grassi, E., Quaglino, E., Turco, E. and Taverna, D. 2013. miR-214 coordinates melanoma progression by upregulating ALCAM through TFAP2 and miR-148b downmodulation. *Cancer Res.* **73**(13), pp.4098-4111.
Podar, K., Zimmerhackl, A., Fulciniti, M., Tonon, G., Hainz, U., Tai, Y.T., Vallet, S., Halama, N., Jäger, D., Olson, D.L., Sattler, M., Chauhan, D. and Anderson, K.C. 2011. The selective adhesion molecule inhibitor Natalizumab decreases multiple myeloma cell growth in the bone marrow microenvironment: therapeutic implications. *Br J Haematol.* **155**(4), pp.438-448.
Pupovac, A., Geraghty, N.J., Watson, D. and Sluyter, R. 2015. Activation of the P2X7 receptor induces the rapid shedding of CD23 from human and murine B cells. *Immunol Cell Biol.* **93**(1), pp.77-85.
Reis, B.S., Lee, K., Fanok, M.H., Mascaraque, C., Amoury, M., Cohn, L.B., Rogoz, A., Dallner, O.S., Moraes-Vieira, P.M., Domingos, A.I. and Mucida, D. 2015. Leptin receptor signaling in T cells is required for Th17 differentiation. *J Immunol.* **194**(11), pp.5253-5260.
Reiss, K., Maretzky, T., Haas, I.G., Schulte, M., Ludwig, A., Frank, M. and Saftig, P. 2006. Regulated ADAM10-dependent ectodomain shedding of gamma-protocadherin C3 modulates cell-cell adhesion. *J Biol Chem.* **281**(31), pp.21735-21744.
Rosso, O., Piazza, T., Bongarzone, I., Rossello, A., Mezzanzanica, D., Canevari, S., Orengo, A.M., Puppo, A., Ferrini, S. and Fabbi, M. 2007. The ALCAM shedding by the

metalloprotease ADAM17/TACE is involved in motility of ovarian carcinoma cells. *Mol Cancer Res.* **5**(12), pp.1246-1253.
Rubinstein, R., Goodman, K.M., Maniatis, T., Shapiro, L. and Honig, B. 2017. Structural origins of clustered protocadherin-mediated neuronal barcoding. *Semin Cell Dev Biol.* **69**, pp.140-150.
Ryu, J., Koh, Y., Park, H., Kim, D.Y., Kim, D.C., Byun, J.M., Lee, H.J. and Yoon, S.S. 2016. Highly Expressed Integrin-α8 Induces Epithelial to Mesenchymal Transition-Like Features in Multiple Myeloma with Early Relapse. *Mol Cells.* **39**(12), pp.898-908.
Saftig, P. and Reiss, K. 2011. The "A Disintegrin And Metalloproteases" ADAM10 and ADAM17: novel drug targets with therapeutic potential? *Eur J Cell Biol.* **90**(6-7), pp.527-535.
Schalm, S.S., Ballif, B.A., Buchanan, S.M., Phillips, G.R. and Maniatis, T. 2010. Phosphorylation of protocadherin proteins by the receptor tyrosine kinase Ret. *Proc Natl Acad Sci U S A.* **107**(31), pp.13894-13899.
Schichman, S.A., McClure, R., Schaefer, R.F. and Mehta, P. 2004. HIV and plasmablastic lymphoma manifesting in sinus, testicles, and bones: a further expansion of the disease spectrum. *Am J Hematol.* **77**(3), pp.291-295.
Schreiner, D. and Weiner, J.A. 2010. Combinatorial homophilic interaction between gamma-protocadherin multimers greatly expands the molecular diversity of cell adhesion. *Proc Natl Acad Sci U S A.* **107**(33), pp.14893-14898.
Six, E., Ndiaye, D., Laabi, Y., Brou, C., Gupta-Rossi, N., Israel, A. and Logeat, F. 2003. The Notch ligand Delta1 is sequentially cleaved by an ADAM protease and gamma-secretase. *Proc Natl Acad Sci U S A.* **100**(13), pp.7638-7643.
Slomp, A. and Peperzak, V. 2018. Role and Regulation of Pro-survival BCL-2 Proteins in Multiple Myeloma. *Front Oncol.* **8**, p533.
Smulski, C.R., Kury, P., Seidel, L.M., Staiger, H.S., Edinger, A.K., Willen, L., Seidl, M., Hess, H., Salzer, U., Rolink, A.G., Rizzi, M., Schneider, P. and Eibel, H. 2017. BAFF- and TACI-Dependent Processing of BAFFR by ADAM Proteases Regulates the Survival of B Cells. *Cell Rep.* **18**(9), pp.2189-2202.
Sommer, A., Kordowski, F., Büch, J., Maretzky, T., Evers, A., Andrä, J., Düsterhöft, S., Michalek, M., Lorenzen, I., Somasundaram, P., Tholey, A., Sönnichsen, F.D., Kunzelmann, K., Heinbockel, L., Nehls, C., Gutsmann, T., Grötzinger, J., Bhakdi, S. and Reiss, K. 2016. Phosphatidylserine exposure is required for ADAM17 sheddase function. *Nat Commun.* **7**, p11523.
Taddesse-Heath, L., Meloni-Ehrig, A., Scheerle, J., Kelly, J.C. and Jaffe, E.S. 2010. Plasmablastic lymphoma with MYC translocation: evidence for a common pathway in the generation of plasmablastic features. *Mod Pathol.* **23**(7), pp.991-999.
Thordardottir, M., Lindqvist, E.K., Lund, S.H., Costello, R., Burton, D., Korde, N., Mailankody, S., Eiriksdottir, G., Launer, L.J., Gudnason, V., Harris, T.B., Landgren, O. and Kristinsson, S.Y. 2017. Obesity and risk of monoclonal gammopathy of undetermined significance and progression to multiple myeloma: a population-based study. *Blood Adv.* **1**(24), pp.2186-2192.
Tomita, T., Kubota, T., Nakasone, N., Morozumi, T., Abe, D., Maruyama, S., Shimizu, T., Horimizu, M., Saku, T. and Yoshie, H. 2013. Gene and protein localisation of tumour necrosis factor (TNF)-α converting enzyme in gingival tissues from periodontitis patients with drug-induced gingival overgrowth. *Arch Oral Biol.* **58**(8), pp.1014-1020.

Toyoda, S., Kawaguchi, M., Kobayashi, T., Tarusawa, E., Toyama, T., Okano, M., Oda, M., Nakauchi, H., Yoshimura, Y., Sanbo, M., Hirabayashi, M., Hirayama, T., Hirabayashi, T. and Yagi, T. 2014. Developmental epigenetic modification regulates stochastic expression of clustered protocadherin genes, generating single neuron diversity. *Neuron.* **82**(1), pp.94-108.
Trentin, L., Miorin, M., Facco, M., Baesso, I., Carraro, S., Cabrelle, A., Maschio, N., Bortoli, M., Binotto, G., Piazza, F., Adami, F., Zambello, R., Agostini, C. and Semenzato, G. 2007. Multiple myeloma plasma cells show different chemokine receptor profiles at sites of disease activity. *Br J Haematol.* **138**(5), pp.594-602.
Vande Broek, I., Asosingh, K., Vanderkerken, K., Straetmans, N., Van Camp, B. and Van Riet, I. 2003. Chemokine receptor CCR2 is expressed by human multiple myeloma cells and mediates migration to bone marrow stromal cell-produced monocyte chemotactic proteins MCP-1, -2 and -3. *Br J Cancer.* **88**(6), pp.855-862.
Vande Broek, I., Van de Broek, I., Leleu, X., Schots, R., Facon, T., Vanderkerken, K., Van Camp, B. and Van Riet, I. 2006. Clinical significance of chemokine receptor (CCR1, CCR2 and CXCR4) expression in human myeloma cells: the association with disease activity and survival. *Haematologica.* **91**(2), pp.200-206.
Vega, F., Chang, C.C., Medeiros, L.J., Udden, M.M., Cho-Vega, J.H., Lau, C.C., Finch, C.J., Vilchez, R.A., McGregor, D. and Jorgensen, J.L. 2005. Plasmablastic lymphomas and plasmablastic plasma cell myelomas have nearly identical immunophenotypic profiles. *Mod Pathol.* **18**(6), pp.806-815.
Vega-Benedetti, A.F., Loi, E., Moi, L., Blois, S., Fadda, A., Antonelli, M., Arcella, A., Badiali, M., Giangaspero, F., Morra, I., Columbano, A., Restivo, A., Zorcolo, L., Gismondi, V., Varesco, L., Bellomo, S.E., Giordano, S., Canale, M., Casadei-Gardini, A., Faloppi, L., Puzzoni, M., Scartozzi, M., Ziranu, P., Cabras, G., Cocco, P., Ennas, M.G., Satta, G., Zucca, M., Canzio, D. and Zavattari, P. 2019. Clustered protocadherins methylation alterations in cancer. *Clin Epigenetics.* **11**(1), p100.
Vincent, T. and Mechti, N. 2005. Extracellular matrix in bone marrow can mediate drug resistance in myeloma. *Leuk Lymphoma.* **46**(6), pp.803-811.
Wen, G., Wang, W., Zhang, Y., Niu, S., Li, Q. and Li, Y. 2017. Management of extramedullary plasmacytoma: Role of radiotherapy and prognostic factor analysis in 55 patients. *Chin J Cancer Res.* **29**(5), pp.438-446.
Weng, J., Xiao, J., Mi, Y., Fang, X., Sun, Y., Li, S., Qin, Z., Li, X., Liu, T., Zhao, S., Zhou, L. and Wen, Y. 2018. PCDHGA9 acts as a tumor suppressor to induce tumor cell apoptosis and autophagy and inhibit the EMT process in human gastric cancer. *Cell Death Dis.* **9**(2), p27.
Wilmore, J.R. and Allman, D. 2017. Here, There, and Anywhere? Arguments for and against the Physical Plasma Cell Survival Niche. *J Immunol.* **199**(3), pp.839-845.
Winter, O., Dame, C., Jundt, F. and Hiepe, F. 2012. Pathogenic long-lived plasma cells and their survival niches in autoimmunity, malignancy, and allergy. *J Immunol.* **189**(11), pp.5105-5111.
Wolf, M.J., Hoos, A., Bauer, J., Boettcher, S., Knust, M., Weber, A., Simonavicius, N., Schneider, C., Lang, M., Stürzl, M., Croner, R.S., Konrad, A., Manz, M.G., Moch, H., Aguzzi, A., van Loo, G., Pasparakis, M., Prinz, M., Borsig, L. and Heikenwalder, M. 2012. Endothelial CCR2 signaling induced by colon carcinoma cells enables extravasation via the JAK2-Stat5 and p38MAPK pathway. *Cancer Cell.* **22**(1), pp.91-105.

Xu, L., Mohammad, K.S., Wu, H., Crean, C., Poteat, B., Cheng, Y., Cardoso, A.A., Machal, C., Hanenberg, H., Abonour, R., Kacena, M.A., Chirgwin, J., Suvannasankha, A. and Srour, E.F. 2016. Cell Adhesion Molecule CD166 Drives Malignant Progression and Osteolytic Disease in Multiple Myeloma. *Cancer Res.* **76**(23), pp.6901-6910.
Zheng, Y., Wang, Q., Li, T., Qian, J., Lu, Y., Li, Y., Bi, E., Reu, F., Qin, Y., Drazba, J., Hsi, E., Yang, J., Cai, Z. and Yi, Q. 2016. Role of Myeloma-Derived MIF in Myeloma Cell Adhesion to Bone Marrow and Chemotherapy Response. *J Natl Cancer Inst.* **108**(11).
Zingoni, A., Cecere, F., Vulpis, E., Fionda, C., Molfetta, R., Soriani, A., Petrucci, M.T., Ricciardi, M.R., Fuerst, D., Amendola, M.G., Mytilineos, J., Cerboni, C., Paolini, R., Cippitelli, M. and Santoni, A. 2015. Genotoxic Stress Induces Senescence-Associated ADAM10-Dependent Release of NKG2D MIC Ligands in Multiple Myeloma Cells. *J Immunol.* **195**(2), pp.736-748.
Zipursky, S.L. and Sanes, J.R. 2010. Chemoaffinity revisited: dscams, protocadherins, and neural circuit assembly. *Cell.* **143**(3), pp.343-353.